ISSN 0711-6659

canadian acoustics
acoustique canadienne

SEPTEMBER 1991 SEPTEMBRE 1991
Volume 19 -- Number 4 Volume 19 -- Numéro 4

PROCEEDINGS ISSUE

CANADIAN ACOUSTICS WEEK
SEMAINE CANADIENNE D'ACOUSTIQUE

1991

CAHIER DES ACTES

canadian acoustics

acoustique canadienne

THE CANADIAN ACOUSTICAL ASSOCIATION
P.O. BOX 1351, STATION "F"
TORONTO, ONTARIO M4Y 2V9

L'ASSOCIATION CANADIENNE D'ACOUSTIQUE
C.P. 1351, SUCCURSALE "F"
TORONTO, ONTARIO M4Y 2V9

CANADIAN ACOUSTICS publishes refereed articles and news items on all aspects of acoustics and vibration. Papers reporting new results or applications, as well as review or tutorial papers and shorter research notes are welcomed, in English or in French. Submissions should be sent directly to the Editor-in-Chief. Complete instructions to authors concerning the required camera-ready copy are presented on the last page of this issue.

ACOUSTIQUE CANADIENNE publie des articles arbitrés et des informations sur tous les domaines de l'acoustique et des vibrations. On invite les auteurs à proposer des manuscrits rédigés en français ou en anglais concernant des travaux inédits, des états de question ou des notes techniques. Les soumissions doivent être envoyées au rédacteur en chef. Les instructions pour la présentation des textes sont exposées à la dernière page de cette publication.

CANADIAN ACOUSTICS is published four times a year - in March, June, September and December. Publications Mail Registration No. 4692. Return postage guaranteed. Annual subscription: $10 (student); $35 (individual, corporation); $150 (sustaining - see back cover). Back issues (when available) may be obtained from the Associate Editor (Advertising) - price $10.00 including postage.

ACOUSTIQUE CANADIENNE est publiée quatre fois par année - en mars, juin, septembre et decembre. Poste publications - enregistrement n^{o} 4692. Port de retour garanti. Abonnement annuel: $10 (étudiant); $35 (individuel, société); $150 (soutien - voir la couverture arrière). D'anciens numéros (non-épuisés) peuvent être obtenus du rédacteur associé (publicité) - prix: $10,00 (affranchissement inclus).

EDITORIAL

Here it is folks, as promised - the first annual Proceedings Issue of *Canadian Acoustics*. It constitutes the proceedings of the technical sessions of Canadian Acoustics Week 1991 which will be held in Edmonton in October. Two-page summaries were recieved from 56 of the 73 people who will present papers at the conference. Many thanks to everyone who worked hard to produce their summary papers, to submit them on time and to put them in the required format. I think these proceedings are something that we all can be proud of.

Last year I promised to investigate having papers published in Canadian Acoustics cited in the various citation indices. I have written to ten such indexing services and have had responses from five. I am pleased to be able to report that, from now on, *Canadian Acoustics* papers will be cited in the following indices: References to Current Papers on Acoustics (JASA); Acoustics Abstracts; Shock and Vibration Digest; Physics Abstracts; Industrial Hygiene Digest. I will report to you again when I hear from the other citation services.

Between now and the publication of the December issue, your Editor-in-Chief is moving across the country. He has been asked by the Board of Directors, and has accepted, to continue editing the journal. However, this will involve considerable disruption (finding a new printing company, transfering our Post Office account etc.) in publishing the next issue, in which I'll provide details of my move and my new mailing address. I'll do my best to keep publication of on schedule, but please bear with me if necessary.

Tel que promis, voici, chers amis, la première publication du Cahier des Actes de l'*Acoustique Canadienne*. Ce numéro constitue les actes de la Semaine de l'Acoustique Canadienne 1991 qui sera tenue à Edmonton en octobre. Nous avons reçu les sommaires de deux pages de 56 des 73 personnes qui présenteront des communications au congrès. Nous remercions tous ceux qui ont travaillé fort afin de préparer leur sommaire, de le soumettre dans les délais et qui ont respecté le format demandé. Je pense que nous pouvons être fiers de ces actes.

L'année dernière, j'avais promis d'investiguer la possibilité que les papiers publiés dans l'*Acoustique Canadienne* soient cités dans les différents répertoires de citations. J'ai écrit à dix de ces services de répertoires et ai reçu cinq réponses. Je suis heureux de vous faire part que, à partir de maintenant, les articles publiés dans l'*Acoustique Canadienne* seront répertoriés dans: References to Current Papers on Acoustics (JASA); Acoustics Abstracts; Shock and Vibration Digest; Physics Abstracts; Industrial Hygiene Digest. Je vous ferai de nouveau rapport lorsque j'obtiendrai des nouvelles des autres services de citations.

Entre aujourd'hui et la publication du numéro de décembre, votre rédacteur en chef déménagera à travers le pays. Le conseil d'administration lui a demandé de continuer son travail de rédacteur en chef, ce qu'il a accepté. Cependant, ceci risque de provoquer de considérables problèmes (trouver une nouvelle compagnie d'impression, transférer notre compte au bureau de poste, etc.) dans la publication du prochain numéro, dans lequel je transmettrai les détails de mon déménagement et de ma nouvelle adresse postale. Je ferai tout mon possible afin de respecter la date de publication, mais j'apprécierais grandement que vous soyez indulgents à mon égard, si nécessaire.

Superior Instrumentation for Acoustics and Vibration

LARSON-DAVIS LABORATORIES

We have become a new technology leader in acoustics and vibration measuring instruments. Our goal is to provide advanced, precise, high-quality products at very reasonable prices. As the result of a substantial ongoing research program, Larson-Davis products provide versatility and automation untouched by *any* competitive offerings. Our growing product family includes:

- Portable multichannel Real-Time analyzers delivering 1/1, 1/3 and 1/12 octave bands to 125 KHz with future plug-in modules for FFT, acoustic intensity, memory expansion, etc.
- Underwater acoustic analysis equipment.
- Precision sound level meters with computer interfaces and automated control of 1/1 and 1/3 octave filters.
- Data logging noise dosimeters and hand-held sound level meters.
- Environmental and industrial noise monitoring systems.
- Building and architectural acoustics analyzers.
- Vibration measuring and monitoring instruments.
- Audiometric calibration instruments for speech and hearing.
- Network airport noise monitoring systems, with management planning software.
- Precision measuring microphones, preamplifiers, power supplies, instrumentation amplifiers, acoustic intensity probes, calibrators and accessories.

For more information contact the factory.

Dalimar Instruments Inc.

89, boul. Don Quichotte
Suite No. 7
Ile Perrot, Qc
J7V 6X2
Tel.: (514) 453-0033
Fax : (514) 453-0554

PROCEEDINGS OF CANADIAN ACOUSTICS WEEK 1991
ACTES DE LA SEMAINE CANADIENNE D'ACOUSTIQUE 1991

Table of Contents / Table des matières

Comparison of Computational Methods for Rectangular Silencer Insertion Loss Prediction

Ramani Ramakrishnan
41 Watson Avenue
Toronto, Ontario

Robert Stevens and Brian Howe
Vibron Limited
1720 Meyerside Drive
Mississauga, Ontario

1.0 INTRODUCTION

The insertion loss (IL) of duct silencers with absorbent material can be predicted by a number numerical techniques. Two of the most common methods are the Boundary element method (BEM) and the Modal Finite Element Method (FEM). These two procedures are applied to predict the IL of rectangular silences and the comparative results are presented in this paper.

2.0 THEORETICAL BACKGROUND

Example of a typical rectangular silencer is shown in Figure 1. Silencers with sound absorbing baffles are commonly used in HVAC system ducts. The main aim for HVAC system duct designers is to compute the silencer IL spectrum for a given silencer configuration.

The IL of a duct silencer is made of three components namely: entrance loss, exit loss and the loss due to the sound absorbing material. The BEM method can model all the three components whereas the FEM procedure presented here can take into account only the loss due to the absorbing material

2.1 Boundary Element Method

The boundary element method models only the boundary surface of the acoustic region of interest, unlike conventional FEM techniques which subdivide the domain into a mesh of three dimensional brick type elements. The BEM technique considers the problem of an enclosed acoustic domain as a potential field problem and uses Green's theorem to reduce the steady state, three dimensional Helmholtz equation (1) to a two dimensional surface integral [1].

$$\nabla^2 p + k^2 p = 0 \qquad (1)$$

where p is the sound pressure,
$k = \omega/c$ is the wave number
and c = speed of sound in air.

The BEM model consists of two dimensional plate type elements forming an enclosing surface. The dimensions of each element must be less than approximately one quarter of the wavelength of interest. (See Figure 2. Note - only half of the silencer boundary is modelled, since the BEM algorithm can take advantage of the symmetry of the silencer in the width direction.)

At each surface element (including the plane of the outlet), the specific acoustic impedance, Z_S, is specified. Assigning each element a Z_S value implicitly makes the assumption that the absorptive surfaces are locally reacting. The Z_S values for the sound absorbing material are derived from characteristic impedance and propagation constant obtained from Bies and Hanson [2]. Over the inlet elements, a unit normal particle velocity condition is specified.

The BEM algorithm then numerically solves the reduced Helmholtz equation over the boundary surface at the frequency of interest using a Gauss quadrature integration technique.

2.2 Finite Element Method

The acoustical evaluation follows conventional methods [3,4,5]. The methodology requires a complete description of the sound absorbing material. The material is considered to be homogeneous, isotropic and made up of either fibrous or foam type material. It is also considered to be bulk reacting unlike the locally reacting model assumed by the BEM model. The propagation in the material is thus included with proper accounting of the bulk properties of the acoustic material.

The sound field in the duct is evaluated by the following set of wave equations:

$$\frac{\partial^2 p}{\partial z^2} + \frac{\partial^2 p}{\partial x^2} - \frac{1}{c_1^2}\frac{\partial^2 p}{\partial t^2} = 0 \qquad (2)$$

$$\frac{\partial^2 p}{\partial z^2} + \frac{\partial^2 p}{\partial x^2} - \frac{1}{c_2^2}\frac{\partial^2 p}{\partial t^2} = 0 \qquad (3)$$

Equation (1) is valid in the open airway with c_1 being the sound speed and equation (2) is valid in the sound absorbing material with a complex sound speed of c_2. Pressure and velocity continuity are applied at two interfaces between the absorbing material and the open airway. The two equations are solved for the common axial wave number k_z by applying a cubic finite element algorithm [6]. The characteristic impedance and propagation constant in the sound absorbing material are obtained from Bies and Hanson [2] and Beranek [7]. The real part of the axial wave number k_z is directly proportional to the attenuation rate per unit length of the silencer.

All possible modes up are evaluated at each frequency of interest. Only those modes with slow rates of attenuation are summed to determine the final decay rate per unit length by assuming that these modes carry equal amount of the incident sound energy.

The silencer shown in Figure 1 consists of two section: the straight portion and a tapered divergent diffuser section. The decay rate calculated in the straight section is multiplied by its length to predict the IL of the straight section. The modes are evaluated at two additional points, the mid-section and the tail end of the diffuser. The averaged decay rate (average of the three final decay rates) is multiplied by the length of the diffuser section to predict the diffuser IL. The silencer IL is the sum of the above two predictions.

3.0 RESULTS AND DISCUSSION

IL values for two typical silencers were modelled for four octave bands (ranging from 125 to 1000 Hz) using BEM and FEM. The results are presented in Table I. Also given in Table I, are IL values from ASTM standard test E477-90. The predictions agree reasonably well with test data. The silencers employed fibreglass fill with a flow resistivity of 20 000 mks rayl as the absorptive medium.

The agreement between BEM predictions and test data becomes poorer at frequencies approaching 1 kHz or greater. This may be explained by the fact that the assumption of locally reacting sound absorbing material tends to become inaccurate as frequency increases [5]. The high frequency accuracy can be improved by constructing a multi-domain BEM model which treats the absorptive material as a separate domain, taking into account the bulk reacting properties of the material. The multi-domain approach would, of course, increase computation time.

Difference between FEM predictions and test data can be attributed primarily to the fact that the FEM model does not account for entrance and exit effects at the inlet and outlet of the silencers. Correction factors can be added to the FEM prediction to improve agreement with tests.

The computation time for both techniques were comparable; one to two hours to obtain IL values in each of four octave bands for each silencer configuration. The algorithms were executed on a PC/386 type machine. The BEM computation becomes increasingly slower as the test frequency increases, since the mesh dimensions must always be less than approximately one quarter wavelength of the test frequency.

4.0 CONCLUSIONS

BEM and FEM models were applied to the problem of predicting rectangular silencer insertion loss. The results were found to be in reasonable agreement with test data.

The BEM method was found to be best suited to low frequency applications, (i.e., f ≤ 500 Hz) in which the absorptive material may be considered to be locally reacting and computation speed is greatest.

The FEM technique, while its accuracy and computation time are less sensitive to frequency, does not consider entrance and exit effects. The FEM approach is practical if proper corrections for entrance and exit effects are added to the predicted insertion loss.

5.0 REFERENCES

1.0 C.Y.R. Cheng and A.F. Seybert, "Recent Applications of the Boundary Element Method to Problems in Acoustics", Paper presented at the 1987 SAE Noise and Vibration Conference, Traverse City, MI April (1987).

2.0 D.A. Bies and C.H. Hanson, *Engineering Noise Control: Theory and Practice*, Appendix 3. (Allen and Unwin, Winchester MASS 1988).

3.0 R. Ramakrishnan and W.R. Watson, "Design Curves for Rectangular Splitter Silencers", Presented to Applied Acoustics Journal for publication, (1990).

4.0 R. Ramakrishnan and W.R. Watson, "Acoustic Performance of Multi-Unit Splitter Silencers", Canadian Acoustics Journal, 18(3), 3-12 (1990).

5.0 R.A. Scott, "The Propagation of Sound between Walls of Porous Materials", Proceedings, Physical Society, London, Vol. 58, 358-368 (1946).

6.0 W.R. Watson and D.L. Lansing, "A Comparison of Matrix Methods for Calculating Eigenvalues in Acoustically Lined Ducts", NASA Technical Note, TN D-8186, (1976).

7.0 L.L. Beranek, *Noise and Vibration Control*, 245-269 (McGraw-Hill, New York, 1971).

Figure 1. Cut-away Showing Rectangular Silencer Construction

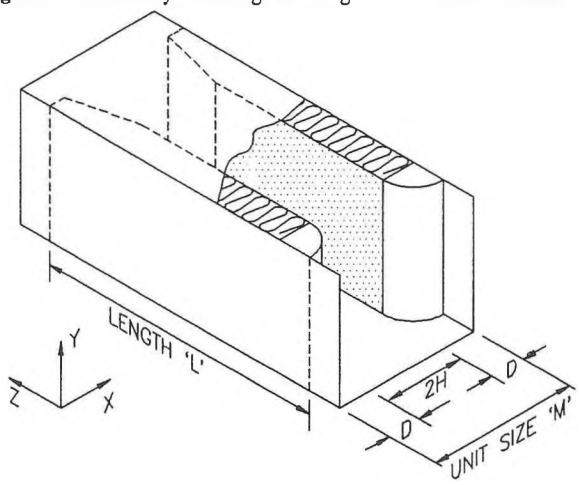

Figure 2. BEM Model S1 - 91 Elements

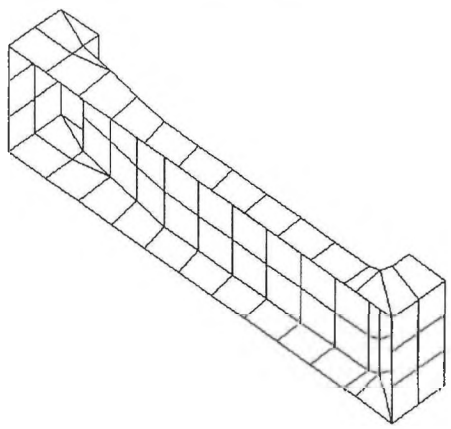

Table I

Model # M, mm	D/H	L mm		Insertion Loss, dB in Octave Bands 2	3	4	5
S1 458	1.13	1525	Test	5	12	20	26
			BEM	6	12	17	28
			FEM	6	14	21	29
S2 305	1	1525	Test	4	12	27	41
			BEM	3	9	22	33
			FEM	4	12	26	44

BAGPIPES A PROGRAM FOR ANALYZING ACOUSTIC TRANSMISSION IN DUCTWORK

P. Fuchshuber and A. Craggs
Department of Mechanical Engineering
University of Alberta
Edmonton, Alberta T6G 2G8

Introduction

The finite element method provides an effective means for modelling acoustic propagation in HVAC systems and pipe networks. However, due to extensive lengths of ducting and the degree of mesh refinement required to model high frequency sound transmission, resulting systems of equations can be very large. It is essential to reduce their size so that computer memory limits are not exceeded and computation time is reduced.

In BAGPIPES, system equations are generated automatically in the form of duct superelements. During generation, the superelements are formed by successively enclosing layers of elements, so that the complete superelement is described by only the number of nodes needed to describe a single layer. Consequently the interior nodes, which are not required for superelement conductivity, do not add to the size of the system. Limits on the model size arise from the number of superelement nodes required for connectivity.

Once the superelements have been assembled, nodes which are not required for the application of boundary conditions and sound sources, or for the solution output are condensed from the system. The result of these reductions in savings in run time and the ability to model far larger systems than would otherwise be possible within the confines of a personal computer.

The program has been used to model several fittings commonly found in HVAC systems. In addition, a network including a plenum chamber was modelled and results compared with a complementary experimental study of the acoustic transmission through the network.

Theory

This section contains an outline of the finite element acoustic theory utilized in the program. The matrix methods for substructuring and application of boundary conditions are described.

The finite element equations for modelling an acoustic volume have been derived previously and are given by Craggs [1]. At frequency λ the nodal system of equations has the form

$$([K] - \lambda^2[P])\{p\} = \{Q\}$$

where

[K] and [P] are square symmetric matrices derived from the kinetic and potential energy, respectively

{p} and {Q} are vectors containing the nodal pressures and volume source terms, respectively.

In the following the frequency dependent coefficient matrix ({K} - λ^2[P]) will be represented by the single stiffness matrix [S].

Substructuring

When the nodal pressure and sources at interior nodes in a length of duct may be eliminated from the system, the duct length can be modelled as a single "superelement". The advantage of this approach is that the superelement has only as many nodal variables as the number of nodes lying on the end planes of the duct.

In addition, for prismatic ducts where the geometric changes are one dimensional, the duct superelement can be generated by assembling an element representing a single layer of the duct and cascading this layer sequentially n times to generate 2^n layers. This applies to duct segments consisting of straight sections or arc sections. When the layers differ, a new layer must be formed and cascaded with the previous assemblage each time. This applies to sections containing bends or where the dimensions of the layers parallel to the duct axis is non-uniform.

The procedure is summarized as follows. For two duct segments A and B the system of nodal equations are:

$$\begin{bmatrix} S_{11}^A & S_{12}^A \\ S_{21}^A & S_{22}^A \end{bmatrix} \begin{Bmatrix} p_1^A \\ p_2^A \end{Bmatrix} = \begin{Bmatrix} Q_1^A \\ Q_2^A \end{Bmatrix}$$

$$\begin{bmatrix} S_{11}^B & S_{12}^B \\ S_{21}^B & S_{22}^B \end{bmatrix} \begin{Bmatrix} p_1^B \\ p_2^B \end{Bmatrix} = \begin{Bmatrix} Q_1^B \\ Q_2^B \end{Bmatrix}$$

Where the subscripts 1 and 2 denote nodes on the endplanes and p_2^A is synonymous with p_1^B and Q_2^A with Q_1^B.

The system of equations representing the coupled model is

$$\begin{bmatrix} S_{11}^A & S_{11}^A & 0 \\ S_{21}^A & D & S_{12}^B \\ 0 & S_{21}^B & S_{22}^B \end{bmatrix} = \begin{Bmatrix} p_1^A \\ p_2^A \\ p_1^B \end{Bmatrix} \begin{Bmatrix} Q_1^A \\ Q_2^A \\ Q_1^B \end{Bmatrix}$$

where $D = S_{22}^A + S_{11}^B$

Solving for p_2^A from the second row

$$p_2 = -D^{-1}S_{21}^A p_1^A - D^{-1}S_{21}^B p_2^B$$

and eliminating p_2 from the third row results in the condensed system

$$\begin{bmatrix} S_{11}^A - S_{12}^A D^{-1} S_{21}^A & -S_{12}^A D^{-1} S_{12}^B \\ -S_{21}^B D^{-1} S_{21}^A & S_{21}^B - S_{21}^B D^{-1} S_{12} \end{bmatrix} \begin{Bmatrix} p_1^A \\ P_2^B \end{Bmatrix} = \begin{Bmatrix} A_1^A \\ Q_2^B \end{Bmatrix}$$

or

$$[S^*]\{p\} = \{Q\}$$

If the layers are all equal the procedure is

1. Form $[S^A] = [S^B]$
2. Form $[S^*]$ n times, each time setting $[S^A] = [S^*]$ to form a superelement consisting of 2^n layers.

If the layers differ the procedure is, for n-1 layers

1. Form $[S^A]$
2. Form $[S^B]$

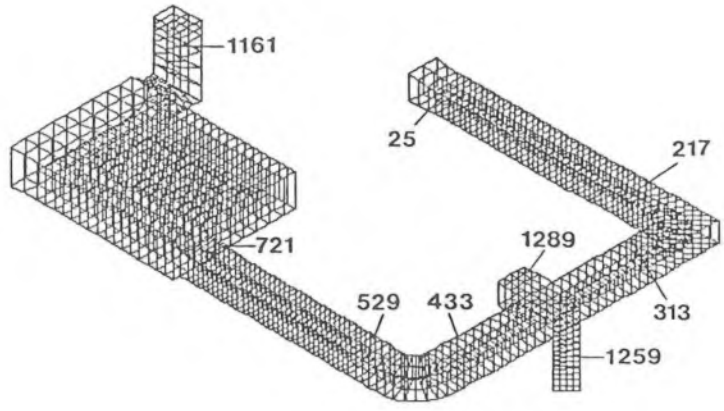

Figure 1

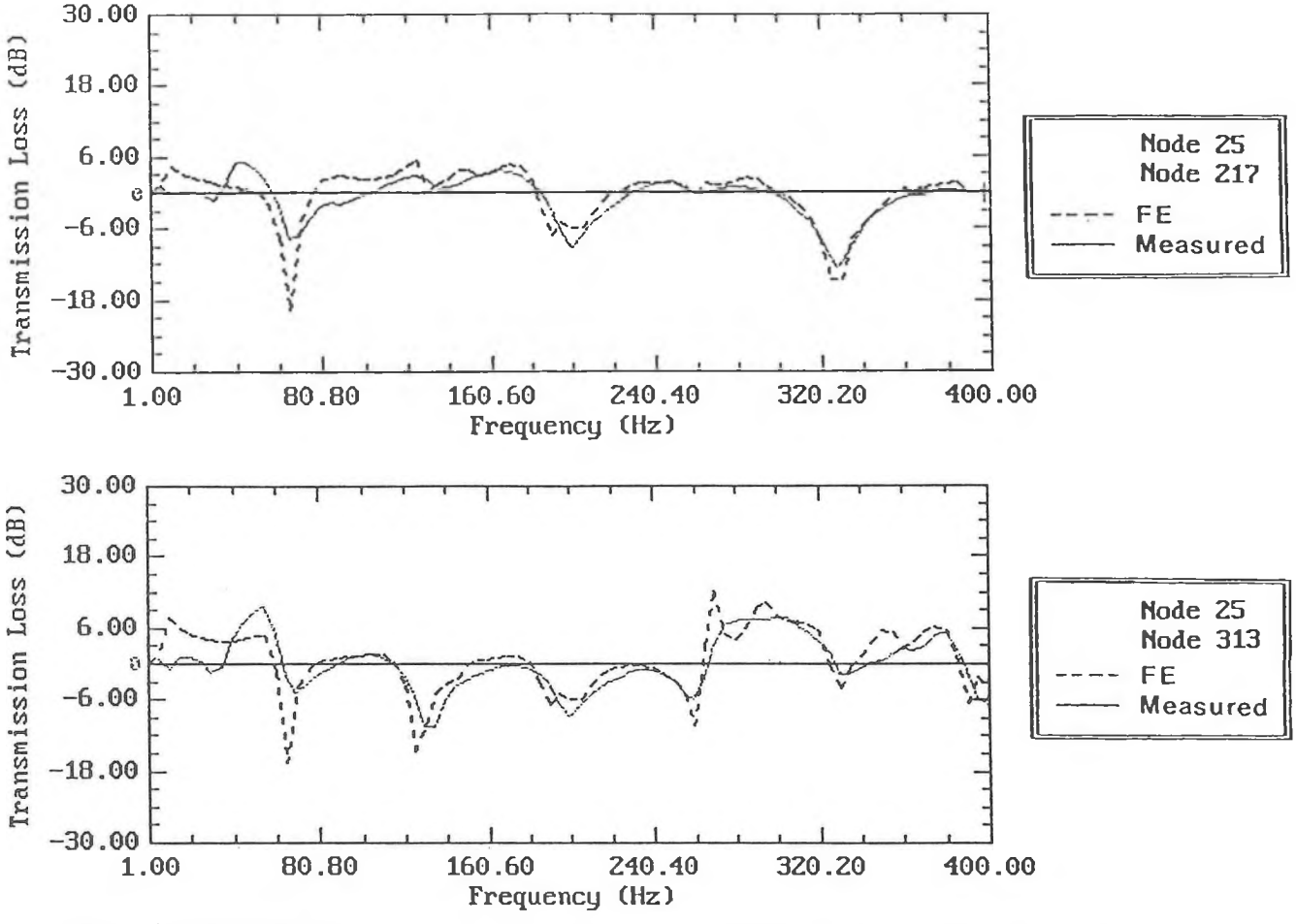

3. Form $[S^*]$ and set $[S^A] = [S^*]$

4. Form $[S_B]$

These procedures allow very large systems to be represented without having to generate the huge matrices which would be associated with the standard finite element methods.

Experimental Validation of Program

A three dimensional duct rig was specially built in order to provide test data to compare with the computer model results. The right was modular in construction so that bends, junctions and plenum chambers could be tested separately. A complete network finite element model is shown in Figure 1. Results for the transmission loss at various points in the network are shown. There is very good agreement.

References

Craggs, A. (1972) "The Use of Simple Three-Dimensional Acoustic Finite Elements for Determining the Natural Modes and Frequencies of Complex Shaped Enclosures", Journal of Sound and Vibration, 23(3), p. 331-339.

Craggs, A. and Fuchshuber, P.J. (1990) BAGPIPES, A Finite Element Program for Pipe Acoustics", Dept. of Mechanical Engineering Report #75, University of Alberta.

PC. CIRCLE
Circular Duct Silencer Performance Prediction Software

Ramani Ramakrishnan
41 Watson Avenue
Toronto, Ontario

Norman Ball
114 Queenmary Street
Ottawa, Ontario

1.0 Introduction

Design curves for lined circular silencers are available in the literature [1,2]. Extensive set of design curves for circular and annular duct silencers were made available recently [3,4]. The generation of a design curve to predict the silencer insertion loss spectrum for each application is a time consuming effort in a personal computer environment. A computer software for DOS machines was developed and released by Ramakrishnan and Ball for conventional rectangular duct silencers [5]. The software eliminated the tedious effort required for the generation of the theoretical prediction scheme for each individual silencer configuration. The development of a software for circular and annular duct silencers is presented in this paper.

2.0 Theoretical Background

Examples of silencer configuration are shown in Figure 1. Circular silencers with sound absorbing centre bullets are more commonly used in HVAC system ducts than simple lined circular ducts. Simple lined ducts are also shown in Figure 1. for completeness. The main aims for HVAC system duct designers are twofold, namely, to compute the silencer insertion loss spectrum for a given silencer configuration and to calculate the pressure drop across the silencer for a given face velocity.

2.1 Acoustical Evaluation

The insertion loss of a duct silencer is made of three components namely: entrance loss, exit loss and the loss due to the sound absorbing material [6]. The procedure presented in this paper is limited to the loss due only to the absorbing material. Proper adjustments would have to be added to account for the entrance and exit losses.

The acoustical evaluation follows conventional methods [7]. The methodology requires a complete description of the sound absorbing material. The material is considered to be homogeneous, isotropic and made up of either fibrous or foam type material. It is also considered to be bulk reacting unlike the locally reacting model assumed in references 1 and 2. The propagation in the material is thus included with proper accounting of the bulk properties of the acoustic material.

The sound field in the duct is evaluated by the following set of wave equations:

$$\frac{\partial^2 p}{\partial z^2} + \frac{\partial^2 p}{\partial r^2} + \frac{1}{r}\frac{\partial p}{\partial r} + \frac{1}{r^2}\frac{\partial^2 p}{\partial \phi^2} - \frac{1}{c_1^2}\frac{\partial^2 p}{\partial t^2} = 0 \qquad (1)$$

$$\frac{\partial^2 p}{\partial z^2} + \frac{\partial^2 p}{\partial r^2} + \frac{1}{r}\frac{\partial p}{\partial r} + \frac{1}{r^2}\frac{\partial^2 p}{\partial \phi^2} - \frac{1}{c_2^2}\frac{\partial^2 p}{\partial t^2} = 0 \qquad (2)$$

Equation (1) is valid in the open airway with c_1 being the sound speed and equation (2) is valid in the sound absorbing material with a complex sound speed of c_2. Pressure and velocity continuity are applied at various interfaces [one for Types (a) and (b) and two for type (c) shown in Figure 1.] between the absorbing material and the open airway. The two equations are solved for the common axial wave number k_z by applying a cubic finite element algorithm [8].

The characteristic impedance and propagation constant in the sound absorbing material are obtained from Beranek [9] and reference 2. The real part of the axial wave number k_z is directly proportional to the attenuation rate per unit length of the silencer.

All possible radial modes up to an azimuthal mode order of 5 are evaluated at each frequency of interest. Only those modes with slow rates of attenuation are summed to determine the final insertion loss by assuming that these modes carry equal amount of the incident sound energy.

2.2 Pressure Drop Evaluation

References 1,2 and 6 had outlined simple methods to estimate the expected pressure drop across the length of the silencer for a given face velocity. The interior details of the silencer are shown in Figure 2.

k_1 through k_5 are the loss coefficients that represent the losses associated with the shape of the silencer restricting the flow. Standard aerodynamic flow equations were used to estimate the loss coefficients. The coefficients depend on the length of the silencer, the open area to total silencer area ratio, radius of the nose cone and the tail diffuser angle of the silencer.

The total loss is represented by,

$$k = k_1 + k_2 + k_3 + k_4 + k_5 \qquad (3)$$

The pressure drop across the silencer is then given by,

$$pd \text{ (inches of water)} = 1/2\ \rho_0\ (v_0)^2 k \qquad (4)$$

where, ρ_0 is the density of the medium and v_0 is the face velocity at the silencer.

3.0 Development of PC. CIRCLE

The theoretical background for the evaluation of silencer insertion loss and pressure drop was presented in Section 2. It is seen that the pressure drop calculations are straight forward once the interior details of the silencer geometry are known. However, acoustic insertion loss calculation time for each individual silencer configuration is considerable (approximately 2.5 hrs in an AT personal computer with a math coprocessor). Enough curves to cover the silencer range of interest can be generated and insertion loss can be estimated by interpolation. The parameters to consider are: silencer overall diameter (from .31m to 1.53m), frequency (from 100 Hz to 10000 Hz), centre bullet size as a percentage of the silencer diameter (usually three sizes are used), liner thickness if used and the sound absorbing material to be used. The required number of design curves is therefore very large.

The required number of curves can be substantially reduced by grouping the design curves. The grouping of the design curves is aided by the fact that the sound propagation in the silencer can be completely described by the following four non-dimensional parameters: $N_1 = d / (2h)$; $N_2 = d / (2t)$; $R = (zd) / (2z_0)$ and $\mu = (fd) / (2c_1)$ where z is the specific flow resistance of the sound absorbing material per unit thickness, f is the frequency and z_0 is the characteristic impedance of the flow medium.

Approximately 600 design curves were generated to cover the range of parameters possible for the three types of conventionally

manufactured silencers for low speed HVAC systems (Fig.1). Instead of solving the wave equations for each individual silencer configuration, i.e., generating a fresh design curve, a linear interpolation scheme is applied to calculate the insertion loss spectrum from the design curve set stored in a large data base.

The scheme is as follows: the four non dimensional parameters are evaluated from silencer details such as overall diameter, bullet size, liner thickness, silencer length, tail diffuser shape and length, and the sound absorbing material type. The closest design curve or curves form the data base are used to perform a linear interpolation and the insertion loss at 18 third octave bands from 100 Hz to 5000 Hz is calculated. Exact shape of the silencer is used in the interpolation scheme, i.e, different values of the non dimensional parameters are used for different sections of the silencer. One set is used for the straight section of the silencer and a minimum of three locations are used to represent the tail diffuser section. The insertion loss values at the 18 bands are calculated by averaging a band of values centred around the third octave frequency [2]. The final insertion loss at the 18 frequencies is calculated by summing the values at each section of the silencer with the appropriate lengths. The results at the 18 bands are then combined together to determine the values at six octave bands from band No. 2 through 7. The evaluation time for each silencer configuration is about 30 seconds.

4.0 PC. CIRCLE

PC. CIRCLE is a computer program for the IBM PC or compatible personal computer that calculates the insertion loss and the pressure drop of a circular/annular duct silencer. The objective of the program is to provide a quick and simple, but comprehensive evaluation tool.

The program is written in the computer languages 'C' and 'FORTRAN'. In addition, FORTRAN links with a copy-righted GRAPHICS package. FORTRAN is used as it can handle mathematical computations in a simple way and is widely available. C language is used for Input/Output and screen presentations as it is versatile and is widely applied. In order to achieve simplicity and clarity, the program is driven through simple in-put menus and pull-down windows.

4.1 Hardware Requirements

Any PC or PC compatible with at least **512K RAM** is sufficient for the execution of the program. A hard disc drive is a must for the smooth execution and for storing all the required Files. The only other necessary requirement is that the machine must be equipped with a Monochrome Graphics or a Colour Graphics Card. **NOTE: The Computer** must have sufficient **RAM memory** available if DOS SHELL is invoked while executing the program.

4.2 Sample Screen Presentation

The program is executed by typing CIRCLE and the return key. The front panel with the Serial No. and the User address will be shown first. The second screen will be as shown in Figure 3. The top line is the Menu-Bar level. The bottom line contains various prompts for the User. Five Menus are available. Display will present graphic details of the silencer and the definitions of the required input variables. Acoustics evaluates the insertion loss and Pressure Drop calculates the pressure drop. Utilities sets the program and hardware requirements. Quit enables to Dos Shell or stop the execution of PC.CIRCLE.

The results of choosing Type 1 Display option are shown in Figure 4. In addition to providing a sketch of the silencer, the details of the necessary parameters are also presented. By appropriate selections of the various menus and windows, the data can be input to the program and the results will then be shown on the screen. The Program can be executed in any sequence, as there are default dummy variables defined within the program.

References

1.0 F. P. Mechel, " Design Criteria for Industrial Mufflers", Proceedings, Inter-Noise '75, 751-760 (1975).

2.0 D.A. Bies and C.H. Hansen, Engineering Noise Control: Theory and Practice, Chapter 9 (Allen and Unwin, Winchester, MASS, 1988).

3.0 R. Ramakrishnan and W.R. Watson, "Design Curves for Circular and Annular Duct Silencers", Proceedings, Inter-Noise '89, 417-419, (1989).

4.0 R. Ramakrishnan and W.R. Watson, "Design Curves for Circular and Annular Duct Silencers", To appear in May/June issue of Noise Control Engineering Journal, (1991).

5.0 R. Ramakrishnan and N. Ball, "PC.BAFFLE, Duct Silencer Performance Prediction Software for a Personal Computer", Paper presented in Acoustics Week in Canada, Toronto, (1988).

6.0 I.L. Ver, "Acoustical Design of Parallel Baffle Mufflers", Proceedings, Nelson Acoustic Conference (1981).

7.0 R.A. Scott, "The Propagation of Sound between Walls of Porous Materials", Proceedings, Physical Society, London, Vol. 58, 358-368 (1946).

8.0 W.R. Watson and D.L. Lansing, " A Comparison of Matrix Methods for Calculating Eigenvalues in Acoustically Lined Ducts", NASA Technical Note, TN D-8186, (1976).

9.0 L.L. Beranek, Noise and Vibration Control, 245-269 (McGraw-Hill, New York, 1971).

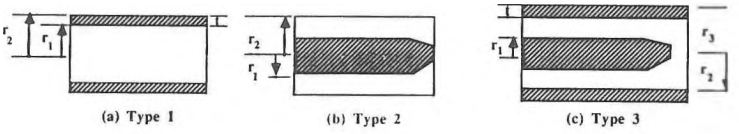

Figure 1. Conventional Circular Duct Silencers

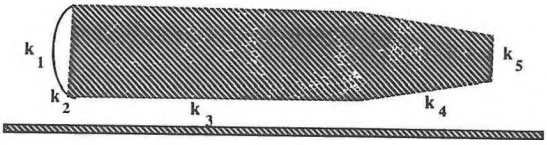

Figure 2. Loss Coefficients for Pressure Drop Calculations

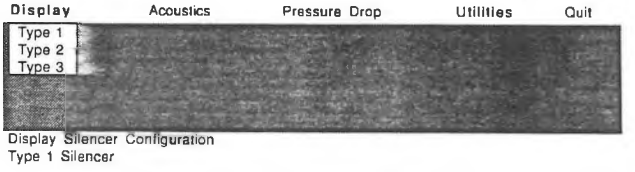

Figure 3. PC. CIRCLE Screen

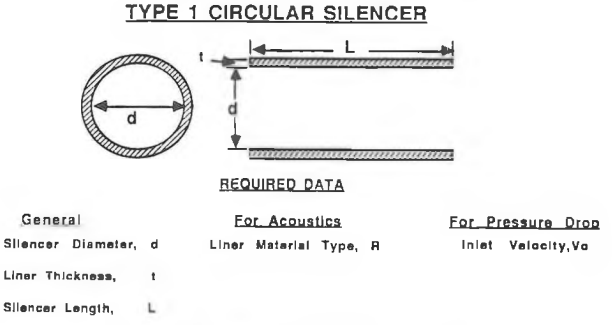

Figure 4. Type 1 - Display Option

EFFECT OF THE BULKHEAD FIXING ON THE NOISE INSIDE THE AIRPLANE CABIN

L. Cheng and J. Nicolas
G.A.U.S., Mechanical Engineering Department, University of Sherbrooke

1. DESCRIPTION OF THE PROBLEM

This paper describes one step of a research program undertaken by the authors to investigate the cabin noise of airplanes (more specifically the Challenger 601-3A made by Canadair). It focuses on the effect of fixing conditions of the Rear Pressure Bulkhead (RPB) on the internal cabin noise. The idealized modal simulating the problem is the radiation of sound from point-driven circular plates into a hard-walled cylindrical enclosure.

Two issues motivated this work. Firstly, for Challenger configuration, preliminary testings on the plane revealed that mechanical excitation is one of the main noise sources. The engines are attached through a beam-like structure to the rear part of the airplane body where the RPB is mounted. Therefore, the RPB which is a circular plate-like structure, may be a strong sound radiator. A throughout understanding of the effects of the boundary conditions of the RPB can , hopefully, help the engineer to reduce the cavity noise. Secondly, the present work is intended to deepen the existing knowledge regarding the general structure-cavity analysis. In fact the literature clearly showed a lack of general formulation and understanding of the boundary conditions effects on the induced cavity sound field.

2. OUTLINE OF THE MODEL AND THE THEORY

The model used for this study is a circular plate backed by a circular cylindrical cavity. The plate is driven by an external point-force and is elastically supported by rational and translational springs along its edge. With this model, both classical boundary conditions and intermediate cases can be easily simulated by making different combinations of the elastic constants of the spring. A variational formulation associated with a Rayleigh-Ritz approach is used in the analysis of the plate by choosing simple polynomials as trial functions. For the cavity, the hard-walled cavity modes are used as a decomposition basis of the sound pressure and also for obtaining the cavity Green's function. The resulting couplings equations, in which full interactions between the structure vibration and the internal cavity pressure field are taken into account, are then solved. Details about the formulation are available in the references given.

3. PRINCIPAL FINDINGS

1). In the theory formulated above, the plate-cavity coupled system is described in terms of the natural modes of its two uncoupled subsystems: the in vacuo plate and the acoustically hard-walled cavity. It is shown that the normal modes of the coupled system can be divided into three groups: plate-controlled modes, cavity-controlled modes and well-coupled modes, depending on whether the modes are dominated by plate vibration, cavity sound field or both. In particular the concept of so-called "pumping mode " of the free plate is put forward.

2). Taking a simple-supported plate and a free plate, both being driven by a point force, it is illustrated that the overall vibration levels of the two plates are not much affected by boundary conditions of the plates. However, except at very low frequencies, the free plate radiates much less than a simply supported one. The nuance occurs at the low frequency range, where the free plate gives a stronger sound field than a simply-supported one. This is due to the previously named pumping mode .

3). It is shown that the translational stiffness of the contour supports is a key factor in the radiation behavior of the plates into the cavity. The concept of "Radiation Efficiency into Cavity"(REC) is defined as the ratio between the acoustic energy in the cavity to the kinetic energy of the plate. This parameter represents the radiation capacity of each structural mode into the cavity.

4).Using this concept, this observed phenomenon is shown to be due to the low radiation capacity of the flexural modes of the free plates. This observation is consistent with previous one made for the far-field sound radiation from the baffled plates except that the piston motion, which is the main radiator for the free plate, is no longer true in cavity configuration. This is mainly because the flexural modes, which may generate evanescent waves in far-field radiation case, become significant contributors to the sound field within an enclosure.

5). Elastical supports of the plates are investigated, showing two interesting phenomena: Firstly, in comparison with the free cases, a limiting frequency seems to exist

for each elastical support, above which the plate behaves roughly like a free plate. indicating therefore a significant reduction in induced sound pressure. Secondly, in the frequency range below this value, a softer support does not always guarantee a sound reduction. The reason is that different supporting conditions modify the structural modes, the consequence of which can further change the modal structural-cavity coupling. As a result, in some frequency ranges, the cavity sound pressure may be amplified. Combining these two observations, one concludes that the stiffer the support is, the higher is this limiting frequency and, consequently, the higher is the frequency range where the beneficial effect is expected.

6). Using the model, a prediction is made for a 1/4 scale model of the airplane mentioned at the beginning of the paper. The cabin is faithfully scaled in every respects, Whereas the rear pressure bulkhead is simulated by a 3 mm thick plate. Fig.1 illustrates the cabin noise level in one-third octave band radiated by bulkheads with three different supports in translation. Three stiffnesses chosen are respectively infinite, $100K_p$ and $1000K_p$. K_p is the aerostatic stiffness of the cavity which one can calculate easily. It is concluded that a softer translational support of this bulkhead improves significantly the cabin noise.

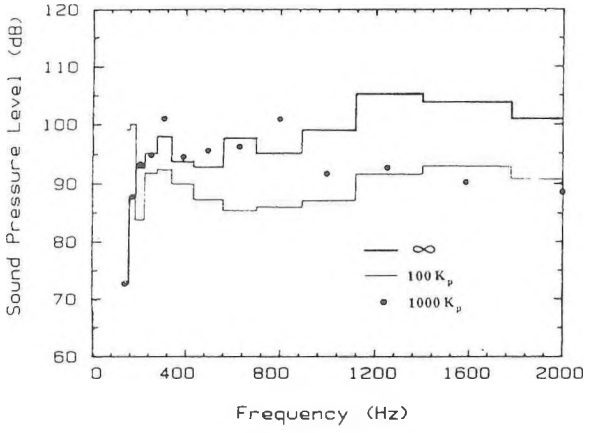

Fig. 1. Sound pressure level inside the cabin of a 1/4 scaled airplane model. Three fixing conditions of the RPB are considered

ACKNOWLEDGMENT

This work was supported by Canadair, Aerospace Group, Bombardier Inc.

REFERENCES

1 L. Cheng and J. Nicolas, "Free vibration analysis of a cylindrical shell-circular plate system with general coupling and various boundary conditions", to appear in J. sound and vib.

2 L. Cheng and J. Nicolas, "Radiation of sound into a cylindrical enclosure from point-driven end plate with general boundary conditions", to appear in J. Acous. Soc. Am.

OPTIMUM POSITIONING OF DUCT SILENCERS IN SOUND-RATED CONSTRUCTION

Mei Q. Wu, Tom Paige and Donald L. Allen
Vibron Limited, 1720 Meyerside Drive, Mississauga
Toronto, Ontario, L5T 1A3

1.0 Introduction

In sound-sensitive spaces, particularly sound studios constructed with high transmission loss partitions and ceilings, penetrations for mechanical system air-handling ducts are an important concern. Typically, duct silencers are provided at or near the penetrations to maintain the STC ratings of the walls and ceilings. This paper looks at factors related to the optimum location of duct silencers between spaces requiring sound-rated constructions. The constructions studied are based on the actual constructions used in the CBC Broadcast Centre in Toronto.

2.0 Scope of the Study

Two configurations were studied. The first case is shown in Figure 1. An air-handling duct penetrates a wall separating a noisy space and a quiet space, such as a studio, in order to supply air to the quiet space. A duct silencer is used to attenuate the noise which breaks into the ductwork inside the noisy space. If the silencer is located completely inside the noisy room, then the noise breaking into the ductwork or the silencer close to the wall will not be attenuated. If the silencer is located completely inside the quiet space, then the noise can break out from the silencer into the quiet space before it is attenuated.

The second case, as shown in Figure 2, is similar to the first case. However, in this case, the duct does not terminate in the quiet space. Instead, it runs through the quiet space and terminates in the next room. Noise intrusion in the quiet space is caused by noise breaking out of the duct into the room. The objective of the study is to determine for each configuration, the optimum position of a duct silencer to minimize noise transmitted to the quiet space.

3.0 Analysis Methodology

A computer program was developed to calculate the resultant noise levels inside the quiet space under various assumed parameters. The program was developed based on the noise calculation methods provided in the ASHRAE Handbook and prominent noise control books (Ref.'s 1, 2 and 3).

The following base parameters were assumed in the calculations:

* noise levels in the noisy room are 80 dB in each octave band;
* the thickness of the wall separating the noisy and quiet space is negligible;
* the duct dimensions are 30" x 14";
* there is 20 feet of duct in the noisy room and 10 feet (case 1) or 20 feet (case 2) of duct in the quiet room;
* the duct and silencer are both made of 22 gauge galvanized steel;
* the silencer is 5 feet long and has insertion losses of 4, 7, 14 and 25 dB in the first four octave bands, respectively.

The effects of varying silencer wall thickness and insertion loss were also investigated.

4.0 Summary of Results

4.1 Case 1; Duct Terminating in Quiet Space

a) Lower noise levels can be achieved in the quiet space when the silencer is located completely inside the quiet space. This conclusion is expected because when the duct terminates in a space, the break-out noise is usually negligible compared to the noise radiated from the termination. When break-out noise is not of concern, a longer run of silencer in the quiet room will provide more attenuation and will result in a lower noise level in the room.

b) When the silencer has high insertion loss (e.g. 8, 14, 25 and 40 dB in the first four octave bands respectively), the difference between locating the silencer completely inside the quiet space and locating the silencer completely inside the noisy space can be 6 dB in the first octave band and 14 dB in the fourth octave band.

c) When the silencer has a thicker wall (e.g. 14 gauge galvanized steel), the difference between silencer locations will be less than 1 dB.

In summary, the silencer performance is maximized by placing it in the quiet room, although sensitivity to silencer location is reduced with increased silencer wall thickness.

4.2 Case 2; Duct Passing Through Quiet Space

a) Above and including the second octave band, break-out noise levels are lower when the silencer's centre is at the wall compared to other silencer locations. The difference in the resultant noise levels is in the range of 2 to 7 dB. The difference is higher when the silencer has higher insertion loss and the lower when the silencer has a thicker wall.

b) First octave band noise levels are minimized if the silencer is completely located inside the quiet space. The noise levels can be 3 to 4 dB lower than if the silencer is located completely inside the noisy room. This noise level difference does not depend much on the silencer insertion loss or the silencer wall thickness.

In summary, the silencer should be placed symmetrically between rooms for optimum performance, unless the noise in the noisy room is predominantly first band, in which case silencer placement inside the quiet room is optimal.

5. Conclusions

An optimum silencer location can usually be found to minimize noise transmitted between spaces. The optimum location depends on many factors including silencer wall thickness and insertion loss. The optimum location of each individual case should be calculated based on the ductwork configuration and other parameters of that individual case. The above investigation provides only general guidelines for selecting the silencer location under some typical conditions.

6. References

1. American Society of Heating, Refrigeration and Air-Conditioning Engineers, ASHRAE Handbook, Chapter 52 Sound and Vibration Control.

2. Cyril. M. Harris, Handbook of Noise Control. McGraw Hill, New York.

3. Leo L. Beranek, Noise and Vibration Control. McGraw Hill, New York.

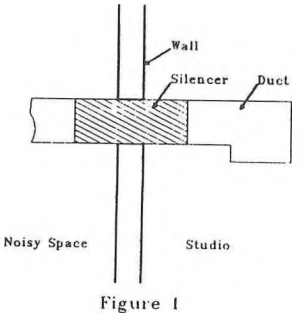

Figure 1

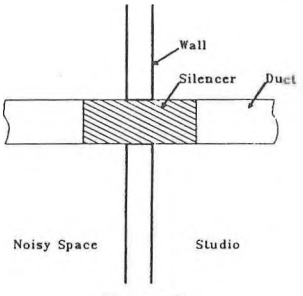

Figure 2

ACOUSTIC PULSATIONS IN RECIPROCATING MACHINERY

Brian C. Howes, M.Sc., P.Eng. - Chief Engineer
Shelley D. Greenfield, P.Eng. - Supervisor - Acoustical Analysis
Christine K. Schuh, E.I.T. - Project Engineer
Beta Machinery Analysis Ltd., 300, 1615 - 10th Ave S.W., Calgary, AB, T3C 0J7

1.0 Introduction

High vibration in reciprocating machinery is a common occurrence. Vibration produces alternating stresses in the material. Alternating stress levels beyond the endurance limit of the material causes fatigue failure. Failures of this type can be catastrophic. Consequently, measures are taken to avoid high vibration. Vibrations can usually be attributed to either the mechanical or **acoustical** design. One key to controlling vibration is the understanding and manipulation of each systems' unique acoustical characteristics.

2.0 Background

Beta Machinery Analysis Ltd. (BMA) began 24 years ago as an engineering consulting firm troubleshooting machinery problems. After several years of field experience, BMA discovered that many problems encountered with reciprocating machinery, and the attached piping, were due to pressure pulsations. In 1972 the company began the development of an acoustical modelling method using a digital computer. Since 1974, we have been providing a digital acoustical analysis service (MAPAK) for reciprocating compressors and pumps. MAPAK (Mechanical and Acoustical PAcKage) analyses two causes, acoustical and mechanical, of vibration and makes recommendations to eliminate potential problems.

3.0 Discussion

Pressure pulsations are generated by the reciprocating action of a piston or plunger. Considering the discharge side of a cylinder, the piston or plunger moves to compress the fluid. Regions of compressed fluid are released into the system when the valves are open and regions of rarefaction are formed when the valves are closed. The same phenomenon occurs on the suction side when the fluid is being drawn into the cylinder. Pressure waves always travel away from the source at the speed of sound of the fluid, regardless of the direction of fluid flow. Because of the cyclic nature of the machinery, compression and rarefaction waves, or pulsations, are sent into the system at regular intervals. Thus, pulsations are inherent to all reciprocating systems and cannot be completely eliminated.

3.1 Effects of Pulsations

High pulsations can affect valve performance, metering accuracy, and system pressure drop.

Pressure pulsations influence the motion of compressor, or pump, valves, and under certain conditions cause erratic valve behaviour. Phenomena such as improper opening and closing events, and valve flutter are typical symptoms of high pulsation. Such phenomena can distort the pressure-volume (P-V) curve and affect compressor performance. Some of the negative effects of high pulsation at the compressor valves are degraded compressor performance, and hence capacity, and increase maintenance costs due to premature valve failures.

Pressure pulsations are accompanied by fluctuating flow. Excessive flow fluctuation at orifice flow measuring devices cause inaccurate readings. Readings from such meters are often used to determine the amount of gas bought or sold. Thus inaccurate metering can result in substantial monetary losses.

Another consequence of high fluctuations in the flow is increased system pressure drop. Even though the average line flow of a system with high pulsations is the same as one without pulsation, the oscillating flow component of the high pulsation system produces more pressure drop (due to the squared relationship between flow rate and pressure drop). The greater the pressure and flow pulsations, the harder the driver has to work to produce the throughput of a system with low pulsation.

3.2 Effects of Pulsation on Vibration

Pulsations travelling away from the source are reflected at the discontinuities in the system (i.e. at changes in cross-section, entrances to volumes, dead legs, changes in density, etc.) to form standing waves. Depending on the geometry, and pulsation frequency, amplitude and phase, the pulsation standing wave will either be greater or less than the initial travelling pulsation wave. However, high pulsations do not normally damage a piping system. The interaction of the piping system with the pulsations result in unbalanced forces. These unbalanced forces cause vibration and the vibration in turn produces stress. Alternating stresses beyond the endurance limit will in time cause fatigue failures.

In some cases high vibrations may be acceptable from a stress point of view but are considered unacceptable from a phycological point of view. High vibration, resulting in alternating stresses below the endurance limit, can create an air of 'unsafe' conditions making operators working in the area feel uncomfortable.

3.3 Digital Computer Modelling

Once the system geometry and operating conditions are known, MAPAK can be used to calculate the magnitude and phase of the impedances, pulsations, and volume velocities over the frequency range of concern. Acoustical input is generated at multiples of compressor run speed or plunger passing frequency.

The predicted pulsations, unbalanced forces and metering error can then be compared to guideline levels. If necessary, pulsation suppression devices such as orifice plates, choke tubes and volumes can be added to the system to modify the acoustical characteristics to within guideline. The pressure drop, and hence horsepower loss, introduced into a system by pulsation suppression devices must also be considered.

By using a computer model the best balance of the above guidelines can be determine for the full range of operating conditions expected for the life of the installation. For the installations where not all the guidelines can be satisfied, the initial capital costs and long term operating costs must be evaluated. Based on the economics of the installation it can be determined which of the guidelines is least important.

BMA's computer model makes use of the simplifying assumptions of plane wave acoustical theory and an ideal valve model. The plane wave acoustical theory is valid in confined piping systems. At extreme pulsation levels, the acoustical pulsation assumption is not valid. However, as more pulsation control is added the model becomes more accurate. For engineering purposes an ideal valve model is sufficient. Any non-ideal valve behaviour can be corrected outside the computer model. With these assumptions, field data compare closely to predicted pulsations, as shown below.

4.0 Field v.s. Predicted Comparison

The following comparison is for the second stage discharge system of a two stage, two throw, 400 HP reciprocating compressor. The pulsation test point is located just after the cooler. The cylinder passage design was proposed by the manufacturer to act as a pulsation dampener.

Special care was taken in modelling the cylinder passages because of their unique design. This is the only area which was given special attention, the remainder of the system was modelled based on standard techniques employed by BMA in performing an acoustical study.

The first graph is the measured pulsations encountered in the field. The following graph shows the MAPAK predictions. The third graph is the MAPAK model of the same system with the addition of a mild orifice located between the cylinder and bottle nozzle connection. This was added to reduced the pulsations at the higher frequencies.

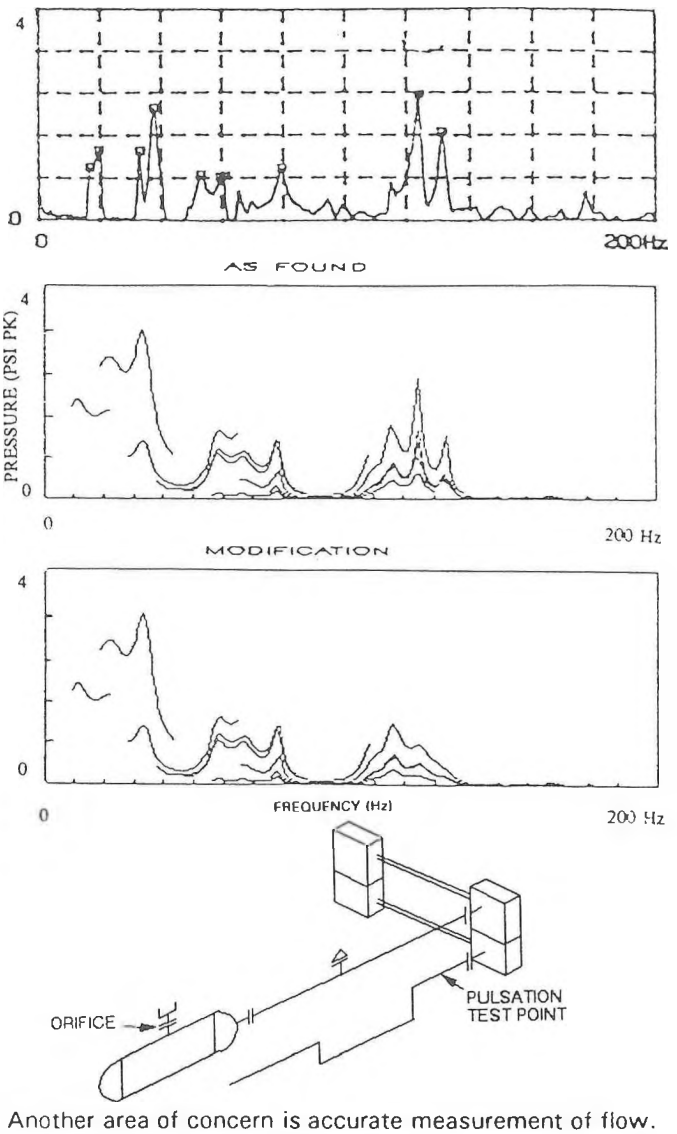

Another area of concern is accurate measurement of flow. Using MAPAK to determine what volume velocities will occur at a metering device enables the metering error due to pulsations to be predicted. The following comparison is for a single stage, two throw, 1680 HP reciprocating compressor.

Metering error varies with speed. Depending where in the speed range the compressor is operating, the metering error may be high or low. In this case, at 710 RPM, the metering error corresponds to what was measured in the field.

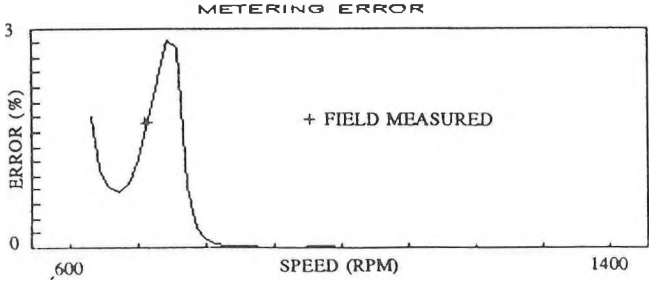

SIMULATION OF THE ORIFICE GAUGE LINE EFFECT IN PULSATING FLOW

W.M. Jungowski, G. Petela
NOVA HUSKY Research Corporation

1. Introduction

Gauge line response to pressure pulsation at the orifice plate taps distorts pressure signals and affects pressure difference applied to the diaphragm of a differential transmitter (Fig. 1). This response depends on gauge line length L, volume V_o of the transmitter chamber, pulsation frequency f, and amplitude $|P_p|$. Distortion of the pressure difference ($\Delta p = p_{p1} - p_{p2}$) by the gauge line obviously affects accuracy of flow rate metering. In order to eliminate significant errors, the gauge line response was simulated with lumped parameter model and plane wave model. Connectors on the gauge line, however, constitute abrupt variation of the inside diameter, affecting propagation and attenuation of the disturbances. Moreover with high velocity amplitudes turbulent regime occurs. These factors preclude pure theoretical description of the gauge line response and make some empirical contribution necessary. Utilizing experimental results damping coefficients were determined for two models with various gauge line length, chamber volume, pulsation frequency, and amplitude. Oscillating pressure difference across the orifice plate was simulated and compared with the monitored one.

2. Experiment

Frequency and amplitude of pressure pulsation was controlled by flow velocity in the test line and by the speed of a rotating disc installed on the line. Oscillating pressures were monitored with four high frequency response transducers (Endevco). The measurements were taken with three gauge lines of a different length L (0.166, 1.118 and 3.118 m) and in the frequency range 5 - 180 Hz.

3. Theory

Lumped Parameter Model

In this model [1] the tube and volume are regarded as capacitance, momentum equation takes into account inertance and resistance, and boundary conditions are nonlinear. Differential equation of forced vibration was obtained

$$(1) \quad d^2p_t/dt^2 + 2\theta|dp_t/dt|dp_t/dt + \omega_o^2 p_t = \omega_o^2 p_p \ ,$$

where damping factor

$$(2) \quad \theta = (1 + L_o/L)(1 + \zeta + \lambda L/d)/4\gamma p_o \ ,$$

natural frequency of undamped oscillation

$$(3) \quad \omega_o = 2\pi f = a_o \Big/ \left[L(1 + L_o/L)^{1/2}\right], \qquad L_o = 4V_o/\pi d^2 \ ,$$

ζ - coefficient of inlet pressure loss, λ - coefficient of friction, γ - isentropic exponent, p_o - mean gas pressure and a_o - mean sound speed.

Plane Wave Model

Transfer matrix for the tube of L length yields the oscillating pressure ratio

$$(4) \quad P_p/P_t = \cosh(ikL) + (ikL)(L_o/L)\sinh(ikL)$$

where according to Kirchoff's derivation $ik = \alpha_L + i(k_o + \alpha_L)$, $k_o = 2\pi f/a_o$ and

$$(5) \quad \alpha_L L = (k_o L)^{1/2}\left[(2L/d)/Re_a\right]^{1/2}\left[1 + (\gamma - 1)/Pr^{1/2}\right]$$

$Re_a = \rho_o a_o d/\mu$, ρ_o - mean gas density, μ - dynamic viscosity and Prandtl number $Pr = \mu c_p/K$. Omission of damping in (4) and introduction of resonance condition provides natural frequency of oscillation

$$(6) \quad (k_o L)\tan(k_o L) = L/L_o$$

4. Numerical Simulation

For simulation purpose the complex geometry of the system was simplified by substituting the gauge line with the variable cross-section by the uniform cross-section tube with the equivalent diameter.

Lumped Parameter Model

The coefficients θ and ω_o were calculated from Eq. (1) using pressure-time traces measured in the transducer chamber and pipe. The multilinear regression method was applied to obtain coefficient values which ensure the best fit (minimum standard deviation) between both pressure signals. Natural frequency ω_o depended only on the system geometry, i.e. on the transducer chamber volume, length and equivalent diameter of the gauge line, what is in agreement with the theory. Attenuation coefficient θ was little dependent on the frequency and amplitude of pressure oscillation, as well as on the gauge line length (Fig. 2). Simulated and measured pressure p_{p1} (Fig. 3) and pressure difference Δp across the orifice plate agreed within ~1%. It was found that model accuracy only slightly decreased with the increasing frequency and amplitude of pressure oscillation but it deteriorated completely for the longest gauge line.

Plane Wave Model

In order to take into account the turbulent damping, the laminar attenuation coefficient was replaced by the effective coefficient $\alpha = n \cdot \alpha_L$ in Eq. (4), and calculated using the amplitude ratio of the first harmonics measured in the pipe and transducer chambers. For the lowest frequency and the shortest gauge line multiple α values occurred for a given pressure ratio. The value with the best approximation of the phase angle between the pipe and transducer pressures was selected for further calculations. As Fig. 4 shows, increasing attenuation suppressed $|P_t/P_p|$ and shifted it to lower k_oL value. Maximum α/α_L increased with the gauge line becoming shorter (Fig. 5). Simulated and measured pressure differences Δp are compared in Fig. 6. The model gave good prediction of the pipe pressure amplitudes, but not always accurate estimation of phase angles.

5. Conclusions

Numerical simulation showed different assets and limitations of both models:

- Lumped Parameter Model considers the overall oscillating pressure level and is not restricted to a single harmonic. However, its range of application is limited to a short or medium length of gauge lines ($L \leq 1.2$ m)
- Plane Wave Model simulated only the amplitude of the first pressure harmonic. Its application was not constrained by the length of the gauge line. Disadvantage results from a low accuracy of the phase shift prediction and omission

of higher harmonics what affects particularly Δp calculation

- Accuracy of both models declines with increase in frequency, but was not affected by the pressure amplitude in the range monitored.

Generally, simulation with high accuracy of the pressure in the pipe using the pressure signals measured in the transducer chamber was feasible for some ranges of basic parameters.

6. References

1. Nagao, F. and Ikegami, M., "Errors of an Indicator Due to a Connecting Passage", Bulletin of JSME, Vol. 8, No. 29, 1965, pp. 98 - 108.
2. Tijdeman, H., "On the Propagation of Sound Waves in Cylindrical Tubes", J.S.V., Vol. 39, No. 1, 1975, pp. 1 - 33.

Acknowledgement

This article is based on a research project performed for NOVA Corporation of Alberta. Permission to publish the results is gratefully acknowledged.

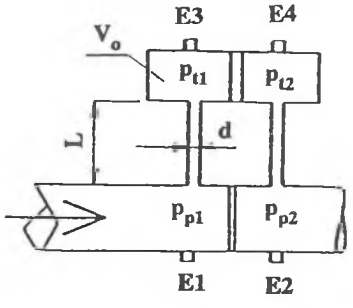

Fig. 1

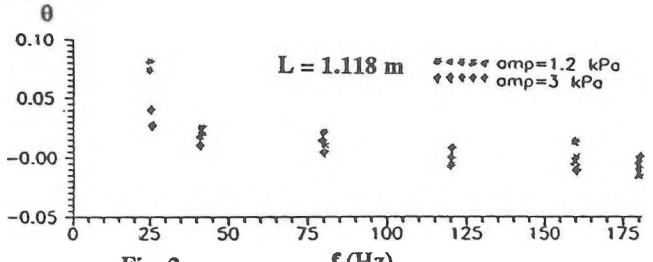

Fig. 2

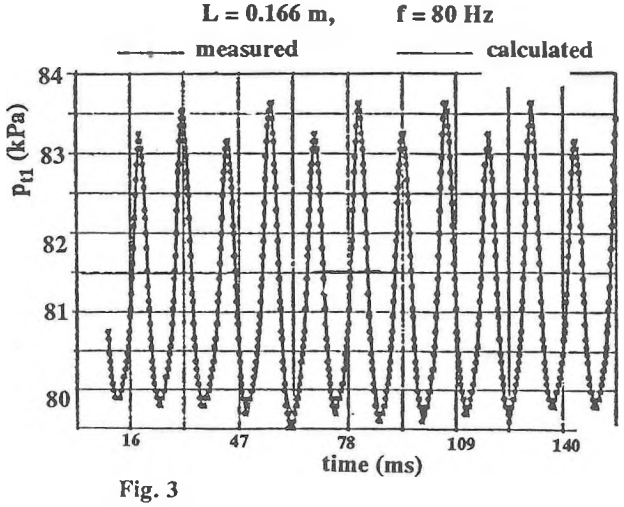

Fig. 3

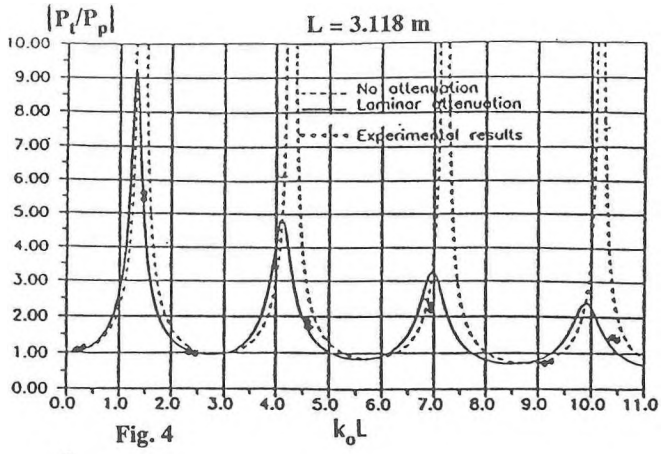

Fig. 4

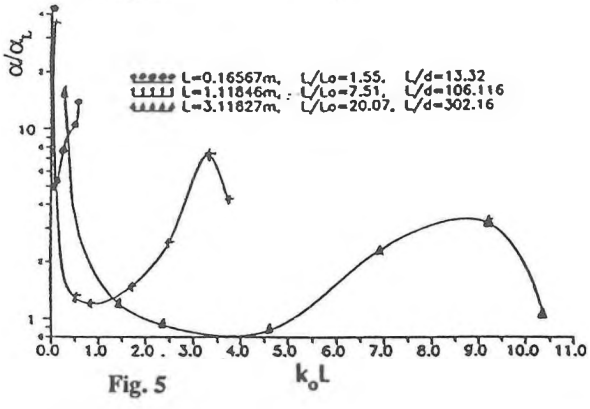

Fig. 5

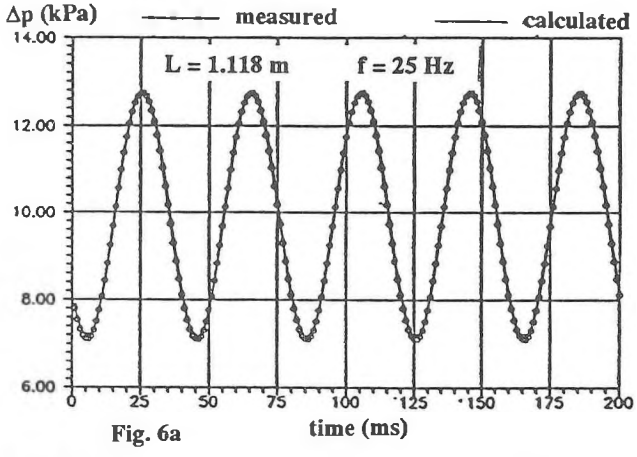

Fig. 6a

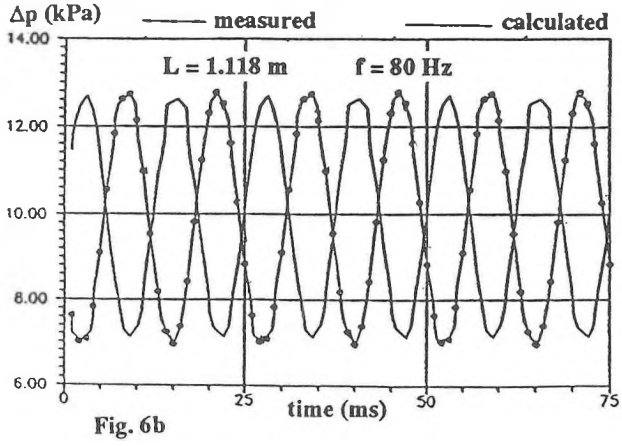

Fig. 6b

REVERBERATION CHAMBER MEASUREMENT OF THEATRE CHAIR ABSORPTION

J.S. Bradley
Institute for Research in Construction
National Research Council, Ottawa, Canada, K1A 0R6

1. Introduction

In most auditoria, theatre chairs and their occupants are the major source of sound-absorbing material. Knowledge of their sound-absorbing properties is critical to the acoustical design of an auditorium. Although the effects of the chairs and their occupants were first predicted in terms of the total absorption per chair, Beranek has suggested that it is better to describe the effects in terms of the absorption coefficients of the audience seating areas.

The results of reverberation chamber tests on small samples are used to estimate the sound absorbing-properties of materials in rooms. Such tests have been found to overestimate the effects of standard porous absorbing materials due to both edge absorption and diffraction effects. For these simple materials, the measured absorption coefficients have been found to relate approximately linearly to the ratio of perimeter/area, P/A, of the samples, as indicated by equation (1).

$$\alpha = \beta \bullet P/A + \alpha_{\infty} \qquad (1)$$

where:

α = sound absorption coefficient of a finite sample
β = regression constant
P/A = perimeter/area of the sample, m^{-1}
α_{∞} = absorption coefficient of an infinite sample

The intent of this work was to verify that more accurate predictions of chair absorption in auditoria could be made by measuring absorption coefficients as a function of P/A in a reverberation chamber and then extrapolating to larger sample sizes using equation (1). In addition, other more approximate approaches are also compared.

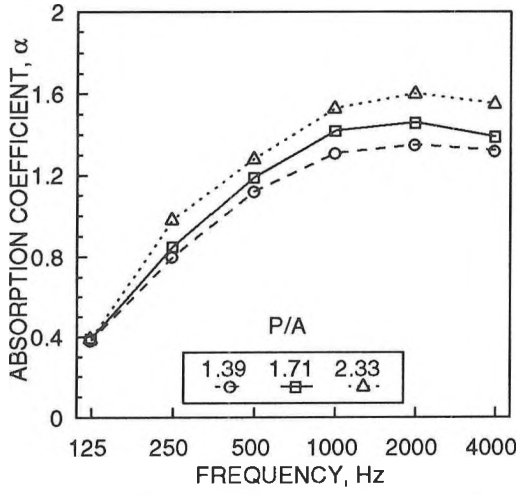

Figure 1. Measured sound absorption coefficients of unoccupied type E chairs for three different P/A values. Chair edges exposed.

2. Reverberation Chamber Measurements

The absorption coefficients of various groups of up to 18 upholstered theatre chairs were measured in a large reverberation chamber. Figure 1 gives examples of measured absorption coefficients versus frequency for three different P/A values. Smaller samples with higher P/A values have higher absorption coefficients, and the effect is strongest at higher frequencies.

In Figure 2, the measured absorption coefficients are plotted versus sample P/A value. The slope β of the regression lines tends to increase with frequency. By extrapolating to a P/A value of 0, the infinite area absorption coefficients α_{∞} are obtained. These results clearly demonstrate that the absorption coefficients of samples of upholstered theatre chairs vary considerably with sample size. Thus, measurements of a small sample (e.g. two rows of four chairs, P/A = 2.0) would not accurately predict the expected effect of the larger blocks of chairs found in most auditoria.

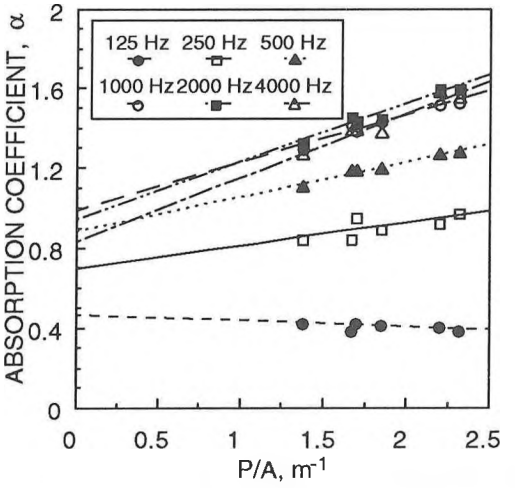

Figure 2. Measured absorption coefficients versus sample P/A for unoccupied type E chairs. Chair edges exposed.

3. Validation in Auditoria

The results of the previous section suggest that one could best predict the absorption of large blocks of chairs from extrapolations from measurements of samples of varied P/A. This concept was tested in halls that were undergoing renovations that included removing the chairs. The absorbing properties of four different sets of chairs were tested both in the reverberation chamber and in the auditorium. The effect of each type of chairs in each auditorium was predicted from the reverberation chamber measurements using data similar to that shown in Figure 2 and regression equations of the form of equation (1). These predictions were then compared with the absorption coefficients of the chairs obtained from reverberation time measurements in the auditorium with and without the chairs in place.

Figure 3 illustrates the comparison of measured and predicted chair absorption coefficients for one of the sets of chairs. The other comparisons also gave good agreement between measured and predicted values. In some cases, differences were a little larger at some frequencies due to uncertainties in the effects of construction materials that were present during measurements and unknown changes in the auditoria. The results confirmed that extrapolations

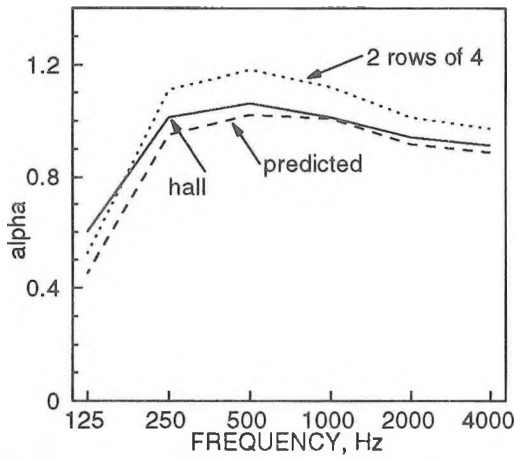

Figure 3. Comparison of sound absorption coefficients for type A chairs, measured in the hall and estimated from reverberation chamber tests for two rows of four chairs (P/A = 2.0) and for a hall sized sample (P/A = 0.8).

to smaller P/A values from reverberation chamber measurements led to better predictions than using the results of smaller samples directly.

4. Other Approaches

While the use of extrapolations from smaller samples is thought to be the most accurate method for predicting the absorption of theatre chairs in auditoria, other more approximate methods were also considered.

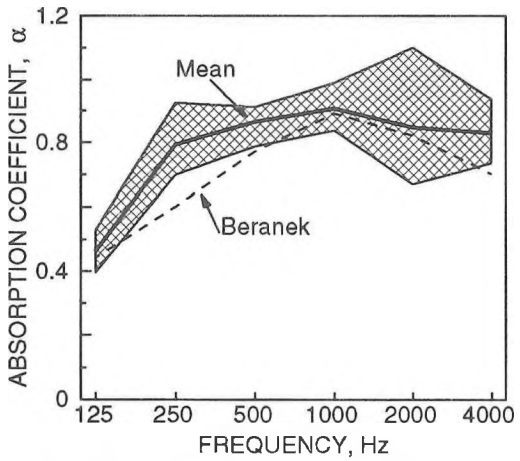

Figure 4. Comparison of the mean and range of values of the estimated infinite area sound absorption coefficients with Beranek's average upholstered chair absorption coefficients.

The simplest approach is to use one average absorption coefficient characteristic to represent all types of upholstered theatre chairs, as suggested by Beranek. The mean and range of absorption coefficients for infinite samples are compared to Beranek's data in Figure 4. The means of the five quite different types of chairs are similar to Beranek's values, but particular types of chairs can be considerably different. Thus, the use of a single set of average absorption coefficient values is a valid but approximate approach.

It has been suggested that in reverberation chamber absorption tests, the absorptive edges of chairs should be screened. This would be expected to reduce the edge absorption of the sample but not the diffraction effects. Figure 5 compares measured absorption coefficients versus P/A with and without the edges screened. The screening of the edges is seen to reduce the variation with P/A but does not eliminate it. The addition of the screens produces anomalous effects at low frequencies that lead to negative absorption coefficients.

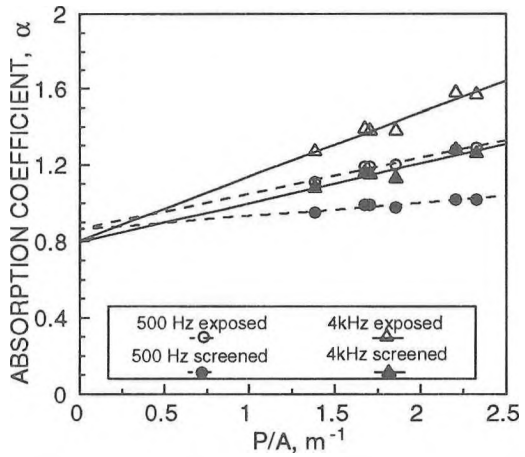

Figure 5. Comparison of measured sound absorption coefficients versus sample P/A for chairs with edges screened and exposed at 500 and 4000 Hz.

As a compromise approach, one could use average β values to extrapolate from a single measurement sample to the larger areas of chairs found in auditoria. The average β values could be based on measurements of chair samples with the edges either exposed or screened. The β values for the edges screened case are smaller and hence should lead to smaller prediction errors. Figure 6 compares β values versus frequency for occupied and unoccupied chairs with their edges screened. Also shown is Hegvold's data for simple model listeners and an average design curve.

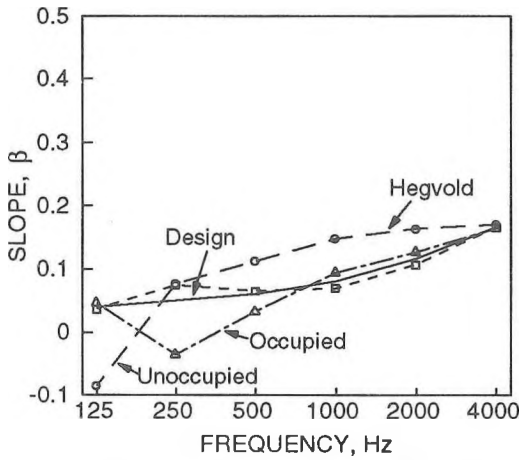

Figure 6. Calculated β values for upholstered theatre chairs with edges screened for occupied and unoccupied type E chairs. Also shown is a design curve approximating the calculated values and Hegvold's simple model audience results.

5. Conclusions

The results confirm that one can most accurately predict the absorption of upholstered theatre chairs in auditoria by extrapolating from measurements of samples of varied P/A. Other more approximate methods can be used to reduce the number of reverberation chamber sound absorption tests that are required, but with increased prediction errors.

MODERN ACOUSTIC MEASUREMENTS ON CANADIAN STAGES

John P.M. O'Keefe and Marc Bracken
Barman Swallow Associates,
1 Greensboro Drive, Rexdale, Ontario. M9W 1C8

INTRODUCTION

The acoustic requirements of listeners and performers are not the same. Over the past decade, a number of acoustical measurements have been derived to quantify the conditions preferred by performers. Broadly speaking these measurements are divided into two groups: SELF and OTHER. This reflects the fundamental dilemma of stage acoustics - the conflicting needs of a performer to hear both himself and the other musicians.

Gade[1] has proposed a ratio of reflected to direct sound as quantifier of SUPPORT, i.e. a performer's need to hear herself:

$$ST_x = \frac{\int_0^x p^2(t)\,dt}{\int_0^{10ms} p^2(t)\,dt}$$

The upper limit of integration in this parameter, x, was originally set at 100 ms. Gade later found that a 200 ms limit provided a better correlation with subjective response.

Naylor[2] found that the Modulation Transfer Function (MTF) was a good model for what he called Hearing of Other (HOO). He established that a correlation existed between MTF and HOO, much like the speech intelligibility curves developed by Houtgast and Steeneken.[3]

Other researchers, notably Meyer[4] and Marshall et al.[5] have found that the direction of sound arriving at a performer is important. None of the existing acoustical parameters however account for directionality.

MEASUREMENTS

To perform our measurements we used a Maximum Length Sequence System Analyzer manufactured by DRA Laboratories. Measurements were performed using a Maximum Length Sequence of order 15, i.e. 32,767 points per period. The stages were insonified with a single dodecahedron source complete with 12 75 mm diameter loudspeakers. Stage responses were measured with an omni-directional microphone.

Measurements were performed at and between five locations on the stages, roughly corresponding to positions in the violin, viola, horn and bass sections. The fifth position was between the conductor's podium and the violin section, roughly corresponding to the location of a soloist.

SELF measurements were performed *at* a given location, for example in the violin section with the microphone located 0.5 m from the loudspeaker. OTHER measurements were performed *between* two locations, for example between the violin and horn sections. The SELF measurements follow Naylor's practice, i.e. the microphone is located 0.5 m from the source. Gade used a 1 m source/receiver distance. For consistency with his data, our ST100 and ST200 measurements employ a +6 dB correction.

MTFs were measured in third octave modulation frequency intervals from .2 to 20 Hz. The results are expressed as an unweighted average of the third octave band data. Other parameters that we measured include: Level Difference, Clarity (C80), Centre Time (ts) and Early Decay Time (EDT).

RESULTS

Some of the results of our measurements are shown in the tables on the following page.

Our most interesting results were in the Centre in the Square, Kitchener Ontario. This is a multi-purpose hall with a large, single component reflector above the stage. The reflector height can be adjusted from 8.5 to 14.5 m. Measurements were taken with the reflector at three different heights: 8.5 m, 14.5 m and the height chosen by the resident conductor, 11 m.

The accepted wisdom is that stage reflectors or ceilings should be between 8 and 10 m high. It is intriguing that, given a choice, a conductor should set the reflector higher than this. ST100 measurements, shown in Figure 1, indicate levels close to Gade's proposed optimum when the reflector is 8.5 m high. Levels decrease significantly when the reflector is raised above this height. The ST100 measurements would therefore seem to support the 8 to 10 m height postulate.

So why was the reflector set at a height that our "rule of

thumb" and the stage measurements tell us is less than ideal? Figure 1 also shows the EDT data for each of the three reflector heights. At the 11 and 14.5 m heights the EDTs are about 0.5 seconds longer. This represents a significant increase in perceived reverberance. It would appear that the conductor's criterion for the reflector height is based more on listeners' requirements (reverberance) than it is on the performers' (Support).

CONCLUSIONS

The purpose of this study was to add to the database of stage acoustics measurements proposed by Gade and Naylor. Some of our results are shown in the tables below. A fundamental conflict in stage acoustics is the performer's need to hear both herself and her colleagues. In a hall where an orchestra was provided with significant control of the stage acoustics, our measurements indicate that these conflicting requirements were superseded by the listeners' desire for greater reverberance.

REFERENCES

1. Gade, A.C., Acustica Vol 69 (1989) pp. 193-262
2. Naylor, G.M., Acustica Vol. 65 (1988) p. 127
3. Houtgast, T., Steeneken, H.J.M., Acustica Vol. 28 (1973) pp. 66-73
4. Meyer, J., 12th ICA Vancouver (1988) pp. 33-38
5. Marshall, A.H., Gottlob, D., Alrutz, H., J. Acoust. Soc. Am., Vol. 64 (1978) pp. 1437-1441

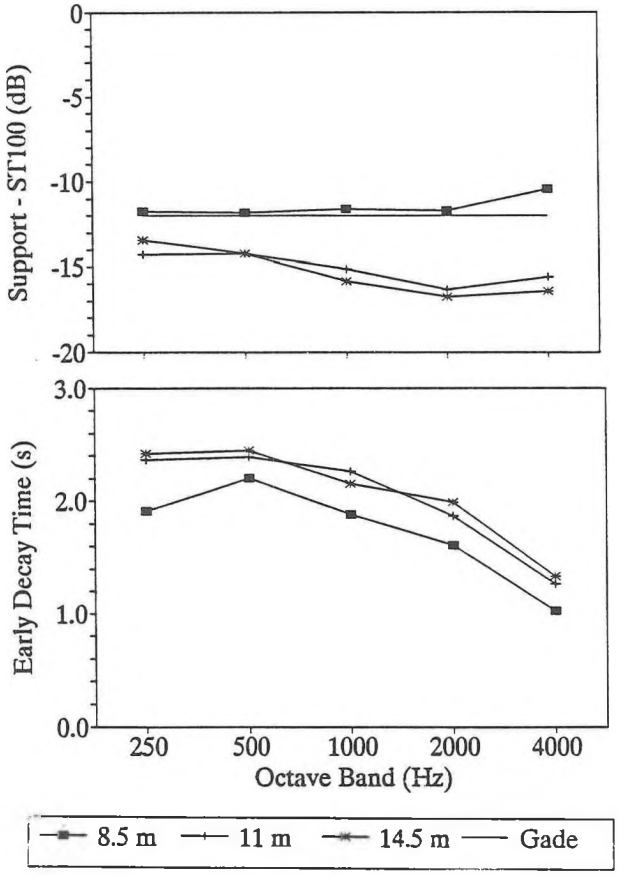

Figure 1. 100 ms Support and Early Decay Times for varying stage reflector heights at the Centre in the Square, Kitchener, Ontario.

Hall	City	Type	Seats
Cardinal Carter Academy	North York	Theatre	750
MacMillan Theatre	Toronto	Theatre	1000
Centre in the Square	Kitchener	Multi	2000
Massey Hall	Toronto	Concert	2200

Hall	MTF
Carter	0.66
MacMillan - Stage	0.83
MacMillan - Pit	0.80
Centre - Theatre	0.83
Centre - Concert (11 m)	0.64
Centre - Concert (8.5 m)	0.80
Massey	0.65

	EDT (s) - Other				
Hall	250	500	1000	2000	4000
Carter	1.25	1.23	1.33	1.15	0.88
MacMillan - Stage	1.26	1.30	1.37	1.21	1.04
Centre - Theatre	1.64	1.63	1.76	1.69	1.53
Centre - Concert (11 m)	2.37	2.39	2.26	1.87	1.27
Massey	2.14	2.40	2.32	2.14	1.79

	ST100 (dB) - Self				
Hall	250	500	1000	2000	4000
Carter	-12.7	-13.3	-14.6	-15.4	-14.2
MacMillan - Stage	-13.8	-15.8	-15.2	-16.2	-16.7
MacMillan - Pit	-9.0	-10.0	-11.1	-12.5	-12.2
Centre - Theatre	-19.5	-19.2	-19.8	-20.1	-18.5
Centre - Concert (11 m)	-14.3	-14.2	-15.1	-16.3	-15.6
Massey	-13.1	-14.3	-15.5	-16.6	-15.6

	ST200 (dB) - Self				
Hall	250	500	1000	2000	4000
Carter	-11.9	-12.9	-13.8	-14.1	-13.9
MacMillan - Stage	-12.5	-13.9	-13.4	-14.8	-15.2
MacMillan - Pit	-8.5	-9.5	-10.5	-11.9	-11.7
Centre - Theatre	-14.9	-15.6	-16.2	-17.1	-15.7
Centre - Concert (11 m)	-12.7	-13.0	-13.8	-15.0	-14.7
Massey	-10.9	-11.6	-11.9	-13.3	-12.7

A COMPARISON OF SUBJECTIVE SPEECH INTELLIGIBILITY TESTS IN REVERBERANT ENVIRONMENTS

K. Kruger
Alberta Public Works
Acoustics Section

K. Gough
University of Alberta
Dept. of Eduational Psychology

P. Hill
Educational Consultants
for the Sensory Impaired

INTRODUCTION

Subjective speech intelligibility tests are not often used because of their time consuming nature. However, a lack of accurate objective measurement techniques requires that a subjective approach be used in many critical situations. This is especially true in large reverberant spaces where the primary sound source is a loudspeaker system.

For subjective evaluation of articulation it is necessary to use a test that is reasonably simple to conduct, is sensitive to changes in the acoustical parameters that affect intelligibility and is indicative of intelligibility of running speech occurring under realistic conditions. Other studies[1,2,3] that have investigated the effects of reverberation and signal-to-noise on intelligibility have used a variety of subjective measurement instruments including Fairbanks Rhyme Test, Modified Rhyme Test, Phonetically Balanced Word Tests, CVC Word Tests and spondaic word tests. It is recognized that the various tests lead to different results but the intrinsic relationship between them has not been clearly established for the case where the primary distorting factor is reverberation. It is often assumed that reverberation affects discrimination in a similar manner as signal-to-noise ratio.

This study compared intelligibility scores for three subjective test methods against a wide range of reverberant conditions. The three subjective methods were CID Phonetically Balanced Word Test (PB), Modified Rhyme Test (MRT) and CID Test Sentences. Reverberation times varied from approximately 1 second to 6 seconds. Other aspects, not typically explored in previous studies, included a rating scale of difficulty, a measure of the subjects comprehension of speech, and a phonemic analysis of PB wordlist errors.

PROCEDURE

The stimuli for each test were recorded in near anechoic conditions using a single male speaker. Reverberation was added to the signal upon presentation to the listeners by routing the pre-recorded signal through a digital multi-effect processor. With the processor it was possible to control the relative intensities of the direct sound, early and reverberant energy and the latter portion of the decay. It was decided to simulate an ideal exponential decay as closely as possible. Figure 1 illustrates the reverberation time versus frequency for the various test conditions.

Five subjects, 22 - 28 years old, were screened for normal hearing and speech discrimination. All pure tone threshold scores fell within a range of 0 dB to 20 dB (ISO). Speech discrimination scores using PB-50 word lists were 100% across all subjects.

The articulation tests were presented through headphones. Subjects first listened to samples of each speech stimulus and were given the opportunity to adjust the loudness to their Most Comfortable Level (MCL).

During the administration of PB words, subjects were required to state aloud the perceived stimulus words which were recorded as correct or incorrect by the test administrator. Subjects responded to the MRT stimuli by circling the perceived word on a response sheet that listed the target word with 5 distractors per stimulus. Each subject responded to the Sentence test by repeating the sentence which was transcribed by the administrator as well as being recorded on audio-tape for future reference. Each test (PB words, MRT, and Sentence test) was administered at each of five reverberant conditions. This generated fifteen different listening tasks which were presented to the subjects in a randomly assigned order.

At the completion of the tests, subjects were asked to judge the level of difficulty they experienced in performing the task. In addition, the subjects comprehension of speech was determined through their responses to questions on short anecdotes presented at each reverberant condition.

RESULTS AND DISCUSSION

Figure 2 shows the mean discrimination scores for each of the three articulation tests. The indicated reverberation times represent the averages over the 500 Hz to 2000 Hz one-third octave bands with the characteristics shown on Figure 1. The PB and Sentence tests indicate the greatest sensitivity to increases in reverberation time. Of the two, the PB test was also found to have the least variability in scores at each condition. The MRT showed minimal sensitivity. Over the extreme range of reverberant conditions, the modified rhyme scores varied by only 13%. The PB and Sentence tests in contrast varied by 49% and 38% respectively.

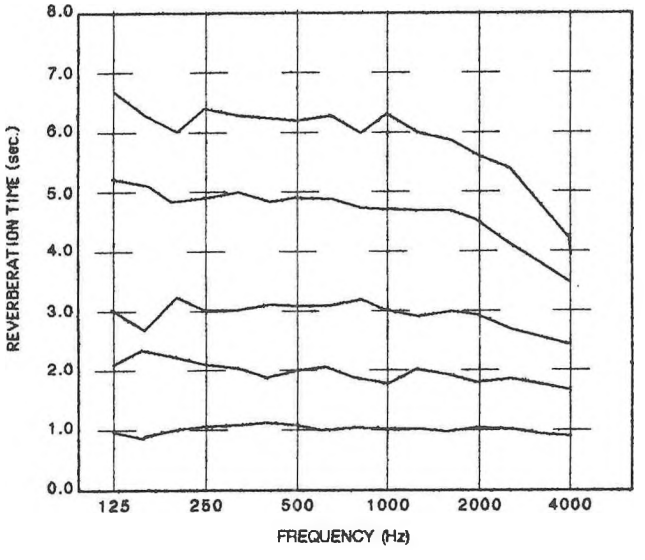

Figure 1 Reverberation time versus frequency for five test conditions.

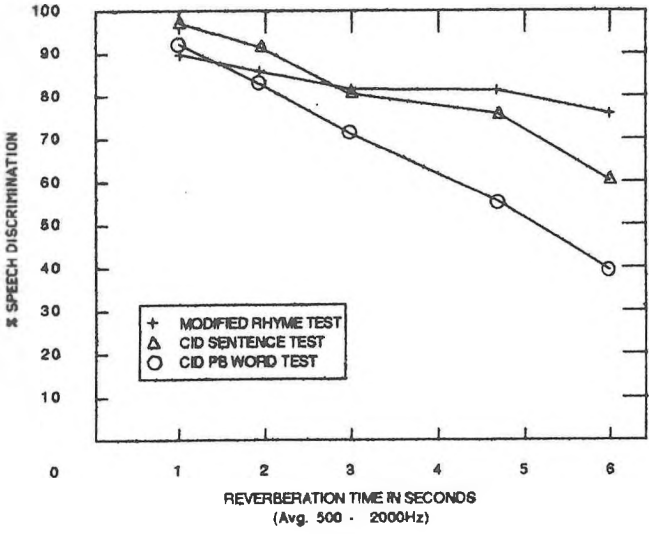

Figure 2 Mean speech discrimination scores versus reverberation times for various articulation tests.

Figure 3 shows the relationship between the same tests but under various signal-to-noise conditions[4]. It appears that there are both similarities and differences between the articulation tests for contaminating factors of background noise and reverberation. In both cases the PB and Sentence tests are the most sensitive to changes. Also the Sentence test scores are consistently higher for all conditions. The marked difference relates to the curves for the MRT. In the case of noise, the MRT displays reasonable sensitivity over the S/N conditions and the absolute value of the discrimination scores tends to be less than the Sentence test. Under reverberation, however, the MRT differentiates very little over a wide range of conditions. It is hypothesized that the MRT exhibits this characteristic because of two reasons. Firstly, the MRT does not have a carrier phase so that there is no reverberant masking from previously spoken words to interfere with discrimination. Secondly, 50% of the test word groups requires that the listener correctly identify the initial phonemes. Since there is no self masking taking place during the initial word pulse there are no contaminating factors to inhibit correct identification.

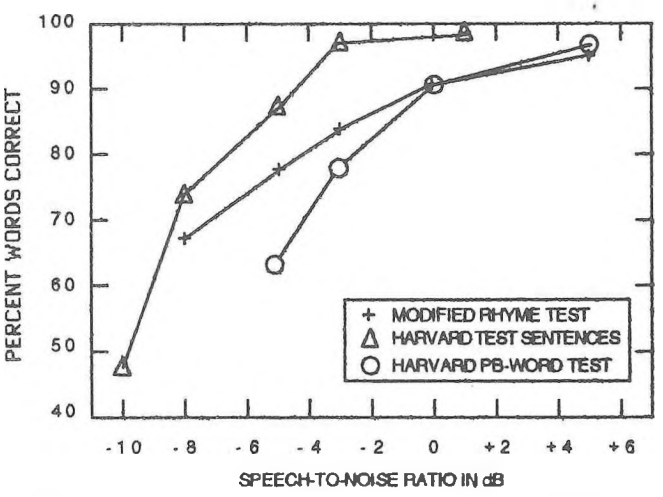

Figure 3 Discrimination score versus speech-to-noise ratio for various articulation tests. [4]

PB word tests appear to be sensitive to both noise and reverberation conditions, particularly when the listeners are responding to 50-word lists. Typically the scoring protocol simply involves determining the percentage of words correctly identified. This scoring system does not indicate, however, the number and type of phonemic errors. This type of analysis may provide more specific information on the effects of reverberation and background noise. From the results of the PB tests, the specific phonemic elements of the incorrect words were categorized in terms of phoneme class for the consonants and vowels under each of the reverberant conditions Figure 4 presents the overall vowel and consonant errors.

The difficulty test scale rated from 1 (no diffculty) to 5 (extreme difficulty) showed, not surprisingly, that difficulty increased for all tests as reverberation increased. The judgments of least difficulty were attributed to the MRT where the highest difficulty level was 3 compared to 5 for the PB and MRT at the extreme reverberation time. The anecdotal test of comprehension indicated the highest correlation with the PB test scores.

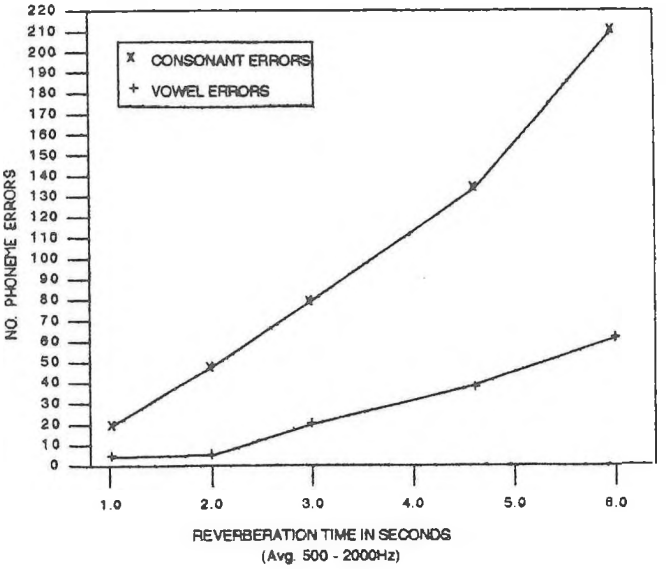

Figure 4 Phonemic errors from PB word test.

CONCLUSION

Of the three subjective measurement instruments considered in this pilot study, the PB word test was the most responsive to changes in reverberation. This finding agrees with studies that found similar results under signal to noise conditions. The Sentence test compares favourably in terms of sensitivity with the PB word tests and closely resembles the trends found under noise conditions. The MRT was determined to be a poor indicator on the effects of reverberation on speech intelligibility. The study also provided information on aspects of intelligibility not usually considered in studies of this type. This included listeners' subjective impressions of level of test difficulty, auditory comprehension under reverberant conditions and a phonemic analysis of subjects' responses to PB tests. Further support for the PB test as the best of the three measures of intelligibility was indicated by these results.

REFERENCES

1 Nabelek, A.K. and Robinson, P.K. Monaural and Binaural Speech Perception in Reverberation for Listeners of Various Ages.
J. Acoust. Soc. Am. 71(5), 1242 - 1248 (1982)

2 Houtgast, T. and Steeneken, H.J.M. A Multi Language Evaluation of the RASTI - Method for Estimating Speech Intelligibility in Auditoria, Acustica 54(4) 185 - 199 (1984)

3 Bradley, J.S. Uniform Derivation of Optimum Conditions for Speech In Rooms, National Research Council Canada, BRN 239

4 Williams, C.E. and Heckler, M.H.L. Relation Between Intelligibility Scores for Four Test Methods and Three Types of Distortion, J. Acoust. Soc. Am. 44(4), 1002 -1006 (1968)

THÉATRES MODERNES OU ANCIENS, SALLES SYMPHONIQUES, SONORISATION DE GRANDS LOCAUX - UTILISATION DE L'INDICE RASTI ET DU TEMPS DE RÉVEBÉRATION INITIAL POUR L'ANALYSE DES PROBLEMES D'ACOUSTIQUE ARCHITECTURALE

Jean-Gabriel Migneron (*) et Christian Martel (**)

(*) Laboratoire d'acoustique, CRAD, Université Laval, 1636 Pavillon Félix-Antoine Savard, Québec, Qué., G1K 7P4.
(**) Acoustec, inc., 925 rue Newton, suite 103, Québec, Qué., G1P 4M2.

SUMMARY

Correlation between the Rasti index and the impulse response, namely the EDT-5, EDT-10 and EDT-15 dB, has been analysed, both in laboratory and during experiments conducted in multi-purpose halls and in large amphitheatres equipped with sound reinforcement systems. The close relationship between the Rasti index and the EDT measurements will be demonstrated. We will also show the necessity to measure the EDT's at the same localization and with the same directivity as the normal sources of the hall; for exemple, with the use of a powerful omnidirectional source in order to study the acoustical behavior of orchestra shell (Louis Fréchette Hall of the Grand théâtre de Québec or Albert Rousseau Hall) or with the measurement of impulse response through the sound system of a large amphitheatre (Montreal Olympic Stadium). In addition to provide a better understanding of the parameters governing the intelligibility, the proposed approach could be very helpful to the acoustical design of new and to be renovated halls (New Richmond Theatre, The National Theater Institute of Montreal).

1. INTRODUCTION

Le STI ou la procédure condensée du RASTI constituent une même méthode objective de mesure de la qualité de transmission de la parole qui quantifie particulièrement bien l'intelligibilité; il s'agit de la méthode mise au point par HOUTGAST et STEENEKEN en 1980 [1,2]. Les deux paramètres susceptibles d'influencer le STI (*"Speech Transmission Index"*) ou l'indice simplifié RASTI (*"Rapid Speech Transmission Index"*) sont le niveau du bruit de fond et le temps de réverbération; dans un local réverbérant, ces deux paramètres affectent la dynamique du signal perçu, tout particulièrement au tout début de chacune des décroissances de l'énergie acoustique. Pour l'obtention de l'indice RASTI, le signal de test utilisé consiste en deux octaves de bruit rose, centrés sur les bandes de 500 Hz et 2 KHz; les niveaux, dans ces bandes d'octave, étant choisis pour être représentatifs du niveau moyen de la voix (sonorisée ou non). Les modulations de basses fréquences présentes dans la voix humaine sont simulées par neuf fréquences discrètes de modulation. Les mesures RASTI consistent en une analyse du signal résultant à la position d'écoute, de façon à calculer le facteur de réduction du niveau de modulation pour chacune de ces neuf fréquences de modulation. Si le rapport signal sur bruit devient prédominant la fonction de transfert de modulation MTF donne une réponse plate, c'est-à-dire que toutes les fréquences de modulation sont affectées de la même manière; par contre, si c'est le temps de réverbération qui domine, la fonction de transfert de modulation présente une pente négative, parce que la réverbération affecte les fréquences de modulations les plus hautes.

Il a été démontré, également, une cohérence évidente avec d'autres méthodes consacrées aux salles de concert comme le *"Clarity Index"* (C_{80}, de REICHARDT, 1981), indice qui peut être complété par la modélisation de l'intelligibilité de BRADLEY[3,4]. Néanmoins, le paramètre de la réverbération initiale EDT apparaît plus facile à obtenir et à modéliser dans le contexte d'une réverbération variable, à la fois temporellement au long de la décroissance et spatialement, comme celui qu'on retrouve généralement dans un grand local très réverbérant, puisque ce paramètre ne s'attache pas à l'énergie tardive.

2. RELATION ENTRE L' INDICE RASTI ET LE TEMPS DE RÉVERBÉRATION INITIAL

L'utilisation de l'indice RASTI et de la réponse impulsionnelle, notamment la détermination exacte et précise des indices EDT -5, EDT -10 et EDT -15 dB a été valorisée ces dernières années, tant en laboratoire qu'au cours de différentes expertises dans plusieurs salles de spectacle, dédiées ou non à la musique, ou dans de grands locaux sonorisés (à l'aide des nouveaux analyseurs rapides et d'un échantillonnage au 1/3 d'octave au 1/128 sec.).

Afin d'éclairer cette relation de dépendance entre l'intelligibilité et le EDT, il avait été fait état au congrès d'Halifax [5] d'une expérience menée dans un local vide de plus de 50 m de long, avec une répartition homogène de l'absorption et de la diffusion; cette expérience ayant consisté à mesurer simultanément l'indice RASTI et le temps de réverbération initial EDT, à -5, -10 et -15 dB, pour les bandes d'octave de 500 et 2000 Hz, la source impulsive utilisée ayant une directivité peu prononcée.

Après avoir calculé les valeurs des temps de réverbération initiaux EDT susceptibles de redonner l'indice RASTI obtenu (à partir des fonctions de transfert de modulation réellement mesurées), il avait été vérifié que la régression la plus proche dans les deux bandes de fréquence était bien EDT -5 dB. Suite à ces résultats, il apparaisait donc nécessaire de mesurer la toute première décroissance de l'énergie, pour pouvoir modéliser convenablement l'indice RASTI.

3. DIFFÉRENTS EXEMPLES DE SALLES DE SPECTACLE OU DE CONCERT

Comme le montre, à titre d'exemple, le tableau n°1, relevé dans la salle de l'École Nationale de Théâtre à Montréal, avant sa rénovation, cette étroite relation, entre l'indice d'intelligibilité RASTI obtenu à partir des pertes de modulation et les valeurs réellement mesurées du EDT, a été documentée et mise en évidence, dans différentes expertises d'analyse acoustique de salles de spectacle ou de concert.

De même, la nécessité d'acquérir les temps de réverbération initiaux à partir des mêmes localisations que les sources ordinaires des salles de spectacle analysées et avec la même directivité que ces sources sera démontrée; d'où l'emploi d'une source omnidirectionnelle de forte puissance pour l'étude du comportement des conques d'orchestre (salle Louis Fréchette du Grand-Théâtre de Québec et salle Albert Rousseau) ou bien la mesure de la réponse impulsionnelle

TABLEAU Nº1:*Mesure des temps de réverbération initiaux EDT -5, -10 et -15 dB et de l'indice RASTI en %*

Localisation	Rasti tot.	EDT 500 Hz			Rasti 500	EDT 1000 Hz			EDT 2000 Hz			Rasti 1000
parterre	%	- 5 dB	- 10 dB	- 15 dB	%	- 5 dB	- 10 dB	- 15 dB	- 5 dB	- 10 dB	- 15 dB	%
3 ème rangée	63	0.28	1.17	1.50	61	0.38	1.50	1.63	0.24	0.94	1.28	65
Centre parterre	53	0.44	1.91	1.99	46	0.75	1.67	2.17	0.56	1.08	1.38	58
Fond du parterre	54	1.12	1.41	1.88	42	0.94	1.59	1.66	0.47	0.80	1.25	65
Balcon	48	1.31	1.56	1.66	44	0.23	0.33	1.33	0.56	1.41	1.62	52

au travers du système de sonorisation d'un grand local (Stade Olympique de Montréal). En plus de mieux comprendre les paramètres responsables de l'intelligibilité, les approches proposées peuvent aider grandement dans le design des nouvelles salles ou la rénovation des salle de spectacle plus anciennes; des exemples seront présentés et discutés comme ceux des figures nº1 et 2 (théâtre neuf de New-Richmond, théâtre National de Montréal, en rénovation).

4. SIMULATION DE L'INTELLIGIBILITÉ A PARTIR DE EDT MESURÉS

L'influence de la directivité de la source sur les temps de réverbération initiaux a été clairement mise en évidence: une grande directivité entraîne nécessairement une part de champ diffus plus importante, pour les points qui ne sont pas dans le champ direct de la source et, réciproquement, le niveau relatif du son direct est plus élevé pour les points directement exposés.

La recherche a démontré que pour mettre au point une procédure de modélisation convenable de l'intelligibilité pour les nouveaux systèmes de sonorisation dans des locaux fortement réverbérants, il faut idéalement disposer du temps de réverbération initial EDT, suivant la localisation du point source et avec une directivité, similaires à celles des futurs haut-parleurs. Cependant, la modélisation de l'intelligibilité devrait rester significative avec une connaissance plus fragmentaire du champ réverbéré (puisque le véritable EDT local ne peut être directement mesuré sans les futurs haut-parleurs). On peut envisager ainsi de calculer l'intelligibilité à partir d'une connaissance spatialement limitée du EDT -5 dB, soit en interpolant les valeurs les plus proches de la source et en tenant compte de sa directivité.

Par exemple, lors de tests préliminaires sur le rendement des nouveaux haut-parleurs du Stade Olympique de Montréal [6], en plus des mesures de pression et de RASTI, il avait été procédé à une analyse de la réponse impulsionnelle à travers le système sonorisation, soit avec la localisation et la directivité quasi-définitives des nouveaux haut-parleurs; l'introduction dans le modèle informatique des valeurs mesurées de EDT - 5dB a permis de simuler, avec une grande précision cette fois, les valeurs de l'indice RASTI escomptées. Ce résultat est fort encourageant, puisqu'il laisse apparaître à la fois la complexité du problème et une solution possible à la modélisation exacte de l'intelligibilité.

5. CONCLUSION

Dans une salle existante, que ce soit pour l'intelligibilité de la voix proprement dite ou pour la qualité de l'écoute en général, fusse-t-elle musicale, l'emploi complémentaire des indices RASTI et EDT -5,-10 et -15 dB permet d'éclairer, de façon utile et, surtout, très analytique, le comportement acoustique, qu'il s'agisse d'une salle de spectacle ou de n'importe quel grand local sonorisé. Ces indices peuvent être mesurés seuls ou bien coordonnés, avec la réponse impulsionnelle conventionnelle et la détermination d'un indice tel que C 80 msec. (dans une salle symphonique notamment).

Pour cerner complètement les résultats obtenus, il faut s'assurer que tous ces paramètres sont bien mesurés à partir d'un point source représentatif d'un usage bien déterminé de la salle et avec une directivité similaire à celle des sources réellement en présence, lors d'un spectacle ou d'un concert.

Au plan prédictif, la détermination du EDT (à l'aide d'un tir de rayon par exemple) pourra permettre de déduire avec une précision suffisante l'intelligibilité escomptée. Enfin, en matière de sonorisation, pour les grands locaux très réverbérant, la simulation exacte du STI ou de l'indice RASTI exigera non seulement une connaissance précise de la réverbération locale au point d'écoute, mais également de l'influence de la directivité des haut-parleurs sur la réponse impulsionnelle résultante.

6. RÉFÉRENCES

[1] HOUTGAST, T., STEENEKEN, H.J.M. et PLOMP, R.: "Predicting speech intelligibility in rooms from the modulation transfer function in room - 1. General room acoustics", pp. 60-72, in Acustica, vol.46, 1980.

[2] HOUTGAST, T. et STEENEKEN, H.J.M.: "A review of the MTF concept in room acoustics and its use for estimating speech intelligibility in auditoria", pp.-1069-1077, in Journ. of Acoust. Soc. Am., vol. 77, 1985.

[3] BRADLEY, J.S.: "Predictors of speech intellligibility in rooms", pp. 837-845, in Journ. of Acoust. Soc. Am.,vol.80, nº 3, 1986.

[4] BRADLEY, J.S. et HALLIWELL, R.E.: "Making auditorium acoustics more quantitative", pp. 16-23, in Sound & Vibr. vol.23, nº 2, 1989.

[5] MIGNERON, J.-G. et LECLERC, D.: "Modélisation de l'intelligibilité pour le nouveau sytème de sonorisation du Stade Olympique de Montréal", pp. 39-45, in Proceedings, Semaine canadienne d'acoustique, Halifax, octobre 1989.

[6] MIGNERON, J.-G.: "Modélisation de l'intelligibilité dans les locaux réverbérants", pp. 49-55, in Proceedings, Semaine canadienne d'acoustique, Montréal, octobre 1990.

[7] MIGNERON, J.-G. et LECLERC, D.: "Modélisation de l'intelligibilité et sonorisation du Stade Olympique de Montréal", pp.1093-1096, in Colloque de physique , tome 51, février 1990.

[8] MIGNERON, J.-G.: "Analyse acoustique du Stade Olympique de Montréal", 16 p. in Proceedings, Semaine canadienne d'acoustique, Toronto, octobre 1988.

ACOUSTIC STRATEGY: PUBLIC WORKS CANADA

Greg E. Clunis, P.Eng.
Interior Environmental Engineer
Public Works Canada
Sir Charles Tupper Building
Riverside Drive
Ottawa, Ontario
K1A 0M2

Background

Public Works Canada (PWC) is the federal government's custodian of real property, and is celebrating its 150th anniversary this year. PWC provides roads and bridges, canals, locks, and manages building accommodation for many federal operations, providing office space for Canada's 250,000 civil servants. PWC directly owns 400 buildings, and serves as property manager for several thousand more. The average age of PWC buildings is 40 years.

PWC is organized into six operational Regions, managed by a Headquarters unit providing overall direction and managing/conducting technology development activities.

Overview

This paper focuses on PWC office space, and presents an overview of the Acoustic Strategy which has been developed by PWC to act as a plan for ongoing activities to develop technologies in supporting the improvement of PWC buildings. Three strategic thrusts are presented, each supported by a series of tactics. The overall PWC goal is to provide an appropriate acoustical environment for tenants.

Acoustic Objectives

In a reasonable acoustical environment for the office worker there would be privacy and freedom from distraction in the office areas, and good speech intelligibility in meeting rooms. Acoustic security would be provided where required.

In open office areas this is achieved with a moderate level of background noise which masks transient noises, and yet provides a pleasant environment when combined with other factors which limit noise transmission between workstations. This appropriate level of background noise will maximize the potential for speech privacy between workstations, but not be so loud as to be distracting or cause occupants to raise their voices.

In closed offices the walls provide privacy and freedom from distraction. The background noise should therefore be lower, allowing for easier communication within the room. In meeting rooms the provision of low background sound levels and appropriate reverberation times allow for good communication.

Since too much noise, as well as too little, are each potential detractors to productivity, PWC has set target upper and lower limits on noise levels in the workplace.

PWC's first priority is to bring PWC buildings into line with established target levels. This requires that the status of the inventory be reviewed and appropriate actions determined based on technical deficiencies and costs. The strategy described in this paper concentrates on the development and provision of technologies which are required to achieve this priority. In addition, PWC will be working closely with the National Research Council (NRC) in the development and application of acoustical technology.

In order to put acoustic knowledge and technologies into practice, PWC needs to ensure that Regional staff are provided with the tools: procedures, resources, training; and thus expertise to control, measure and assess acoustics issues.

Strategic Thrusts

The three strategic thrusts are:

A. MEET CURRENT PWC COMMITMENTS
PWC has target levels of acoustic performance. PWC should know that it is meeting those targets.

B. DEVELOP FUTURE TARGETS
PWC needs to explore additional elements of the acoustic environment for which it may wish to establish targets.

C. IMPROVE KNOWLEDGE FLOW
Information needs to flow both into and out of HQ to the Regions, to ensure that the information produced is useful, and being used.

Tactics

The first strategic thrust requires the study of the acoustic performance of the inventory, from both the occupant perception perspective and the purely technical viewpoint. This includes enhancing the manner in which PWC receives and collates complaint data, and measures acoustics in buildings as a whole, and at individual workstations. PWC requires hard data on deficiencies: their nature and the technology required to achieve rectification and costs associated therewith. This information will be the basis for the direction of ongoing activities. PWC must ensure that tenants are informed, and that operations, maintenance, and all projects, are progressed in a manner sensitive to acoustics issues. The following tactics have been adopted:

A1. Receive and analyze acoustic data;
A2. Develop and implement repeatable test procedures;
A3. Assess inventory performance;
A4. Advise tenants about their impact on acoustics;
A5. Ensure acoustics issues are reflected in the documents supporting all stages in the process of space delivery.

These tactics are supported by a set of activities which include monitoring the existing complaint tracking system, and recommending enhancements where appropriate. Comprehensive test kits are now provided for every two Regions, and a wide range of acoustics instrumentation is available for loan from HQ. An expansion of the Regional capability with greater distribution of more basic instrumentation, specifically type 2 sound level meters, is being considered.

PWC will be able to take a more pro-active approach to assessing workplace acoustics. The impact of tenant noise, and the vital role that the tenant plays in maintaining good acoustics must also be explored. Tenant departments must realize that PWC alone cannot guarantee good acoustics without their support.

While PWC has set targets for background noise levels, it would like to explore other target areas as it moves towards an improved acoustical environment. The setting of additional targets requires long lead times. It is anticipated that several years into the implementation of this strategy we will be in a position to recommend additional targets for consideration.

The second strategic thrust is supported by the following tactics:

B1. Develop future acoustical targets, and assess their validity in terms of achieving occupant satisfaction, and cost effectiveness;
B2. Initiate and continue technology development activities.

Since PWC only specifies targets for background noise levels, noises that are superimposed by the tenant are not accounted for. While PWC cannot control the actions of tenant departments, it can help these departments tailor their own environment by controlling noise sources and appropriately designing office facilities.

New technologies need to be developed which are sensitive to the diversity of the inventory, and the fiscal constraints currently facing the federal government. Three areas are currently being explored:

Slab to slab construction, while traditionally accepted as the only way to provide acoustic privacy between closed offices, is costly and inflexible. PWC in partnership with the NRC have developed the fuzzwall technique, which uses a stack of fibreglass insulation over the tops of partitions in the ceiling plenum, to act as an acoustic barrier. While limited in ultimate isolation ability, this technique provides a marked improvement over the open plenum. PWC is currently developing this technique for wide application, by addressing air handling and air quality implications as well as life cycle costs.

Door systems are often a problem when high acoustic security is required. While usually effective upon installation, PWC experience has been that many high acoustic security doors degrade over time. Longevity is an important issue to PWC.

Sound masking is also an emerging technology which is being explored by PWC, with wider application anticipated.

The third strategic thrust relates to the improvement of knowledge flow, both into and out of Headquarters. PWC needs to ensure that every opportunity to provide positive and useful guidance on acoustics issues to those directly responsible for the delivery of space is exploited. This includes existing and new initiatives. It is also essential that the ability of PWC HQ, to receive information both about the inventory and also the knowledge of other agencies, is enhanced and maintained. HQ cannot make informed decisions in a vacuum.

The following tactics have been adopted:

C1. Maintain a close working relationship with NRC, and monitor industry and other agencies for developments;
C2. Develop acoustics training programs for Regional staff;
C3. Investigate and act on other mechanisms to transfer knowledge to the Regions.

PWC recognizes that most acoustics technology is developed by other agencies, and has formally recognized the need to keep abreast of these developments. Much acoustics technology exists, often however only at the research and scientific level and not necessarily in the format for common understanding or field application. Difficulties with acoustics in the Regions have been attributed to insufficient knowledge, especially of newly emerging technologies, by those directly responsible for the delivery of space. A common complaint from field personnel regarding acoustics is the frustration of not knowing about, and thus not being able to avoid errors in acoustics design, construction and operation. In particular, the following issues are considered critical: how to assign and specify acoustic requirements; how to design for these; how to build, inspect and test for acoustics; and how to maintain acoustic performance over time.

Training programs for Regional staff are periodically revised and presented, and other mechanisms to transfer knowledge to the Regions are continuously being sought.

Summary

The discussion presented above provides an overview of PWC's acoustical technology development strategy. For senior decision makers this provides the overall direction and means to assess all activities which together will move PWC closer to the departmental objective of improved office acoustics. The overall objective is to maximize the return on expenditures to improve acoustic performance. In the current climate of fiscal restraint it is even more critical that all activities are complementary, and that an appropriate balance exists between competing demands for resources.

Numerical Methods for Solving Acoustic Radiation Problems

Luc J. J. Cremers and Ken R. Fyfe
Department of Mechanical Engineering, University of Alberta, Edmonton, Alberta

1. Introduction:

In solving acoustic radiation problems, different numerical methods can be used. The conventional finite element (CE) method can model the near field if proper boundary conditions are applied, simulating a region extending to infinity. The so-called Sommerfeld radiation condition, simulating an outgoing travelling plane wave, can be appropriately imposed at a large distance from the radiating body.

Often though, one is interested in the acoustics of the far field. For this, boundary element (BE), infinite element [1] and infinite wave envelope (WE) element formulations may be used. The BE method requires only a discretisation of the sound radiating boundary and allows one to calculate the acoustic variables at an arbitrary field point. A major disadvantage however, is that the formulation yields a full complex system of non-symmetric matrices as opposed to the banded symmetric FE matrices, resulting in higher computing times and data storage problems.

Both the infinite and infinite wave envelope element are special elements that are matched onto a conventional finite element mesh modelling the near field. The infinite element is a conventional finite element where the shape functions are modified by adding a wavelike variation $\exp(-ikr)$ and where the computational domain in the radial direction is mapped to infinity. However because of the exponential factor, special integration procedures are needed, other than the Gauss Legendre quadrature formula, in calculating the system matrices.

The infinite wave envelope element differs from the infinite element in the use of the complex conjugate of the shape function as a weighting function in a modified Galerkin procedure [2]. Therefore the exponential factor vanishes, allowing the use of the Gauss Legendre quadrature formula in the evaluation of the appropriate system terms. A disadvantage is that the symmetry of the banded system matrices is destroyed.

In the following work, an n^{th} order infinite wave envelope element will be presented. With this element, an arbitrary number of acoustic degrees of freedom can be specified. Results from both 2D and axisymmetric models are presented.

2. Formulation:

In Figure 1, the geometry mapping of the infinite wave envelope element is shown for 2D and axisymmetric problems. Mapping functions $M_i(s,t)$ are defined [3] which map the unbounded real element onto a unit parent element, such that the inverse mapping along each infinite radial edge yields:

$$t = 1 - \frac{2a_i}{r} \qquad i = 1,2$$

Where a_i indicates the distance from the element to the source of the outgoing travelling wave.

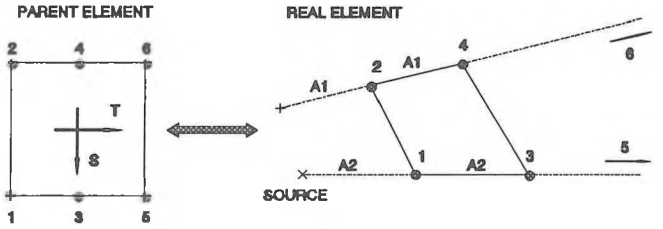

Figure 1 Geometry mapping of the WE element.

The shape functions are chosen to be linear in the angular s-direction $S_i(s)$, while in the radial r-direction a shape function of order n can be specified. These n^{th} order functions are generated in the parent element by adding acoustic nodes between the geometry nodes, 1-3 & 2-4, and forming the Lagrangian polynomials $T_i(t)$ for the respective nodes. Due to the geometry mapping a n^{th} order polynomial in the parent element will render a function of the form:

$$\frac{a_1}{r} + \frac{a_2}{r^2} + \ldots + \frac{a_n}{r^n}$$

in the radial direction of the real element, which appropriately models the amplitude decay of an outgoing travelling wave in 3D. Since the amplitude decay in 2D is approximately $1/\sqrt{r}$, the radial portion of the shape function is corrected by a factor of $\sqrt{r}$ [1].

The total n^{th} order shape function then becomes:

$$N_i(s,t) = S_i(s)\ T_i(t)\ \exp\left(-ik\,a(s,t)\frac{1+t}{1-t}\right)$$

Finally by using the complex conjugate of these shape functions as weighting functions, the acoustic mass and stiffness matrices can be evaluated following the conventional finite element procedures.

3. Discussion and Results:

As a first example, an axisymmetric model of scattering of a plane acoustic wave from a rigid sphere is studied. The left side of Figure 2 shows a mesh using only 20 wave envelope elements, while on the right a fine mesh is shown using 6 additional layers of conventional finite elements. For comparison, an equivalent BE mesh is indicated by the thick nodes on the left hand mesh.

In Figure 3, results are presented by means of a polar plot of $|P_s|/|P_i|$ at a distance of $r = 5a$. These are shown together with the analytical and BE (20 linear elements) solution. The 2nd order WE element, used in the coarse mesh (i.e. with no conventional acoustic elements), is able to model the correct general shape of the directivity pattern, but the magnitude is not very accurate in some regions. The 20 node boundary element model is slightly more accurate than the low order WE model, but it should be noted that the WE calculation time was 25 times faster

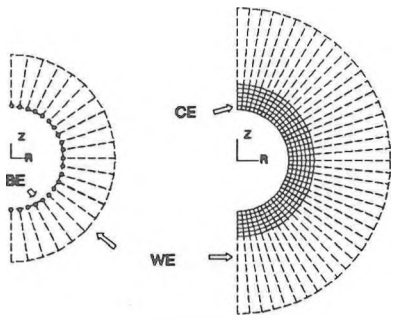

Figure 2: Axisymmetric meshes for rigid sphere.

than that for the BE solution.

Using the fine mesh, it is seen that the 5th order WE element solution matches the analytical solution very well, and was still 2.5 times faster than the BE solution.

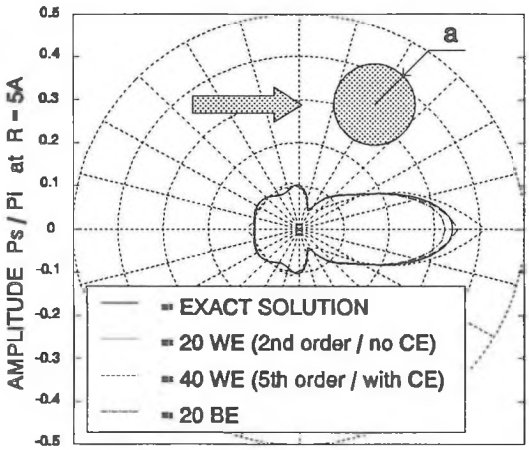

Figure 3: Scattering of an acoustic plane wave from a rigid sphere @ka = 4.

In a second example, the 2D acoustic pressure field generated by simple radiator is presented. The calculational mesh is shown in Figure 4 along with the superimposed real velocity boundary condition on the central panel. The panel is of length a, and the calculational frequency was specified at $ka = 10\pi/3$.

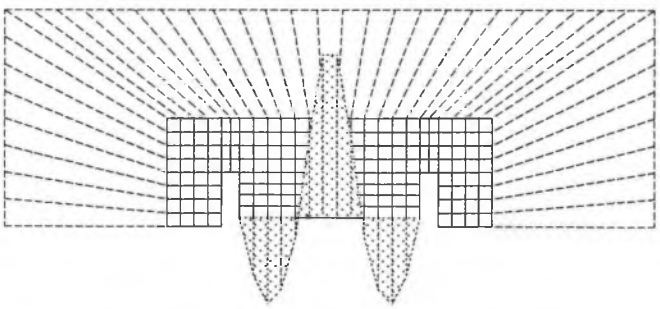

Figure 4: Simple radiator: WE mesh and velocity b.c.

The contour lines of constant pressure magnitude are shown in Figures 5 and 6 for the BE method and 7th order WE element calculation respectively. Very good comparison is obtained between the two pressure patterns, but again the WE calculation shows great speed; almost 5 times faster than the BE method.

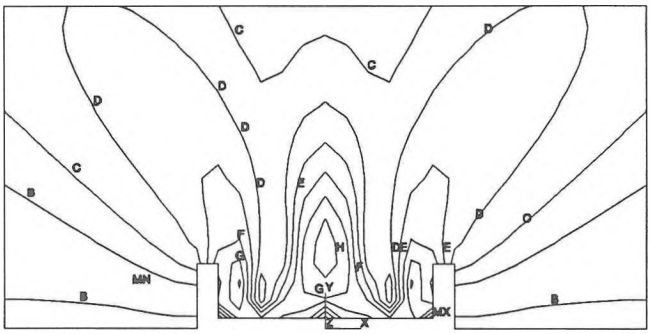

Figure 5: Simple radiator: BE solution.

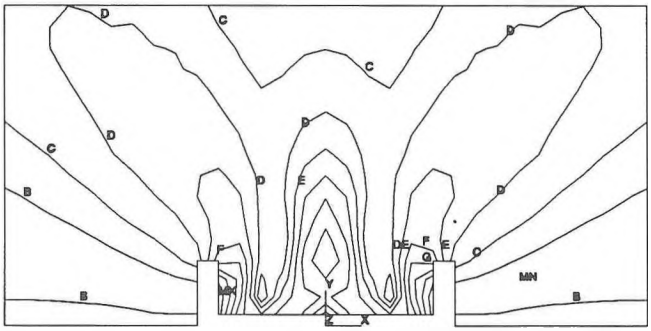

Figure 6: Simple radiator: 7th order WE solution.

4. Conclusions:

The infinite wave envelope formulation has been shown to be able to accurately model different types of acoustic radiation problems. The large calculation speed advantage over the BE method has been demonstrated. In a WE solution, normally both CE and low order WE elements are used for high accuracy solutions. Moving to higher order elements allows the element to better model the acoustic near field, and in some cases the need for CE is eliminated.

5. Acknowledgement

The authors wish to thank J.P. Coyette of N.I.T. (Leuven, Belgium) for valuable discussions in the preparation of this work.

6. References:

1) O.C. Zienkiewicz, K. Bando, P. Bettess, C. Emson, and T.C. Chiam, *Mapped Infinite Elements for Exterior Wave Problems*, Int. J. Num. Meth. Eng., vol.21,1229-1251(1985).

2) R.J. Astley and W. Eversman, *Finite Element Formulations for Acoustical radiation*, J. Sound & Vibration, 88(1), 47-64 (1983).

3) J.M.M.C. Marques and D.R.J. Owen, *Infinite Elements in Quasi-static Materially Non-linear Problems*, Computers & Structures 18, 739-751 (1984).

Vibro-acoustic behavior of a plane radiator in the case of impact excitation

D. Trentin, F. Laville
GAUS, Génie mécanique, Université de Sherbrooke, Sherbrooke (Qc) J1K 2R1 Canada

1. Introduction

In order to understand and reduce impact generated noise, the acoustic radiation due to the impact of a sphere on a plane, semi-complex structure (plate with general boundaries where point masses and stiffeners can be added) has been modelled. First, the force generated during impact is obtained with a time domain approach because of the non linearity of the problem. Second, a variational approach in the frequency domain allows the impact response and sound radiation from the structure to be calculated. The theoretical formulation is given in section 2. The experimental validation of the developed model is presented in section 3. Then, a first application case to a plastic granulator is given in section 4: the theoretical model enables to design a special impact reduction structure (thin street metal + elastic layer) and a noise reduction of 8 dB(A) was obtained.

2. Theoretical formulation

This structural acoustic radiation case involves coupling between excitation source (sphere impact) and receiving structure (planar radiator). The radiation problem is solved in two steps.

The first step is the calculation of the force input into the structure. The elastic deformation d(t), the structural impact displacement w(t) and then the impact force f(t) are obtained through a numerical resolution of the following system of equations [1]:

- Hertz law for the elastic deformation during impact:

$$F(t) = k\,(d\,(t))^{3/2} \qquad (1)$$

- Newton law for the movement (w(t) + d(t)) of the projectile of mass m:

$$\frac{d^2}{dt^2}\,(w(t) + d(t)) = -\frac{F(t)}{m} \qquad (2)$$

- Movement of the structure at impact point obtained with the structure impulse response M(t):

$$w(t) = \int_0^t M\,(t - \tau) \cdot F(t)\,d\tau \qquad (3)$$

The second step enables to obtain sound radiation from the structure with the input force. A variational approach [2] in the frequency domain is used in order to consider a semi-complex structure.

3. Experimental validation

Because the structural radiation problem for a semi-complex structure has been already validated [2], the validation concerns the computation of the force generated during the impact. Two cases of receiving structure are considered: a semi-infinite structure and a clamped rectangular plate.

3.1 Case of a semi-infinite receiving structure

This experience serves to validate the hertz contact law. A steel sphere is dropped directly on a force transducer attached to a heavy steel structure. The results are shown in Figure 1. There is good agreement between theory and experiment. The continuing oscillation of the impact force observed in the experience is due to the transducer resonance.

3.2 Case of a clamped rectangular plate

This experiment serves to validate the complete force calculation model in a case where coupling effects between excitation source and receiving structure can't be neglected. A steel sphere is dropped onto a clamped rectangular plate whose motion is measured with a laser vibrometer. A laser vibrometer was used in order to measure the very high frequencies in structure velocity generated by the impact and to avoid mechanical coupling problems between the structure and the vibration transducer. Figure 2 gives the experimental results. There is good agreement between theory and experiments.

4. Application to a plastic granulator

The developed model was used to reduce the noise generated by plastic parts projections on the inside wall of a plastic granulator. A special impact reduction structure (thin sheet metal + elastic layer) was designed to cover the inside of the granulator (see Figure 3). An interesting result from the computation was that the important parameter for impact force reduction was the thickness of the thin sheet metal (the thinner the better) and the characteristics of the elastic layer did not matter much. Figure 4 shows the obtained noise reduction of 8 dB(A). This solution has several advantages over classical enclosure type solutions: it is low cost and does not interfere with production and maintenance operations.

5. Bibliography

[1] W. Goldsmith, Impact, London: Edward Arnold, 1960.

[2] A. Berry et al., J.A.S.A., 88(6), 1990.

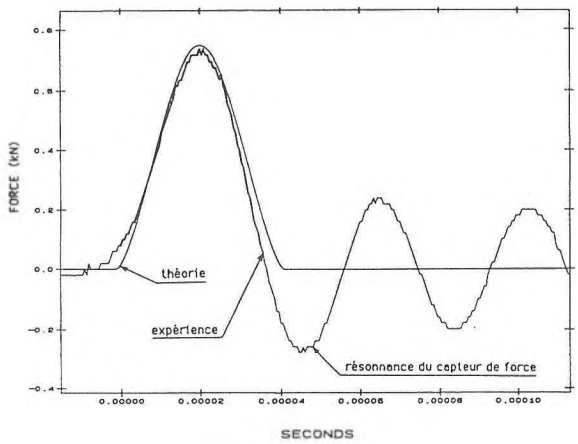

Figure 1: Impact force generated in the case of a semi-infinite receiving structure

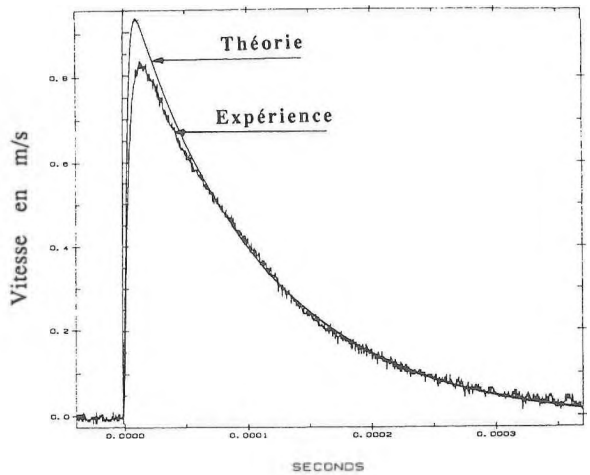

Figure 2: Structure velocity for a clamped rectangular plate

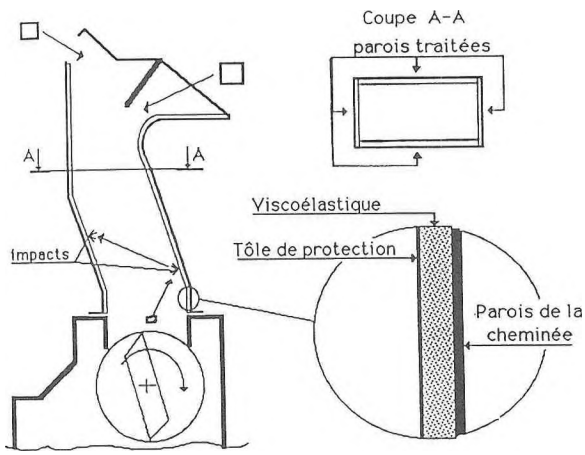

Figure 3: Special impact reduction structure for a plastic granulator

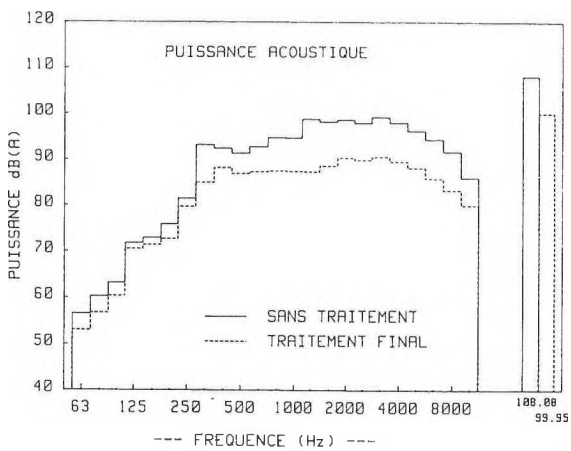

Figure 4: Noise reduction of 8 dB(A) obtained with the special impact reduction structure installed on the plastic granulator

Simulation of the acoustic radiation emitted by vibrating structures

J. Nicolas, A. Berry, D. Trentin, F. Laville
GAUS, Génie mécanique, Université de Sherbrooke, Sherbrooke (Qc) J1K 2R1 Canada

1. Introduction

Challenge of noise control for the nineties will be to leave out trial and error methods which have proven to be efficient only in specific and well known situations in order to tackle the difficult and complex, but inevitable, problem of structural acoustic and vibrations.

In order to control noise at source during the designing phase, a radiation model of a semi-complex structure has been developed. Based on analytical approach using a variational method, this model allows to predict the effects of the boundary conditions [J. Acoust. Soc. Am., 88(6), 1990] as well as stiffeners and added masses with force or moment type of excitation. To meet industrial applications, calculations have been extended to mechanical sources of vibrations (electric motor, engine) which are attached to large thin structure and act as noise radiator. A theoretical analysis of the problem is presented. The actual force input into the structure is the boundary result of both the output impedance of the source and the input impedance of the structure. A quadripole approach for the source assembly enables to calculate the force input, the kinetic energy, the radiation efficiency and the overall sound power. The key novelty of this method lies in its capacity to predict, a priori, the radiated noise in various configurations allowing the designer to rationally choose the best configuration in terms of noise control. Some applications will be presented. In general, guidelines for optimal acoustic conception, at designing stage, will be suggested.

2. Basic theory

Structural acoustic and vibration behaviors of a structure can generally be described by Figure 1.

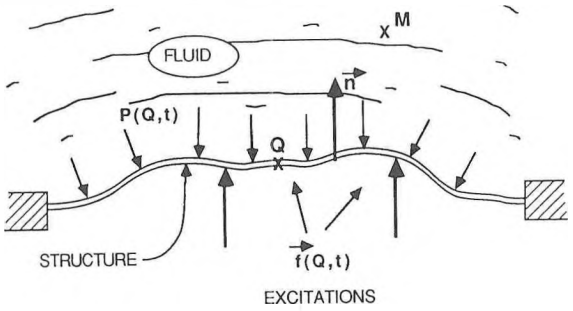

W(Q,t) = normal displacement of the structure
P(M,t) = acoustic pressure

Figure 1. Main parameters in structural acoustic and vibration problems

Usually this fluid structure interaction problem is described by the following equations:

For the structure
- Dynamic response

$$\rho_s \frac{\partial^2 w}{\partial t^2}(Q,t) + L_e(w(Q,t)) = \vec{f}(Q,t) \cdot \vec{n} - p(Q,t) \qquad (1)$$

L_e : Space differential $\vec{f}$: Excitations p: Fluid loading operator

- Boundary conditions (2)

For the fluid
- Wave equation

$$\nabla p^2(M,t) - \frac{1}{C_o^2}\frac{\partial^2 p}{\partial t^2}(M,t) = 0 \qquad (3)$$

- Sommerfeld condition (4)

$$-\rho_o \frac{\partial w}{\partial t}(Q,t) = \vec{\nabla}\, P(Q,t)\, \vec{n}(Q,t) \qquad (5)$$

with a $e^{-j\omega t}$ frequency dependance the (3), (4), (5) lead to (6)

$$p(M) = -\rho_0 \omega^2 \int_{(s)} G(Q',M)\, w(Q')\, dQ' \qquad (6)$$

which introducing (6) into (1) bring to:

$$-\rho_s \omega^2 w(Q) + L_e(w(Q)) = \vec{f}(Q)\vec{n} + \rho_o \omega^2 \int_{(s)} G(Q',Q)\, w(Q')\, dQ'$$

The displacement of a given structure, in the presence of the fluid, is the solution of integro-differential system.

Under this form one may easily understand why so many approaches tend to simplify the problem. It is not an easy one. However, if one wants to solve it as rigorously as possible, there will be essentially two choices:

3. Generalized analytical approach

The method used to obtain the structural acoustic and vibration behaviors of the plate is based on a variational approach with a discretisation of the solution which is using polynomial function such as

$$\{\phi_m(x) \cdot \phi_n(y)\} = \left\{ \left(\frac{2x}{a}\right)^m \left(\frac{2y}{b}\right)^n, \begin{array}{l} n = 0 \ldots N; \\ m = 0 \ldots N \end{array} \right\}$$

The system of equations to be solved are the following
- Equation of motion of the structure
- Boundary conditions along structure contour
- Equation of motion of the surrounding acoustic media
- Sommerfeld conditions

This leads to a linear system which is

$$\{-\Omega[M_{nmpq}] + [K_{nmpq}]\}\{a_{nm}\} = \{F_{nm}\} + j\,\Omega[Z_{nmpq}]\{a_{nm}\}$$

where Ω is the pulsation, M_{nmpq} the generalized mass, K_{nmpq} the generalized stiffness, F_{nm} the mechanical forces, and the last term the acoustic pressure $\{a_{nm}\}$ are the unknown modal

coefficient of displacement. This acoustic pressure is calculated with the Rayleigh integral. More details are given in Berry's paper [1]. It is worth noticing that the variationnal approach permits to add several degrees of complexity on the structure. The most important features are described in figure 2.

The coupling between the source excitation and the structure is made through a similar approach of the one used by Snowdon. This allows to take into account the interaction between the impedance of the input system and the local mechanical impedance of the plate.

4. Results

The modal permits a very interesting and meaningful parametric study. The key informations are the force transmissibility, the quadratic velocity, the radiation factor and the overall acoustic power. The type of excitation can vary, the plate can have any type of boundary conditions with added mass and added stiffeners. To show the importance of the coupling interaction between the excitation source and the structure, a basic example is given in figure [3]. One could see that classical force transmissibility described in textbook with the hypothesis of an infinite mechanical impedance of the supporting structure (fig. 3.a) is far more different than the actual value transmissibility (fig. 3.b). More complex phenomena will be exposed in the presentation.

5. Conclusions

A general analytical approach describing the vibro-acoustic behavior of a semi-complex system has been developed. It allows to understand the physical phenomema involved, gives quantitative results and reveals a good tool for engineers who want to make acoustic design a priori.

6. Bibliography

[1] A. Berry, J.-L. Guyader and J. Nicolas, "A general formulation for the sound radiation from plates with arbitrary boundary conditions", J.A.S.A., 88(6), 1990.

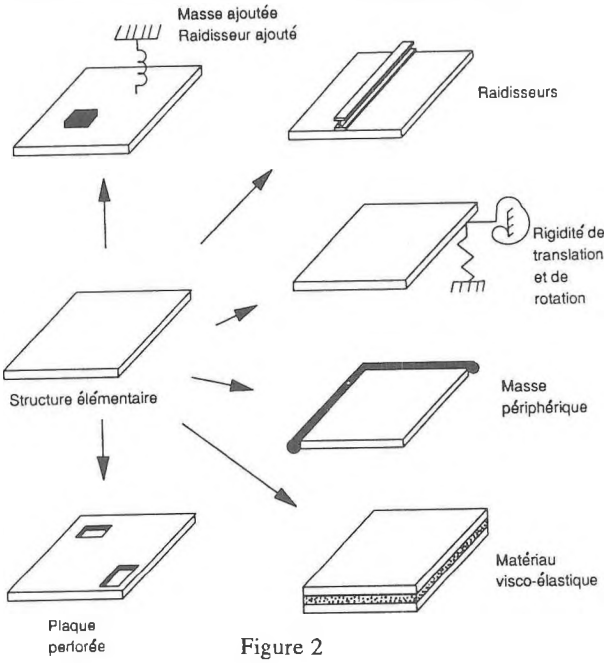

Figure 2

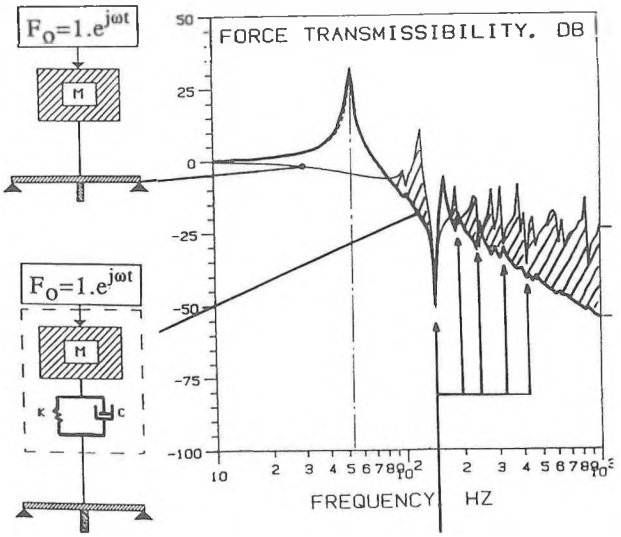

Figure 3.a: Force transmissibility with a rigid structure (infinite impedance)

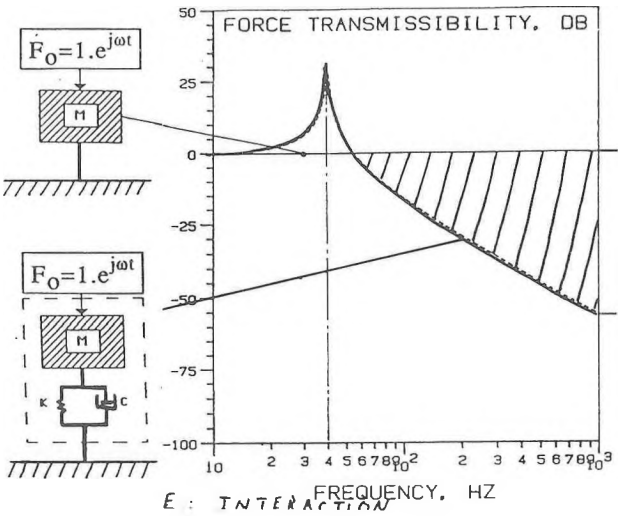

Figure 3.b: Force transmissibility with structure interaction (finite impedance)

ACOUSTIC AUGMENTATION OF THE ENTRAINMENT COEFFICIENT OF AXISYMMETRIC FREE AIR JETS

P.J. Vermeulen, P. Rainville, V. Ramesh and Wai Keung Yu
Department of Mechanical Engineering
The University of Calgary
Calgary, Alberta, Canada T2N 1N4

Introduction

The entrainment by steady turbulent axisymmetric free gaseous jets may be subdivided into entrainment in the initial zone, up to about 15 diameters axially downstream of the jet orifice; and by entrainment in the fully developed zone, ie., greater than about 15 diameters axially downstream of the jet orifice. The first direct measurements of fully developed entrainment were made by Ricou and Spalding (1) and Hill (2) extended the technique to make direct measurements of the local entrainment rate in the initial zone. These measurements showed that the entrainment coefficient varied non-linearly from 0.11 at one diameter downstream of the jet nozzle orifice, to the fully developed constant value of 0.32 at about 13 diameters.

Jet flow mixing plays a major role in the performance of combustors of the gas turbine type and jet entrainment is responsible for the mixing produced by a jet. The possibility of increased jet entrainment and mixing by acoustically pulsing the jet flows, thereby improving combustor performance, is therefore of important technical interest. Responding to this possibility Vermeulen, et al. (3) made the first direct measurements of fully developed entrainment by acoustically pulsed air jets, and found that the entrainment was increased by up to six times. They adapted the Ricou and Spalding technique for these measurements, and just recently by extending Hill's work Vermeulen, et al. (4) made the first direct measurements of the local entrainment rate in the initial region of pulsed jets.

Consider a normal local slice of thickness ΔX, between the jet orifice exit plane and the fully developed region, with $\Delta \dot{M}_e$ as the corresponding local entrainment mass flow rate. Then the entrainment coefficient C_e can be shown to be approximately expressed by

$$C_e \approx \frac{D}{\dot{M}_j}\left(\frac{\rho_j}{\rho_s}\right)^{\frac{1}{2}} \frac{\Delta \dot{M}_e}{\Delta X}$$

where D is the jet orifice diameter, $\dot{M}_j$ is the jet mass flow rate at the orifice, ρ_j is the jet density at the orifice and ρ_s is the density of the surrounding fluid. C_e varies with X, the axial distance to mid point of slice ΔX from the nozzle orifice exit plane, as was shown for steady jets by Hill (2). This equation is the basis for the direct measurement of the entrainment coefficients of steady and pulsating jet flows. The novel experiments on pulsating jets discussed in this work were designed to investigate the influence on C_e of geometry, Reynolds number Re, acoustic driver power or pulsation strength U_e/U_j (U_j is the steady jet velocity and U_e the jet velocity pulsation amplitude) and Strouhal number St. In essence this paper is a consolidation of ASME references (3) and (4).

Experimental

Figure 1 shows the apparatus was essentially a ΔX thick porous walled entrainment chamber which can move coaxially about the jet flow. A loudspeaker driver of 250 W capacity was used to pulse the jet flow. Air was supplied to the chamber such that the porous walled cylinder pressure was atmospheric with uniform radially inward flow and with no axial pressure gradient. Thus free-jet flow conditions were established and the measured supplied air mass flow rate to the chamber was equal to the local entrainment mass flow rate of the jet. This measurement method was used for jets with or without acoustic drive.

Figures 2 and 3 present typical experimental C_e versus X/D data for two nozzle sizes, for low and medium Reynolds numbers, and Strouhal numbers were almost identical. The system had a strong response at 163 Hz producing the good range of pulsation strength effect exhibited. As shown the entrainment coefficient varied strongly with X/D and pulsation strength. The acoustic drive considerably increased the entrainment coefficient as well as extended the developing zone. The fully developed value for C_e at a particular U_e/U_j magnitude could not be established because of measurement difficulties at the extended X/D values required.

All the available data at X/D = 10, 163 Hz, are summarised in Figure 4, showing C_e versus U_e/U_j with Re and St as parameters. There was no clear effect due to Strouhal number, therefore, an optimum jet response Strouhal number value cannot be deduced.

Conclusions

The acoustic drive considerably increased the entrainment coefficient C_e by up to 4.5 times greater than the "no-drive" case at X/D = 10.0, and by up to 5.2 times at X/D = 17.5, for a driver power of 246 W at 163 Hz. The extent of the initial development zone of the jet was significantly increased, however, measurement difficulties prevented fully developed values of C_e being obtained. There was only a tendency for C_e to increase with the Strouhal number, and therefore, an optimum value for jet response could not be discovered.

References

1. Ricou, F.P. and Spalding, D.B., "Measurements of Entrainment by Axisymmetrical Turbulent Jets", Journal of Fluid Mechanics, Vol. 11, 1961, pp. 21-32.

2. Hill, B.J., "Measurement of Local Entrainment Rate in the Initial Region of Axisymmetric Turbulent Air Jets", Journal of Fluid Mechanics, Vol. 15, Part 4, 1972, pp. 773-779.
3. Vermeulen, P.J., Ramesh, V., and Yu, Wai Keung, "Measurements of Entrainment by Acoustically Pulsed Axisymmetric Air Jets", ASME Journal of Engineering for Gas Turbines and Power, Vol. 108, No. 3, July 1986, pp. 479-484.
4. Vermeulen, P.J., Rainville, P. Ramesh, V., "Measurements of the Entrainment Coefficient of Acoustically Pulsed Axisymmetric Free Air Jets", 36th ASME Gas Turbine and Aeroengine Congress and Exposition, Paper No. 91-GT-235, 3-6 June 1991, Orlando, Florida, pp. 1-8.

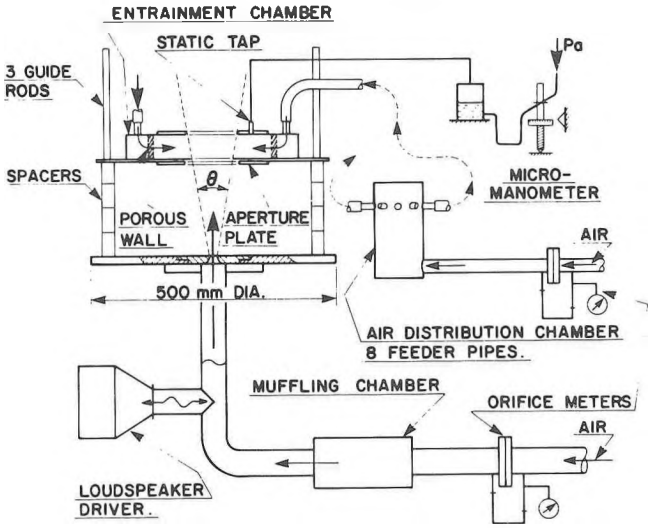

FIGURE 1 - SCHEMA OF APPARATUS FOR MEASUREMENT OF LOCAL ENTRAINMENT MASS FLOW RATE.

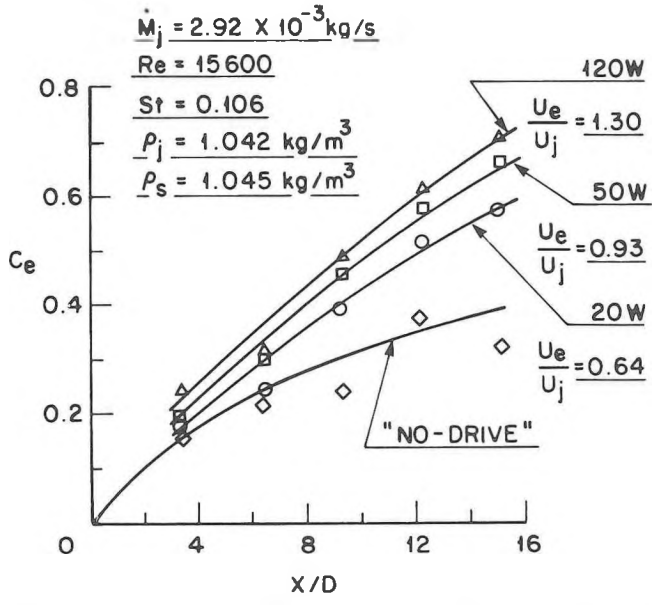

FIGURE 3 - VARIATION OF ENTRAINMENT COEFFICIENT WITH AXIAL DISTANCE AND PULSATION STRENGTH, D = 12.70 mm DIA., U_j = 19.6 m/s, f = 163 Hz.

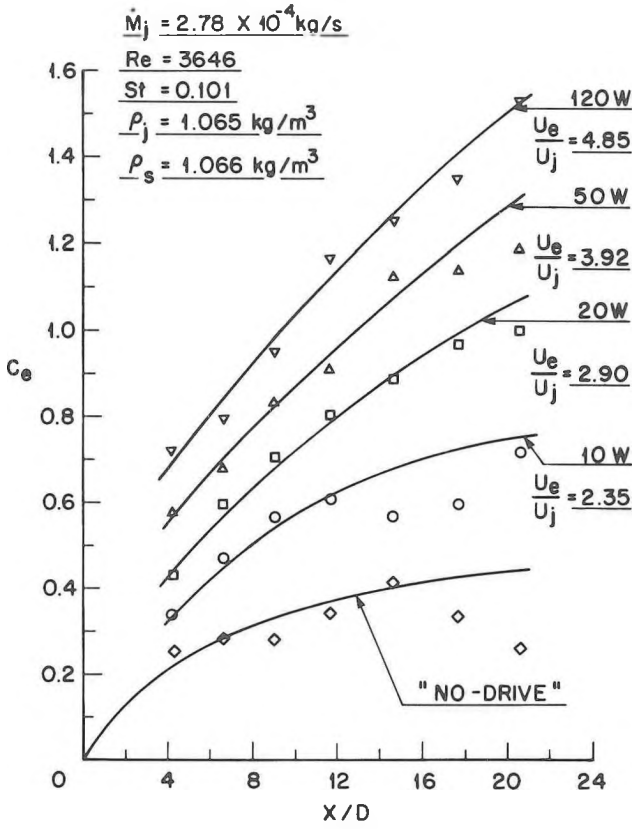

FIGURE 2 - VARIATION OF ENTRAINMENT COEFFICIENT WITH AXIAL DISTANCE AND PULSATION STRENGTH, D = 6.35 mm DIA., U_j = 10.3 m/s, f = 163 Hz.

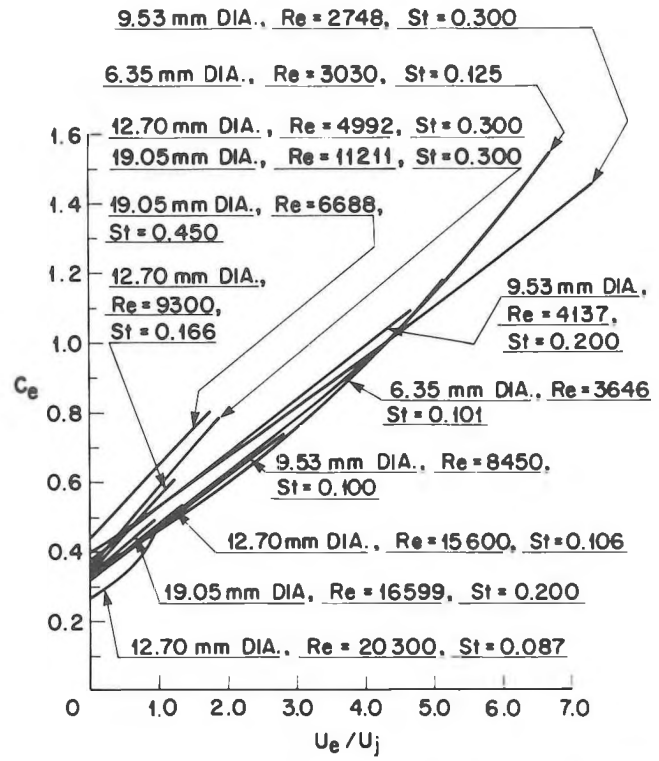

FIGURE 4 - VARIATION OF ENTRAINMENT COEFFICIENT WITH PULSATION STRENGTH FOR THE VARIOUS NOZZLES, f = 163 Hz, X/D = 10, ρ_s = 1.04 kg/m³.

EXPERIMENTS ON ACTIVE POWER MINIMISATION

M.E. Johnson and S.J. Elliott
Institute of Sound and Vibration Research, University of Southampton, England.

1. INTRODUCTION

Active control of sound has been proven as a viable method of controlling low frequency, tonal noise in enclosures[1,2]. This method of sound control has thus far relied on a strategy of direct minimisation of the acoustic potential energy present in the enclosure. This paper suggests an alternative approach to active control. Here we consider the power outputs of sources and attempt to manipulate them to produce a desired result.

Because of their nature, these two strategies require different types of information to achieve control. The direct minimisation of energy requires information about the field as a whole using an array of microphones, typically sixteen to thirty two in number. The minimisation of total power output, however, is concerned with information purely local to the sources themselves (i.e., pressure and source strength) and does not concern itself with information general to the field. Although these approaches appear different in nature, they produce very similar results.[3]

2. THEORY

2.1 Power Outputs of Sources

The power output of a harmonic point monopole source is given by $W = \frac{1}{2}\mathrm{Re}\{q^*(\omega)p(\omega)\}$ where $q(\omega)$ is the complex strength of the source, $p(\omega)$ is the complex acoustic pressure at that source and Re denotes the real part of the bracketed quantity. If we consider a single channel active control system, i.e., one primary source and one secondary source, we can define the pressures at these sources in terms of their source strengths and transfer impedances, as

$$p_p = Z_{ps}q_s + Z_{pp}q_p \tag{1}$$

$$p_s = Z_{sp}q_p + Z_{ss}q_s \tag{2}$$

where q_p and q_s are the source strengths of the primary and secondary, Z_{pp} and Z_{ss} are the radiation impedances of the primary and secondary, respectively, and Z_{sp} and Z_{ps} are the transfer impedances between the sources ($Z_{sp} = Z_{ps}$ due to reciprocity).

We can combine these equations with that for the power to give expressions for the power outputs of the two sources in terms of their source strengths and their radiation and transfer impedances. The impedances are split into their real and imaginary components such that $Z = R$ and jX:

$$W_p = \frac{1}{2}[|q_p|^2R_{pp} + \frac{1}{4}q_s^*Z_{sp}q_p + \frac{1}{4}q_sZ_{sp}q_p^*] \tag{3}$$

$$W_s = \frac{1}{2}[|q_s|^2R_{ss} + \frac{1}{4}q_s^*Z_{sp}q_p + \frac{1}{4}q_sZ_{sp}q_p^*] \tag{4}$$

The total power of the two sources can now be written as output:

$$W_T = \frac{1}{2}[|q_p|^2R_{pp} + |q_s|^2R_{ss} + q_s^*R_{sp}q_p + q_sR_{sp}q_p^*] \tag{5}$$

2.2 Optimal Secondary Source Strength

To actively control the sound field, we vary the strength of the secondary source to minimise the total power output. The optimal values of secondary source strength to produce this result is given by setting the differentials of W_T with respect to the real and imaginary parts of q_s to zero, which gives[3]

$$q_s = q_{s0} = \frac{-q_pR_{sp}}{R_{ss}} \tag{6}$$

If we substitute this optimal value of q_s (equation (6)) into the expression for secondary power (equation (4)), we arrive at a very interesting result. That is, under these conditions the secondary power output becomes exactly zero.[3]

$$\text{If } q_s = q_{s0}, \quad W_s = 0. \tag{7}$$

There are an infinite number of other combinations of the real and imaginary parts of the secondary source strength ($q_s = q_{sr} + jq_{si}$) which also produce zero power output of the secondary source in the presence of the primary source. If q_p is assumed real, the values of q_{sr} and q_{si} which satisfy the condition $W_s = 0$ can be written, from (4), as

$$q_{sr}^2 + q_{si}^2 + q_{sr}\left(\frac{q_pR_{sp}}{R_{ss}}\right) + q_{si}\left(\frac{q_pX_{sp}}{R_{ss}}\right) = 0 \tag{8}$$

which is plotted in Figure 1. The centre and radius of this circular contour are the values of q_s which maximise the power *absorption* of the secondary source:[3] $q_{sa} = -q_pZ_{sp}/2R_{ss}$.

It is important to note here that the secondary source strength which minimises total power output q_{s0} is entirely out of phase with the (real) primary source strength q_p, equation (6). This value of q_s must thus be given by the non-trivial intersection of equation (8) with the q_{sr} axis, as illustrated in Figure 1. If q_s is thus arranged to be out of phase with q_p and its source strength gradually increased, it initially absorbs sound power. If the magnitude of q_s is further increased, the amount of absorbed power is decreased until its power output is exactly zero when $q_s = q_{s0}$, in which case the total power output of the two sources is optimally reduced.

3. EXPERIMENTS

The experiments were conducted with a pure tone excitation frequency of about 90 Hz in an enclosure of approximate dimensions 6 m × 2.2 m × 2.2 m. The volume velocity of two loudspeakers acting as the primary and secondary sources were monitored using the method described in reference 4. The primary source was driven at a constant level and the phase of the secondary source adjusted to be 180° with respect to that of the primary. The power output of the two sources was measured by monitoring the average product of their volume velocity with their near field pressures.[4] The measured values of W_s and W_T as the secondary source amplitude was gradually increased are shown in Figure 2, together with J_p, the level of the sum of the squared outputs of 32 monitor microphones also deployed in the enclosure. It can be seen that W_s initially is negative but then rises to a positive value, as expected. The value of q_s for which $W_s = 0$ corresponds closely to the minimum in the measured values of W_T, confirming the prediction above. This minimum in total power output also coincides with the minimum in the mean square pressure in the enclosure J_p indicating that minimising W_T does achieve global control, even though only measurements local to the secondary source are used in achieving this minimum.

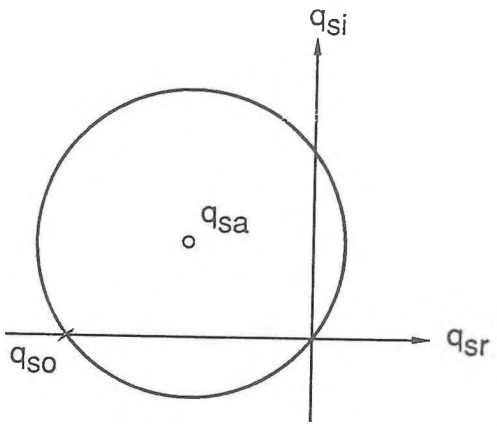

Figure 1. Locus of real and imaginary components of the secondary source strength (q_{sr} and q_{si}) which cause its power output to be zero in the presence of a primary source.

REFERENCES

1. S.J. ELLIOTT *et al* 1988 *Proc. of Inter-Noise '88*, 987-990. The active control of engine noise inside cars.
2. A.J. BULLMORE 1987 *Ph.D. Thesis, University of Southampton*. The active minimisation of harmonic enclosed sound fields with particular application to propeller-induced cabin noise.
3. S.J. ELLIOTT *et al* 1991 *ISVR Technical Report no.* 191(to be published in JASA). Power output minimisation and power absorption in the active control of sound.
4. D.K. ANTHONY and S.J. ELLIOTT 1991 *J. Audio Eng. Soc.* **39**, 355-366. A comparison of three methods of measuring the volume velocity of an acoustic source.

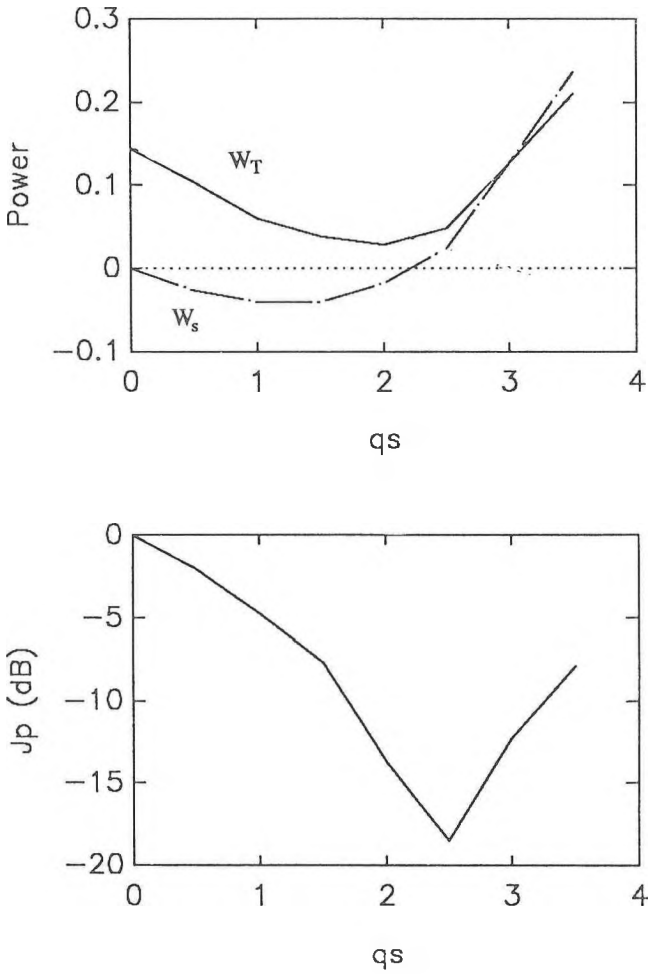

Figure 2. Power output of secondary source W_s (-·-·) total power output of primary and secondary sources W_T (___), and mean square pressure J_p in the experimental enclosure as the secondary source strength was increased.

ELECTROMAGNETIC ACOUSTIC NOISE AND VIBRATIONS OF ELECTRICAL MACHINES; THEIR PRODUCTION AND MEANS OF REDUCTION

S.P.VERMA and A.BALAN
Department of Electrical Engineering
University of Saskatchewan
SASKATOON, CANADA S7N 0W0.

1. INTRODUCTION

The increasing applications of electrical machines have resulted in a growing awareness of the problem of noise produced by them. In motors upto 150 kW capacity, lowest cost per unit output has been the principal design criterion. Owing to the increasing economic pressures, modern electrical machine design trends are towards the use of higher currents and flux-densities. To keep the machine size to a minimum and maximize the efficiency, high speed motors are used wherever possible. Such motors are inevitably a source of considerable magnetic, windage and mechanical noise [1].

Mounting criticism of ambient noise levels, even in traditionally noisy environments, has led to increasing attention being focused on the noise emitted by electric motors. Stricter regulations are now being enforced to protect people from a noisy environment. It has, therefore, become necessary for machine manufacturers to specify the noise produced by their products, and try to make them quieter than those of their competitors.

Vibrations and consequently the noise produced by a machine can be reduced to a large extent if the forces produced during their operation are not allowed to excite any resonances of the machine-structure. Accurate determination of the exciting forces and the resonant frequencies are of paramount importance. It is also becoming necessary for a designer to be able to predict the noise produced by a machine from its design data. This is especially significant in the case of large machines where it is not practical to build prototypes and it is expensive to employ external means of noise control.

2. REVIEW OF INVESTIGATIONS

Squirrel-cage induction motors are by far the most commonly used motor for industrial drives. Extensive investigations were conducted to understand the nature and mechanism of production of electromagnetic acoustic noise from squirrel-cage induction motors [2-6]. Detailed theoretical and experimental investigations were conducted to determine the resonant frequencies and the vibrational behaviour of electrical machine stators of different sizes. During the course of the study of resonant frequencies and the nature of the vibration at resonance, the effects of the frame, laminations, dynamics of the teeth and windings were critically examined. Further, investigations were conducted on the electromagnetic excitation forces that induce vibrations in the machine during its operation. These forces produce cyclic deformations of the stator and the rotor, and they generally occur at predictable frequencies. The electromagnetic radial-forces depend on the nature of the magnetic field in the air-gap of a machine. A detailed study was done to examine the effects of various parameters on the magnetic field and the radial-forces [6]. A simple and elegant technique is developed to predict the various frequency components in the audible noise spectrum.

3. RESONANT FREQUENCIES AND VIBRATION BEHAVIOUR OF STATORS

Several analyses have been developed over the years to analytically determine the resonant frequencies and the vibration behaviour of stators. The stator core was treated as a thin shell by many investigators. Such an approximation can be erroneous for stators with thick cores, as in the case of turbogenerators and machines where the core radial-thickness-to-radius ratio may well exceed a value of 0.2. Further, many investigators considered only the lowest resonant frequency of a particular mode to be significant. Although this may be true for small machines, it is certainly not true for large machines where several resonant frequencies for each mode of vibration may lie within the critical frequency range of noise production.

In reference [2], the authors developed an analysis, based on the three dimensional elasticity theory and Flugge's theory of thin shells for the frame, to determine the resonant frequencies and vibration response of stators of encased construction. This analysis while treating the stator core and frame rigorously, treats the teeth and windings as an additional mass. The complex boundary conditions in the presence of both teeth and windings, along with the free end conditions of the stator, posed considerable difficulties in the formulation of the frequency equation. In a revised analysis [3], the general frequency of the stator was derived using the three dimensional theory of elasticity, an energy-method and the principle of Rayleigh-Ritz. By using the energy-method, the problem of satisfying the boundary conditions along the junctions between the various components of the stator was avoided. The assumptions made in the analysis are those related to the homogeneity and linearity of the materials involved. The analysis was further extended in reference [5], to include the more complex configurations of a stator with outside cooling ribs,

and a stator core supported by a frame with internal longitudinal ribs. The general frequency equation obtained is equally applicable to all circumferential mode of vibration, including the breathing and the beam-type modes of vibration. It predicts two set of resonant frequencies for circumferential modes, one which is associated with symmetric longitudinal modes and the other with antisymmetric longitudinal modes.

Extensive experimental investigations were conducted on several models to confirm the validity of the analysis. The models were designed to have an increasing degree of complexity in construction such that each model examined the validity of a particular aspect in the analysis. Details of the various models can be found in reference [2-5]. Further experimental investigations were also carried on a 7.5 hp and a 125 hp induction motor stator. The salient findings of this study will be presented by the authors.

4. ELECTROMAGNETIC EXCITATION

The prediction of the vibration behaviour, and the sound radiated from electric machines require accurate determination of the exciting radial-forces. A better understanding of the noise producing radial-forces will definitely help in achieving a good sonic design. A variety of undesirable phenomena such as parasitic torques, stray losses and magnetic noise associated with electrical machines are produced due to the presence of harmonic fluxes in the air-gap. The harmonics in the air-gap field are produced due to the spatial distribution of the current carrying conductors, slotting of the stator and rotor surfaces and magnetic saturation of the iron [6]. Another inadvertent source of harmonic production is the eccentricity of the rotor. The radial forces that act on the stator and rotor are produced by the Maxwell's stresses associated with the magnetic fluxes entering or leaving the iron surfaces. These stresses that act on the stator and rotor surfaces are proportional to the square of the air-gap flux-density.

The significance of a force component depends on the magnitude, frequency and the mode of vibration associated with it. In the event of the exciting force-frequency coinciding with a resonant frequency, even a small exciting force can give rise to appreciable vibrations. At conditions different from that at resonance, the amplitude of the forced response will be determined by the magnitude of the exciting force. Further, it should be emphasised that the flexural rigidity posed by the stator and rotor increases to the forces which induce higher modes of vibration. Consequently, in such a case the dynamic deflections produced will be small. Some results from theoretical and experimental study conducted on squirrel-cage induction machines, will also be presented.

5. MEANS TO REDUCE NOISE

As a first step towards noise reduction, the mechanical structure must be designed in such a way that preferably no exciting force-frequency coincides with a resonant frequency of the machine. Secondly, a stiffer construction may be used to attenuate the vibration response to the various electromagnetic exciting forces.

Most of the secondary phenomena associated with electric motors, such as noise and vibrations, are largely influenced by the winding disposition and the slotting of the stator and rotor surfaces. Since some of the design requirements to diminish these effects are mutually incompatible, design compromises are essential. Magnetic noise is critical with respect to the correct choice of the slot ratio. A prudent slot combination with an appropriate stator winding arrangement will help alleviate the problem by mitigating the effects of some of the important noise producing electromagnetic radial-forces.

6. REFERENCES

1. Wernick, E.H. (1978) "Electric Motor Handbook", McGraw-Hill book company Ltd., U.K.
2. Verma, S.P., & Girgis, R.S. (1973) "Resonance frequencies of electrical machine stators having encased construction, I.E.E.E. Trans. PAS-92, pp. 1577-1585.
3. Girgis, R.S., & Verma, S.P., (1981) "Method for accurate determination of resonant frequencies and vibration behaviour of stators of electrical machines", I.E.E. proceedings, Vol. 128, pp. 1-11.
4. Verma, S.P., & Girgis, R.S. (1981) "Experimental verification of resonant frequencies and vibration behaviour of stators of electrical machines", Part 1 and 2, I.E.E. proceedings, Vol. 128, pp. 12-32.
5. Verma, S.P., Williams, K., & Singal,R.K (1989) "Vibrations of Long and Short laminated stators of Electrical machines", Part I, II and III, Journal of Sound and Vibration, Vol.129(1), pp. 1-44.
6. Verma, S.P., & Balan, A., (1990) "Air-gap field harmonics and radial-forces of induction motors", proceedings of the International conf. on Electrical Machines, M.I.T. (Boston, U.S.A.), pp. 474-479.

SYMPHONIC BELLS OF 'FANTASTIC' PROPORTION

Daryl Caswell
University of Calgary
Mechanical Engineering Dept.
2500 University Dr. N. W.
Calgary, Alberta

1. THE PROBLEM:

Producing the sound of large church bells in an orchestral setting is often referred to as the last unsolved problem of the orchestral percussionist. The problem is as old as the symphonic orchestra and has resulted in many amusing and often musically disastrous attempts at finding a solution. Among the more successful attempts (ranging from an eight foot long tubular chime played from a step ladder, to throwing open the back door of the concert hall and playing the local church carillon at the prescribed moment in the score) is the use of flat metal plates. The disadvantages of using metal plates to imitate the sound of church bells centre on the difficulties encountered in accurately predicting the natural frequency of the plate, achieving sufficient amplitude and avoiding unharmonious overtones.

2. THE USUAL SOLUTION:

The free vibration of plates under every conceivable method of support has been the subject of countless publications and research projects in the last 100 years. [ref. 1-8] Mathematical analysis requires the solution of the differential equation of motion:

$$D\nabla^4\omega + \rho\frac{\partial^2\omega}{\partial t^2} = 0$$

where ω is the transverse deflection and ∇ is the biharmonic differential operator.

$$D = \frac{Eh^3}{12(1-\upsilon^2)}$$

is the flexural rigidity where E is Young's modulus; h is the plate thickness; υ is Poisson's ratio. Mass density per unit area of plate is represented by ρ and t is time.

At first glance, the problem merely requires the researcher to plug the proper numbers into one of the many methods stemming from the work of Rayleigh and Ritz near the turn of the century. However, the results are unsatisfactory because of the following difficulties:

a. The theory assumes that the plate is thin. However, the fundamental frequency of a thin plate will not dominate acoustically when a freely suspended plate is struck. One or more of the harmonics will be louder than the natural or fundamental frequency.

b. There is no theoretical method to predict the strength of the sound and match it to that of a real bell.

c. While plate theory permits the determination of the frequency content of a given plate, the reverse is not true. Given the frequency content of a bell there is no means to determine the plate dimensions which will yield an approximation to the desired response.

d. Until recently, the freely suspended plate was subject to large errors in frequency analysis (>6%) because of the difficulty in correctly modelling the boundary conditions.

3. THE 'MUSICAL' SOLUTION:

Given the serious difficulties encountered in attempting a purely mathematical solution, I decided to develop an artistically driven method by allowing competent musicians with an extensive knowledge of the problem to guide the necessary experimentation. Foregoing the use of acoustical analyzers which are at best averaging instruments, the musicians verbally described the sound they were looking for and, with the help of our musically inclined shop technicians, isolated the most appropriate plate material, the optimum thickness for proper amplitude, and the approximate length to width ratio which seemed to give a bell-like frequency response.

Now it was possible to go back to the analyzers, the mathematics and the computer to determine what it was about the 'subjective' input of the musicians that resulted in the final choice of material, thickness and shape. Analysis showed that the solution existed in a very narrow window of dimension which lies between a thin plate and a thick plate as well as between a plate and a beam. The mathematical disadvantage is that the assumption of thinness is lost but this was compensated for by the fact that the plate could be treated as a beam as far as determining the fundamental frequency. This resulted in improved accuracy. Arising from this artistically driven analysis was the interesting observation that there is a critical length to thickness ratio below which the fundamental frequency of a plate will not dominate in the frequency response.

4. RESULTS:

Employing the information gained from quantifying the musical appropriateness of the chosen plate parameters, a set of bell plates has been produced for performances of Berlioz's 'Symphonie Fantastique' by the Calgary Philharmonic and the Vancouver Symphony. The final movement of the work requires the tolling of distant church bells calling the witches back from their revel. Further experimentation produced a gong-like sound for the Calgary Opera's production of Puccini's 'Madame Butterfly' as well as the church bell signalling the lover's meeting time in Verdi's Falstaff.

5. REFERENCES

1. **Gorman, Daniel J.** 1982 'Free Vibration of Rectangular Plates' (Elsevier, New York).
2. **Leissa, A. W.** 1969 NASA SP-160 'Vibration of Plates'.
3. **Leissa, A. W.** 1973 Journal Of Sound And Vibration 31(3), 257-293. The Free Vibration Of Rectangular Plates.
4. **Rayleigh, Lord** 1894 'Theory of Sound', vol. 1, second edition (Macmillan and co., London).
5. **Ritz, W.** 1909 Annalen der Physik, fourth series, vol.28, p. 737, 'Theorie der Transversalschwingungen einer quadratischen Platte mit freien Randern'.
6. **Timoshenko, Stephen, D. H. Young, and W. Weaver,** 1990 'Vibration Problems in Engineering', fifth edition (Wiley, New York).
7. **Waller, Mary D.** 1961 'Chladni Figures, A Study in Symmetry' (G. Bell and Sons Ltd., London).
8. **Warburton, G. B.** 1954 Proceedings of the Institute of Mechanical Engineers, ser. A,168,371-384. The Vibration Of Rectangular Plates.

INCREDIBLE VERSATILITY

At Only 2.2 lbs.

RION

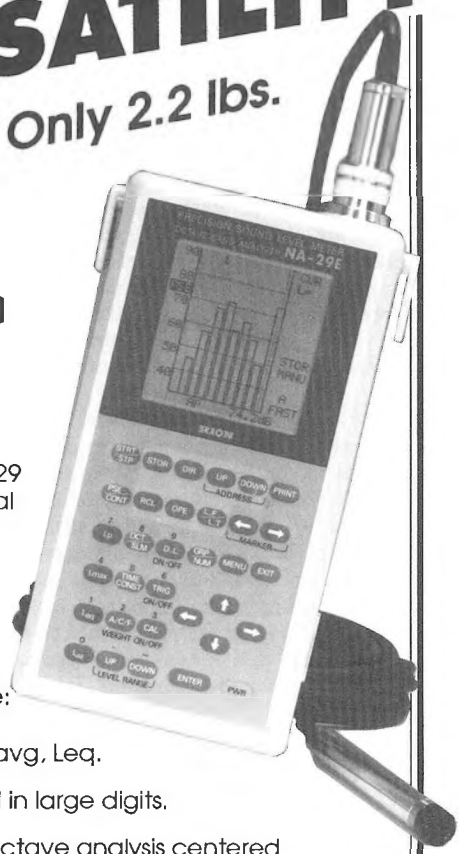

Rion's new NA-29 provides unusual capabilities for a pocket-size acoustical analyzer weighing only 2.2 lbs. It's displays include:

- ❑ Lmax, Ln, Lavg, Leq.
- ❑ Sound level in large digits.
- ❑ Real-time octave analysis centered 31.5 Hz. through 8000 Hz.
- ❑ Level vs. time, each frequency band.
- ❑ 1500 stored levels or spectra.
- ❑ Spectrum comparisons.

It also features external triggering, AC/DC outputs, and RS-232C I/O port. A preset processor adds additional versatility for room acoustics and HVAC applications. To minimize external note taking, users can input pertinent comments for each data address. Specify the NA-29E for Type 1 performance or the NA-29 for Type 2.

Our combined distribution of Norwegian Electronics and Rion Company enables us to serve you with the broadest line of microphones, sound and vibration meters, RTAs, FFTs, graphic recorders, sound sources, spectrum shapers, multiplexers, and room acoustics analyzers, plus specialized software for architectural, industrial and environmental acoustics. You'll also receive *full* service, warranty and application engineering support. Prepare for the '90s.

Call today. (301) 495-7738

SCANTEK INC.

Norwegian Electronics • Rion

916 Gist Avenue • Silver Spring, MD 20910

PALM SIZE FFT

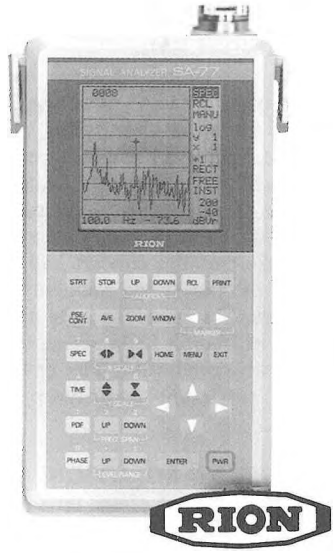

RION

Amazingly smaller and lighter than a lap-top

Our new SA-77 FFT Analyzer is a true miniature. Yet it is very big in capability.

- 0 – 1 Hz to 0 – 50 kHz.
- Zooms to 800 lines.
- FFT, phase and PDF analysis and time waveform.
- External sampling for order analysis.
- Stores 150 screen displays plus 30K samples of time data.
- Single/double integration or differentiation.
- Arithmetic/exponential averaging or peak-hold.
- Built-in RS-232C.
- $8\frac{1}{4}$ X $4\frac{3}{8}$ X $1\frac{1}{2}$ inches.
- 23 ounces.

Call today. Discover how much noise, vibration and general signal analysis capability you can hold in the palm of your hand. And at how reasonable a cost.

SCANTEK INC.

Norwegian Electronics • Rion

916 Gist Avenue, Silver Spring, MD, USA 20910 • (301) 495-7738

PROGRESS ON THE DEVELOPMENT OF STANDARDS FOR SOUND INTENSITY MEASUREMENTS

G. Krishnappa
Institute for Mechanical Engineering
National Research Council, Ottawa, Canada

Introduction

Sound intensity measurements are increasingly being employed in machinery and industrial noise assessment and control. Using sound intensity measurements sound power levels of noise sources can be determined in their normal operating environment, without the requirement of special facilities. The international and ANSI standards organizations have been involved in developing both instrument and calibration standards, and procedural standards to determine sound power. The sound power document based on discrete point measurements, developed by the ISO, has already become an approved standard. The ANSI sound power draft is expected to receive final approval in a short time. Both the ANSI and IEC working groups are striving hard to develop instrument standards. The progress has been rather slow due to difficulties associated in standardizing many types of instruments and the lack of appropriate calibrating procedures.

This paper discusses the progress made by the ANSI and international standards working groups, highlighting the differences between the two approaches.

Instrument Standards

The instrument standards that are being prepared by the ANSI and IEC working groups are in the final stages of development. Due to insufficient progress on the techniques relating to the performance evaluation of pressure/velocity probes, both the working groups decided to develop standards for the two microphone probe. The approaches taken by both the working groups are similar, with small variations in some sections. The probe and the processor forming the sound intensity instrument, are treated separately and together. Requirements and tolerance limits are based on the current state of technology. Performance verification requirements are written in terms of type tests to be carried out by the manufacturers, and periodic calibrations to be performed either by the manufacturer or in an accredited laboratory, as they require high degree of specialized knowledge and facility. Simple field checks of the instruments are also required to be carried out during the measurements. Important performance indicators of the instruments are the residual intensity-pressure index, performance of the probe under free field condition and inside standing wave apparatus. The methods and procedures to carry out these performance tests are specified in the documents.

Sound Power Standards

The standards developed by ANSI and ISO, specify methods for determining the sound power of noise sources from sound intensity measurements on a surface enclosing the source. The standards contain information on the procedures for the selection of measurement surface, methods for sampling sound intensity on the measurement surface, and procedures for the calculation of sound power levels and achieving the desired grades of accuracy. The approved ISO standard is based on the measurements at discrete points, and the uncertainties are determined by certain ancillary tests using indicators. The procedures prescribed in this standard is rather complex and time consuming, and sometimes lead to too many points. Now this working group is involved in developing a much simpler scanning document. The ANSI draft, which is currently being balloted for the second time for adaptation as an approved standard, includes both fixed point measurements and the scanning of the measurement surface. The required measurement points are determined by successively doubling the number of points on the measurement surface until the specified convergence index for each frequency band is less than the tolerance value. The uncertainties in the scanning method is evaluated either by using the data indicators, given in an appendix, or by varying the scanning rate and pattern.

References

IEC 1043, *Instruments for the Measurement of Sound Intensity*, Second Committee Draft, July 1991.

ISO 9614, *Determination of Sound Power Levels of Noise Sources Using Sound Intensity - Part 1: Measurement at Discrete Points*, April 1990.

ANSI S12, 12-199X, *Engineering Method for Determination of Sound Power of Levels of Noise Sources Using Sound Intensity*, April 1991.

ELECTROACOUSTICAL RESEARCH AND ACOUSTICAL CALIBRATIONS AT INMS

George S. K. Wong,
Institute for National Measurement Standards
National Research Council Canada, Ottawa, Ontario, K1A 0R6.

1. INTRODUCTION

Since the formation of the Institute for National Measurement Standards (INMS) at the National Research Council to replace programs in the previous Division of Physics and Division of Electrical Engineering, substantial changes have been made to the operational structure of NRC. INMS has the responsibility over a wide spectrum of Primary Standards that are maintained in Canada, and has a leadership role in national and international standards activities. The Institute also provides calibration services that are traceable to the Primary Standards. The aim here is to present a concise picture on the current research on electro-acoustics and the acoustical calibration and standards activities within INMS. The Acoustical Standards Group which is one of the ten groups in INMS, is responsible for the maintenance of the Primary Acoustical Standards and has been given a new mandate to develop Ultrasound Standards.

2. ELECTROACOUSTICAL RESEARCH

Electroacoustical research is a continuing activity of the Acoustical Standards Group. It includes up dating the semi-automatic acoustical instrument calibration system when new acoustical measuring instruments are submitted for calibration, low-frequency high sound pressure microphone calibration, phase match of microphones (for sound intensity measurements and research), new measuring techniques and instrument development. In view of a limited human resource, the current activities are selected to satisfy immediate needs :

(A) Coupler methods for phase match of microphones :

The design and development of a new three-port coupler [1] has enable NRC to have the capability to phase match microphones precisely. Current research indicates that the phase match uncertainty is less than $\pm$ 0.05 deg.; and depending on the type of microphones, the operating frequency range of the coupler can be extended to beyond 6.3 kHz. There are three variations of the coupler method :

With the Direct Method, the phase match arrangement requires two independent electronic channels i.e. two preamplifiers and two measuring amplifiers. The measurement is based on a microphone interchange procedure [1]. With the Substitution Method, only one electronic channel is required; whereas with the Comparison Method, two preamplifiers and one measuring amplifier are needed. The Direct Method has been automated with the operation under the control of a computer.

(B) Precision measuring amplifier :

The precision measuring amplifier [2] developed at NRC has been redesigned to incorporate new programmable features such as high pass and low pass filters; linear, A, B and C weightings; input and output gain stage selection, or with auto range; direct and preamplifier inputs; various response time constants; peak and hold, and data averaging.

3. CALIBRATION ACTIVITIES

Apart from routine calibrations, the Acoustical Standards Group is constantly upgrading and improving the capability of their calibration facilities.

(A) Primary acoustical standard :

The Canadian primary acoustical standards arrangement has been moved to a more spacious location. The reciprocity calibration system, including all the environmental controls for temperature, humidity and pressure, is being automated. The final arrangement will enable NRC to investigate into the effects of the environment on microphone sensitivity and frequency response.

(B) Accelerometer calibration :

A system for the absolute calibration of accelerometers is under development. The system consists of an electro-dynamic shaker to which the test accelerometer is attached, an interferometer to measure the movements of the accelerometer, together with an electronic counter to register the phase transition of the interference fringes, and a precision AC voltmeter to record the rms voltage from the accelerometer. Current investigation is focused on the shaker head movement orthogonality that contributes to nearly 40 % of the uncertainties in the calibration of an accelerometer.

(C) Ultrasound standards :

With the mandate to develop ultrasound standards to satisfy Canadian needs, the Acoustical Standards Group is making arrangements to implement initially, a high power ultrasound standard to cover the power range from approximately 0.5 W to 30 W ; and then a low power ultrasound standard to cover the range below 0.5 W.

The ultrasound standard consists of a tethered float suspended in water. The ultrasound beam from the test transducer displaces the hollowed cone shaped float from its initial position. By measuring the vertical displacement that has been calibrated with known weights applied to the float, the ultrasound power generated by the test transducer can be deduced from the product of the force acting on the float and the wave velocity.

4. CALIBRATION SERVICES

The acoustical calibration service is under review. New calibration services will include microphone phase match, filter sets, accelerometers, and partial check of sound level meters. INMS has recognised that the total cost for a relatively comprehensive calibration of a sound level meter may be out of reach for some smaller organizations, and consultants. Therefore, to provide a partial check that includes only attenuators or weighting net works together with sound pressure level sensitivity at a reference frequency, at a much lower cost can be more attractive. The above partial check rationale is based on the fact that some sound level meter features may not require annual calibration.

Calibration of commercial and special acoustical instruments pertaining to national and international standards are some of the on-going activities; and advice and information pertaining to acoustical standards, and technical aspects of noise measurement are usually available from the Acoustical Standards Group.

5. REFERENCES

[1] G. S. K. Wong, "Precision method for phase match of microphones," J. Acoust. Soc. Am. 90, September (1991).

[2] G. S. K. Wong, "Precision ac-voltage-level measuring system for acoustics," J. Acoust. Soc. Am. 65, 830-837 (1979).

CONSEQUENCES OF NYQUIST THEOREM FOR ACOUSTIC SIGNALS STORED IN DIGITAL FORMAT

Marek Roland - Mieszkowski and Wayne R. Young
School of Human Communication Disorders, Dalhousie University
5599 Fenwick Street, Halifax, Nova Scotia, B3H-1R2, Canada.

The calculation of functions in digital domain from analogue acoustic signals involves a two-step process which includes analog to digital (A/D) conversion and digital calculations performed on digitized acoustical signal. Function V(t) will be represented digitally without any loss of information as long as sampling occurs in accordance with the Nyquist criteria [1-9]. How can we determine the values of digitized function for points between samples when we have only N samples available ? The Nyquist formula requires an infinite number of samples to accomplish this task. In situations when digital samples are sufficiently dense, one can approximate many continuous functions with their discrete formulations. Errors generated in these cases will be small, since they depend on spacing between samples. The situation will be different, however, when samples are coarsely spaced.. For example, a sinusoidal tone of frequency f=20,000 Hz sampled at $f_{sampling}$=44,100 Hz is represented by only 2.205 samples per period. Calculation of many functions (for example RMS values) may lead in this case to some errors. Finite duration sampling of continuous signal results in errors caused by our limited knowledge of the function for all points in time.It turns out that the more samples we have around the region of interest, the more accurately we are able to reproduce the function there. This paper investigates the error caused by truncation of the Nyquist sampling formula with the aim of quantifying it and establishing ways to minimize its effect.

Nyquist Theorem

According to the Nyquist theorem [1-9] the discrete time sequence of a sampled continuous function { $V(t_n=n\cdot T_s)$ } contains enough information to reproduce the function V=V(t) exactly provided that the sampling rate ($f_s=1/T_s$) is at least twice that of the highest frequency contained in the original signal V(t):

$$V(t) = \sum_{n=-\infty}^{+\infty} V[n] \cdot \frac{\sin[\pi \cdot f_S \cdot (t - n \cdot T_S)]}{\pi \cdot f_S \cdot (t - n \cdot T_S)} \qquad (1)$$

where:
$f_S = 1 / T_S$ - sampling frequency
V(t) - value of signal (voltage) at arbitrary time t
$V[n] = V(n \cdot T_S)$ - value of signal at time $t = n \cdot T_S$

Nyquist Theorem's consequences

It is worth noting that information about the signal V=V(t) at any given moment in time $t \neq n \cdot T_S$ is distributed among all discrete samples { V[n] } with appropriate weights (see eq. (1)). Realistically, we are never presented with an infinite discrete time sequence and are therefore forced to perform the summation over a finite range. This is equivalent to a loss of information about the function V=V(t) not only before and after our time window (which is understandable), but also at the time points between the sampling points. This can introduce errors into the process of reconstructing the function. Let assume that we have available to us N digital samples of function V=V(t) (this is illustrated in fig. 1):

$$V[n] = V(t=n \cdot T_S) \quad \text{where: } n = 0,1,2.....(N-1) \qquad (2)$$

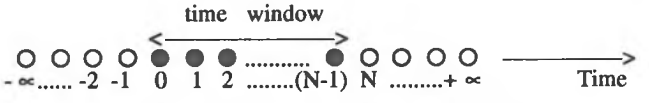

● - known and ○ - unknown values of function V[n]

Fig.1. Illustration of available values V[n] in the time window $[0, (N-1)\cdot T_S]$

Values of the function V=V(t) for the times $t \in [\,0 \cdot T_S\,;\,(N-1)\cdot T_S]$, can be estimated by a truncated version of formula (1) :

$$V(t) = \sum_{n=0}^{N-1} V[n] \cdot \frac{\sin[\pi \cdot f_S \cdot (t - n \cdot T_S)]}{\pi \cdot f_S \cdot (t - n \cdot T_S)} \qquad (3)$$

The errors resulting from truncation are $\varepsilon_{LEFT}(t)$ and $\varepsilon_{RIGHT}(t)$. They represent the "LEFT" and "RIGHT" portions of the sum (with respect to the time axis) in eq. (1) that are omitted in eq.(3), and can be represented mathematically by the following formulas :

$$\varepsilon_{LEFT}(t) = \sum_{n=-\infty}^{-1} V[n] \cdot \frac{\sin[\pi \cdot f_S \cdot (t - n \cdot T_S)]}{\pi \cdot f_S \cdot (t - n \cdot T_S)} \qquad (4\,a)$$

$$\varepsilon_{RIGHT}(t) = \sum_{n=N}^{+\infty} V[n] \cdot \frac{\sin[\pi \cdot f_S \cdot (t - n \cdot T_S)]}{\pi \cdot f_S \cdot (t - n \cdot T_S)} \qquad (4\,b)$$

The sum truncation error is generated when eq.(3) is used instead of eq.(1), and is given by the following formula :

$$\varepsilon_{TOTAL}(t) = \varepsilon_{LEFT}(t) + \varepsilon_{RIGHT}(t) \qquad (5)$$

where:
$\varepsilon_{LEFT}(t)$ - "LEFT" error (due to truncation to the left where values of V[n] are unknown)
$\varepsilon_{RIGHT}(t)$ - "RIGHT" error (due to truncation to the right where values of V[n] are unknown)

In the next section we will try to evaluate the sum truncation error for different cases.

Evaluation of sum truncation error

● If a priori information is given, that $V(t) = 0$ for $t \notin [0;(N-1)T_S]$ then $\varepsilon_{TOTAL} = 0$ (since $\varepsilon_{LEFT} = 0$ and $\varepsilon_{RIGHT} = 0$) and we can use with full confidence the truncated version of the Nyquist sum (eq. (3)). Otherwise using the sum from eq. (3) is equivalent to the zero-extension (or zero-padding) method [3,5].

● If a priori information is given, that function V = V(t) is periodic (ie. $V(t) = V(t+ T)$) then this information can be used in formula (1). In the special case when the function period $T= N_0 \cdot T_S$, where $N_0 \leq N$, one can use formula (1) directly since all values of function V[n] are known for $n \in (-\infty\,;\,+\infty)$. In this case one can also use the Discrete Fourier Transform (DFT) on N_0 consecutive data points (from the available N data points V[n] where n=0,1,2.....(N-1)) to calculate amplitudes A_i , and phases ϕ_i, of the periodic signal and then use the formula :

$$V(t) = A_0 + \sum_{i=1}^{M} A_i \cdot \sin(2\pi f_i \cdot t + \phi_i) \qquad (6)$$

where:
A_0 - DC component of the periodic signal V = V(t)
A_i - amplitudes calculated from DFT
ϕ_i - phases calculated from DFT
$f_i = (i / N_0) \cdot f_S$ - frequencies available in periodic signal V = V(t)
$M = INT(N_0 / 2)$ - number of the highest possible harmonic (since $f_i < f_S / 2$)

● When a priori information is not available about the function V=V(t) then direct use of the truncated Nyquist sum (eq. (3)) is going to lead to truncation error ε_{TOTAL} given by eq. (4) and (5). Values V[n] in eq. (4 a) and (4 b) can be any arbitrary numbers, since we do not have any a priori information about the signal. In the next section we will investigate this in greater detail to estimate values of possible errors.

Estimation of truncation error for general case

Let's consider for simplicity the "LEFT" error given by eq. (4 a) (estimation of "RIGHT" error is performed in identical way). Total error given by eq. (4 a) is a sum of contributions from data points V[n] where n=-1,-2,-3.....- ∞.

Error contribution from the n-th point is given by :

$$\varepsilon_n(t) = V[n] \cdot \frac{\sin[\pi \cdot f_s \cdot (t - n \cdot T_s)]}{\pi \cdot f_s \cdot (t - n \cdot T_s)} \qquad (7)$$

where:
$t \in [0 ; (N-1) \cdot T_s]$
n=-1,-2,-3.....- ∞ for "LEFT" errors
n= N, (N+1),.....+ ∞ for "RIGHT" errors

The function sin (x) /x (where $x = \pi \cdot f_s \cdot (t - n \cdot T_s)$) is equal to 0 at time points $t = m \cdot T_s$; m=0,1,2,3.....(N-1) (which are the sampling points in our time window). Therefore there is no contribution to the error in V(t) at sampling points due to truncation. Also the function sin (x) / x has local max. and min. approximately at the middle points between adjacent sampling points in our time window. This can be proved easily by taking first derivative of function sin (x) / x. The approximation gets better for larger values of x. Therefore from now on we will consider the error at the middle points between samples V[n] in our time window (see fig.1.) :

$$t = (m + 1/2) \cdot T_s \qquad (8)$$

Substituting time t from eq (8) into formula (7) we get:

$$\varepsilon_n[m + 1/2] = V[n] \cdot \frac{(-1)^{(m-n)}}{\pi \cdot [(m + 1/2) - n]} \qquad (9)$$

where:
m=0,1,2,3.....(N-2) - indexing of middle points between adjacent samples in the time window
n =-1,-2,-3.....- ∞ - indexing of points on the left of the time window (see fig.1)

● An interesting question to ask is how large the value of index "m" in eq.(9) must be in order for the absolute value of error $\varepsilon_{LEFT}[m+1/2]$ to be equal or smaller then 1/2 of the quantization step Δ , which is defined as a difference between quantization levels [1,3,8,9]. This is a reasonable comparison since all samples V[n] have quantization error inherent to the process of A/D conversion [1,3,8,9]. Quantization error is uniformly distributed in the range $[-\Delta/2 ; \Delta/2]$, where Δ is a step size in the A/D converter [1,3,8,9]. From eq. (9) we have for n=-1 and $V[-1] = V_{MAX} = 2^{B-1} \cdot \Delta$ (where V_{MAX} is the max. possible signal amplitude in the A/D converter and B is the No. of bits in the A/D converter) :

$$m \geq 2^B / \pi - 3/2 \qquad (10)$$

From inequality (10) we get (times are calculated for f_s = 44,100 Hz):

for B = 8 bit : m ≥	80	(0.001 sec	inside sound file)
for B = 10 bit : m ≥	325	(0.007 sec	inside sound file)
for B = 12 bit : m ≥	1,303	(0.030 sec	inside sound file)
for B = 14 bit : m ≥	5,214	(0.118 sec	inside sound file) (11)
for B = 16 bit : m ≥	20,860	(0.473 sec	inside sound file)
for B = 18 bit : m ≥	83,442	(1.892 sec	inside sound file)
for B = 20 bit : m ≥	333,771	(7.569 sec	inside sound file)

Results in (11) show that if we have no information about the signal before our time window, then in order to avoid errors associated with the unknown values of function V[-1], V[-2], V[-3]....., one has to be " m" samples deep inside of the time window. We can then use the formula (3) for any time t as long as we stay away from the ends of the time window by " m " samples ($t \in [m \cdot T_s ; (N-1-m) \cdot T_s]$).

● Another interesting question to ask is which sequence of samples V[-1], V[-2], V[-3].....will generate the largest error at the middle points in our time window ? Taking the summation of eq. (9) from n=-1 to m=- ∞ we get :

$$\varepsilon_{LEFT}[m + 1/2] = 1/\pi \cdot (-1)^m \cdot \sum_{n=-1}^{-\infty} V[n] \cdot \frac{(-1)^{-n}}{(m + 1/2) - n} \qquad (12)$$

If we take the sequence of samples $V[n] = V_{MAX} \cdot (-1)^n$ then we get from eq (12) :

$$\varepsilon_{LEFT}[m + 1/2] = 1/\pi \cdot V_{MAX} \cdot (-1)^m \cdot \sum_{n=-1}^{-\infty} \frac{1}{(m + 1/2) - n} \qquad (13)$$

Unfortunately our choice of { V[n] } in eq. (13) was inappropriate because the sum of this series diverges to ∞. As a matter of fact this happened since this particular series corresponds to the digital representation of a sine wave with the Nyquist frequency $f = f_s / 2$. Such a frequency can't exist in the digital domain, since it can't be recorded via A/D conversion. A realizable choice of samples would be, for example, one which represents sinusoidal wave with frequency $f < f_s / 2$:

$$V[n] = V_{MAX} \cdot \sin[2 \cdot \pi \cdot f \cdot n \cdot T_s + \phi] \qquad (14)$$

where :
$\phi = \pi / 2 + 2 \cdot \pi \cdot f \cdot T_s$ - phase angle chosen to maximize error for n = -1 ($V[n=-1] = V_{MAX}$)

Substituting (14) in eq. (12) we get : (15)

$$\varepsilon_{LEFT}[m+1/2] = 1/\pi \, V_{MAX} \, (-1)^m \sum_{n=-1}^{-\infty} \sin[2 \cdot \pi \cdot f \cdot n \cdot T_s + \phi] \frac{(-1)^{-n}}{(m+1/2) - n}$$

Computer calculations of error were performed using formula (15) for m=1000 (calculations of error in middle point between 1000 and 1001 sample in time window) . Results were as follows :

(16)

for $f = 0.250 \cdot f_s$: S(1)=3.18 E-04 $\cdot V_{MAX}$; S(10000)=1.45 E-04 $\cdot V_{MAX}$
for $f = 0.300 \cdot f_s$: S(1)=3.18 E-04 $\cdot V_{MAX}$; S(10000)=1.45 E-04 $\cdot V_{MAX}$
for $f = 0.350 \cdot f_s$: S(1)=3.18 E-04 $\cdot V_{MAX}$; S(10000)=1.45 E-04 $\cdot V_{MAX}$
for $f = 0.400 \cdot f_s$: S(1)=3.18 E-04 $\cdot V_{MAX}$; S(10000)=1.45 E-04 $\cdot V_{MAX}$
for $f = 0.450 \cdot f_s$: S(1)=3.18 E-04 $\cdot V_{MAX}$; S(10000)=1.48 E-04 $\cdot V_{MAX}$
for $f = 0.490 \cdot f_s$: S(1)=3.18 E-04 $\cdot V_{MAX}$; S(10000)=2.24 E-04 $\cdot V_{MAX}$
for $f = 0.499 \cdot f_s$: S(1)=3.18 E-04 $\cdot V_{MAX}$; S(10000)=7.23 E-03 $\cdot V_{MAX}$

where:
S(1) represents first term in eq.(15) (contribution from the V[-1])
S(10000) represents summation of first 10000 terms in eq. (15)

Results (16) show, that max. error is obtained when frequency f approaches the Nyquist frequency $f_s / 2$. The value of the error from the first term (V[-1]) is larger then from the sinusoidal wave as long as frequency f is smaller then about $0.490 \cdot f_s$ (which is 98 % of Nyquist frequency= $f_s / 2$). This seems reasonable since the input antialiasing filter would usually eliminate all frequencies above $0.46 \, f_s$ (see for example data for PCM or DAT recorders). The errors resulting from sinusoidal waves are similar to the error contribution from V[-1], therefore we expect that the recommendation given in (11) should be valid for any arbitrary sequence V[-1],V[-2],V[-3] .., since such sequence is a linear combination of pure tones according to the Fourier Theorem. However, further investigation and computer simulations are required to substantiate this claim.

Conclusions

In this paper we investigated the errors due to finite duration sampling of continuous signal and determined that this error can be considerable at the beginning and near the end of the sampling time window. These errors had a tendency to get larger at higher frequencies as they approach the Nyquist frequency ($f_s / 2$) for signal near the inside boundaries of the time window . At this time however, we don't know which physically realizable sequence of samples V[-1], V[-2], V[-3].....will produce the largest error inside of the time window. Further tests and computer simulations are required.

References :

[1] Nakajima et al., "The Sony Book of Digital Audio Technology", published by TAB Books Inc.,1983.
[2] Papoulis Athanasios, "Circuits and Systems, A Modern Approach", Holt, published by Rinehart and Winston Inc.,1980.
[3] Oppenheim Alan V., Schafer Ronald W., "Discrete-Time Signal Processing", published by Prentice Hall Inc., 1989.
[4] Jayant N. S., Noll Peter, "Digital Coding of Waveforms, Principles and Applications to Speech and Video", published by Pretice-Hall Inc., 1984.
[5] Jackson Leland B., "Digital Filters and Signal Processing", published by Kluwer Academic Publishers, 1989.
[6] Press William et al., "Numerical Recipes", published by Cambridge University Press, 1987.
[7] Weaver H. Joseph, "Applications of Discrete and Continuous Fourier Analysis", published by John Wiley & Sons, 1983.
[8] Marek Roland-Mieszkowski, "Introduction to Digital Recording Techniques", Proceedings from "Acoustic Week in Canada 1989" - CAA Conference,Halifax,N.S.,Canada,October 16-19,1989, 73-77.
[9] Robert Wannamaker, Stanley Lipshitz and John Vanderkooy, "Dithering to eliminate quantization distortion", Proceedings from "Acoustic Week in Canada 1989" - CAA Conference, Halifax, N.S., Canada, October 16-19, 1989, pp. 78-86.

DIGITAL GENERATION OF THE HIGH QUALITY PERIODIC AUDIO SIGNALS WITH THE AID OF A D/A CONVERTER AND COMPUTER

Marek Roland - Mieszkowski
School of Human Communication Disorders, Dalhousie University
5599 Fenwick Street, Halifax, Nova Scotia, B3H-1R2, Canada.

Very often in many areas of acoustics, sound engineering, psychology, psychoacoustics, audiology etc. there is a need for high quality sinusoidal, square wave, series of clicks and other types of periodic signals.

A computer - based digital function generator can generate any arbitrary type of signal in the frequency range from 0 Hz to 20,000 Hz, S/N = 95 dB and with no harmonic or intermodulation distortion (when based on 16 bit, 44.1 kHz D/A converter) . Frequency stability is determined by a quartz clock in the D/A converter which has an accuracy in the order of $1/10^6$.

Methods for sinusoidal signal synthesis

Generation of sinusoidal waves is of primary importance, since due to the Fourier theorem any periodic wave may be synthesized via additive synthesis of pure tones with appropriate amplitudes and phases. There are many alternative methods to digitally generate pure tones [1,2,3].

Very often real-time synthesis is accomplished on DSP (Digital Signal Processing) chips by using a sine function look-up table stored in the internal ROM (Read Only Memory) [2]. A limitation to this approach is the short length of the sine table (N).
In order to synthesize any arbitrary frequency using the look-up table method, one has to synthesize the values of the sine function using an interpolation process [2]. With linear interpolation between sine samples, this leads to S/N=64 dB for N=64, S/N=76 dB for N=128 and S/N=88 dB for N=256 due to the generation of THD by this algorithm [2]. Also this noise has an undesirable nature, since it is coherent with the generated signal (higher harmonics are generated) [5]. The only way to improve this situation is to use a longer look-up table, or by the filtering of generated signal in the analog or digital domain (which could jeopardize the real-time performance).

Synthesis of more complex signal in real time (combinations of several sinusoids with certain amplitudes and phases) could put too much performance demand on the computer's DSP chip or microprocessor.

RAM-based method for sinusoidal signal synthesis

Another way to generate sinusoidal signal is to generate audio file, which contains appropriate samples in RAM (Random Access Memory) or on the Hard or Optical Disk. Then reading of this file in real time to the D/A converter is performed to generate the desired audio signal [6]. However there is a limit on the duration of this signal due to memory consumption = 88,200 Bytes/sec (for 16 bit, 44.1 kHz D/A converter).

In many situations long durations of signal are required. In this case the most appropriate way to generate sine wave is to construct the audio file in RAM in such a way as to be able to read this file to the D/A converter over and over again (looping). To accomplish seamless (or click-less) looping through the file, the fundamental period of the sine wave must be:

$$T_0 = N\,T_s \quad \text{where: } T_s = 1/f_s \text{ - sampling interval}, \; N = 3,4,5,\ldots \text{etc- length of RAM buffer} \tag{1}$$

Fundamental frequency (first harmonic) generated in this case is :

$$f_0 = 1/T_0 = 1/(N\,T_s) \tag{2}$$

Higher harmonics of fundamental frequency can be also generated:

$$f_m = m \cdot f_0 = (m/N)\cdot f_s \quad \text{where: } m = 1,2,3,\ldots m_{MAX}, \; m_{MAX} = \text{INT}(N/2) \tag{3}$$

m- harmonic number (for fundamental m=1)

Formula for the n-th sample in the RAM buffer, to generate the fundamental or it's higher harmonic is given by:

$$A[n] = A_0 \sin[(2\cdot\pi\cdot m\cdot/N)\cdot n + \varphi_m] + \text{OFFSET} \tag{4}$$

where: A_0 - signal amplitude (represented by real number)
$\pi = 3.14....$
$n = 0,1,2...(N-1)$
φ_m - arbitrary phase (any real number)
OFFSET - number representing offset required by D/A converter (OFFSET=32,767.5 for 16 bit D/A converter)

Sequence of samples going to D/A converter during generation of the sine wave in real-time is as follows:

(5)

A[0], A[1],.....A[N-1], A[0], A[1],.....A[N-1], A[0], A[1],.....etc
first loop second loop third loop --- → time

Eq. (4) and (5) is the basic formula for generation of continuous sine wave.

Note 1: As can be seen from eq. (3) max frequency which could be generated is $f_m \le f_s/2$ (where $f_s/2$ is a Nyquist frequency determined by the sampling frequency f_s)

Note 2: Quantities in eq. (4) should be represented by numbers with adequate precision in order to obtain amplitudes A[n] which exceed the precision required by the D/A converter (for example 24 bit precision for 16 bit D/A converter). Rounding of the A[n] should be the last operation performed before storing them in RAM. Otherwise additional harmonic and nonharmonic (intermodulation) distortion will be generated due to the intermediate round-off errors.

Example: generation of frequencies 1Hz, 2Hz, 3Hz.....20,000Hz

Assume that we have a computer with a 16 bit, 44.1 kHz D/A converter (CD-quality). If we take a RAM buffer size of N=44,100 (88,200 Bytes); then from formula (3) we can see that the available frequencies are:

$$f_m = m \;\; [\text{Hz}] \;\Rightarrow\; f_1 = 1 \text{ Hz}, \; f_2 = 2 \text{ Hz}, \; f_3 = 3 \text{ Hz}, \; \ldots\ldots\ldots\ldots, \; f_{20{,}000} = 20{,}000 \text{ Hz} \tag{6}$$

Note 1: Precision of these frequencies is determined only by the precision of the D/A converter's clock which is in the order of $1/10^6$, and in the case of a 1000 Hz tone this leads to an expected error in the order of ± 0.001 Hz.

Note 2: With RAM buffer size N=441,000 (882,000 Bytes), one can generate all frequencies from 0.1 Hz to 20,000 Hz with 0.1 Hz resolution.

Note 3: Other choices of N and m parameters in eq. (3) will give desired combinations in most practical applications.

Note 4: Generated files with desired frequencies could be stored on the Hard or Optical disk and recovered into RAM prior to generation of sine tone.

This algorithm was the basis for a successful implementation on the AMIGA Computer [6], and is being implemented on the NeXT Computer [7].

Improving Generator through the use of Digital Dither

The only harmonic and intermodulation distortion generated by the above described algorithm is associated with round-off error of final amplitudes A[n] before storing them in RAM (in order to generate integer numbers used by D/A converter - from 0 to 65,535 for 16 bit D/A). However as mentioned previously, due to the signal correlated nature of noise, higher harmonics and intermodulation products with the sampling frequency are generated [4,5].
Elimination of the harmonic and nonharmonic (intermodulation) distortion (which are imposed by the resolution of the D/A converter) may be accomplished by using Digital Dither, with a small white noise penalty (3 dB- for uniform-pdf dither) [5,8], resulting in S/N=95 dB for 16 bit dithered digital generator (theoretical S/N=98.2 dB for undithered 16 bit digital system).
This could be done by adding dither to each amplitude before rounding the number and sending it to the D/A converter:

(7)

$A_D[n] = A[n] + D[n]$ where: A[n] - initial amplitude of sine wave before final rounding
$A_D[n]$- final amplitude of sine wave after adding dither
D[n] - dither amplitude

An example of optimal dither in this case is a sequence of random numbers in the range [-0.5; 0.5] with uniform pdf (probability density function). For other types of dither please see ref. [5,8,9,10].

Generation of Random Digital Dither:
On some hardware, dither words D[n] can be generated in real time. In this case unrounded amplitude A[n] is retrieved from RAM, added to real-time synthesized dither D[n], then rounded and send to the D/A converter. This is the preferable way to use Digital Dither.

Generation of Pseudo-Random Digital Dither:
In the case when the hardware can't generate dither words D[n] in real-time, one can use a random sequence D[n] of the same length as A[n], add them according to eq.(9), and store the rounded value of $A_D[n]$ in RAM for use by the D/A converter. This is not as an effective method as using random digital dither, but for a long enough RAM buffer (value of N), it can decrease the level of harmonic and nonharmonic (intermodulation) distortion [7].

Synthesis of more complex periodic Waveforms

According to the Fourier theorem any bandlimited, periodic function with fundamental period $T_0 = N \cdot T_s$,can be expressed in the form:

$$A_T[n] = \sum_{m=1}^{m_{MAX}} A_m[n] = \sum_{m=1}^{m_{MAX}} A_m \sin [(2 \cdot \pi \cdot m / N)\, n + \varphi_m] + OFFSET \quad (8)$$

where: A_m - amplitude of the m-th component
φ_m - phase for the m-th component
A_T - total amplitude of a synthesized signal

● Formula (8) can be used to synthesize many different types of bandlimited and periodic waveforms. For example: combinations of sinusoidal signals, triangular wave, square wave, series of clicks, frequency modulated signal, amplitude modulated signal etc. However, the period of modulation function is restricted to available periods $T_m = 1/f_m$, given by eq. (3). Also none of the components in eq.(8) can exceed Nyquist frequency = $f_s/2$.
● Synthesis of any arbitrary bandlimited and periodic function can also be accomplished by using any arbitrary sequence of amplitudes A[0], A[1], A[2],.....A[N]. There is $N \cdot 2^n$ of such waveforms for a n-bit D/A converter and N-samples long RAM buffer. For example, pseudo-random noise can be generated in this fashion (pseudo-random due to periodicity).
● Yet another way of synthesis is to take any periodic function (with period $T_0 = N \cdot T_s$) in analytic form A= A(t) and do digital sampling (sampling in the digital domain) according to the formula:

$$A[n] = A(t_n = n \cdot T_s) \quad (9)$$

However in this case one must be certain that the function A= A(t) is bandlimited, otherwise aliasing distortion will occur [4]. If the function A= A(t) is not bandlimited, digital filtering should be performed prior to applying formula (9) in order to eliminate all frequencies above Nyquist frequency = $f_s/2$

Generating stereo signals

The procedures outlined above may be applied for synthesis of multichannel periodic and bandlimited waveforms (for hardware with multiple D/A converters). For example, for stereo (2 channel) synthesis, one can generate different or similar waveforms in each channel by using formula (4) and (8). Phase relationship between waveforms will be maintained during playback. Since phases (φ_m) in formula (4) and (8) are arbitrary real numbers, arbitrary phase shifts between waveforms can be obtained. This could be important for some audiological and psychoacoustic tests [6,11,12].

Conclusions

The most precise digital-domain method for the generation of arbitrary periodic audio signals was presented. Advantages of this method are: highest available precision with a given D/A converter, and low requirement on the speed of hardware and software, because synthesis of waveform is not performed in real-time. Hardware and software only have to be capable of doing real-time looping through sound file generated in the RAM buffer. Details of the waveform synthesis should be sufficient for easy implementation of this algorithm on different computer platforms.

References:

[1] Leland B. Jackson, "Digital Filters and Signal Processing", Second Edition, Kluwer Academic Publishers, Boston, Dordrecht, London, 1989.

[2] Andreas Chrysafis, "Digital Sine-Wave Synthesis Using the DSP 56001", MOTOROLA Inc., Brochure No. APR1/D REV1, 1988.

[3] Waldemar Kucharski, Andrzej Czyzewski, "Implementation of Basic Methods of Sound Synthesis for IBM-PC compatibles", Proceedings of Thirty Seventh Open Seminar on Acoustics, Technical University of Gdansk, September 10-14, 1990, pp. 225-228.

[4] Marek Roland-Mieszkowski, "Introduction to Digital Recording Techniques", Proceedings from "Acoustic Week in Canada 1989" - CAA Conference, Halifax, N.S., Canada, October 16-19, 1989, pp. 73-77.

[5] Robert Wannamaker, Stanley Lipshitz and John Vanderkooy, "Dithering to eliminate quantization distortion", Proceedings from "Acoustic Week in Canada 1989" - CAA Conference, Halifax, N.S., Canada, October 16-19,1989, pp.78-86.

[6] Annabel J. Cohen and Marek Mieszkowski, "Frequency synthesis with the Commodore Amiga for research on perception and memory of pitch", Behavior Research Methods, Instruments, & Computers, 1989, 21 (6), pp. 623-626.

[7] Marek Roland-Mieszkowski, "Digital Generation of the High Quality Periodic Audio Signals with the NeXT Computer", to be published.

[8] John Vanderkooy, Stanley P. Lipshitz, "Digital Dither: Signal Processing with Resolution far below the Least Significant Bit", AES 7th International Conference,Toronto, Ontario, Canada, May 14-17, 1989, paper No. 4.E.

[9] Stanley P. Lipshitz and John Vanderkooy, "The principles of Digital Audio: a Lecture Demonstration", AES 7th International Conference, Toronto, Ontario, Canada, May 14-17, 1989, paper No. 2.B.

[10] S.P. Lipshitz and J. Vanderkooy, "Digital Dither", presented at the 81st Convention of AES, JAES (Abstracts), Vol. 34, p.1030 (1986 Dec), Reprint No. 2412.

[11] John D. Durrant and Jean H. Lovrinic, "Bases of Hearing Science", Second Edition, Williams & Wilkins, Baltimore/ London, 1984.

[12] Brian C. J. Moore, "An Introduction to the Psychology of Hearing", Second Edition, Academic Press Inc., New York, 1982.

ROCK-DRILL HANDLE VIBRATION: MEASUREMENT AND HAZARD ASSESSMENT

S.E. Keith[1, 2] and A.J. Brammer[1]
[1]Institute for Microstructural Sciences, National Research Council, Montreal Road, Ottawa, Ont. K1A 0R6
[2]Department of Mechanical and Aerospace Engineering, Carleton University, Ottawa, Ont. K1S 5B6

Introduction

Despite progress in predicting the risk of developing vibration-induced white fingers (VWF) from exposure to the vibration of power tools, the relative hazard posed by different vibration amplitudes and frequencies remains a subject of debate.[1, 2] The present international standard, ISO 5349 (1986),[3] requires the exposure "intensity" to be derived from orthogonal, component, rms accelerations measured in directions related to the orientation of the third metacarpal, in the frequency range from 5.6 to 1400 Hz. It has been suggested that inaccuracies resulting from application of the ISO procedure are associated with: a) employing a frequency weighting that progressively reduces the contribution to the overall hazard from accelerations at increasing frequencies; b) restricting the frequency range of measurements to an upper limit of 1400 Hz; c) the crest factor of the acceleration waveform; or d) a combination of these factors.

The purpose of this paper is to characterize the handle vibration of a pneumatically-powered jack-leg rock drill commonly used in Canadian mines, and to record its vibration at frequencies above 1400 Hz. The potential health hazard posed by different vibration frequencies may then be explored, by reference to data from medical studies and other types of power tools.

A detailed report of this work will be published elsewhere.

1. Apparatus and Measurements

Three miniature accelerometers (Brüel & Kjær, type 4393), were attached to 10 g weights, and then mounted on a mechanical filter (Brüel & Kjær, type UA 0559). The mechanical filters were, in turn, mounted orthogonally on a prepared steel block welded to the drill handle. By careful positioning of the block, an accelerometer was oriented to record the vibration of the drill along its percussion axis (referred to as "front to rear," or F-R). When drilling horizontally, the handle acceleration was also recorded in the vertical and horizontal directions. The orientation error was less than 15°.

The three vibration components were recorded simultaneously on an FM tape recorder (Brüel & Kjær, type 7006). The frequency limits for the channel recording the F-R acceleration were from 2 Hz to either 1.3 or 10 kHz (± 1 dB). The corresponding frequency limits for the other two channels were 1 Hz, and either 1.6 or 7 kHz.

A retired miner (height 1.70 m, weight 68 kg), drilled horizontal holes (which had been pre-drilled to a depth of ≅ 15 cm) in a near-vertical, exposed rock face of marginally weathered but competent granite. The drill was operated at full throttle, and the penetration time for each 1.2 m of drilling was noted. Some holes were drilled by a second, experienced driller (height 1.83 m, weight 102 kg), to establish whether individual differences in drilling technique influenced the vibration recorded at the drill handles. The effect of hand grip on handle vibration was also explored.

The acceleration waveforms and spectra were monitored during all measurements (Brüel & Kjær, type 2515), to ensure that large-amplitude impacts did not overload the transducers.[4] The apparatus was calibrated both before and after measurements by a portable vibration calibrator (Brüel & Kjær, type 4291). In addition, electronic calibration signals were recorded on each tape. With these precautions, the systematic error of these measurements is believed to be less than 5 %.

The recorded signals were analyzed in the laboratory to yield one-third octave bands (complying with IEC 225-1966 and ANSI S1.11-1966, Class III), by means of a real-time spectrum analyzer. Linear (time) averaging of each signal was performed for 32 s, to accommodate fluctuations in vibration amplitude. Unexplained variations in drill operation that resulted in changes to the percussion frequency of greater than ± 12 % have been excluded from the data analysis.

2. Results

The root mean square one-third octave-band, F-R component acceleration spectrum recorded when drilling with a 1.2 m length drill rod, and the air pressure set to a typical value found within a mine (5.5×10^5 Pa), is shown in figure 1 (expressed in dB re 10^{-6} $m \cdot s^{-2}$). While accelerations of similar magnitude were observed in orthogonal directions at frequencies below 31.5 Hz, it was found that at this, and higher frequencies, the F-R component dominated the handle vibration. Values of the component accelerations frequency-weighted according to the provisions of ISO 5349 (1986) are listed in Table 1, and clearly demonstrate that the F-R component possesses the largest magnitude. The relative magnitudes of the frequency-unweighted acceleration levels, also given in Table 1, suggest this ranking of the handle acceleration components is unlikely to change with hazard weighting schemes that give more emphasis to contributions from higher frequencies.

The spectrum in figure 1 has been constructed from two measurements: one including the complete frequency range, and the other, the range from 5.6 to 1400 Hz. The second measurement was required to detect vibration at low signal levels, which was otherwise lost in tape-recorder noise. Repeated measurement of the F-R component acceleration in this restricted frequency range permitted an estimate of the variation in handle acceleration during normal drilling operations. Below 1400 Hz, values for plus and minus two standard deviations are shown by the dashed lines in the diagram, and are derived from 16 data samples.

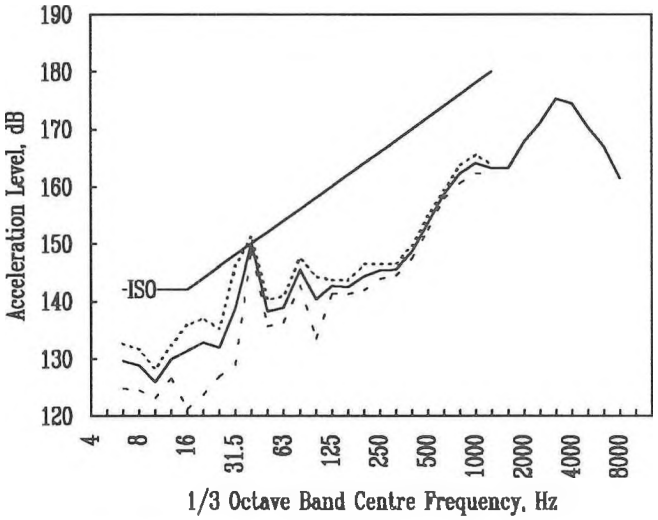

Figure 1: RMS Front to Rear Component Handle Acceleration Level (dB re 10^{-6} m·s^{-2}), using 1.2 m Drill Rod. Also shown are: ± 2 standard deviations (- - -), and ISO weighting.

The F-R component handle acceleration tended to increase at the percussion frequency (≅ 40 Hz) when drilling with a new or re-sharpened bit, and at frequencies between 100 and 400 Hz when drilling with a longer (≅ 2.4 m) drill rod. However, all changes in operating conditions, and operators, led to insignificant variations in handle vibration at frequencies above 400 Hz.

3. Discussion and Conclusions

The insensitivity of handle vibration to changes in drill operating conditions, and driller, at frequencies above 400 Hz, together with the small standard deviations recorded at these frequencies, suggest that the spectrum shown will provide a reasonable first estimate of the dominant acceleration component at all frequencies. Inspection of this diagram reveals the presence of a large acceleration peak at frequencies between 3 and 4 kHz, which is not recorded if handle vibration is measured following the procedure established in the international standard.[1]

Two recent studies of miners in Canada have found that the rate of development of VWF is slower than would be predicted from rock drill handle vibration, when the hazard associated with different frequencies is weighted according to the ISO standard (curve labelled ISO).[5,6] In contrast, the development of VWF in forest workers operating gasoline-powered chain saws with vibration-isolated handles is predicted by the ISO procedure.[7] The handle vibration of such saws is known to decrease with increasing frequency, at frequencies above that corresponding to the engine firing (≅ 150 Hz), which determines the frequency-weighted acceleration. Measurements on the handles of a typical 3 kW saw when cross-cutting wood have recorded unweighted one-third octave-band acceleration levels of 140 dB, or less, at band centre frequencies above 315 Hz.[8] In consequence, the hazard associated with operating jack-leg rock drills relative to that associated with operating chain saws, which is presently overestimated by the ISO procedure,[3] will be additionally overestimated by employing frequency-unweighted accelerations.

Table 1: Mean, RMS Component Frequency - Weighted and Frequency - Unweighted Acceleration Levels (dB re 10^{-6} m·s^{-2})

	Front to Rear	Side to Side	Up and Down
ISO Weighting (5.6 - 1400 Hz)	144.9	141.2	139.3
Unweighted (5.6 - 1400 Hz)	169.4	168.9	164.9
Unweighted (5.6 - 5600 Hz)	180.1	-	-

Furthermore, because of the different spectrum shapes, this overestimate will be increased by increasing the maximum vibration frequency included in the assessment of hazard.

Acknowledgements

This work was performed under contract to Boart Canada. The authors are grateful to the sponsors for permission to publish this paper.

References

1. "Criteria for a Recommended Standard: Occupational Exposure of the Hand to Vibration," DHHS (NIOSH) publication 89-106 (U.S. Dept of Health & Human Welfare, Cincinnati 1989).

2. P.L. Pelmear, D. Leong, W. Taylor, M. Nagalingam and D. Fung, "Measurement of vibration of hand-held tools: Weighted or unweighted," J Occup Med 31, 902-908 (1989).

3. "Mechanical Vibration - Guidelines for the Measurement and the Assessment of Human Exposure to Hand-Transmitted Vibration," International Organization for Standardization, Geneva, ISO 5349 (1986).

4. D.E. O'Connor and B. Linquist, "Method for measuring the vibration of impact tools," in Vibration Effects on the Hand and Arm in Industry, A.J. Brammer and W. Taylor (Wiley Interscience, New York 1982), pp. 97-101.

5. R.L. Brubaker, C.L.G. Mackenzie, S.G. Hutton, "Vibration-induced white finger among selected underground rock drillers in British Columbia," Scand J Work Environ Health 12, 296-300 (1986).

6. P.L. Pelmear, D. Leong, I. Taraschuk, and L. Wong, "Hand-arm vibration syndrome in foundrymen and hard rock miners," J Low Freq Noise & Vib 5, 26-43 (1986).

7. M. Bovenzi, A. Zadini and A. Franzinelli, "Vibration-induced vascular disorders in Italian forestry workers," 23rd Int Congress on Occup Health, Montreal (September 1990), Abstracts p. 87.

8. S.E. Keith and A.J. Brammer, "Current research on chain-saw noise," Pulp & Paper Canada 87, T153-T156 (1986).

Subsynchronous Vibration of an Auxiliary Turbine

B. Alavi and C. Hugh

Ontario Hydro
700 University Avenue
Toronto, Ontario M5G 1X6

Introduction and Background

This paper discusses an auxiliary turbine subsynchronous vibration problem which extended over several years at one of Ontario Hydro's thermal generating station.

The auxiliary turbine is a multi-stage condensing steam type and is used to drive a boiler feed pump via a flexible gear coupling. The turbine rotor is supported by and located in the frame assembly by two cylindrical sleeve bearings, one in the low pressure (L.P.) bearing bracket attached to the frame assembly, and one in the high pressure (H.P.) bearing bracket located in the front standard (Figure 1). Normal operating speed of the unit is at 4250 rpm, and the turbine can run either on main steam or extraction steam.

Since 1984, the auxiliary turbine and the feed pump suffered random subsynchronous vibration problem at high loads, and at speeds approaching normal running speed. The predominant component of these vibrations is "locked in" at 1/2*rpm and the overall vibration levels of up to 150 microns (Pk-Pk) to 200 microns (Pk-Pk) have been observed at H.P. and L.P. bearing pedestals (Figure 2).

In the past, The plant operators were able to reduce the subsynchronous vibration amplitude by dis-engaging and re-engaging the gear coupling. This method appeared to be too inconsistent and the station finally decided to carry out full investigations to resolve the problem. It is important to note that when the subsynchronous vibration was suppressed, the vibration response exhibited peaks at operating speed frequency and its harmonics. In this case, the subsynchronous frequency was present but at much lower amplitude and the operator could run the unit at full load.

During this period, many problems were identified and subsequently rectified, however, the vibration problem still existed. Among those, the most noticeable discoveries were:
Loose interstage diaphragms causing the packing seals to lift and contact the rotor; Boiler Feed Pump/Turbine concrete base was cracked about 4 inches below the top of concrete around the sole plate; Mis-matched gear components; Crack formation on the collar of the flexible gear coupling (near the turbine end); Turbine front standard axial keys were dry and appeared out of position to each other.

Measurements

Detailed noise and vibration measurements were carried out for this unit. In each case, the vibration measurements were taken at the L.P., H.P. and the pump inboard and outboard bearing pedestals. Filtered noise measurements were also taken simultaneously at a distance of 10 inches from the pump and turbine casings at discrete locations extending from the pump inboard bearing to the turbine H.P. bearing (see table 1). Figures 3 and 4 represent a typical noise measurements taken by a real time analyzer. It was noticed in all our measurements that a distinct tone was detectable around the unit at one and two times the rpm when the unit was operating at full load. The noise radiated due to 1*rpm appeared to have maximum amplitude close to the south side of the coupling and the noise radiated at 2*rpm had a maximum level in the close proximity of the third and fourth stage turbine.

Vibration measurements revealed that when the unit was exhibiting the subsynchronous vibration problem, the axial pump inboard and outboard vibration amplitudes were generally low. However, in the case where the subsynchronous vibration was suppressed, the measured pump inboard and outboard axial vibration were excessive with the phase difference of approximately 180 degrees.

Additional phase measurements carried out at full load for the unit using hand held "shaft sticks" or pedestal measurements were not conclusive in identifying the direction of the whirl (either backward or forward precession).

Possible Excitation Phenomena

The subsynchronous vibration problem experienced on auxiliary turbine was generated by one, or more, of the following mechanisms: 1) Hydrodynamic fluid film bearing (Oil Whip); 2) Excessive clearances in the bearings; 3) Incorrect pinch on the bearings; 4) poor bearing foundation tie-down; 5) Defective coupling; 6) Stuck HP front standard axial key; 7) Sub-harmonic whirl instability induced by non-linearity (Mathieu-Hill-Meissner); 8) Aerodynamic induced whirl.

Discussions

The noise and vibration measurements confirmed the existence of coupling unbalance. This occurred due to the mis-match of gear components causing gear mesh position error. In addition, the non-uniform nature of axial vibration and its high magnitude also supported the existence of rotor misalignment. The high noise level detected at close proximity to the turbine casing also indicated the possible misalignment of the pump-turbine rotor.

The subsynchronous vibration was generated above the first critical speed (2600 rpm) and the onset of its formation was too sudden. As the rotor was brought up to speed, we saw no evidence of subsynchronous peak. Only when the shaft speed was near 3900 rpm did this subsynchronous peak occurred. As well, we found no evidence (based on the critical speed data) to support that the critical speed of the system was reduced significantly

rotor speed approached 3900 rpm. therefore, it was assumed that the oil whip was not the cause of this instability.

The concept of support stiffness asymmetry was reviewed after the report of pump pedestal cracking (see above). For this phenomenon to occur, at least two distinctly different critical speeds should have been present reflecting the different stiffness in two different directions. Such a response was not observed and consequently this argument was not supported as the cause of this instability.

The sharp increase in the half frequency component could have also been generated due to aerodynamic steam forces. This was however not supported due to the fact that the subsynchronous vibration was phase-locked and as well the frequency was exactly at 1/2 of the running speed.

Based on our analyses, we concluded that the auxiliary turbine was suffering from two types of instabilities. The first type was the subsynchronous vibration and was generated as a result of "Free Mathieu Effect" and the second type was generated as a result of "Gyroscopic Induced Whirl". The two types of whirl had similar responses in many aspects. The factors that influenced the type of instability were the change of radial load created by turbine-pump rotor alignment and the initial degree of rotor misalignment. The subsynchronous vibration was caused by non-linearity effects. In this case the rotor was displaced sufficiently to hit the stationary parts. This generated a sufficient energy for the rotor to sustain its continuous motion. The rotor displacement was as a result of: a) dynamic shaft bending; b) excessive misalignment of turbine-pump rotor; c) inadequate bearing stiffness.

Second type of vibration normally occurred after the unit has been shut down and re-started and the coupling has been dis-engaged and re-engaged. Because the gear coupling comprised unmatched gear components and the turbine-pump rotor had some misalignment, it was quite possible depending on the relative radial positions of the coupling gears upon re-engagement, the required coupling flexibility might not work. In the event of a locked engagement, an additional radial load was generated which was added to the bearing stiffnesses. In this case, the rotor was constrained to be bowed and the Gyroscopic effect would result in an instability. In this mode, light internal rub did take place and many resonances were excited.

To alleviate the vibration problem, an appropriate course of actions were recommended to the station which will be highlighted during this presentation.

Acknowledgement

The authors wish to thank Tony Florian of Central Production Services of Ontario Hydro for his contributions.

References

1. **Muszynska, A., Franklin, W.D., Hayashida, R.D. "** Rotor-to-Stator Partial Rubbing and its Effect on Rotor Dynamic response", 6th Workshop on Rotordynamic Instability, Texas A&M University, Texas, May 1990.

2. **Allaire, P.E., Lee, C.C. "Vibrations of Rotating Machinery Undergoing Rubs", ROMAC Annual Meeting, June 1987.**

North is perpendicul
to the pap

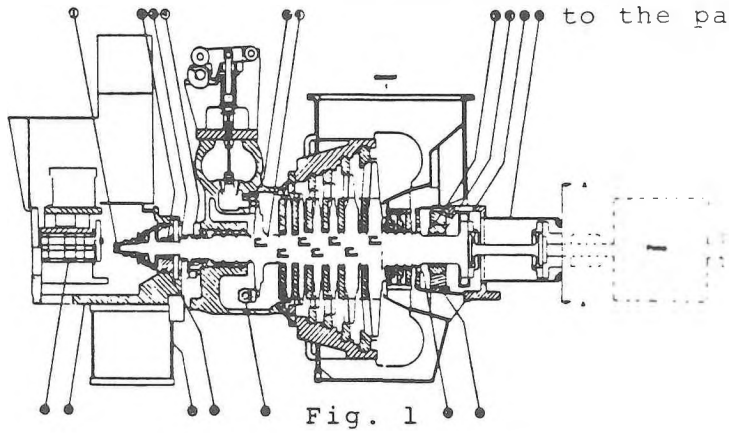

Fig. 1

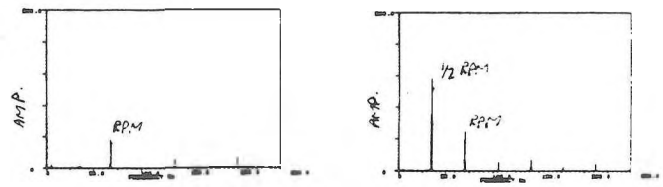

Fig. 2

Position	Approximate Location of Measurement
A	Pump Inboard Bearing
B	Coupling
C	LP Bearing (Perpendicular to Axis of Rotation)
D	LP Bearing (Parallel to Axis of Rotation)
E	Turbine Casing (Close to Coupling)
F	Turbine 7th Stage
G	Turbine 6th Stage
H	Turbine 5th Stage
I	Turbine 4th Stage
J	Turbine 3rd Stage
K	Turbine 2nd Stage
L	Turbine 1st Stage
M	HP Bearing

TABLE 1

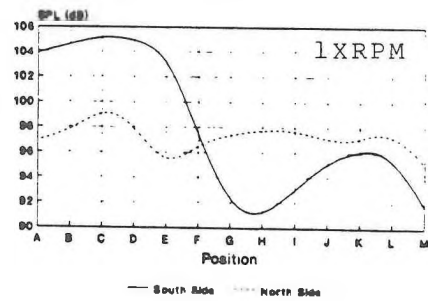

Fig. 3

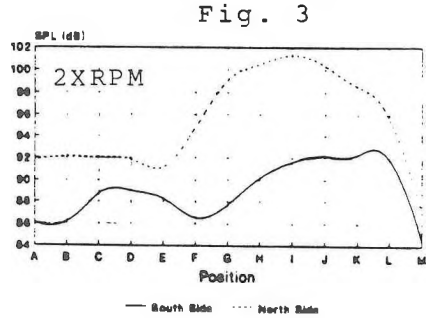

Fig. 4

DEVELOPMENT OF DIESEL GENERATOR ISOLATION SYSTEMS FOR LOW NOISE AND VIBRATION

Greg E. Clunis, P.Eng.
907 Admiral Avenue,
Ottawa, Ontario
K1Z 6L6

Scott J. Bradley, P.Eng.
Senior Engineer Product Support
Boeing Canada Technology Limited
Arnprior Ontario
K7S 3M1

Overview

This paper presents an outline of the engineering design process applied to the development of noise and vibration isolation systems for a 60 kW diesel generator. Two of these DGs are fitted in each of four 35 metre research vessels, currently being procured by the Department of National Defence. The main role for these vessels is sound range support, and thus the greatest emphasis is on low underwater noise levels. Specific issues which are discussed include the specification requirements and process, design requirements, and obstacles to the design process which needed to be overcome. Particular emphasis is placed on the responsibilities and required contributions of the various participants. An outline is provided of the final design details including a discussion of the concept designs which were explored and discounted, finite element assessment, design of all fluid and other flexible connections, design of the acoustic enclosure, and requirements for shipboard interfaces including structure. In conclusion, a discussion of the trials and evaluation process is presented.

Design Objectives

As the primary role for the vessels for which these modules have been designed is underwater noise research and measurements, low underwater noise levels from ship's machinery are critical. The vessel will normally be moored during measurement intervals, and therefore it is only necessary that the auxiliary machinery be isolated to the highest degree. The major items are two 60 kW diesel generators, which provide power for auxiliary systems, and a plethora of scientific instrumentation fitted to the vessels. The DND specified underwater noise levels as a curve of octave band levels not to be exceeded. Further guidance was provided to the builder by the specification of vibration levels at the foundation top, which the DND believed that if met would ensure compliance with the underwater noise level requirements.

The DND had identified that double mounting of the DG would be required using a suitable intermediate raft, with the entire unit enclosed by an acoustic enclosure.

Contractual Considerations

This section will present an overview of the complex contractual arrangements under which this project proceeded. Prime contractor responsibility was awarded to West Coast Manly Shipyard (WCM), of Vancouver, British Columbia, the builder for the vessels. The prime contract specified that WCM must direct the subcontract for design of the DG isolation systems to one of the two agencies which the DND considered to be qualified and experienced for the task, namely BBN or YARD. This requirement was cascaded to the supplier of the diesel generators, Cullen Detroit Diesel/Allison Ltd. of Surrey, B.C., which in turn contracted with YARD Inc. of Ottawa to do the design work. WCM engaged the services of Barron Kennedy Lyzun and Associates Ltd. of Vancouver to monitor and direct all noise and vibration aspects of the vessel design, construction and trials.

It is important to reflect upon these arrangements for a moment and appreciate how important it is that all appropriate contractual requirements are suitably shared by the players. The requirements for underwater noise levels and foundation top vibration levels were passed to YARD, which retained the right to inspect the build, however there were no weight restrictions placed upon YARD's design.

It was agreed between YARD and Cullen that provision of a suitable DG with free vibration levels within specified limits remained the responsibility of Cullen. It was also agreed that Cullen would furnish mounting points for the upper stage mounts at the required locations. WCM supplied compartment arrangement, ship's structure, and ship's services drawings.

The Design

The engine selected by Cullen was the GM 4-60. This is a four cylinder engine, displacing 60 cubic inches per cylinder. The engine is available in both naturally aspirated and turbo charged configurations. For this application only the lowest power rating was required, specifically naturally aspirated with the smallest injector size available. As is typical for many units of this type, the engine was designed for hard mounting to a substantial baseplate, in turn further hard mounted to a concrete slab. Cullen's first attempt at a baseplate utilized an existing design which had given good results previously, but only for hard mount applications. This design was provided to YARD for review. When this baseplate was supported on springs for test, vibration levels were extreme however. Subsequent analysis indicated considerable resonance, and this design had to be discarded.

It then became necessary to explore alternative methods to provide the required mounting point structure from the engine to the upper stage mounts. The preferred design was based on six upper stage mounts, which necessitated that attachment points be identified at the engine front, rear, and under the generator. Symmetry about the centre of gravity was essential, and a wide enough footprint laterally to maintain stability in a seaway. While the engine rear provided good attachment points, both the generator and engine front were rather more complicated, due to complexity of plumbing and other features at the engine front and the lightweight nature of the generator feet. The final design utilized a one inch thick slab under the generator with rails for the mounts, and a complicated bracket at the engine front. This allowed the entire DG assembly to flex relatively unconstrained about its midpoint.

With suitably low vibration levels demonstrated at the Cullen test bed it was now required to design the intermediate raft, acoustic enclosure, and all flexible connection arrangements which must also be two stage.

It was decided to utilize the same mount for both the upper and lower stages, six for the upper as was noted above, and ten for the lower stage which accommodated the extra mass of the raft and enclosure. Mount loading in excess of 80% capacity was achieved for all mounts. The selected mount was the 6A6/900lb from CFTO

D03-003-021/SG-005, the DND's standard for noise, shock and vibration isolation hardware. Figure 1 provides a schematic of the final arrangement.

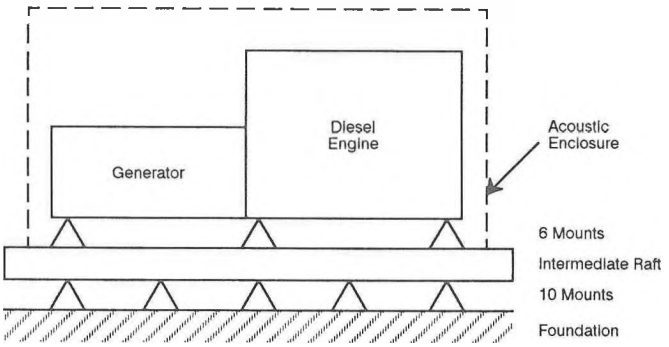

Figure 1: Schematic of Final Arrangement

A concept design for the raft was developed, based upon a solid slab as the main top plate, with longitudinal vertical and horizontal plates to provide lower stage mount attachment points. The structure was stiffened by transverse "T" sections. Once completed to a degree suitable for FE analysis, the design was checked for coincident resonances between engine forcing frequencies, mounting system natural frequencies, and raft structural natural frequencies. A few modifications to the raft design were subsequently implemented. This analysis required that masses, CG's, and moments of inertia be known or estimated for all components.

Flexible connection arrangements were then conceived for all non-structural interfaces including: diesel fuel (in and out); cooling water; exhaust; supply/ventilation air (enclosure only); and all electrical connections. As with the mounts, the fluid connections were selected from the CFTO. Adequate length was necessary to accept the imposed seaway motions, and provide the required degree of isolation. The cooling hoses were designed using an "L" configuration. Dynamic stiffness data on the hoses was compared to that known for the mounts, to confirm that the hoses would not compromise the isolation provided by the mounts. The exhaust connections were particularly challenging due to the larger diameter, stiffer metal hoses required, and the fact that the attachment to the middle stage of the mounting system needed to be achieved at the enclosure top.

To complete the mounting system design YARD was required to assess the ship's structure for suitability for attachment, and propose a foundation design. As the vessel is constructed of 7mm plate, this was not an inconsiderable challenge. The final foundation design utilizes 4*8 inch steel angle, suitably stiffened and gusseted to the ship's structure. This provided a low, squat arrangement, and good dispersion of the point loadings of the mounts out into the lightweight plating. This structure was analyzed by FE as well, the analysis revealing that the areas of plating forming the ship's structure had a tendency to be exited, at a variety of frequencies. Stiffening was proposed to raise these resonances above the range of concern.

The acoustic enclosure was required to provide easy disassembly for maintenance access, and a door with window for local gauge inspection. As was noted above, it was also necessary to provide adequate stiffness at the location at the enclosure top where the exhaust flexible was attached. Calculations showed that more than adequate noise isolation was provided.

Tests And Trials

A comprehensive series of measurements conducted at strategic milestones was necessary to support this design activity. As was noted above, this commenced with Cullen obtaining suitably low vibration levels on a baseplate system supported above resilient mounts. This activity included repeated testing on the original failed baseplate design, and subsequent retest with the final baseplate pieces.

Following this initial testing, the design of the module was completed. Each of the following seven DG sets was also tested to confirm consistency with the vibration levels recorded for the first.

The first complete module constructed, including raft and acoustic enclosure, was tested at the Cullen works, utilizing a dummy foundation attached to the concrete floor of the test bed. While not a true representation of the foundation conditions on board the vessel, the design activity had required/presumed a neutral foundation without significant resonances. Vibration levels were measured on the DG set baseplate above the upper stage mounts, and on the intermediate raft below the upper stage mounts and above the lower stage mounts. See figure 2 for the results. These measurements confirmed that the upper stage of the mounting system was performing as expected, and that no raft amplification resonances existed. Airborne noise measurements around the enclosure confirmed the performance of that aspect. These tests were conducted by Boeing Canada, and witnessed by the DND and the noise and vibration consultant to WCM.

Two of the completed modules were then installed in the first of class vessel. Near-field hydrophone measurements indicated satisfactory underwater noise levels which were later confirmed by sound ranging. The follow on three vessels have since been delivered with similar success.

Summary

It is hoped that this paper has provided an insight into the design process and interrelationships necessary to achieve successful isolation of machinery fitted to a research vessel. Effective cooperation and continued dialogue between the various contributors were essential to the satisfactory completion of this project.

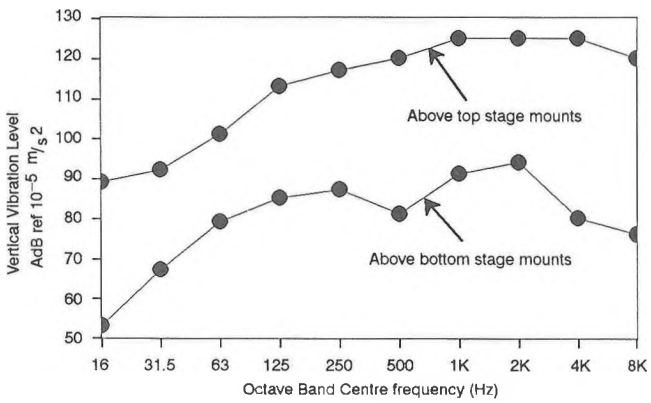

Figure 2: Measured Results, Top Stage

Acknowledgements

The authors wish to express their appreciation for the contributions made to this paper and project by the Department of National Defence, West Coast Manly Shipyard, Cullen Detroit Diesel/Allison Ltd., Barron Kennedy Lyzun and Associates Ltd., YARD Inc. and Boeing Technology Canada Ltd.

Design Optimization of High Speed Axially Loaded Ball Bearings of a Turbo-pump

Behzad Alavi

Ontario Hydro
700 University Avenue
Toronto, Ontario M5G 1X6

Introduction

In the turbo-pump design, the bearings are required to operate at high speed under large misalignment. The misalignment imposed on the bearings is generated by a combination of: 1) Rotor flexibility; 2) Changes in bearing support stiffness due to changes in temperature and vacuum; 3) Geometric tolerance build-up; 4) Unbalance magnetic pull.

This Turbo-pump has a design similar to a multi-stage axial flow compressor and is used to create ultra-high vacuum environment. It consists of a single flexible rotor supported on two precision grease lubricated angular contact ball bearings, and rotates at 52,000 RPM using a three phase induction motor. The bearings are axially preloaded to prevent gross sliding motion, i.e., skidding, between the balls and the raceways. The bearings are supported by rings made of elastomer (inserted between the bearing outer race and the main housing) in order to protect the bearings against lateral vibrations caused by unbalance (during both normal running condition and final stage of balancing).

Frequent failure of one of the bearings was encountered during the development phase of this pump. In all cases, detailed surface analysis revealed that the bearings suffered from excessive friction and heat generation which consequently resulted in a cage failure.

Measurements

Vibration measurements carried out on this pump are presented in figure 1 and 2. Figure 1 shows a typical vibration measurement up to 2.0 KHz frequency range. The existence of spectral peaks at cage frequency, shaft operating speed and its first harmonic are quite apparent. In all our measurements, the amplitude of vibration at cage frequency for one of the bearing was excessive which suggested that the bearing cage was under severe stress. This information was also supported when further measurements were carried out at a higher frequency range (Figure 2).

Attempts undertaken to reduce the cage stresses by re-designing the support flexibility and reducing the geometric tolerances were unsuccessful and a decision was made to look for an alternative bearing design.

Alternative Bearing Design

The bearing selected as a replacement was physically very similar, however, the number of balls, the ball diameter and the raceway curvatures differed substantially. The aim , essentially, was to make the bearing more tolerant to misalignment, without too much sacrifice on life expectancy.

The aim of optimization was to achieve high stiffness, low friction and temperature generation and low vibration levels and still have adequate life. At high speed, the friction was the most important parameter. Bearing life was considered secondary importance and was only checked to ensure it was adequate.

Numerical Results

Detailed computer analysis was carried out for this design to assess the performance of these bearings. To keep data to a minimum whilst still giving a good insight to the effects of the difference of the two bearings, a total of nineteen runs per bearings were carried out. These covered the general operating environment of the bearing when used in the pumpset.

The runs were devised to include the effect of axial and radial loads, speed and angular misalignment on the cage forces and the life expectancy of the bearing.

General Findings

Figure (3) represents the life expectancy of the bearings against the imposed axial loads for no misalignment ($T=0$) and an angular misalignment of $T=0.005$ Rad. It is evident that the original bearing life is substantially higher than the replaced one at low axial loads, however, the advantage decreases as load increases and the life expectancy of the two bearing become very similar. With high misalignment, the original bearing shows no such advantage, and, the replaced one is not substantially affected by tilt.

Figure (4) shows that the contact angle variation is substantially less for the replaced bearing than the original one when operating under high misalignment. The contact angle variation between the outer and inner races is an indication of the amount of spin that the ball experiences during operation. Spin drastically reduces the traction forces in the rolling direction with increased risk of skidding, loss of cage stability and increased temperature generation. Performance improves when the difference between the contacts is a minimum.

Figure (5) shows that the original bearing has a much higher tilt stiffness than the replaced one, specially at high tilts. In this application, this is considered to be a disadvantage. The aim is to allow tilt without increasing resistance to that tilt.

Additional analysis showed that the magnitude of the cage force is reduced by a factor of 4 when the replaced bearing was used under the same degree of misalignment.

Conclusion

Vibration measurements performed on the modified pump (Figure 6) showed that the replaced bearing was much superior to that of the original one with regards to the general parameters used to measure suitability under the adverse conditions. The cage forces were shown to be dramatically reduced in the modified bearing which greatly improved cage performance and reduced wear and excessive torque. In this design optimization, the dynamics of the system was unaffected inspite of the fact that the stiffnesses of the two bearings were different. This was largely due to the fact that the pedestal stiffnesses were very much less stiff and the change in bearing stiffnesses were small in comparison.

References

1. **Harris, T.A.** " Ball Motion in Thrust-Loaded Angular Contact Bearings with Coulomb Friction", Journal of Lubrication Technology, ASME, January 1971.

2. **Dominy, J.** " The Nature of Slip in High-Speed Axially Loaded Ball Bearings", IMechE, 1986.

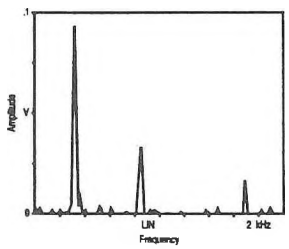

Fig. 1

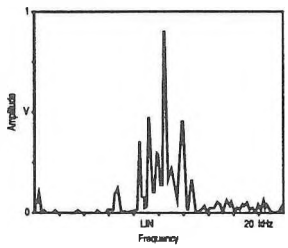

Fig. 2

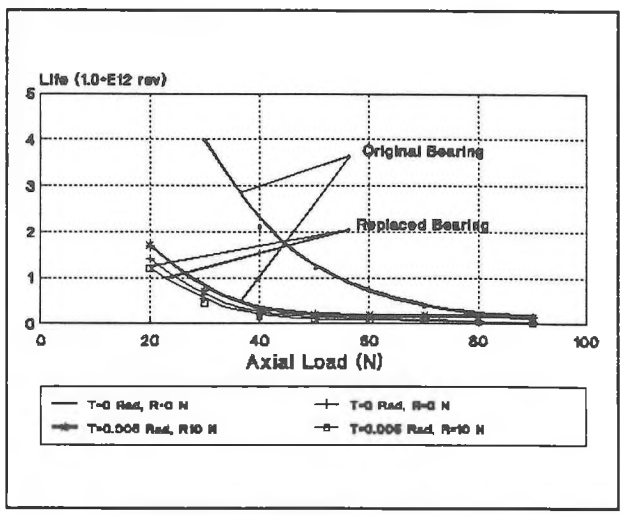

Fig. 3

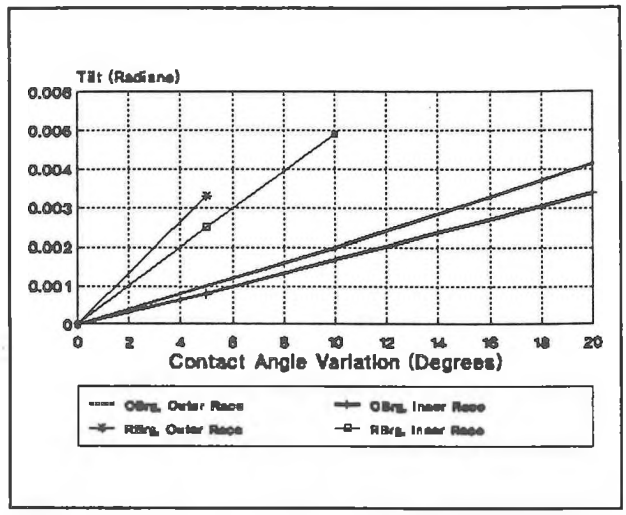

Fig. 4

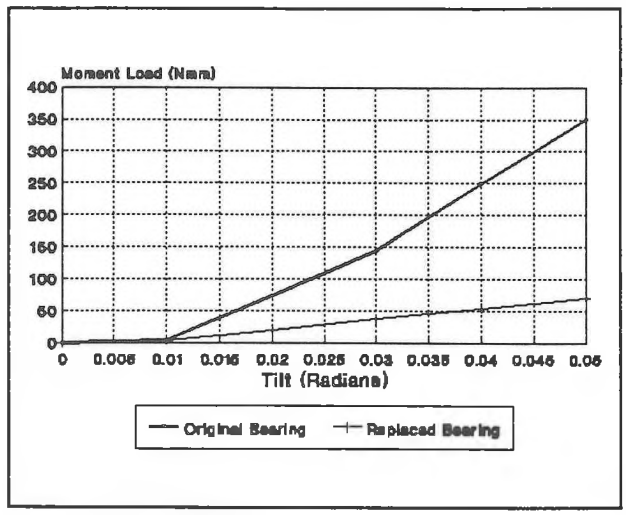

Fig. 5

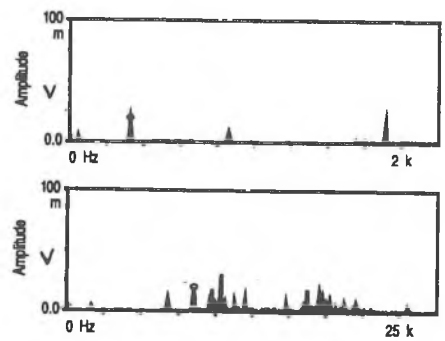

Fig. 6

Computed Order Tracking Applied to Vibration Analysis of Rotating Machinery

Erik D. S. Munck and **Ken R. Fyfe**
Department of Mechanical Engineering, University of Alberta, Edmonton, Alberta

1. Introduction:

Vibration analysis of rotating machinery is an important part of industrial predictive maintenance programs. Accurate determination of machine condition can reduce down time by allowing maintenance to be scheduled and by providing longer intervals between servicing.

When performing vibration analysis on rotating machinery during run-up or run-down, the spectral results are most commonly viewed in the frequency domain, as in Figure 1. This format shows speed-related components as oblique patterns of peaks and fixed-frequency components (eg. structural resonances) as vertical patterns. However, it is often advantageous to view the spectral results in a speed-normalized fashion, known as the order domain (see Figure 2), since the defects of interest (eg. shaft imbalances, wear of bearings and gear teeth) are mostly related to the shaft speed.

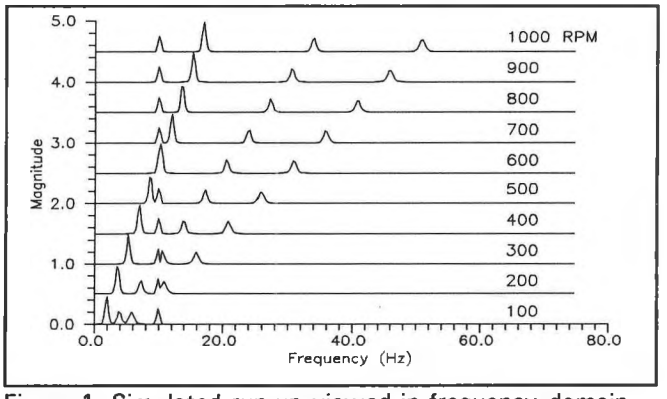

Figure 1: Simulated run-up viewed in frequency domain.

Speed-normalized analysis makes the speed-related vibration components evident, as they are shown as clear vertical patterns of peaks.

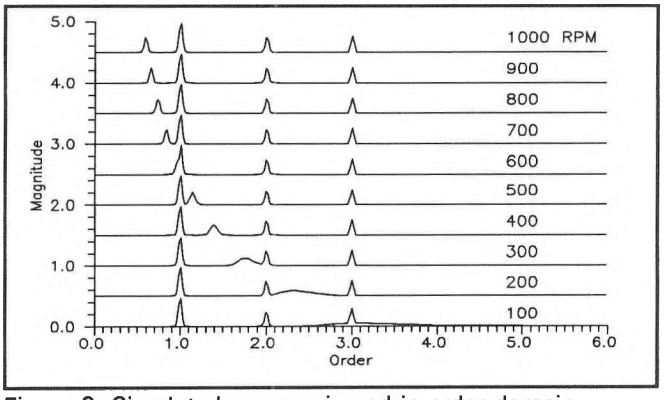

Figure 2: Simulated run-up viewed in order domain.

For spectral analysis to yield results in the frequency domain, the data must be sampled at constant increments of time; to yield results in the order domain, the data must be sampled at constant increments of shaft angle. Figure 3 shows a sine wave of increasing frequency sampled by the two methods. Notice that the constant-angle samples fall on the same location on the wave (peak, trough, etc.), while the constant-time samples change their position relative to the wave's shape.

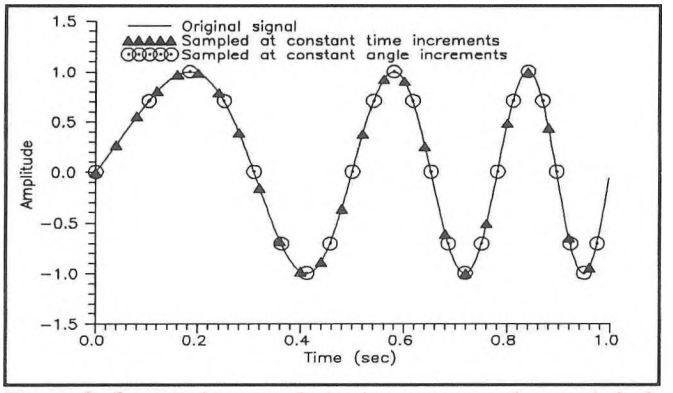

Figure 3: Swept sine sampled using constant time and shaft angle increments.

For order tracking, it is necessary to sample the vibration signal at constant angular increments and hence at a rate proportional to the shaft speed. Historically, this has been accomplished using analog instrumentation to vary the sample rate proportional to some tachometer signal, usually a keyphasor pulse [1]. Two pieces of expensive equipment are required: a ratio synthesizer and an anti-aliasing tracking filter. This is referred to as the classical method for order tracking.

Digital methods have been introduced which can resample a constant-time signal to provide the desired constant-angle data, also based on keyphasor pulses [2,3]. This is referred to as computed order tracking.

2. Procedure:

The two methods of performing order tracking analysis were compared using a computer simulation. To avoid distortion of the results by a low-pass filter, frequencies in excess of Nyquist's criterion were not included in the vibration signal. Both methods assume the keyphasor pulses arrive concurrently with vibration samples.

The varying sample rate of the classical method was approximated by determining the shaft speed each time a new keyphasor pulse arrived, and resetting the sample rate accordingly.

For computed order tracking, the resample times are computed assuming a linear angular acceleration with time, t, so the shaft angle, Φ, can be described by the quadratic equation:

$$\Phi(t) = b_0 + b_1 t + b_2 t^2$$

which is solved for t,

$$t_k = \frac{1}{2b_2}\left[\sqrt{4b_2(\Phi_k - b_0) + b_1^2} - b_1\right] ; \; k=0,1,2...$$

and the values of the coefficients b_0, b_1, and b_2 are found by fitting the keyphasor arrival times, which occur at known shaft angle increments,

$$\Phi(t_1) = \Phi_1 = 0$$
$$\Phi(t_2) = \Phi_2 = \Delta\Phi$$
$$\Phi(t_3) = \Phi_3 = 2\Delta\Phi$$

to the first equation. The resample times are calculated only over the centre half of the interval $0 \leq \Phi \leq 2\Delta\Phi$ to avoid overlap. Thus,

$$\frac{\Delta\Phi}{2} \leq \Phi_k < \frac{3\Delta\Phi}{2} ; \; \Phi_k = k\Delta\Theta$$

where $\Delta\Theta$ is the angular increment desired for resampling. The values for k to be used in the second equation are then found from

$$\frac{\Delta\Phi}{2\Delta\Theta} \leq k < \frac{3\Delta\Phi}{2\Delta\Theta} ; \; k=0,1,2...$$

The constant-time signal is resampled at these times using only linear interpolation; it will be shown in Section 3 that this simplification can cause inaccuracies.

3. Discussion and Results:

Both the approximation of the classical method and the computed order tracking method yield acceptable results, similar to Figure 4.

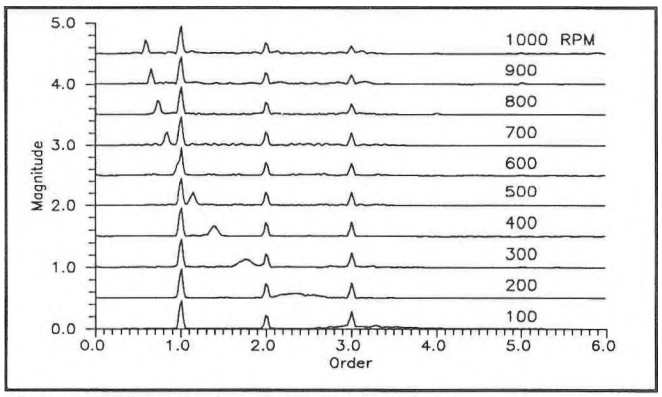

Figure 4: Simulated run-up analyzed by computed order tracking.

The main difference between the two methods is the amount of noise present in the spectra. Figure 5 illustrates that the method of computed order tracking has a noise level approximately one order of magnitude less than the approximation of the classical method.

In the computed order tracking method, linear interpolation works well when the signal is greatly oversampled. However, at sample rates closer to Nyquist's criterion, data resampled by linear interpolation do not coincide with the original signal, as shown in Figure 6. In Figures 5 and 6 only speed related components are shown.

The computed order tracking method assumes that the keyphasor pulses arrive as the shaft angle passes through zero. Notice that, since the keyphasor pulses arrive with the first time signal *after* the shaft passes through zero, a low sampling rate causes the assumption to be erroneous.

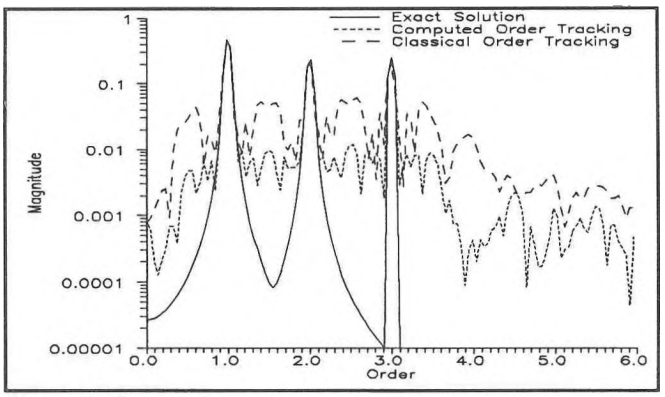

Figure 5: Comparison of typical spectral results.

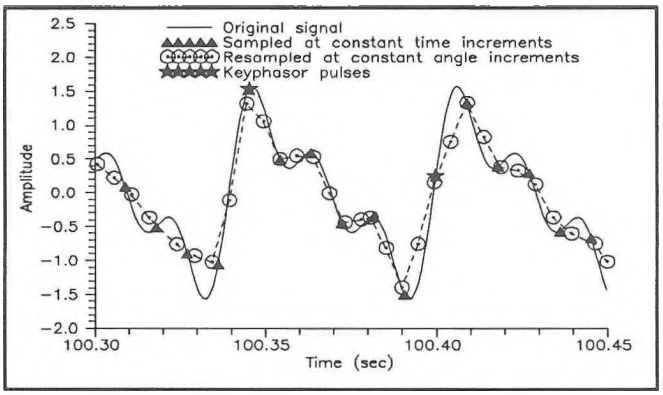

Figure 6: Computed order tracking resampling detail.

The approximation of the classical method has a higher noise level partly because it assumes a linear increase in shaft angle with time. This results in occasional errors in the number of samples taken per revolution, and hence large side lobes appear in the spectra.

4. Conclusions:

Even crude methods of computed order tracking work quite well. Improvements in keyphasor timing (using higher sampling rates or an external keyphasor monitor) and a higher-order interpolation routine would both improve accuracy. For the method to be truly useful, the interpolation method must also provide anti-aliasing filtering of the time signal.

5. References:

1) Hewlett-Packard Application Note 243-1, *Dynamic Signal Analyzer Applications*.

2) Potter, R. and Gribler, M., *Computed Order Tracking Obseletes Older Methods*, SAE Noise and Vibration Conference, May 16-18, 1989, pp. 63-67.

3) Potter, R., *A New Order Tracking Method for Rotating Machinery*, Sound and Vibration, Sept 1990, pp. 30-34

MISE AU POINT D'UNE TECHNIQUE D'INTENSIMÉTRIE POLAIRE PERSPECTIVES D'UTILISATION

Jean-Gabriel Migneron et Pierre Lemieux

Laboratoire d'acoustique, CRAD, Université Laval, 1636 Pavillon Félix-Antoine Savard, Québec, Qué., G1K 7P4.

SUMMARY

A robotic apparatus was designed and developed to take rapidly polar sound intensity measurements. This technique has a double dimension: it entails the expression of the relationship between the polar information and the standard acoustical parameters (pressure, simple vectorial composition of the flux line or complexe temporal and vectorial composition), and secondly, the robotic handling of the sound intensity probe with its two coupled microphones. The robot was built by the CEGEP of Lévis-Lauzon; it can be interfaced, through a PS/2 computer, to the Brüel & Kjaer dual channel third octave real time analyser 2133 or to the 2032 double FFT analyser. The robot can use an orthogonal routine, allowing a fast reading of the three vectorial components in a stationary acoustical mode, and it can be programmed to search automatically the maximum intensity level for the determination of the flux line or, in near field, with the aim of reactive intensity. In addition to conducting polar sound intensity experiments in stationary regime and in laboratory conditions, potential utilization of this technique was developed for complex industrial acoustical fields or for architectural acoustics.

1. RELEVÉ POLAIRE DE L'INTENSITÉ

1.1 Pourquoi effectuer des relevés polaires?

a) Afin d'éviter les confusions possibles

Pour une incidence sonore de 90° (ou 270°) par rapport à l'axe de la sonde intensimétrique, il n'existe théoriquement aucune composante de l'intensité. Or, on constate, en pratique, que la sonde enregistre, sous cet angle d'incidence, des valeurs plus ou moins fantaisistes (point d'ailleurs en partie reconnu par les fabriquants [1]). Cette situation est facilement identifiable lors de la lecture d'un relevé polaire. Par contre, avec un relevé selon trois composantes perpendiculaires, une pour chaque axe de coordonnées (principe des sondes tridimensionnelles avec trois doublets de microphones [7]), il suffit qu'on ait l'une de ces composantes confondue avec cette incidence critique pour que le vecteur intensité ainsi composé soit totalement erroné. On peut d'ailleurs ajouter, que dans la mesure ou le dispositif robotique est suffisamment rapide, il est possible de remplacer avantageusement le capteur à six microphones, ceci à l'aide de trois rotations consécutives.

b) Pour localiser les sources de bruit

Il s'agit d'exploiter le mieux possible les indications de directivité fournies par la nature vectorielle de l'intensité. En déterminant complètement (norme et direction) cette dernière, il est possible de localiser la provenance exacte du champ acoustique étudié et, même, d'estimer sa contribution en énergie dans une direction donnée.

Ces informations seront requises, afin de contrôler efficacement le rayonnement d'une source, qu'on désire renforcer (acoustique architecturale), ou amoindrir (acoustique industrielle). La technique peut s'avérer également utile pour localiser les zones de propagation , ou bien d'ombre, d'un ensemble de sources. De même, elle peut permettre un bilan spatio-temporel autour d'un point de réception déterminé (tel qu'un poste de travail).

c) Pour rechercher automatiquement la ligne de flux

Tel que mentionné dans les prochains points, le dispositif robotique s'est révélé tout à fait opérationnel pour effectuer cette recherche automatiquement, dans des délais relativement courts, ce qui constitue certainement un acquis métrologique important.

1.2 Comment lire un relevé polaire?

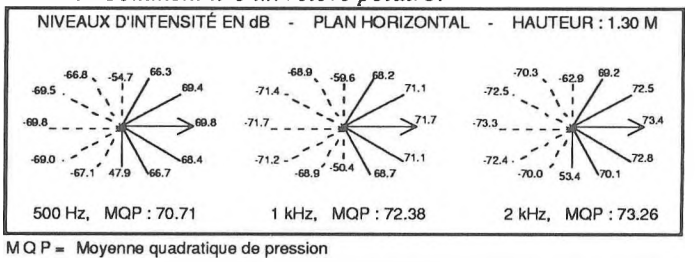

M Q P = Moyenne quadratique de pression

FIGURE N°1: *Présentation d'un relevé polaire*

Un relevé polaire ne peut représenter un ensemble de vecteurs intensités en un point et dans un plan considéré (d'ailleurs le vecteur est unique). Il fournit uniquement le niveau (en décibels) de l'intensité dans l'axe de la sonde, celle-ci effectuant une lecture après chaque rotation de 30°, par exemple. La flèche qui apparait sur le relevé indique une direction de référence choisie par l'utilisateur. La rotation se fait toujours dans le sens trigonométrique: un trait plein indique une intensité *"positive"* et un trait en pointillés indique une intensité *"négative"*.

RASMUSSEN, G. explique que pour décrire un champ vectoriel, on a besoin d'explorer le champ dans toutes les directions, de manière à trouver la lecture maximale[13]. Lorsqu'on effectue un relevé dans un plan considéré, il n'est pas toujours évident, que l'un des axes de mesure soit rigoureusement confondu avec la direction de propagation. En pratique, il paraît convenable de considérer comme direction de propagation (ou direction voisine), dans ce plan déterminé, la direction pour laquelle la plus grande valeur de l'intensité a été enregistrée, les autres n'étant que des composantes de celle-ci. Dans tous les cas, avec la technique polaire, le vecteur intensité sera toujours localisé dans un cône dont l'angle au sommet n'excèdera pas le pas angulaire de mesure.

2. RÉALISATION TECHNIQUE

2.1 Développement du projet de robot

Dans la perspective des besoins du Laboratoire d'acoustique et des projets de recherche en cours, nous avons défini les grandes lignes d'un modèle de robot adapté à la manipulation de la sonde intensimétrique. Après discussion avec l'organisme constructeur, soit le département de robotique du CEGEP de Lévis-Lauzon, nous en sommes

arrivés au concept de la figure nº 2.

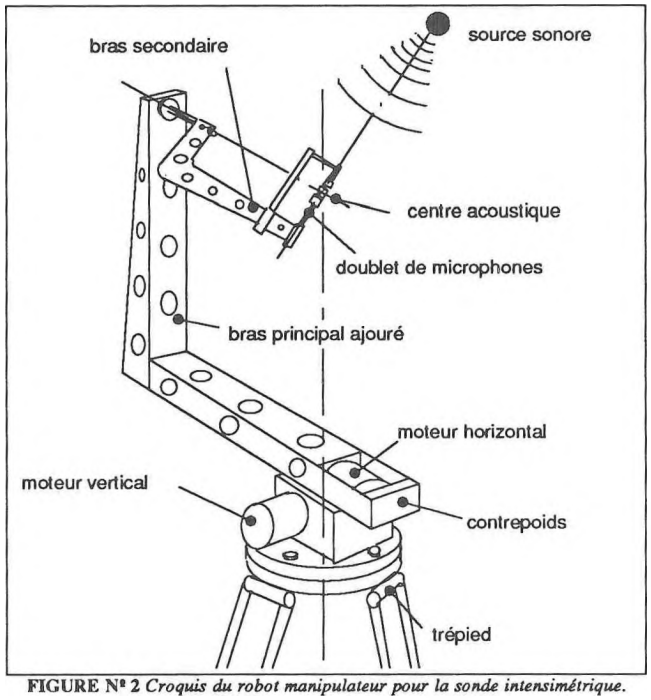

FIGURE Nº 2 *Croquis du robot manipulateur pour la sonde intensimétrique.*

Le robot est construit autour de deux axes de rotation perpendiculaires entre eux, leur intersection étant placée juste au centre acoustique du doublet de microphones de la sonde. Le moteur du bras horizontal est ramené vers la base, afin d'agir comme contrepoids, ceci par l'intermédiaire d'une réduction avec poulies crantées, et le réducteur vertical, destiné à absorber la plus forte inertie, est constitué d'un train d'engrenages avec une vis sans fin. Finalement, le robot repose sur une masse d'inertie démontable, pour faciliter son transport dans l'industrie lors des mesures intensimétriques. Le dégagement vertical est d'environ 500 mm sous la sonde intensimétrique et le dégagement latéral de 250 mm, de façon à ne pas affecter le champ acoustique à mesurer. Toutes les pièces constituant les bras sont percées, pour la même raison, de trous de différents diamètres.

2.2 Principaux éléments du cahier des charges

Les principaux éléments du cahier des charges préparé lors de la commande du robot ont été les suivants: angle de rotation normal suivant les deux axes, 30°, avec la possibilité de programmer d'autres valeurs, telles que 5, 10, 15 ou 90°; couverture complète des 360°, par une cheminement alternatif, vers la gauche puis vers la droite (pour éviter de mêler les câbles); temps moyen de déplacement entre deux positions de mesure: 1 sec.; précision de la position du centre acoustique de la sonde, dans toutes les directions de l'espace, 1 mm.

2.3 Interface ordinateur et analyseur

Le dispositif robotique est piloté par l'intermédiaire d'un ordinateur IBM PS/2. Les deux préamplificateurs de microphones viennent se raccorder à un analyseur bicanal en temps réel, au 1/3 d'octave, de Brüel & Kjaer, modèle 2133, ce qui constitue une chaîne de mesure exceptionnelle, complètement automatisée. L'analyseur est en effet interfacé également au même ordinateur, via un bus IEEE-488.

3. DIFFÉRENTS MODES D'UTILISATION

3.1 Distinction entre champ stationnaire et champ industriel fluctuant

Dans des conditions de laboratoire ou en acoustique des salles, il est possible d'utiliser des sources fixes, de radiation constante dans le temps (en intensité et en directivité), cette situation corrrespond à un champ acoustique stationnaire. C'est certainement dans ces conditions que le robot peut être utilisé le plus rapidement, en réduisant à son minimum le temps d'acquisition des niveaux d'intensité.

Pour certaines situations industrielles, aux perturbations de l'air près, il peut en être exactement de même. Néanmoins, il ne s'agit pas d'un cas général; la plupart du temps, les sources sont variables en durée d'émission, composition spectrale, puissance, directivité, voire même, position géométrique dans l'espace. Les champs acoustiques industriels sont éminemment variables, ils doivent être traités idéalement sur une base statisitque. Au plan pratique, il convient à tout le moins d'augmenter sensiblement le temps de moyennage de l'analyseur bicanal.

3.2 Les déplacements de base

La programmation de base comporte trois déplacements de référence, soit le plan horizontal (12 vecteurs), le plan vertical défini par sa positon angulaire, de - 60° à - 60° du plan horizontal (11 vecteurs), la calotte sphérique supérieure, jusqu'à - 60° du plan horizontal (61 vecteurs), plus une procédure orthogonale rapide.

3.3 La recherche automatique de la ligne de flux

Après quelques mois d'expérimentation, il est déjà acquis que, dans un champ acoustique stationnaire, le robot peut chercher très rapidemment, par optimisations successives, la position exacte de la ligne de flux et procéder ainsi à la détermination du vecteur intensité vrai. C'est d'ailleurs cette procédure itérative, par pas angulaire de 5°, qui est illustrée dans la figure nº 3.

4. PERSPECTIVES DE RECHERCHE

L'optimisation de la technique d'acquisition automatique de l'intensimétrie polaire offre des perspectives de recherche très fructueuses, dont plusieurs aspects dépassent très largement la seule dimension métrologique. Trois aspects sont actuellement en développement, ce sont les suivants:

-la comparaison entre la procédure de mesure triaxiale orthogonale rapide et l'emploi d'une sonde intensimétrique classique à 6 microphones: dans bien des situations, il est fort possible que la procédure d'acquisition robotisée puisse être aussi précise et rapide que l'emploi simultané de trois analyseurs bicanaux ou bien d'un mutiplexeur électronique;

–l'optimisation de la procédure de recherche

SUGGESTIONS FOR CHANGE TO ISO 9614

R.W. Guy & J. Li

Centre for Building Studies
Concordia University, Montréal

1. Introduction

A sound power measurement within a small semi anechoic chamber was undertaken in accordance with ISO Draft Standard 9614 [1] [2] employing a pressure - pressure finite difference probe system with real time band analysis (B & K sound intensity analyzing system type 3360 probe type 4177).

It was found that F_2, designed as an overall surface pressure-intensity indicator, was negative in a particular low frequency band. This result was inconsistent to it's ultimate use within a qualification criterion and in consequence an investigation into the cause was undertaken.

2. The Sound Power Measurement

Sound Power Measurement were undertaken on a small stable rectangular source (0.345m x 0.235m x 0.2m high) located in the centre of a bare concrete floor of a rectangular chamber otherwise lined with acoustic wedges. The chamber dimensions are 2.23m x 3.43m x 2.2m high and a conformai measurement surface 0.7m from each surface of the source was employed with a total measurement array of 320 points.

The acoustic wedges have normal incidence absorption coefficients equal to or greater than 0.97 from 100 Hz upwards, whilst their random incidence absorption is greater than unity.

The test facility is fully described in reference [3], whilst the semi automated measurement procedure employed is fully described in reference [4].

All measurements were undertaken in accordance with the requirements of the Draft Standard 9614, and the indicators prescribed by the standard were evaluated and the 125 Hz third octave band result for F_2 was negative.

The indicator F_2 is prominent in a check for measurement equipment adequacy by way of $L_d > F_2$ for Criterion 1 to be satisfied. L_d is always positive, F_2 is usually positive, but if negative, Criterion 1 is not the qualifying Criterion supposed.

3. Investigation

The most likely cause of F_2 being negative is overestimation of the intensity resulting either from phase mismatch errors or inadequate sampling within a standing wave field. It can be shown that the average Reactivity Index ($I_{avg} - P_{avg}$) resulting from adequate sampling throughout a standing wave may be written as:

$$L_{kavge} = 10 \log_{10} \left[10^{L_{kR}/10} \{1 \pm 10^{-(\delta_{PIO} + L_{kR})/10}\}\right] \quad 1.$$

where δp_{IO} is the pressure intensity index (dB)

$$L_{kR} = 10 \log_{10} \left[\frac{2R}{R^2 + 1}\right] (dB) \quad 2.$$

and R is the standing wave ratio (non dimensional).

Following the phase mismatch analysis of Gade [5] the value L_{kavg} such that phase mismatch errors shall not exceed 0.5 db may be written as:

$$L_{kavge} = 10 \log_{10} \left[(1 \pm 0.1)\ 10^{L_{kR}/10}\right] \quad 3.$$

this relationship shows that L_{kavge} should not exceed 0.4 dB for a maximum average overestimation of intensity, given when R=1. Further, the maximum value of R to cause (assuming adequate field sampling) L_{Kavge} to be + ve is R=1.6, this implies that no one measure within the field should yield $L_K > 2$ dB.

4. Suggested Solution

In the present analysis, F_2 equates to - L_{Kavge}, thus:

a) A lower limit should be imposed for the field indicator F_2 within Criterion 1 as:

   $L_d > F_2$ with $F_2 \geq -0.4$ dB, subsequently,

b) if $-0.4 \leq F_2 \leq 0$,

   then the index ($L_I - L_P$) at any point shall be less than 2 dB in order to qualify the result.

5. References

1. International Standards Organisation (ISO) Draft Standard 9614 "Determination of the Sound Power Levels of Noise Source Using Sound Intensity Measurements at Discrete Points", ISO/DIS 9614-1, 1989.

2. Fahy, F.J., "Sound Intensity" Chapter 8, Pub. Elsevier Applied Science, London, New York, ISBN 1085166-319-3, 1989.

3. Guy, R.W., Li, J., "A Facility and Test Procedure Designed for Sound Power Measurement by the Point Intensity Technique", Applied Acoustics submitted for publication, June 1991.

4. Guy, R.W., "Running a Test in an Intensity Based Measurement Facility", Canadian Acoustics, Vol. 18, No. 3, 1990 p. 31-45.

5. Gade, S. "Validity of Intensity Measurements", Bruel & Kjea, Technical Review No. 4, 1985.

ECKEL

Noise Control Products & Systems

for the protection of personnel... for the proper acoustic environment...

engineered to meet the requirements of Government regulations

Eckoustic® Functional Panels

Durable, attractive panels having outstanding sound absorption properties. Easy to install. Require little maintenance. EFPs reduce background noise, reverberation, and speech interference; increase efficiency, production, and comfort. Effective sound control in factories, machine shops, computer rooms, laboratories, and wherever people gather to work, play, or relax.

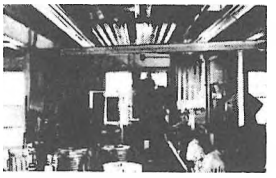

Eckoustic® Enclosures

Modular panels are used to meet numerous acoustic requirements. Typical uses include: machinery enclosures, in-plant offices, partial acoustic enclosures, sound laboratories, production testing areas, environmental test rooms. Eckoustic panels with solid facings on both sides are suitable for constructing reverberation rooms for testing of sound power levels.

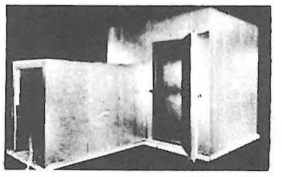

Eckoustic® Noise Barrier

● **Noise Reduction Curtain Enclosures** ● **Machinery & Equipment Noise Dampening**

The Eckoustic Noise Barrier provides a unique, efficient method for controlling occupational noise. This Eckoustic sound absorbing-sound attenuating material combination provides excellent noise reduction. The material can be readily mounted on any fixed or movable framework of metal or wood, and used as either a stationary or mobile noise control curtain.

Acoustic Materials & Products for dampening and reducing equipment noise

Multi-Purpose Rooms

Rugged, soundproof enclosures that can be conveniently moved by fork-lift to any area in an industrial or commercial facility. Factory assembled with ventilation and lighting systems. Ideal where a quiet "haven" is desired in a noisy environment: foreman and supervisory offices, Q.C. and product test area, control rooms, construction offices, guard and gate houses, etc.

Audiometric Rooms:
Survey Booths & Diagnostic Rooms

Eckoustic Audiometric Survey Booths provide proper environment for on-the-spot basic hearing testing. Economical. Portable, with unitized construction.

Diagnostic Rooms offer effective noise reduction for all areas of testing. Designed to meet, within ±3 dB, the requirements of MIL Spec C-81016 (Weps). Nine standard models. Also custom designed facilities.

An-Eck-Oic® Chambers

Echo-free enclosures for acoustic testing and research. Dependable, economical, high performance operation. Both full-size rooms and portable models. Cutoff frequencies up to 300 Hz. Uses include: sound testing of mechanical and electrical machinery, communications equipment, aircraft and automotive equipment, and business machines; noise studies of small electronic equipment, etc.

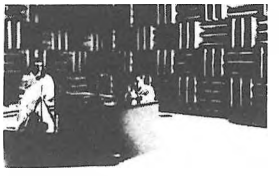

For more information, contact

ECKEL INDUSTRIES OF CANADA, LTD., Allison Ave., Morrisburg, Ontario • 613-543-2967

ECKEL INDUSTRIES, INC.

A SOUND DECISION!

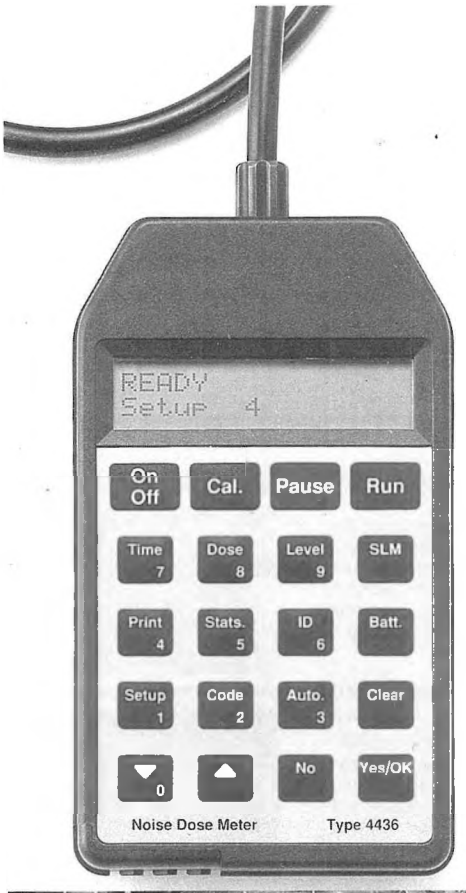

This dose meter withstands the rigors of the modern industrial environment, yet provides accurate and dependable readings.

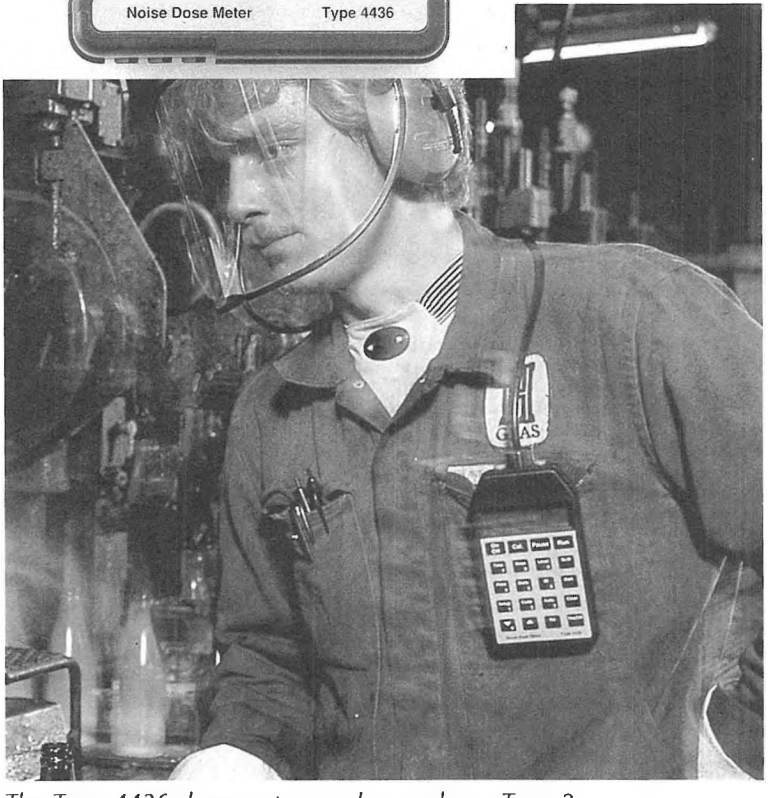

The Type 4436 dose meter can be used as a Type 2 integrating sound level meter.

Put the latest sound technology in your pocket and protect your employees from damaging noise exposure with a dose meter. The Type 4436 incorporates the latest technology and yet is rugged enough to withstand the most hostile industrial environments.

Bruel & Kjaers's Type 4436 microphone is protected inside the instrument casing where the hazards of the workplace cannot reach it. A strong, flexible rubber tube attached to the instrument, guides sounds to the microphone.

Specially-created software, known as the BZ 7028, allows information to be downloaded into a PC for analysis or data logging.

BRUEL & KJAER CANADA LTD.

90 Leacock Road, Pointe Claire, Quebec H9R 1H1
Tel.: (514) 695-8225 Fax: (514) 695-4808 Telex: 05-821691 b k pcir

THE BEST SOFTWARE FOR THE BEST DOSE METER.

Permanent records in two minutes.

Application software BZ 7028 supporting the

Type 4436
Noise Dose Meter

makes for an unbeatable combination.

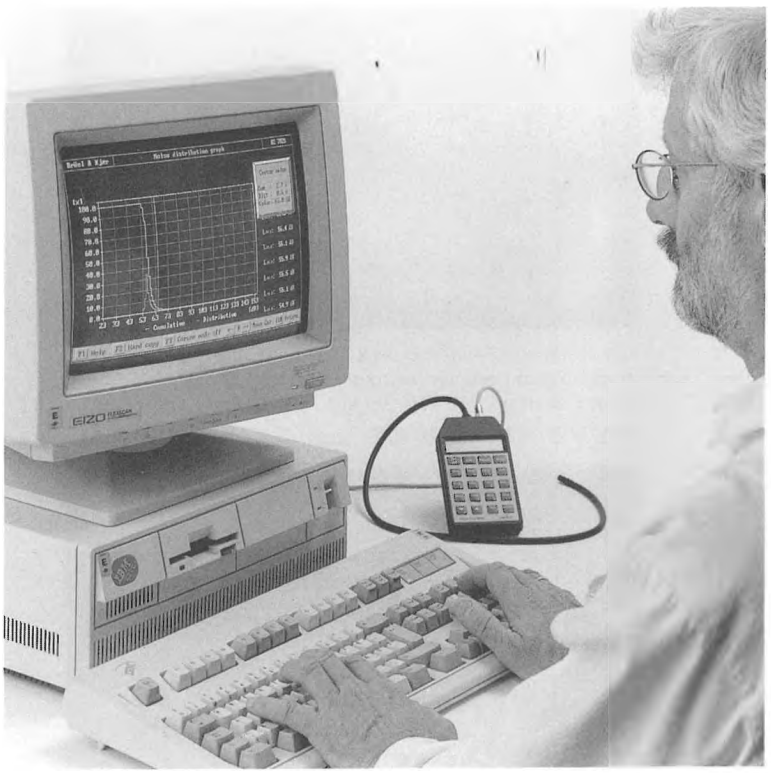

This dynamic new product provides:

- permanent records in two minutes or less.
- color graphs and tables
- time history
- statistical analysis
- cumulative distribution
- level distribution

In short, these are the tools with which you can quickly pinpoint problem noise exposures and provide full documentation.

BRUEL & KJAER CANADA LTD.

90 Leacock Road, Pointe Claire, Quebec H9R 1H1
Tel.: (514) 695-8225 Fax: (514) 695-4808 Telex: 05-821691 b k pcir

Turn your PC into a powerful speech analysis system.

The *Computerized Speech Lab (CSL™)*, Model 4300 is the most powerful computer-based system available for speech acquisition, analysis, editing and playback.

Complete System

CSL comes complete with all hardware (except the computer) and comprehensive software and works on an IBM® PC AT or compatible personal computer. The software operates in a "windows" type environment using pull-down menus. The hardware includes two input channels (each at 50 kHz sampling at 16 bits), digital anti-aliasing filters, a 40 MHz digital signal processor and digital output filters. Microphone, a studio quality speaker and headphones are also included.

Designed for Speech Professionals and Researchers

CSL's software has an extensive array of speech analysis capabilities which are performed with impressive speed because of the two on-board DSP chips. Spectrograms, power spectrum analysis, LPC formant traces, pitch extraction, amplitude traces and waveform analysis can be viewed quickly and simultaneously on a single screen. Signals can be listened to, edited, filtered, annotated with IPA characters or stored for later analysis. Extracted measurements can be conveniently "logged" for statistical analysis.

Flexibility for the Clinic, Research Lab and Classroom

Additional software is available depending on your specific application. For example, voicing parameters (jitter, shimmer and harmonic-to-noise ratio) provide clinicians with quantitative data on their patients' performance. The LPC synthesis program provides linguists, speech scientists and their students with powerful editing capabilities including formant frequency, bandwidth, pitch and temporal modifications. New programs are under development to further enhance CSL's capabilities. The CSL is also an ideal companion for Kay's DSP Sona-Graph™ speech workstation, Model 5500.

CSL with IBM compatible computer, monitor, microphone and mouse.

Call today.
1-800-289-5297
To find out more about the CSL.

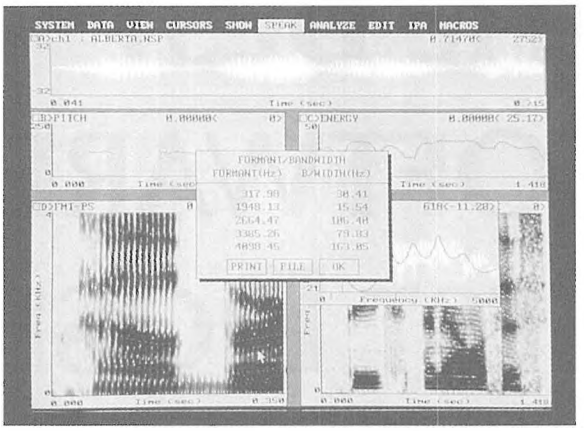

Example of CSL display showing multiple windows of analysis including speech waveform, fundamental frequency contour, energy envelope trace, wideband spectrogram with superimposed formant history (derived from LPC analysis), narrowband spectrogram displaying harmonics and FFT analysis of vowel segment with superimposed LPC analysis. Numerical window shows formants' center frequencies and bandwidths.

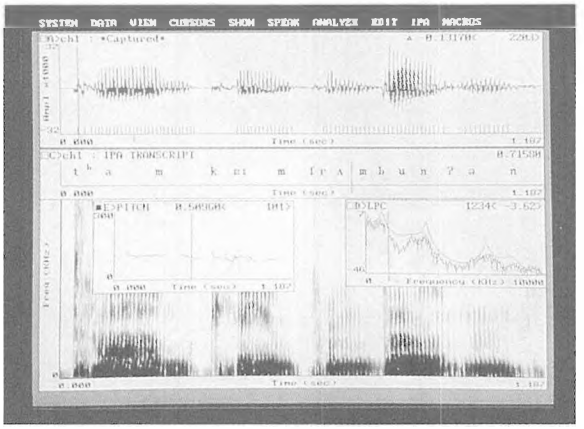

Five windows of analysis with speech waveform, phonetic transcription (time-linked to waveform), wideband spectrogram f_o contour and FFT analysis of vowel segment with superimposed LPC analysis.

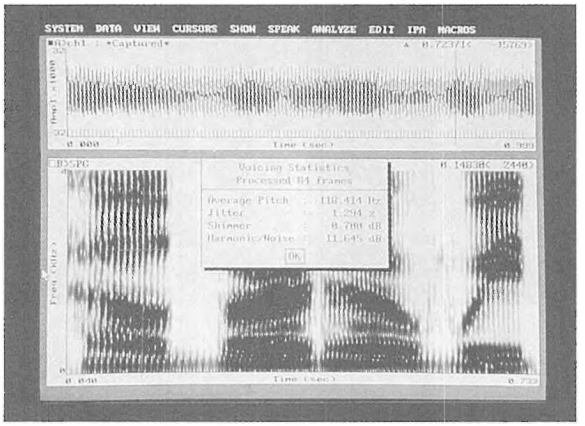

Three windows of analysis with speech waveform, spectrogram and voice parameter analysis including average f_o, jitter, shimmer and harmonic-to-noise ratio.

KAY

Kay Elemetrics Corp
12 Maple Avenue, PO Box 2025
Pine Brook, NJ 07058-2025
TEL: (201) 227-2000, FAX: (201) 227-7760
TWX: 710-734-4347

Predicting Acoustic Radiation from Coupled Fluid/Structure Systems : A Comparison of Two Computer Codes

L.E. Gilroy
Defence Scientist, Defence Research Establishment Atlantic, Dartmouth, N.S.

D.P. Brennan
Project Engineer, Martec Limited, Halifax, N.S.

1 Introduction

Predicting the acoustic radiation arising from fluid/structure interaction can be a difficult problem particularly when the acoustic medium is a dense fluid. This area has been studied extensively at both Defence Research Establishment Atlantic (DREA) and Martec Limited (under contract to DREA) resulting in the development of two suites of computer codes for the prediction of radiated noise from vibrating submerged structures. Both use finite element methods to model the structure and either finite element or boundary element methods to model the surrounding fluid.

The program COUPLE [1, 2, 3] has been developed at DREA and is used in conjunction with the finite element analysis program, VAST (Vibration And STrength) [4], and the boundary element code, BEMAP (Boundary Element Method for Acoustic Prediction) [5]. The program AVAST (Acoustic VAST) has been developed at Martec Ltd. under contract to DREA and is also used with VAST.

2 Theory

COUPLE

In the COUPLE suite of programs, VAST is used to create the matrices for a finite element model of the structure, resulting in the structural dynamics equation

$$[\mathbf{K} - \omega^2 \mathbf{M}]\,\{\delta\} = \mathbf{L}\,\mathbf{p} + \mathbf{f}_s \tag{1}$$

where $\mathbf{M}$ and $\mathbf{K}$ are the discretized mass and stiffness matrices, $\mathbf{L}$ is an interface matrix relating surface pressures to structural forces and $\mathbf{f}_s$ represents the externally applied structural loads. A finite element model of the fluid surrounding or contained in the structure is also generated using equations based on the classical wave equation in pressure. COUPLE assembles this fluid model into the fluid dynamics equation

$$[\mathbf{H} - \omega^2 \mathbf{Q}]\,\mathbf{p} = \rho\omega^2 \mathbf{L}^T \{\delta\} \tag{2}$$

where $\mathbf{H}$ and $\mathbf{Q}$ are the fluid 'stiffness' and 'mass' matrices, $\mathbf{p}$ is the fluid pressure vector, and $\{\delta\}$ is the structural displacement vector. COUPLE then provides the means to combine these two equations. When combined (with $\mathbf{f}_s$=0), (1) and (2) form the unsymmetric system:

$$\left[\begin{bmatrix} \mathbf{K} & -\mathbf{L} \\ \mathbf{0} & \mathbf{H} \end{bmatrix} - \omega^2 \begin{bmatrix} \mathbf{M} & \mathbf{0} \\ \rho\mathbf{L}^T & \mathbf{Q} \end{bmatrix}\right] \begin{Bmatrix} \delta \\ \mathbf{p} \end{Bmatrix} = \begin{Bmatrix} \mathbf{0} \\ \mathbf{0} \end{Bmatrix} \tag{3}$$

which must be symmetrized to maintain compatibility with the VAST eigensolver used. One symmetrical system available in COUPLE, which can easily be derived from the above equation, is:

$$\left[\begin{bmatrix} \mathbf{K} & \mathbf{0} \\ - & \frac{1}{\rho}\mathbf{Q} \end{bmatrix} - \omega^2 \begin{bmatrix} \mathbf{M} + \rho\mathbf{L}\mathbf{H}^{-1}\mathbf{L}^T & \mathbf{L}\mathbf{H}^{-1}\mathbf{Q} \\ - & \frac{1}{\rho}\mathbf{Q}\mathbf{H}^{-1}\mathbf{Q} \end{bmatrix}\right] \begin{Bmatrix} \delta \\ \mathbf{p} \end{Bmatrix} = \begin{Bmatrix} \mathbf{0} \\ \mathbf{0} \end{Bmatrix} \tag{4}$$

This combined dynamics eigenproblem is output from COUPLE and solved using the VAST solvers. The resulting eigenvectors of the fluid/structure system, together with an applied dynamic load vector, are used by the VAST frequency response module to generate the surface velocities on the fluid/structure interface.

The COUPLE suite uses these surface velocities as input boundary conditions to the program BEMAP. BEMAP uses the Helmholtz integral relation,

$$\alpha p(q) = \int_S \left\{ p(\zeta) \frac{\partial G(\zeta, q)}{\partial n_\zeta} + i\omega\rho v(\zeta) G(\zeta, q) \right\} dS_\zeta \tag{5}$$

where G is the Green's function:

$$G(\zeta, q) = \frac{e^{ik(q-\zeta)}}{(q-\zeta)} \tag{6}$$

and

$$\alpha = \left\{ \begin{matrix} 4\pi & (q \text{ exterior}) \\ 2\pi & (q \text{ surface}) \\ 0 & (q \text{ interior}) \end{matrix} \right\} \tag{7}$$

to predict the acoustic radiation from a vibrating surface, S_ζ, at any point, q, in the acoustic field. In order to avoid numerical difficulties at characteristic wave numbers, BEMAP overdetermines the surface Helmholtz equations with a series of interior equations (CHIEF method [6]).

AVAST

The AVAST suite of programs also uses VAST as a basis to establish a finite element model of the structure under consideration. AVAST uses the modal characteristics of the dry structure to establish a mobility matrix, $\mathbf{M}(\omega)$, relating surface nodal velocities ($\mathbf{v}$) to applied structural loads ($\mathbf{f}$):

$$\mathbf{v} = \mathbf{M}\mathbf{f} \tag{8}$$

Using this expression, an equation relating the normal velocity at the surface ($\mathbf{v}_n$) with the surface pressures ($\mathbf{p}$) and the externally applied loads is constructed:

$$\mathbf{v}_n = \mathbf{T}\,[\mathbf{M}\mathbf{f}_s + \mathbf{M}\mathbf{T}\mathbf{Q}_T\mathbf{p}] \tag{9}$$

where the matrix $\mathbf{Q}_T$ provides a transformation from surface pressures to nodal forces and T is a coordinate transformation matrix.

AVAST also uses the Helmholtz integral relation as described by equation (5); however, AVAST uses a set of exterior equations to overdetermine the system [7] [8]. From the Helmholtz equation, AVAST constructs the surface relation

$$\mathbf{Ap} + \mathbf{Bv}_n = \mathbf{0} \tag{10}$$

and the exterior pressure field relation

$$\mathbf{Dp} + \mathbf{Ev}_n = \mathbf{p}_e \tag{11}$$

where

$$\mathbf{A} = \int_S \frac{\partial G}{\partial n} dS - \mathbf{C} \qquad \mathbf{B} = i\omega\rho \int_S G dS \tag{12}$$

$$\mathbf{D} = \frac{1}{4\pi} \int_S \frac{\partial G}{\partial n} dS \qquad \mathbf{E} = \frac{i\omega\rho}{4\pi} \int_S G dS \tag{13}$$

and where

$$\mathbf{C} = 4\pi + \int_S \frac{\partial}{\partial n}\left(\frac{1}{r}\right) dS \tag{14}$$

Since the surface pressures are initially unknown, some form of approximation is required and the one chosen for this method is the plane wave impedance relationship:

$$\mathbf{p} = \rho c \mathbf{v}_n \tag{15}$$

Substituting (15) into equation (9) and solving for $\mathbf{v}_n$ yields:

$$\mathbf{v}_n = [\mathbf{I} - \rho c \mathbf{TMQ}]^{-1} \mathbf{TMf}, \tag{16}$$

The resulting normal velocities may be substituted into equations (10) and (11) and the interface pressures may be solved for in a least squares sense by solving the following overdetermined system of equations:

$$\begin{bmatrix} \mathbf{A} \\ \mathbf{D} \end{bmatrix} \mathbf{p} = \begin{Bmatrix} -\mathbf{Bv}_n \\ \mathbf{p}_e - \mathbf{Ev}_n \end{Bmatrix} \tag{17}$$

The surface pressures calculated in (17) may now be substituted into (9) and the updated normal velocities compared to the original. AVAST then iterates, assuming the velocities are different, through equations (10), (11), (17), and (9) until convergence.

3 Numerical Modelling Results

A model of a cantilevered flat plate vibrating in air was chosen as one of the test cases for comparing the two codes. The model consisted of an aluminum plate (305mm × 254mm × 13mm) clamped in a rigid base as shown in Figure 1. A sinusoidal point load was applied as shown and the resulting directivity patterns at various frequencies determined. One such pattern, measured at 3092 Hz with a load applied at the same frequency, is shown in Figure 2. As can be seen from the figure, the results from the two different codes match extremely well. They also compare well with experimentally measured values.

Another test case to be used for comparison is a submerged cylinder with an internal dynamic load. This model incorporates the more difficult case of a dense fluid. One such model is shown below in Figure 3.

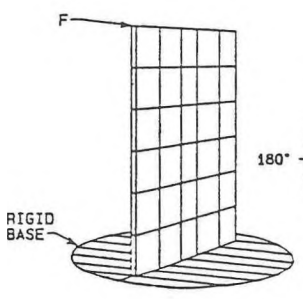

Figure 1: Flat Plate Model

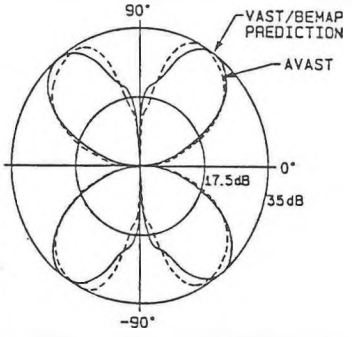

Figure 2: Directivity Pattern

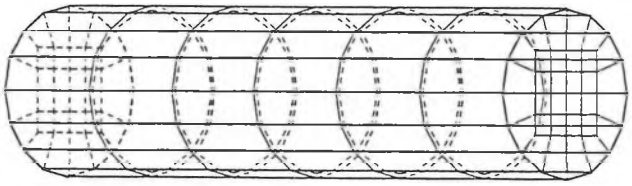

Figure 3: Ring-Stiffened Cylinder Model

4 Conclusions

Two suites of computer codes have been developed to predict acoustic radiation from vibrating structures submerged in a fluid. Results from test cases in air have agreed well with each other and with experimental results. A sufficient number of test cases has not yet been run to determine which suite uses the least computer time. Problems involving structures submerged in a dense fluid are currently being examined, but there appears to be a lack of experimental data for verification.

References

[1] Vernon, T.A., "Finite Element Formulations for Coupled Fluid/Structure Eigenvalue Analysis," DREA Technical Memorandum 89/223, 1989.

[2] Vernon, T.A., Tang, S., "Prediction of Acoustic Cavity Modes by Finite Element Methods," DREA Technical Communication 89/302, 1989.

[3] Gilroy, L.E., Tang, S., "An Improved Finite-Element Based Method for Coupled Fluid/Structure Eigenvalue Analysis," DREA Technical Memorandum 91/209, 1991.

[4] "Vibration and Strength Analysis Program (VAST) : User's Manual Version 6.0," Martec Ltd., Halifax, Nova Scotia, 1990.

[5] Seybert, A.F., Wu, T.W., "BEMAP User's Manual - Version 2.4," Spectronics, Inc., Lexington, Kentucky, 1989.

[6] Schenck, H.A., "Improved Integral Formulation for Acoustic Radiation Problems," J.A.S.A., Vol. 44, 1968.

[7] Vernon, T.A., "An Overdetermined Method for the Prediction of Acoustic Radiation from Submerged Structures," DREA Note H/89/2, Informal Report.

[8] Piaszczyk, C.M., Klosner, J.M., "Acoustic Radiation from Vibrating Structures at Characteristic Frequencies," J.A.S.A., Vol. 75, 1984.

Vibration and sound radiation of a double-plate system

A. Berry, F. Laville, J. Nicolas
GAUS, Génie mécanique, Université de Sherbrooke, Sherbrooke (Qc) J1K 2R1 Canada

D. Stredulinsky
Defence Research Establishment of Atlantic, P.O. Box 1012, 9 Grove Street, Dartmouth, Nova Scotia, B2Y 3Z7 Canada

1. Introduction

Most ship structures can be regarded as a radiating envelope (hull) connected at the vibrating internal structures through the vibration isolators. A simplified analysis of the problem may be done by considering two parallel elastic plates connected through four suspensions. This communication deals with the vibrations of a combined system and the sound radiation of the bottom plate when the top plate becomes excited by a point force in low- and mid-frequency ranges. In order to reduce the size of the linear system to be solved, the structure is divided into six sub-structures which are the two plates and the four suspensions and for which mechanical impedances must be determined. The mechanical impedances of both plates were obtained from a variational method general enough to include arbitrary boundary conditions, point-masses and stiffeners on either plate. The mechanical impedances of the suspensions were calculated with a four-pole network approach. The model is used to investigate the efficiency of suspensions and the effect of structural changes on either plate in order to minimize the radiated power.

2. Theoretical approach

The studied system consists of two thin plates connected through four suspensions which include a spring and a dashpot. The top plate (internal structure) is excited by a mechanical force F_1 and the bottom plate (external radiating structure) is located in an infinite baffle and is surrounded by a semi-infinite medium of low density. Each of these two plates may have any type of boundary conditions. More details on the theoretical calculation are given in [1].

The complete system can be subdivided into six sub-elements (two plates, four suspensions) which permits us to reduce the dimensions of the system to be solved and has the advantage of giving the force transmissibility through the suspension directly.

If $F_i^{(1)}$ is the force applied to the suspension i by the top plate and $F_i^{(2)}$ is the force applied to the bottom plate by the suspension i, one obtains the following relations for the velocity of each plate at the junctions, where the cross mechanical impedance $Z_{ij}^{(k)}$ may be obtained from [1].

$$v_j^{(1)} = \frac{F_1}{Z_{1j}^{(1)}} - \sum_{i=2}^{5} \frac{F_i^{(1)}}{Z_{ij}^{(1)}} \qquad j = 2, \ldots 5 \qquad (1)$$

$$v_j^{(2)} = \sum_{i=2}^{5} \frac{F_i^{(2)}}{Z_{ij}^{(2)}} \qquad j = 2, \ldots 5 \qquad (2)$$

$$\begin{Bmatrix} F_i^{(1)} \\ v_i^{(1)} \end{Bmatrix} = \begin{bmatrix} A_i B_i \\ C_i D_i \end{bmatrix} \begin{Bmatrix} F_i^{(2)} \\ v_i^{(2)} \end{Bmatrix} \qquad (3)$$

The terms A_i, B_i, C_i and D_i are the four-pole parameters representing suspension i which can be a simple spring and dashpot in parallel or a more complex system of springs and dashpots. The relations (1), (2) and (3) gives a system of 16 linear equations with 16 unknowns $F_i^{(1)}$, $V_i^{(1)}$, $F_i^{(2)}$, $V_i^{(2)}$. For example with a spring dashpot system the values of the matrix coefficient are the following:

$$A_i = D_i = 1;\ B_i = 0;\ C_i = \left(\frac{k}{j\omega} + c\right)^{-1}$$

where ω is the pulsation, k is the spring stiffness, c is the damping coefficient.

The dynamic response of the two plates is obtained by calculating the extremum of the Hamilton functional of each plate in vacuo. The acoustic radiation of the bottom plate is obtained by the double spatial Fourier transformation of the velocity profile of that plate. Details can be found in [2].

3. Results

The results are presented in Figure 1 for two steel plates (size 0.45 m x 0,37 m x 1 mm) connected through four springs symmetrically distributed. The top plate is guided and excited by a 1N force at its centre; the bottom plate is simply supported. Figure 1 shows the effect of stiffeners added either on the upper or lower plate. The interesting parameters, as a function of frequency, are the force transmissibility (Fig. 1a) the quadratic velocity Fig. 1b) the radiation efficiency (Fig. 1c) and the radiated power (Fig. 1d).

The solid line shows the case without stiffeners. The dotted and dashed lines are the cases with four stiffeners added on the bottom and the top plates, respectively. It is worth noting the complex vibratory and acoustic behaviours of the system. In particular one can note that the addition of stiffeners decreases the structural vibration level, as expected, but increases the radiation efficiency. Both contrary phenomena lead to almost no change on the overall radiated power at medium and high frequencies.

4. Conclusions

Scientifically speaking, this new approach allows one to quantitatively predict the complex vibro-acoustic behaviour of a typical suspension system. The benefit of using an analytical method is quite obvious in terms of physical interpretation, as well as parametric study. Technically speaking it opens the door to new tools for minimizing radiated noise.

5. Acknowledgements

This work has been done under the D.R.E.A. contract 0SC89-00545. Investigations into radiation in water are being done under contract W7707-0-1291/01

6. Bibliography

[1] A. Berry, J.-L. Guyader, J. Nicolas, "A general formulation for the sound radiation from rectangular, baffled plates with arbitrary boundary conditions, J.A.S.A., 88(6), 1990.

[2] A. Berry, J. Nicolas, "Acoustic radiation from a coupled planar structure", Contract report, DREA LR 91/425, March 1991.

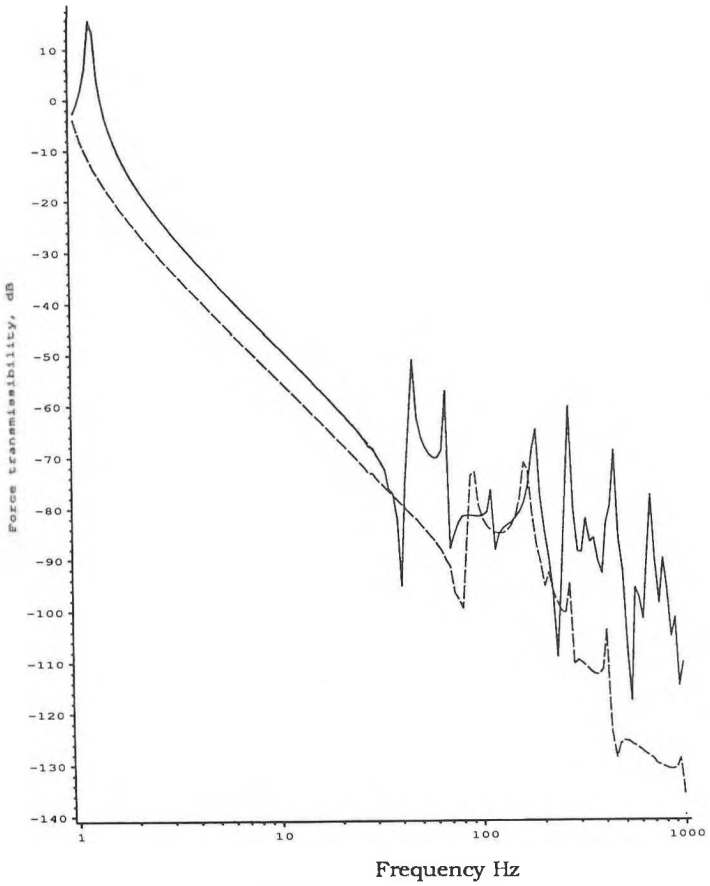

Fig. 1 a : Force transmissibility

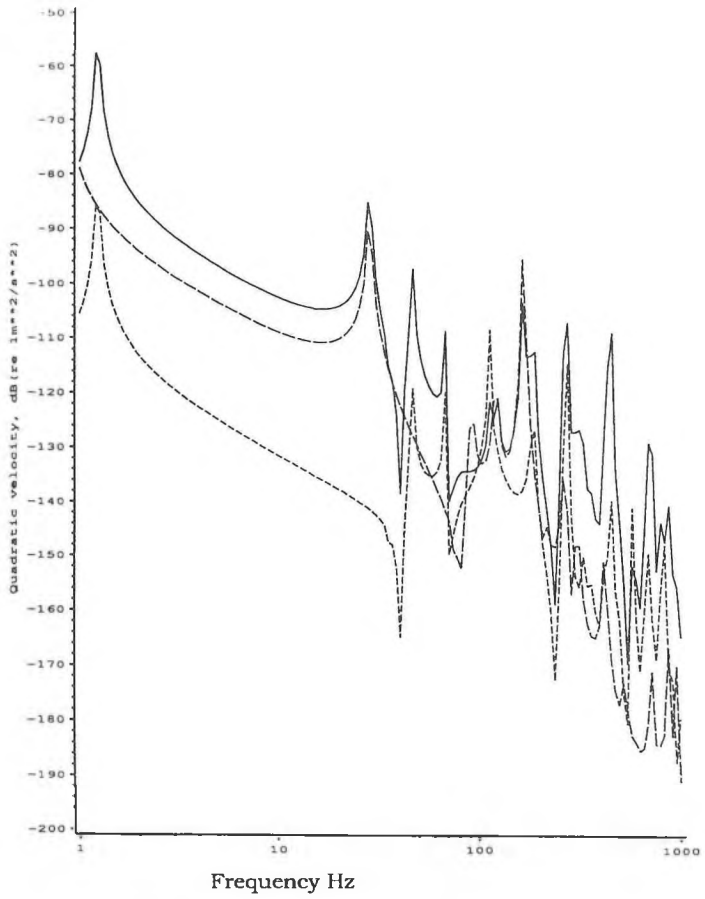

Fig. 1 b : Quadratic velocity

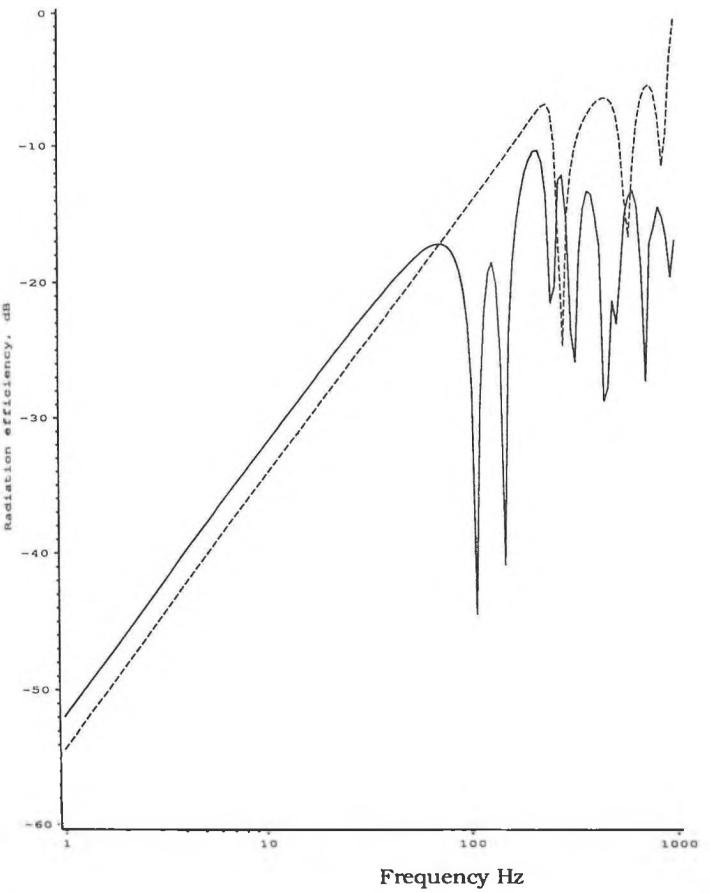

Fig. 1 c : Radiation efficiency

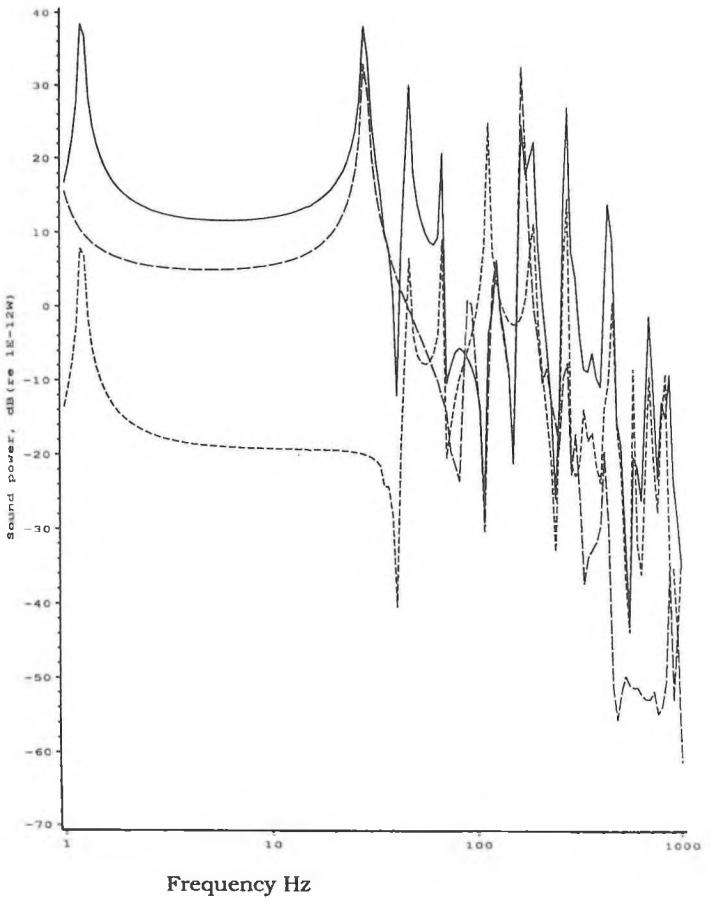

Fig. 1 d : Sound power

Fig. 1 : Numerical results for various stiffeners installation
_____ no stiffener; - - - - - four stiffeners, top plate; ..... four stiffeners, bottom plate

ACOUSTIC BACKSCATTERING FROM CYLINDERS: NEAR-FIELD CORRECTIONS

David M.F. Chapman and F.D. Cotaras
Defence Research Establishment Atlantic, P.O. Box 1012, Dartmouth, N.S., B2Y 3Z7

1. Introduction

To design active sonars, one needs to know how strongly the intended target forms an echo from the incident sonar ping. This target characteristic is called the *target strength* (TS) and is defined to be the reflected intensity at 1 m from the target divided by the incident intensity, expressed in decibel units. In this paper, we are interested only in the *backscattered* TS; that is, the source and the receiver are co-located. For reference, a perfectly reflecting sphere 4 m in diameter has a TS of 0 dB if the wavelength is much smaller than the sphere diameter.

Although theoretical TS formulae exist for simple shapes, there is no substitute for accurate measurement. Fig. 1 is a schematic diagram of the TS measurement procedure. In the course of making TS measurements of hollow aluminum cylinders of length 91 cm and diameter 28 cm in the frequency range 30-36 kHz, we realized that our measurements were being corrupted at beam aspect because the source and receiver were in the near-field of the target. Fortunately, we were able to increase the range and reduce this effect, but we also derived a correction to the near-field TS measurements that could be applied if sufficient range were unavailable. The derivation and application of this beam-aspect TS correction is the subject of this paper.

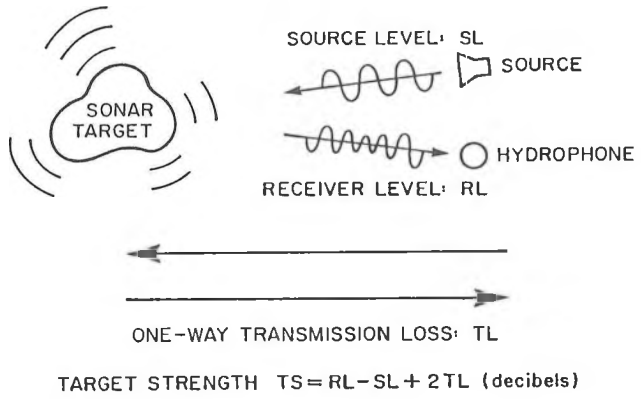

Figure 1 *Schematic diagram of target strength measurements.*

2. Target Strength Measurements at Two Ranges

Fig. 2 shows measured TS vs. aspect angle at 36 kHz for the test cylinder at 17 m range. Note the highlights at end aspect and beam aspect, caused by strong reflections at the flat end caps and straight cylinder sides, respectively. Also, note that the highlights are fairly narrow and high. Fig. 3 shows a similar measurement of the same target, but at a shorter range of only 6 m. The highlights are noticeably broader and lower.

3. Theory: Deriving the Correction

Consider a line source of length L with a receiver situated a distance R along the perpendicular bisector, as shown in Fig. 4. If R is large enough, the waves from all points of the line arrive in phase, and the received intensity is enhanced according to the ratio L/λ. As the receiver is brought nearer to the source, the distance from the ends becomes longer than that from the middle. When the phase difference is of the order $\lambda/4$, there will be noticeable destructive interference, and the received intensity is reduced. This happens when $R \approx L^2/2\lambda$. If there is a source located with the receiver, and if the line is a scattering target, a similar analysis applies, but the phase difference is doubled.

If one sums all the contributions along the cylinder length

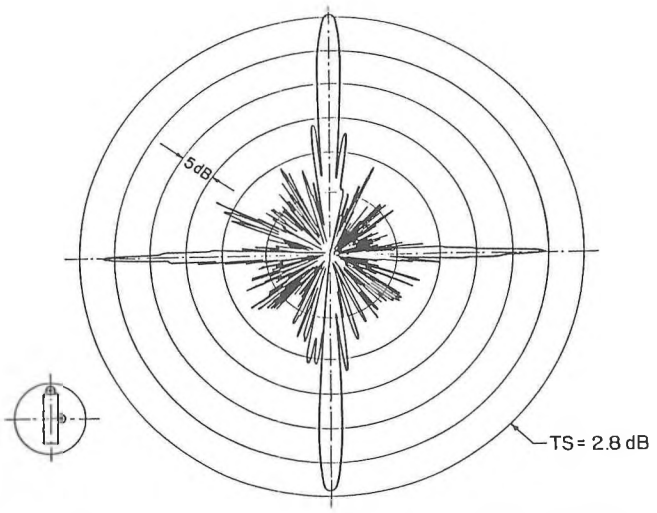

Figure 2 *Target strength vs. aspect angle at 36 kHz for the test cylinder at 17 m range.*

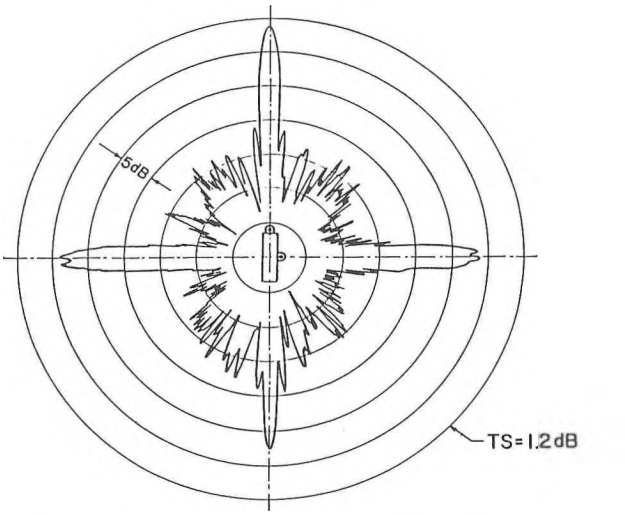

Figure 3 *Target strength vs. aspect angle at 36 kHz for the test cylinder at 6 m range.*

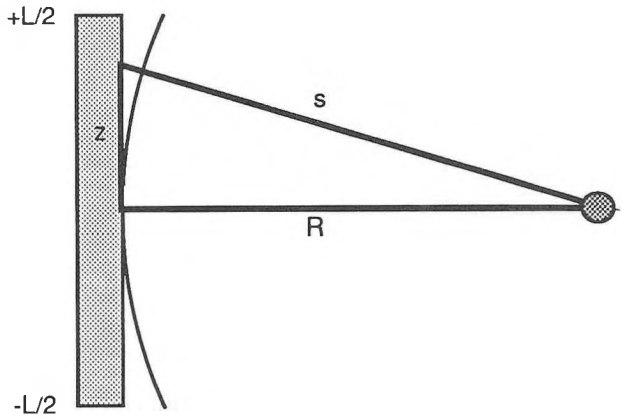

Figure 4 *Geometry for the near-field TS correction.*

coherently, the following correction to the near-field beam-aspect target strength is found:

$$\Delta TS = 20 \log \left| \frac{e^{-i2kR}}{L} \int_{-L/2}^{+L/2} e^{i2ks(z)}\, dz \right|, \qquad (1)$$

in which k is the acoustic wavenumber and $s = \sqrt{R^2 + z^2}$. When z«R, then $s \approx R + z^2/2R$, and a constant phase term can be factored out. Then, the integral can be written in the form

$$\Delta TS \approx 10 \log \left(p^{-2} \left[C^2(p) + S^2(p) \right] \right), \qquad (2)$$

in which $p = L/(\lambda R)^{1/2}$ and C(p) and S(p) are Fresnel sine and cosine integrals[1], respectively The parameter p determines whether the target is in the far field or not. The correction factor ΔTS is plotted vs. the parameter p in Fig. 5. Note that the correction is less than 1 dB if p<1, but it increases rapidly for p>1. We can say that the sonar is in the far field of the target if p<1, that is, if $R > L^2/\lambda$. A related near-field correction for transducer calibration is discussed by Bobber[2] and for radio antennae by Bickmore[3].

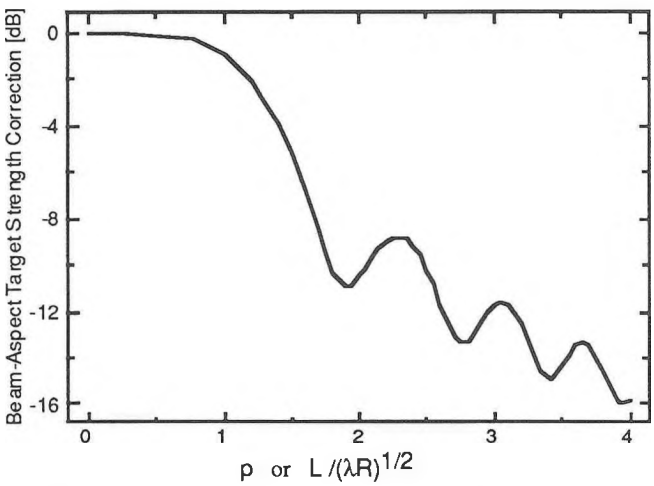

Figure 5 *Near-field reduction of cylinder TS at beam aspect.*

	30 kHz	33 kHz	36 kHz
R = 6 m	-8	-10	-7
R = 17 m	0	0	0

Uncorrected Measured Beam-Aspect TS [dB]

+

	30 kHz	33 kHz	36 kHz
R = 6 m	9.0	9.6	10.4
R = 17 m	1.1	1.2	1.5

Calculated Near-Field Correction [dB]

=

	30 kHz	33 kHz	36 kHz
R = 6 m	+1	-0.5	+3.5
R = 17 m	+1	+1	+1.5

Corrected Measured Beam-Aspect TS [dB]

≈

30 kHz	33 kHz	36 kHz
+0.5	+1.0	+1.5

Theoretical Beam-Aspect TS [dB]

Figure 6 *The correction of near-field beam-aspect target strength measurements for the test cylinder.*

4. Calculations: Applying the Correction

Fig. 6 demonstrates the correction of near-field beam aspect target strength measurements for the test cylinder at three frequencies. Notice that the corrected values are more alike than the uncorrected values and they agree favourably with the theoretical values calculated from Urick[4].

5. Conclusions

Theoretical analysis of the near-field of a line source produced a correction term that helps to explain the discrepancy between near-field beam-aspect target strength measurements and the theoretical TS formula. This reconciliation between theory and experiment gives us the confidence to apply the theoretical TS expression to other targets.

---

[1] Abramowitz, Milton, and Irene A. Stegun, *Handbook of Mathematical Functions* (Dover, 1965), p. 300.

[2] Bobber, Robert J., *Underwater Electroacoustic Measurements* (Naval Research Laboratory, Washington, 1970).

[3] Bickmore, Robert W., "On focusing electromagnetic radiators," Can. J. Phys. 35, 1292-1298 (1957).

[4] Urick, Robert J., *Principles of Underwater Sound, 3rd Edition* (McGraw-Hill, New York, 1983).

THE EFFECT OF SEDIMENT LAYERING ON OCEAN BOTTOM REFLECTION LOSS

Francine Desharnais
Defence Research Establishment Atlantic, P.O. Box 1012, Dartmouth, N.S., B2Y 3Z7

1. Introduction

DREA has produced several analyses of acoustic data for northern ocean areas, in particular analyses of acoustic bottom reflection loss vs grazing angle. The data from one station in Baffin Bay presented some interesting features that were discussed by Desharnais (1990): the data showed that, at high grazing angles, bottom loss at high frequencies (630 Hz) was several dB lower than bottom loss at lower frequencies (20 Hz). The low-loss interval was concentrated in a broad band centred around 600 Hz. The data was successfully modelled using normal geo-acoustic parameters for the ocean sediments of that area, with the addition of a thin high impedance layer near the sediment-water interface. The layer structure is thought to be associated with periodic sediment deposition influenced by ice-rafting and turbidity currents.

Other authors presented bottom loss data with similar low-loss bands at high frequencies. Among others, Holthusen and Vidmar (1982) analyzed sites in the western Nares Abyssal Plain (North Atlantic Ocean), and Hastrup (1969) analyzed a site in the Small Tyrrhenian Abyssal Plain (Mediterranean Sea). Both references estimated the low-loss frequency band to be somewhere between 1400 and 1600 Hz. Core samples were available for these two areas, and the presence of turbidity currents was verified. A semi-periodic layered sediment structure is characteristic of turbidity currents, and these authors used such a layering to explain the behaviour of their data at high frequencies. It is known (Brekhovskikh,1980) that constructive interference can occur between the acoustic reflections from each layer of a periodic system, and that reflection loss can be greatly reduced in specific frequency bands. These low-loss frequency bands are closely related to the periodic structure.

Comparison of the data from different areas shows that the centre frequency of the low-loss frequency band can differ greatly between areas. If a semi-periodic layered structure produces an increase in bottom reflectivity for a particular frequency band, it should be possible to associate the centre frequency to the structure, and to the geological area.

This paper discusses how core samples can be easily analyzed to estimate the centre frequency of those low-loss bands. Modelling trials will be presented to emphasize the layer parameters that are closely related to low-loss frequency bands, and how the low-loss frequency bands could possibly be associated to different geological areas.

2. Theory of the half-wavelength layer

For a periodic system consisting of 2 alternating layers of different acoustic impedance (see Figure 1), it can be shown that the reflection coefficient of the system at normal incidence will be minimum at an acoustic wavelength (λ) equal to twice the thickness of the two basic layers (D). The reader is referred to Hastrup (1969) for the derivation of the basic equations. For a system such as shown in Figure 1, the reflection loss will have a minimum at:

$$f = \bar{c} / \lambda = \bar{c} / 2D \qquad (1)$$

where $\bar{c}$ is the average sound speed through the layer.

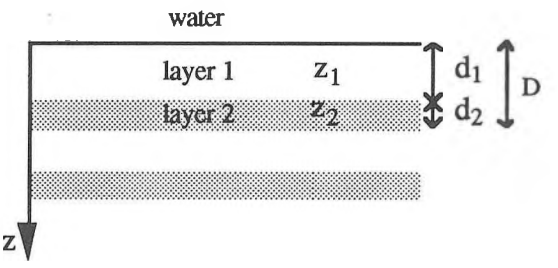

Figure 1. *Layers of alternating impedance.*

Figure 2 shows the density profile from a real core sample that will be used as a test case for the discussion that follows. An average sound speed of 1600 m/s was used to convert the density profile to an impedance profile. This approximation does not affect the conclusions presented below.

Modelling of the reflection loss vs frequency for a bottom of this type can be done with an acoustic propagation model like SAFARI (Seismo-Acoustic Fast field Algorithm for Range-Independent environments; Schmidt, 1988). Figure 3 shows a plot of smoothed reflection loss as a function of frequency for the SAFARI model using the density profile given in Figure 2, for a near-vertical grazing angle of 88°. A five-point moving average (corresponding to a moving window of 25 Hz) was applied to smooth the modelled data.

A decrease of reflection loss is noticeable at approximately 1535 Hz. The low-loss band is defined as that where the reflection loss is within 2 dB of the minimum value.

For a sediment structure of undefined periodicity as the core shown in Figure 2, a Fourier transform analysis can be done on the impedance profile (after subtracting the average impedance) to determine the main periodicity of the first few meters of sediments. The input series to the Fourier transform is a series of impedance values vs depth, and the spectrum obtained is therefore a function of the spatial periodicity of the impedance.

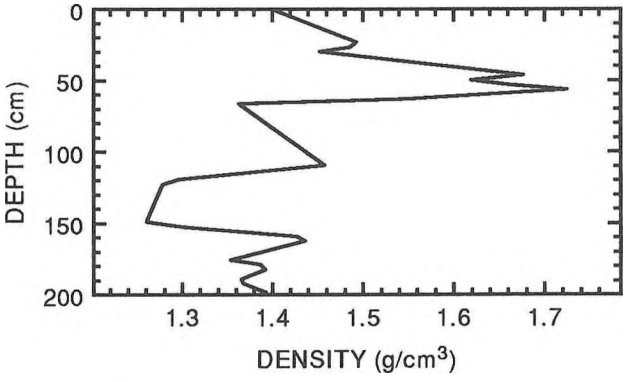

Figure 2. *Density vs depth of a core sample (Hastrup, 1969).*

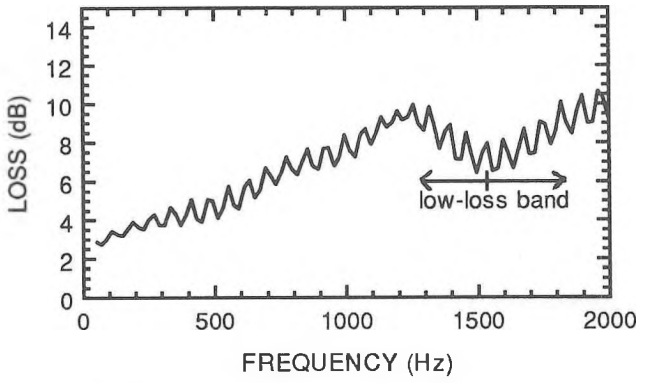

Figure 3. *Calculated reflection loss vs frequency, from SAFARI, showing centre frequency and bandwidth of the low-loss band.*

The spectrum of the test case is shown in Figure 4. The associated frequencies, as defined by equation (1), are noted on the upper axis of the spectrum. It is observed that the main periodicity of the core is approximately 55 cm, which is associated to a low-loss frequency band centred at 1460 Hz (the error bar drawn in Figure 4 defines the area where the amplitude is within 2 dB of the maximum value). The centre frequency of 1460 Hz agrees with the frequency of 1535 Hz indicated by SAFARI, as shown by the overlapping error bars (Figures 3 and 4).

3. Modelling of periodic structure

The analysis presented in the previous section allowed us to estimate the centre frequency of the low-loss band (if any) of a particular area for which core samples are available. The low-loss centre frequency can therefore be estimated without a complete bottom loss analysis.

To analyze the effect of the sediment layering on the low-loss centre frequency, modelling of different types of sediment layering was investigated. A Fourier transform was done on the impedance profile to find out the periodicity of the system, and reflection loss modelling with SAFARI was done to see the effect on the low-loss frequency band . The main results are here summarized:
For a periodic system of two layers of identical thicknesses, the centre frequency of the reflected band is proportional to the average sound speed of the two layers; the amplitude at the peak period of the spectrum is directly proportional to the impedance contrast between the two layers. A high amplitude in the spectrum indicates a broader reflected frequency band. If the thicknesses are identical, the peak amplitude is independent of $\bar{c}$. If the two layers are semi-periodic, meaning periodic with a gaussian variability in thicknesses, the results will be the same as above.

The system seems to require a minimum of 4 double layers in order to show the low-loss frequency band, or else the peak associated with the low-loss band will be lost in the background features of the spectrum. The frequency band also diminishes if the layers are covered by several wavelengths of regular sediment of constant impedance.

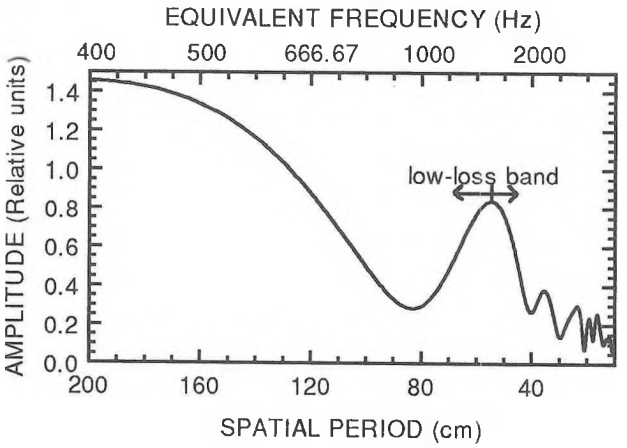

Figure 4. *Spatial frequency spectrum of the impedance profile.*

Therefore, the most important factors affecting the low-loss frequency band are the impedance contrast between the layers, and the average sound speed of the layers.

4. Conclusions

Various sets of bottom loss data from areas with turbidity currents indicate high acoustic reflectivity at a certain frequency band. The centre frequency of the band varies with the geographical location.

Different sedimentation processes affect the average speed of the sediments at a particular site and the vertical distribution of the layers. Turbidity currents, contour currents and ice-rafting all can create an alternation of layers of different impedances by the sediment-water interface. If the impedance contrast is large between the different layers, the bottom loss decrease at high frequencies will be more manifest.

It was shown that core samples could potentially be used to estimate the centre frequency of the low bottom loss frequency band. Statistics of core properties of different areas with known sedimentation could improve the knowledge of bottom losses for remote areas.

5. References

Brekhovskikh, L.M. (1980). *Waves in Layered Media.* London. Academic Press.

Desharnais, F. (1990). "Bottom loss in areas with ice-rafted sediments". Proceedings, Acoustics Week in Canada.

Hastrup, O.F. (1969). "The effect of periodic bottom layering on acoustic reflectivity", SACLANTCEN Report TR-149.

Holthusen H., Vidmar, P.J. (1982). "The effect of near-surface layering on the reflectivity of the ocean bottom", in: *J. Acoust. Soc. Am.*, v.72, pp. 226-234.

Schmidt, H. (1988). "SAFARI - Seismo-Acoustic Fast field Algorithm for Range-Independent environments - User's guide", SACLANTCEN Report SR-113.

COMPARISON OF NOISE EXPOSURE LEVELS BETWEEN WORKPLACES

Alberto Behar, P.Eng., C.I.H.
Ontario Hydro, 757 McKay Road, Pickering, Ontario L1W 3C8

Project Summary

1.0 Introduction

As an essential part of any hearing conservation program, noise exposure levels of workers are measured to assess their risk of hearing loss. Whenever the legal limit is exceeded (e.g., 85 dBA, 90 dBA, etc.), measures have to be done to eliminate or reduce the risk. To do so, work practices are re-examined, hearing protection is introduced and/or engineering controls are put in place to reduce noise levels, and consequently, noise exposure levels.

Any of the above measures requires use of resources, that are usually at a high demand and short supply.

This paper presents a process by which several indices are calculated using:

(a) the average noise exposures of the different work groups (L_{Trade}) (e.g., 85-90 dBA, 90-95 dBA, etc.).

The indices calculated using this method can be used in isolation or combined, so that a more complete picture (more representative rating) be obtained.

2.0 The Process

2.1 Ranges of Noise Exposures

The first step in the process is to choose ranges of noise exposures the data will divide. The first range usually has the lower limit of 85 dBA, since lower noise exposure levels do not present risk of hearing loss. Because in most cases 90 dBA is the limit when engineering noise control are recommended, the first range can be 85-90 dBA. The next can be 90-95 dBA, etc.

2.2 Collective Noise Exposure

The term "collective noise exposure" is defined as the sum of the products of the number of workers in each trade times their L_{Trade}. In other words, if there are two trades of 20 and 25 workers each and their L_{Trade} are 85 and 90 dBA respectively, the collective noise exposure for that workplace will be:

$$(20 \times 85) + (25 \times 90) = 3950 \text{ person x dBA}$$

2.3 Average Noise Exposure Level

The average noise exposure level (ANEL) for each noise exposure range is calculated by dividing the sum of the collective noise exposures within each range by the number of workers within the same range. The ANEL represents roughly the average noise exposure of a worker within the noise exposure range.

2.4 Normalized Average Noise Exposure Level

The normalized average noise exposure level is obtained by subtracting 85 dBA from the average noise exposure level. This is done to enhance differences between noise exposure levels from the different workplaces: it is easier to "see" a difference between 2 and 5 dB, than between 87 (85+2) and 90 (85+5) dB.

By subtracting 85 dBA (accepted as a "safe" limit), the normalized level can also be used as an estimate for the risk of hearing loss.

2.5 Maximum Collective L_{Trade}

Another estimate that can be used for inter-workplaces comparison is the maximum collective L_{Trade}. This is the collective noise exposure for the trade with the highest L_{Trade} within each noise exposure range.

NUMBER OF NOISE EXPOSED STAFF

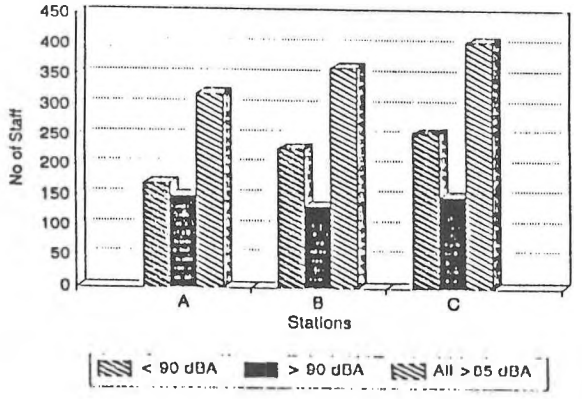

COLLECTIVE NOISE EXPOSURE

LTrade x No of Staff

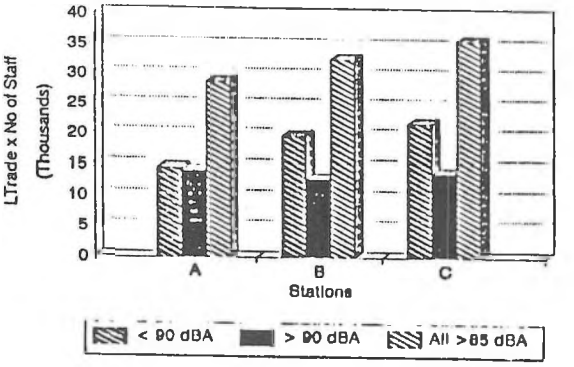

NORMALIZED NOISE EXPOSURES

(Coll Ltrade/No of Staff)/ - 85 dBA

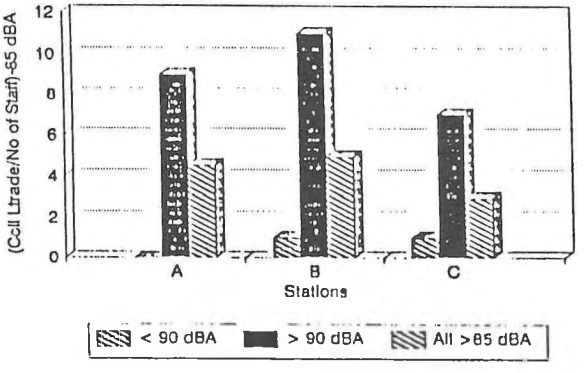

MAXIMUM COLLECTIVE L Trade

LTrade x No of Staff

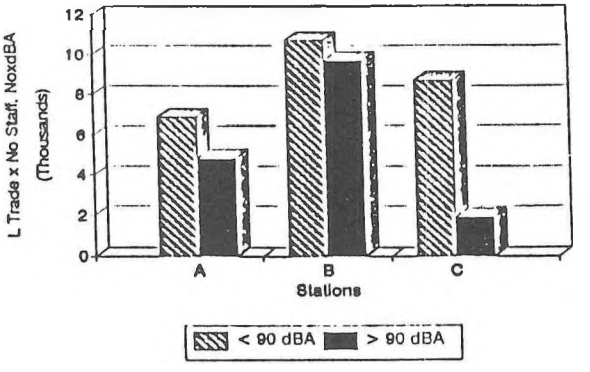

Example of the indices calculated on staff from three work stations

THE EFFECTS OF MUSIC TECHNOLOGY ON HEARING: A CASE STUDY OF ST. JOHN'S BARS

Shawn DeLay, Stephen Hiscock, Tracey Koopmans, Stephen Lenser, Emad Rizkalla and Donald Tulk
Faculty of Engineering and Applied Science
Memorial University of Newfoundland

1. Introduction

In many of today's popular bars and dance clubs, music is played at levels which may contribute significantly to permanent hearing loss. This is disturbing, considering that many young people spend a great deal of time in these establishments. Of particular concern is the risk that loud music poses to bar employees who are regularly exposed to this excessive noise for long periods of time.

A recent study conducted in Halifax [Whitehead, 1989] found that many bars maintained music levels capable of inducing hearing damage after only a few minutes of exposure. This raised questions about the noise levels in St. John's bars. Consultations with audiologists, and other experts indicated that a potential health hazzard exists, and that an investigation was warranted.

2. Study Outline

The study examined the relationship between hearing loss and loud music levels in bars. This relationship was investigated through the use of sound intensity readings and public opinion surveys conducted in the George Street bar district of St. John's, Newfoundland.

An important aspect of the research was to establish if bar patrons and bar employees are putting themselves at risk by spending long hours in a bar. In order to determine this, a sound level survey was conducted in fifteen popular bars and dance clubs. Readings were taken on several weekend evenings with a portable audio spectrum analyzer and a sound level meter. No advanced warning was given to bar management so as to prevent deliberate adjustment of sound levels. Peak readings were recorded using both "A" and "C" scale weightings. These results were later correlated with accepted industry standards for allowable unprotected exposure times.

In conjunction with the sound readings, three opinion surveys were conducted. Bar patrons, employees and management were surveyed to gauge each group's awareness of and concern towards the effects that loud music may have on hearing. One hundred bar patrons were interviewed using a random survey on several busy nights in St. John's major bar district. In addition, interviews were conducted with twenty bar employees and fifteen bar managers/owners who worked in the fifteen bars that were monitored. The surveys also addressed the following issues: the symptoms of temporary threshold shift experienced by employees and patrons; the frequency and effectiveness of patron complaints; the ability of bar owners to monitor sound levels; and the adequacy of the provincial government's noise regulations for bars.

3. Summary of Results

3.1 Sound Monitoring

a) Sound level measurements taken in fifteen bars revealed that twelve (80%) exceeded the ACGIH 1 hour exposure time limit.

b) Average measured sound intensity levels were 111 dB C and 101.8 dB A. This corresponds to a safe unprotected exposure limit of 49 minutes.

3.2 Opinion Surveys

a) Sixty percent of bar patrons admitted that they experience a "ringing" sensation after leaving a bar (temporary threshold shift (TTS)).

b) Seventy percent of bar employees experience "ringing" after completing their work shift.

c) Seventy-eight percent of bar patrons did not believe that loud music can have a permanent effect upon hearing.

d) Sixty percent of bar employees responded positively to the introduction of more stringent noise regulations, however, the majority of patrons and bar owners were not in favour of any new regulations.

4. Conclusions

The measured sound levels, as well as the high incidence of TTS, suggest that a potential hazard exists for bar patrons and employees alike in St. John's. However, the opinion surveys indicated that there is a definite lack of awareness of the potential negative effects that loud music may have on hearing. This lack of awareness was reflected in the existing noise standards which do not adequaltely regulate noise levels in bars. Aside from municipal by-laws for bars near residential areas, there does not appear to be any effecitve regulations for sound levels within the bars themselves.

5. Bibliography and Resources

American Conference of Governmental Industrial Hygienists. (1990). Threshold Limit Values and Biological Exposure Indices for 1989-1990 (Second Printing). Cincinnati, Ohio: Author.

American National Standards, ANSI S1.4. (1971). Specification for Sound Level Meters. New York: American National Standards Institute.

American National Standard, ANSI S3.20. (1973). Psychoacoustical Terminology. New York: American National Standards Institute.

Friend, B. (1990, January 31). Hear Today ... Nursing Today, p. 21.

Goodman, R. (1980). Output intensity of home stereo headphones. Ear, Nose, Throat Journal, 59, pp. 330-333.

Health and Welfare Canada. (1988, January). Acquired Hearing Impairment in the Adult. Ottawa: Minister of Supply and Services Canada.

Hodges, D. A. (Ed.). (1982). Handbook of Music Psychology. National Association for Music Therapy.

Leonard, J. (1990, November 20). Newfoundland Coordinating Council on Deafness. Personal Interview.

Parrott, V. (1990, November 19). Newfoundland Hearing Health Centre: Audiologist. Personal Interview.

Phillips, S. (1990, November 16). Worker's Compensation Commission of Newfoundland and Labrador. Personal Interview.

Sataloff, J. (1966). Hearing Loss Second Edition. J.B. Lippincott Company.

Supic, I. (1987). Music in Society: A Guide to the Sociology of Music. New York: Pendragon Press.

West, P. & Evans, E. (1990). Early detection of hearing damage in young listeners resulting from exposure to amplified music. British Journal of Audiology, pp. 89-103.

Whitehead, G. & Mieszkowski, M. (1989). Live music performance intensity levels. Nova Scotia Speech and Hearing Clinic.

Williams, C. R. (year unkown). Principle of Noise Measurement in Industrial Deafness.

Worker's Compensation Commission. (1990, February 7). Operations Manual: Subject: Hearing Loss (Policy: CL-01(R)). St. John's: Author.

Zagorski, M. (1990). Review of Goose Bay EIS. Memorial University of Newfoundland.

ELECTROACOUSTICAL AND REAL-EAR COMPARISONS OF ASSISTIVE LISTENING DEVICES

Peter A. Dobbins and Sheila M. Douglas
St. Joseph's Hospital, Guelph, Ontario, Canada

Purpose

To compare electroacoustical characteristics and real-ear insertion gain levels of commercially available personal assistive listening devices (ALDs), equipped with supra-aural headphones and earbud-type transducers.

Methodology

Four ALDs (Radio Shack Stereo Amplified Listener, Williams PockeTalker II, Whisper 2000, Audex Soundirector), two of which had tone adjustments as well as volume controls, were analyzed electro-acoustically and in-situ. Electroacoustical analyses were carried out on a Fonix 5500-Z Hearing Aid Analyzer, under conditions adapted from ANSI (1976) standards for linear output hearing aids. With the ALDs fitted to their supplied or recommended supra-aural headphones, the cushion from the left headphone was removed and the remaining transducer affixed to an HA-1 2 cc coupler with Blu-Tack. For each device, the saturation output (90 dB SPL input), full-on gain (60 dB SPL input), and frequency response were determined, along with second harmonic distortion levels at 500, 800, and 1600 Hz.

In-situ (real-ear) measurements were performed on a Madsen IGO 1500 Insertion Gain Optimizer. Maximum available insertion gain (i.e., volume control set just below the point of feedback) was determined for each device with ten adult listeners, using left pocket ALD/microphone placement, left ear probe placement, and a sweep stimulus level of 50 dB SPL. These measures were repeated, without changing volume control settings, with all ALDs coupled to a pair of earbud-type transducers (Radio Shack #33-8104) in place of their headphones. Where possible, additional available earbud insertion gain at higher volume control settings was also determined.

Results

In the 2 cc coupler, all ALDs had saturation output levels comparable to powerful ear-level hearing aids. Peak saturation levels all exceeded 135 dB SPL at 1000 Hz. All devices also exhibited peak gain levels of at least 50 dB, broad-band frequency responses, and negligible distortion levels. At 1000 Hz, input-output linearity was observed up to an input level of 90 dB SPL.

Except for one device with four listeners, maximum real-ear insertion gain with headphones never exceeded 20 dB at or below 2000 Hz. Peak insertion gain, typically observed in the 3 - 4 kHz region, was consistently less than 30 dB. Means and typical findings (five of six curves) from a single listener are shown in Figure 1.

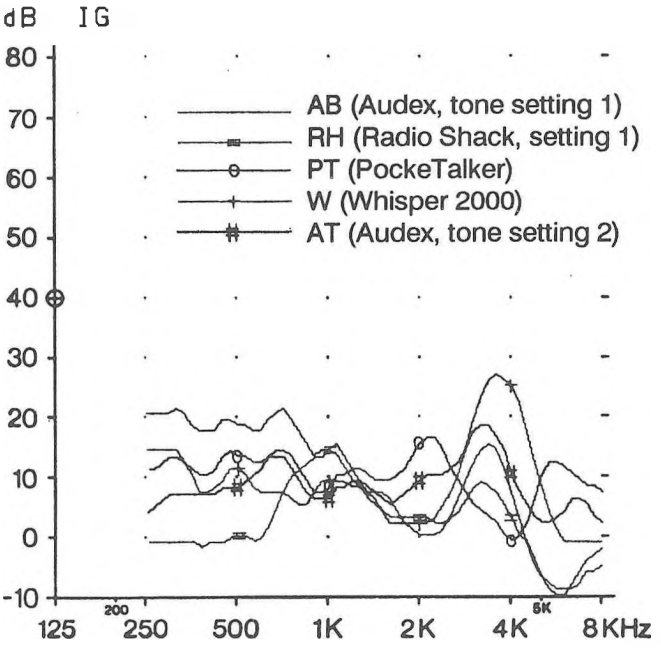

MEAN MAX. HEADPHONE I.G.(dB)

ALD	AT 1000 HZ	PEAK I.G.
AB	12.8	20.2
AT	8.2	20.5
PT	10.6	23.6
RH	12.7	13.5
RS	10.9	11.7
W	2.8	21.9

Figure 1

Typical single-listener findings (graph) and overall means (table) of maximum ALD insertion gain with headphones.

All ALDs provided more low-frequency gain with earbuds. Peak insertion gain was typically found at 355 Hz, where 14 - 34 dB more gain was observed than with headphones. For those devices that could not be worn at full-on with headphones, additional gain of up to 14 dB was available at higher volume control settings with earbuds. However, gain in the 3 - 4 kHz region still tended to be lower than that available with headphones (see Figure 2). This may be due to the greater canal occlusion created by earbuds, or possibly to a limitation of the earbuds used in this study.

Discussion

Examination of the single-listener curves in Figures 1 and 2 shows that the insertion gain available from an ALD depends primarily on the output transducer employed. While one device consistently provided the most gain for all listeners (with earbuds), there was no consistent rank order among the others. Between-subject variability was also observed, suggesting that external ear differences also influence ALD efficacy.

For various reasons, ALDs may be considered as potential substitutes for conventional hearing aids. However, one ALD will not be equally suitable for all wearers with hearing losses. It is suggested that an ALD should be selected and/or modified for an individual according to some fitting criteria, even if it cannot meet such criteria closely because of limited flexibility. Research into further output modifications of ALDs, whether by electronic or non-electronic means, is also warranted. Finally, the input-output linearity of these devices is of particular concern, since their output levels may potentially exceed listeners' tolerance levels and/or levels considered hazardous by health and safety standards.

Bibliography

Bebout, J.M. Non-hearing aid amplification devices: Competition or complement for hearing aids? The Hearing Journal, 1988, 41, No. 5, 7-12.

Brooks, W.S., & Grimes, A.M. Real-ear assessment of personal communication devices. Poster presented at 1989 ASHA Convention, St. Louis, MO.

Pruitt, J.B. Assistive listening device versus conventional hearing aid in an elderly patient: Case report. Journal of the American Academy of Audiology, 1990, 1, 41-43.

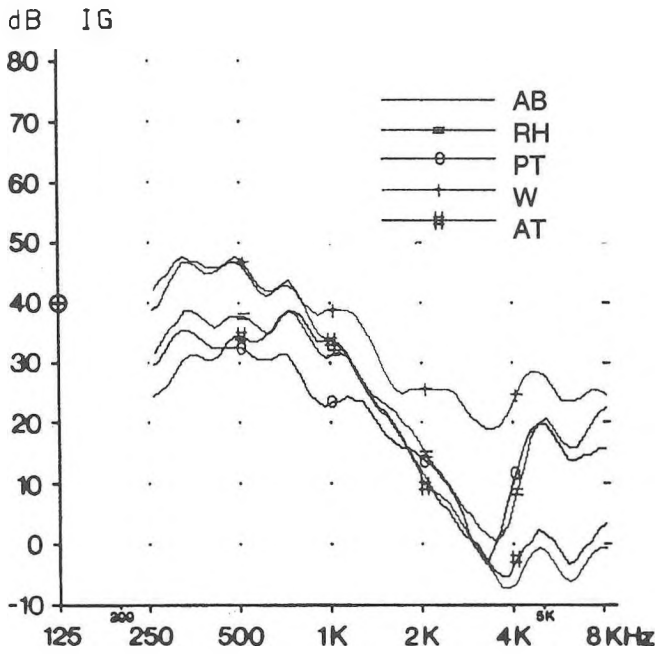

MAXIMUM AVAILABLE EARBUD I.G.(dB)

ALD	≃355 Hz	1 kHz	≃3 kHz	8 kHz
AB	41.3	22.4	–4.6	8.3
AT	28.2	24.4	–4.5	11.1
PT	32.7	14.1	0.8	26.1
RH	33.4	23.8	6.0	12.3
RS	33.5	22.1	0.7	16.9
W	42.2	29.0	17.8	18.8

Figure 2

Typical single-listener findings (graph) and overall means (table) of maximum ALD insertion gain with earbuds.

≃ using maximum and minimum gain values in these respective frequency regions.

SIGNAL DETECTION AND SPEECH PERCEPTION WITH LEVEL-DEPENDENT HEARING PROTECTORS

Sharon M. Abel, Nadine M. Armstrong and Christian Giguère
Hearing Research Laboratory
Samuel Lunenfeld Research Institute
Mount Sinai Hospital
Toronto, Ontario, Canada

PROJECT SUMMARY

1. Introduction

Hearing protective devices (HPDs) are the mainstay of industrial hearing conservation programmes for the prevention of noise-induced hearing loss. Conventional muffs and plugs are level-independent devices, i.e., they reduce all sounds by the same amount regardless of decibel level. As a result, they may interfere with speech communication and acoustic cues to occupational hazard, particularly in individuals with pre-existing hearing loss. The present research was undertaken to determine whether level-dependent protectors might provide a more suitable alternative for this group. These newly-marketed HPDs either reduce sounds minimally or amplify them at low levels, depending on the design, and attenuate maximally at high levels judged hazardous to hearing. Signal detection and speech perception were assessed in quiet and in noisy surroundings with the ears unoccluded and protected with the two types of muffs. The effect on protected listening of ageing, as well as hearing loss, was assessed.

2. Experimental Design

Two level-dependent ear muffs (E-A-R 9000 and BILSOM 2390) and two level-independent ear muffs (E-A-R 3000 and BILSOM 2315) were evaluated. The E-A-R 9000 exemplifies a passive level-dependent design concept. The change in sound attenuation with level is accomplished without electronics. Sounds below 120 dBA are attenuated by 25 dB over the audible frequency range. Higher level sound impacts, however, create turbulent airflow within precision orifices in the cup that impedes sound, resulting in an additional 10 dB of attenuation. In contrast, the BILSOM 2390 houses a limiting electronic amplifier, and exemplifies an active level-dependent design concept. Sounds below 85 dBA are passed with a gain of 5-10 dB. Between 85 and 120 dBA, the level at the ear will remain constant at 85 dBA. The two conventional level-independent HPDs, E-A-R 3000 and BILSOM 2315, have the same style earcups and cushions as their level-dependent counterparts. They provide a constant attenuation of about 25 to 35 dB.

Three groups of twenty subjects participated, two with normal hearing, aged 25 to 35 years and 40 to 60 years, and one with mild bilateral sensorineural hearing loss, aged 40 to 70 years. In each subject, the detection thresholds for 1/3 octave noise bands, centred at 0.5, 1, 2 and 4 kHz, consonant discrimination and word recognition were measured. The speech materials were presented at an intensity of 80 dB SPL. The three types of measurements were made in quiet and in a background of continuous cable swager noise (75 dB SPL).

3. Summary of Results

a) In quiet surroundings, neither age nor hearing loss affected the sound attenuation achieved with the conventional level-independent HPDs (E-A-R 3000 and BILSOM 2315) or with the passive level-dependent muff (E-A-R 9000). The active level-dependent amplifying muff (BILSOM 2390) afforded the hearing-impaired listeners a small advantage (i.e., negative attenuation) at the mid-frequencies.

b) Signal detection in noise was unaffected by the wearing of muffs in the two normal-hearing groups. This was also true for the hearing-impaired group in their range of normal hearing (.5 to 2 kHz). However, at 4 kHz, the region of dysfunction, all four HPDs raised the threshold significantly, the three attenuating HPDs (E-A-R 3000, E-A-R 9000 and BILSOM 2315) more so than the amplifying HPD (BILSOM 2390). For the former set of devices, the thresholds in noise were similar to the thresholds in quiet, suggesting that the wearing of these protectors virtually eliminated the perceptual effect of the noise in the hearing-impaired subjects.

c) In normal-hearing subjects, none of the four HPDs affected consonant discrimination in quiet. Word recognition, however, was adversely affected by attenuation. In contrast, the wearing of the attenuating muffs was beneficial in noise, while the amplifying muff had no effect or a deleterious effect, depending on the task.

d) In the hearing-impaired subjects, speech perception was impeded by all four HPDs. The amount of additional impairment, relative to unoccluded listening, was positively related to the degree of attenuation, in the

quiet condition. There was no difference due to protector type in noise. The protected detection threshold at 2 kHz was a good predictor of intelligibility.

4. Conclusions

A level-dependent HPD which amplifies low sound levels will aid mid-frequency detection in quiet in hearing-impaired listeners and will improve their high-frequency detection in moderate noise, relative to devices which attenuate sound. Also, speech intelligibility in quiet for this group will be close to the result for unoccluded listening, although there is little or no advantage in noise. In normal-hearing listeners, attenuating protectors result in better speech perception in noise, compared with unoccluded listening, likely because these devices can improve the speech-to-noise ratio. The degree of this benefit will, in general, depend on the noise spectrum.

5. Acknowledgements

This program was supported by Applied Research Award #234/R from the Ontario Ministry of Labour.

6. References

Abel, S.M. (1986). "Noise-induced hearing loss and hearing protective devices." Canad. J. Pub. Health, 77, Suppl. 1, 104-107.

Abel, S.M., Alberti, P.W., Haythornthwaite, C. and Riko, K. (1982). "Speech intelligibility in noise: Effects of fluency and hearing protector type." J. Acoust. Soc. Am. 71, 708-715.

Abel, S.M., Krever, E.M. and Alberti, P.W. (1990). "Auditory detection, discrimination and speech processing in ageing, noise-sensitive and hearing-impaired listeners." Scand. Audiol. 19, 43-54.

Acton, W.I. (1987). "History and development of hearing protection devices." J. Acoust. Soc. Am. 81, Suppl. 1, S4.

Allen, C.H. and Berger, E.H. (1990). "Development of a unique passive hearing protector with level-dependent and flat attenuation characteristics." Noise Control Eng. J. 34(3), 97-105.

Dorey, A.P., Pelc, S.F., Rawlinson, R.D. and Wheeler, P.D. (1978). "Evaluation of an active noise reduction system for use with ear defenders." IEE Conf. Pub. No. 162, 374-377, London, England.

Durkin, J. (1979). "Effect of electronic hearing protectors on speech intelligibility." U.S. Dept. of the Interior, Bureau of Mines, Report No. 8358.

Giguère, C. and Abel, S.M. (1990). "A multi-purpose facility for research on hearing protection." Appl. Acous. 31, 295-311.

Maxwell, D.W., Williams, C.F., Robertson, R.M. and Thomas, G.B. (1987). "Performance characteristics of active hearing protection devices." Sound Vib. 21(5), 14-18.

Wheeler, P.C. and Halliday, S.G. (1981). "An active noise reduction system for aircrew helmets." AGARD, CP-311, paper 22, Soesterberg, The Netherlands.

DIGITAL HEARING AIDS - THE WAY OF THE FUTURE

Marek Roland - Mieszkowski and **Steven D. Clements**
School of Human Communication Disorders, Dalhousie University
5599 Fenwick Street, Halifax, Nova Scotia, B3H-1R2, Canada.

First developments in digital processing of speech sound were done in 1960's in Bell Laboratories [29]. In recent years, the use of digital components in the design of **hearing aids (HA's)** is fast becoming a standard rather than an exception. Various HA's on the market, that utilize digital circuits, have proven to provide increased flexibility and efficiency in both fitting and hearing aid evaluation [1,2,25]. Although the availability of **digital signal processing (DSP)** techniques that are applied to the incoming signal do not vary much in the commercially available units, it is evident that research in DSP is the most promising area in future hearing aid development. Already new generation of HA's brings higher levels of satisfaction from the end user-hearing impaired [2,17,24,26].

Signal Processing can be viewed as any manipulation of a signal that alters its characteristics; whether extracting, enhancing or otherwise modifying said information [3,4,30]. These changes are conducted in order to help the hearing aid wearer to better discriminate between speech and noise; essentially then to increase **signal to noise ratio** (S/N). To achieve these results the consumer has available to him/her two basic approaches: automatic/adaptive digitally controlled analogue systems, and digitally programmable HA's. It should be noted that however complex a HA may seem, generally five approaches to signal processing are in use: variable gain, equalization, compression, limiting, and steady state noise reduction [8]. Following is a description of the major types of DSP on the market.

Automatic/Adaptive DSP circuits

This form of DSP; decreasing certain frequencies, while trying to leave the so called speech frequencies untouched, has been shown to increase speech intelligibility by 15% in the presence of low frequency noise [3], but so far gives no increased benefit to the HA wearer while in the presence of competing noise of similar broadband spectra, such as cafeteria noise [7].

The **Argosy Manhattan II Circuit** automatically alters its frequency response as a result of continuous sampling of sounds in the environment. As the noise SPL increases, high frequency gain decreases and low frequency output also decreases. Adjustments to the low frequency potentiometer provides up to 40 dB of gain reduction at 500 Hz [4].

The **Siemens 283** changes its overall frequency response to compensate for the loss in speech intelligibility caused by low frequency noise. The incoming signal is divided into two channels, the low frequency; up to 800 Hz which contains a compression circuit and the linear high frequency channel, which contains an adjustable high-pass filter from 800-1600 Hz [3].

From **Intellitech** the **Zeta Noise Blocker II**, a digital microchip integrated into a hearing aid circuit, samples incoming signals and analyzes the rate of frequency change, becoming active when the presence of noise is detected and applying digitally controlled attenuation by four analog filters. This circuit has been shown to be more effective in increasing S/N in the presence of high frequency competition [1,9].

Although the **K-AMP** is an amplifier, it does adaptively affect the linearity of a signal, offering approximately 25 dB maximum gain for sounds below 40 dB SPL, with gain gradually reduced to 0 dB as input level increase. The K-AMP will operate to 110 - 115 dB SPL input without distortion, and is noted as only amplifying quiet sounds. Loud transient sounds that represent a problem to many HA users are passed without amplification. These transients cause the **Telex Communication Adaptive Compression Circuit ®**, included in the K-AMP, to quickly drop to 0 dB, with a recovery time almost as fast; resulting in little affect on the ongoing gain [5,6].

Digitally Programmable HA's

Digitally programmable HA's process sound in the analogue domain, but are controlled by digital circuitry. They have the ability to be reprogrammed by an external unit, thus allowing quick caparisons of different settings in order to determine patient's preferences [1,10]. Paired-comparison techniques can be used with these types of HA's to improve the fitting process [22].

The **Audiotone System 2000** (from **Dalberg "The Dolphin System™"**) was the first programmable unit available on the market (1988). Its programming features include, maximum output, gain, high frequency cut (25 dB at 5 kHz), low frequency cut (30 dB at 500 Hz), input compression and frequency dependent output limiting [1,11].

The **Maico/Bernafon PHOX** (programmable hearing operation system) allows the programmability of the following features: gain, high and low frequency cut, slope of the high and low frequency response, a high frequency emphasis filter (cuts gain below 1500 Hz), a 3 kHz peak to emulate the canal resonance, option X a patient-activated noise reduction system, which cuts high and low frequency gain an additional 18 dB per octave, and an **automatic gain control** (AGC) input compression circuit [1,11,12,13,25].

Siemens Triton 3000 is a three channel compression HA. Ability is provided to program the gain in each channel (up to 36 dB), the AGC in each channel as well as two crossover points (300-1400 Hz & 1-5 kHz) with a minimum bandwidth of 1 octave and maximum of 3 octaves [1,11,25].

Resound's Personal Hearing System (PHS) offers a programmable two channel compression unit,with a compression range of 3:1 - 1:1, and an ultrasonic remote control for reprogramming. Programmable crossover frequencies for the high and low frequency bands are between 400-4000 Hz, with gain variable from 0 - 40 dB for each band. Fitting information can be stored in memory cartridge, as well as transferred to a PC. ReSound also incorporates an input compression limiter to control maximum output [1,11,14,25].

3M Corporation offers the **Memory Mate**, a programmable two channel compression HA. Programmable functions include; overall gain, dispenser-adjustable crossover frequency between 500-4000 Hz, and an eight memory client selected RAM. The RAM stores different frequency responses, for different environments [1,11,25].

The **Widex Quattro** allows for programmability of gain, maximum power output, output compression on/off, low and high-cut filters, plus an additional low-cut filter, the inverse presbycusis adaption filter. The HA also contains four memory choices selectable from a small FM remote control, which also operates as a programming unit, with the insertion of a programming key [1,11,15,16,25].

The **Ensoniq Sound Selector HA** has a programmable thirteen band equalizer that is adjustable in 1 dB increments up to 40 dB in each band and up to 60 dB overall gain. The thirteen bands are divided as such: lowest two in 1 1/2 and 1 octave bands respectively, the next three are 1/2 octaves, and the following eight are 1/3 octave bands. This is noted to generate a smooth response virtually free of distortion caused by resonance peaks. Also standard is 2:1 frequency-independent input compression and a directional microphone [1,11,17,18,19,25].

The **Nicolet Phoenix**, the only fully digital HA, has been taken off the market. Based upon the fitting, different frequency response characteristics, and a noise reduction algorithm were programmed (by the manufacturer) into the HA. The user was then able to select one of three "modes", by selecting one of three buttons on the aid, each set up for different listening environments. The **Phoenix VP** (variable processor) has five frequency response curves programmed into the first button, five degrees of noise reduction in the second, and the third button set to reverse the effect of the first two. The **Phoenix Plus** offers an additional 15 dB of gain [1,24].

Other programmable hearing instruments are offered by:

Audioscience (2-channel), **Beltone Electronics Corp.** (1-channel), **GN Danavox** (3-channel), **Philips Hearing Instruments** (3-channel), **Rexton Inc.** (1-channel) and **Starkey Laboratories Inc.** (1-channel) [25].

Conclusions

● In the past decade digital HA research and development has resulted in a number of improvements in clarity and S/N ratio (in certain environments). Most of current **ASP (automatic signal processing)** devices are still limited however by the number of frequency bands; thus are generally only effective in the presence of low frequency competition. All but Ensoniq have limited their approach to a few distinct processing channels . We should note when considering masking by noise, it is well accepted that the frequency range of the human auditory system is divided into 24 discreet channels, or critical bands (for each ear) [20] and each cochlear neuron responds to a narrow range of frequency stimuli [21]. It would seem appropriate then to at least separate the frequency range into like divisions. Philips has recently developed the Digital Compact Cassette (DCC), which utilizes 32-band digital processing for perceptual coding of audio signals [27]. This technology could be very easily adopted to make 32-band HA's. However, DCC will not be accepted as a new recording format, since recordable optical discs will be released soon to the consumer market.

● We still lack sufficient understanding as to the nature of many hearing impairment problems and their relationship to one another [2,5,29].Generally hearing problems are divided into: conductive, cochlear, eighth nerve and central nervous system disorders [2]. However the number of the distinctive disorders may reach easily into the hundreds [2], and each may require a specific signal processing algorithm [2,24]. Further research is still needed to explore the usefulness of compression systems [23]. Information theory can be applied to calculate inherent channel capacity for the ear [28]. On the basis of this theory analysis of a hearing impaired communication channel could be performed and the most appropriate information coding obtained.

● Digital Signal Processing workstations (for example NeXT computer) should be used to perform further psychoacoustic tests in order to learn more about the human auditory system. Also a Digital Master HA can be simulated on these types of computers and used to design and check different DSP strategies to be used in HA's.

● The complexity of processing which is needed to address many hearing disorders requires highly sophisticated signal processing. DSP offers substantial improvements over analog techniques [30] along with unmatched flexibility and precision to adopt the processing to individual requirements of each patient [2]. Also the paired-comparison judgment technique may be used more effectively with this technology for precise HA fitting [22].

● DSP should complement rather then substitute for signal processing which is performed in the auditory system (in other words it should be transparent when not needed). This will allow the best signal processor so far- the human brain - to extract information most efficiently [18].

● The following DSP techniques could be used in future HA's : arbitrary filtering and frequency shaping, arbitrary gain (as function of frequency and signal amplitude), frequency shifting, feedback control, noise reduction (various techniques), peak clipping or limiting etc [24,30]. Also multichannel, parallel processing can be done with DSP improving speed and sophistication of sound processing. "Smart HA's" with adaptive algorithms and performing logical operations can be build around DSP technology to further improve HA's capabilities.

In our opinion DSP is still an underexplored technology in the area of HA's, but this may change in the near future with anticipated benefits to the hearing impaired.

HA's however sophisticated never would be a panacea for hearing impairment. Hearing impairment reduces information channel capacity (from outside world to auditory system) and this can't be restored with a hearing aid. HA's can only help to better utilize the remaining information channel capacity.

References:

[1] Sammeth Carol A. PhD, "Digital Hearing Aids", Seminars In Hearing, Vol. 11, No. 1, 1990.
[2] Hecox Kurt E. MD PhD and Miller Eric, MSPA," Foundations for the introduction of new hearing instrument technologies", Hearing Instruments, Vol. 38, No. 11, 1987.
[3] Kates James M.," Signal processing for hearing aids", Hearing Instruments, Vol. 37, No. 2, 1986.
[4] The Manhattan II Circuit specification book, Argosy Electronics, Minneapolis MN 55495-0156.
[5] Killion Mead C. PhD," An "acoustically invisible" hearing aid", Hearing Instruments, Vol. 39, No. 10, 1988.
[6] Killion Mead C. PhD," A high fidelity hearing aid", Hearing Instruments, Vol. 41, No. 8, 1990.
[7] Chiasson Carl R., MA, and Davis Robert I., PhD, "A comparison of DAF and HPF hearing instruments on speech discrimination", Hearing Instruments Vol. 41, No. 1, 1990
[8] Sweeny Dan, "Parallel Universes - DSP for the hearing impaired", Audio Magazine, September 1990.
[9] Taylor Richard R., "Sorting through the capabilities of noise reduction approaches", Hearing Instruments Vol. 39, No. 3, 1988.
[10] Conger Chris, MSEE, "Understanding digital technology in hearing instruments", Hearing Instruments Vol 41, No. 3, 1990.
[11] "Programmable Hearing Aids, A thumbnail-sketch of the programmable instruments currently or soon to be commercially available", The Hearing Journal, Vol. 42, No. 5, May 1989.
[12] The Digitally Programmable Hearing Instrument: Technical articles received from PHOX Minneapolis MN 55459-0156.
[13] Herbst Gerd PhD, "The digitally programmable hearing instrument Part II: The PHOX", Hearing Instruments, Vol. 40, No. 3, 1989.
[14] Hall Mike C. MA, and Jacobs Elise L. MA, "A review of a digitally programmable, full dynamic range hearing device", Hearing Instruments, Vol. 42, No. 4, 1991.
[15] Hayes Donald MA, CCA, "Clinical trial of the Widex Quattro Multichannel, Hearing Aid", OSLA Newsletter, Vol. 6, No. 4 December 1990.
[16] Sandlin, Robert E. PhD, and Andersen Henning H., MScEE, "Development of a remote-controlled, programmable hearing system", Hearing Instruments, Vol. 40, No. 4, 1989.
[17] Rapisardi Doris MA, "Bridging the gap between product R & D and the consumer", Hearing Instruments, Vol. 40, No. 10, 1989.
[18] Gauthier E.A., "Bringing High Fidelity Out of the Lab And Into the Dispenser's Office", The Hearing Journal, Vol. 42, No. 9, September 1989.
[19] Roeser Ross J. PhD, and Taylor Kenya EdD, "Audiometric and field testing with a digital hearing instrument", Hearing Instruments, Vol. 39, No. 4, 1988.
[20] Fielder Louis D., "Human Auditory Capabilities and their consequences in Digital-Audio converter design", Conference paper presented at AES 7th International Conference in Toronto,1989.
[21] Harrison R.V. PhD, "The Physiology of the Normal and Pathological neurons - some recent advances", The Journal of Otolaryngology 15:1 1986.
[22] Neuman Arlene C. et al.,"An evaluation of three adaptive hearing aid selection strategies", J. Acoust. Soc. Am. 82 (6), December 1987, 1967-1976.
[23] Lippmann R.P. et al., "Study of multichannel amplitude compression and linear amplification for persons with sensorineural hearing loss", J. Acoust. Soc. Am. 69 (2), Feb. 1981, 524-534.
[24] Hecox Kurt E. MD PhD, Miller Eric MSPA, "New hearing instrument technologies", Hearing Instruments, Volume 39, No.3, 1988.
[25] "1991 Buyer's Guide to Programmable Hearing Instruments", The Hearing Journal, Vol.44, No.5, May 1991, 37-41.
[26] Hall Mike C. MA, Jacobs Elise L. MA, "Evaluation of a digitally programmable full dynamic range hearing device", Hearing Instruments, Vol.42, No.6, June 1991, 18-19.
[27] Fox Barry, "DCC: Mono fools", in "Studio Sound" Magazine, April 1991.
[28] Corliss Edith L.R., "The Ear as a Mechanism of Communication", J. Audio Eng. Soc., Vol.38, No.9, September 1990, 640-652.
[29] Levitt Harry PhD, "Digital hearing instruments: A brief overview", Hearing Instruments, Vol.39, No.4, 1988, 8-12.
[30] Roland-Mieszkowski M., "Introduction to Digital Recording Techniques", invited paper-demonstration, "Acoustic Week in Canada" - CAA Conference, Halifax, N.S., Canada, October 16-19, 1989, Proceedings, 73-77.

UPDATE TO NOISE CONTROL DIRECTIVE ID 88-1

Dave DeGagne
Richard Wright
Energy Resources Conservation Board

Introduction

The ERCB has authored and enforced a number of Noise Control Directives for the energy industry since 1973. The most recent of these is Interim Directive ID 88-1. This Directive evolved from a common realisation that previous directives were too simplistic with their singular maximum day and night-time sound levels. The development of ID 88-1 sought to incorporate input from all appropriate stakeholders in noise problems generated by energy industry developments in the province of Alberta. To accomplish this, a committee comprised of members from the public, industry, acoustical consultants, university academics and governmental agencies was struck with co-ordination provided by the ERCB. The resulting Directive tries to take a balanced viewpoint of all these potential players through a reasonable unbiased policy.

The new Noise Control Directive and its accompanying handbook Guide G-38 were issued at the end of September 1988 with the specified condition that it must be reviewed after a 2-year period. The complexity of the Directive required this test period, so that flaws and shortcomings in the workability and effectiveness of the Directive would be identified and brought back to committee for review and change, if necessary.

Highlights of the Noise Control Directive

The predecessors to the existing Directive were ID 73-1 and later ID 80-2 which gave 65 dBA day-time and 50 dBA night-time maximum noise levels measured in proximity to a complainant's residence. These were one-page documents while today's Directive is nine pages long with an accompanying guide that is thirty pages long. Determining whether a facility is in violation of the Noise Control Directive is not as simple as taking a number of spot noise level readings and matching these against some scale but rather following a step process which assesses the extent of the problem using a number of applicable criteria.

To give you some insight into how this is achieved, it is necessary to first calculate the Permissible Sound Level. The Permissible Sound Level as defined in the Directive represents the "maximum allowable sound level emanating from the facility measured 15 metres from the nearest or most impacted dwelling in the direction of the source". This calculation starts with the Basic Sound Level determination using a table, representing the night-time values, which evaluates the residence on its proximity to sources of transportation noises and dwelling unit density. In addition, there is a 5 dBA allowance incorporated into the Basic Sound Level to account for industrial presence. If day-time noise is an issue, a value of 10 dBA can be added realizing that this is typically noisier than night-time. There are then two sets of adjustments that can be added, one for specific aspects of the facility and environment and the second adjustment for whether or not the noise source is of a temporary duration. All values are presented in dBA Leq and can vary significantly depending on the above criteria.

Of these sets of adjustments, the Class A adjustment takes into consideration three factors. The first is a seasonal assessment for predominantly winter-time noises, the second is applicable only when audible characteristics of a permanent facility are absent of both tonal and impulse/impact components and the third one is an ambient monitoring adjustment which allows for an incremental change of the Basic Sound Level to reflect characteristics of the actual ambient sound environment. This third factor can be used only when it is proven through a 24-hour continuous sound monitoring survey that the Basic Sound Levels assumed for the area are significantly different than the true ambient sound levels measured through the survey.

The second set or Class B adjustment values involves the duration of the noise source. For short duration activities, specifically those of either less than 1 day, 1 week or 2 months, a factor can be added to allow for the temporary nature of the noise source. A maximum Permissible Sound Level is subsequently derived not to exceed 66 dBA after all adjustments have been taken into consideration. The only exception to this is that the Permissible Sound Levels do not apply for an emergency situation which are "unplanned events requiring immediate action to prevent loss of life or property".

The Directive is very explicit in the way it is to be applied. In the case of a complaint, the Comprehensive Sound Level from the suspect energy facility must be determined using appropriate measurement instrumentation and techniques. It must also be of a certain duration in length, no less than 6 hours and no more than 24 hours, as well as being performed under representative portions of the time of day or night on typical days when the noise causing the complaints occur.

Also contained in the Directive is the option to use an appropriate isolation analysis technique when it appears the facility's noise contribution to the Comprehensive Sound Level may be in fact below the Permissible Sound Level. If this were the case, further action may not be required by the facility owner.

Finally, the Directive notes that some "grey" areas may exist and there will be situations which do not fit into the categories that have been identified. These exceptional cases will be reviewed by the ERCB on an individual basis and if necessary, alter the Permissible Sound Level to a higher or lower limit accordingly. In all situations, the results of the Comprehensive Sound Level Survey as compared to the calculated Permissible Sound Level establishes whether or not a facility is in compliance with the Directive.

Directive Review Process

Since the Directive has been in effect, industry and the ERCB have jointly dealt with approximately 150 noise complaints. In the course of dealing with these, a great deal of experience in working with this Directive has been gained with the realization that some refinements are in fact required. The original working committee was reconvened in mid-January 1991. A complete review of the Directive was initiated looking at all facets and assumptions used in the so-called pass/fail criteria. The overall consensus is that all parties are satisfied that the table format and the numbers in them are working reasonably well. There were, however, a number of concerns which will need to be addressed, the most important of these are:

- Many of the committee's participants felt that there were too many uncontrollable or unknown factors that affect noise survey results especially where a facility either marginally fails or passes. Again, it was felt that the Directive should more clearly spell out what would happen on these marginal cases including some kind of mechanism for resolutions. The ERCB recognizes that marginal cases do exist and will have to be dealt with under a dispute resolution process. The ERCB's Legal Department will advise what mechanisms are available in its mandate to accommodate this. The results of this review may be incorporated into the Directive.

- The night-time starting point should be changed from the present 2200 hours to 2100 hours.

- The wording around the isolation analysis technique should be made more explicit so that everyone can understand the rules. A subcommittee was struck to look at the wording and recommend appropriate changes.

- Informing the public of the existence of the Directive. The ERCB will consider a pamphlet describing the Noise Directive which could be either handed out or included as additional information in other relevant publications.

- A major concern dealt with expertise not only in industry but at the ERCB. The ERCB is committed to maintaining a high degree of expertise in noise control and will actively promote training and development of its head office and field staff in this area in order to enforce the Directive in a fair and credible manner. The same commitment is expected from the energy industry.

- The adjustment for tonal component was recommended to be measured on the A-weighted scale instead of the linear scale. Even though it has been used infrequently to date, industry does not want to see this adjustment disappear. The committee agreed with both these recommendations.

- The maximum wind speed value specified by the Directive of 15 kilometres per hour is seen by some as too high and having a more pronounced effect on measured sound levels than previously anticipated. The concern is with the effect a 5 to 10 kilometres per hour wind can have on sound levels if one measures upwind versus downwind. The subcommittee looking at isolation analysis techniques will also investigate some workable solution to aid in understanding this problem.

- The Directive is only to be used in cases where a complaint has been filed or when new facilities are being planned. Some in industry would like to see a grandfathering clause for all pre-1988 facilities allowing them to add an adjustment for facilities built before issuance of this Directive. This is a concern because there is little protection afforded industry, should residents encroach upon an existing facility. Industry has also suggested that there be a way to identify new residential developments before subdivisions applications are approved or building permits are issued. It is felt however that this would pose a very cumbersome and slow process. As an alternative, it was suggested that a 6 dBA increase for each halving of the distance between the facility and the original closest residence be assigned. This would only be a stop gap measure until the basic question of encroachment is addressed. The ERCB has agreed to take this issue under advisement and intends to propose to committee a method to deal with it.

- There is a concern that the effect of noise control should not adversely affect other environmental-related emissions. For example, the use of electric-driven motors, while quieter, increases the generation of electricity by coal which increases CO_2 emissions. It may be more appropriate for industry associations to raise this at more applicable forums.

- A unanimous resolution was that the document needs clarification as opposed to simplification. The industry associations will endeavour to find an editor who will do an initial attempt on this clarification.

In addition to these specific items discussed in committee, ERCB staff are also considering several additional issues which may have to be addressed in the revised Noise Control Directive. These relate to vibration as it may need to be recognized as a negative impact on the quality of life some people enjoyed prior to living near large low-frequency sound emitting sources. Another is the need to put in place guidelines as to how extended duration sound monitoring results will be averaged to arrive at an appropriate day-time or night-time Leq value. The Directive presently has a 24-hour limit set on monitoring length requirements while some cases may warrant extending this limitation.

Conclusion

Because of the hard work and dedication of many key individuals, Alberta's citizens and energy industry have a Noise Control Directive that is a fair and equitable piece of legislation. It is designed to protect the public and industry alike using the most up-to-date knowledge in the measurement and effects of industrial noise. Further modifications to the Directive will eventually be required as experience grows or advancements in technology become known.

A proposal for a new federal regulation on noisy toys.

Tony Leroux and Chantal Laroche
Sonométric Inc., 5757 Decelles Ave., Suite 514, Montréal (Québec) H3S 2C3

1. Introduction

The Federal Act prohibiting sale of hazardous products limits the sound level emitted by toys to 100 dB [1]. A review of the literature shows that this criteria is not safe for children regarding the risk of developing hearing loss [2]. Based on a world wide accepted safe limit of 75 dBA [3], more than 85 % of the toys available on the canadian market are not safe and may induce hearing loss and other adverse effects on the long term [4]. This needless risk for children health could be avoided by having a more adequate federal regulation.

2. Inefficiency of the actual regulation

Two factors can explain the inefficiency of the current law.

The actual limit for sound level is too lax. The literature tends to demonstrate that children's inner ears are more sensitive to noise exposure and may develop hearing loss with noise dose that are safe for adults [5,6,7,8]. In the light of those findings the current limit of 100 decibels appears to be by far too high.

Toys emitting noise from explosive source (firecrackers and cap gun for example), can be very harmful to hearing after one short exposure [9]. These toys are beyond the scope of the current Act and are covered by the federal Act on Explosives which equally regulates industrial explosives.

On the other hand, the federal regulation does not include a precise and specific method for determining the sound level produce by a given toy. The actual legal text does not precise the frequency weighting to be used for dB nor any other technical specifications for determining the sound level, for instance:

a) type of experimental room,
b) type of noise produced by the toy and
c) nature of the toy

Morever, actually there is no systematic way to test a toy manufactured in Canada or entering into this country. In fact, the actual Act authorizes the sale of hazardous noisy toys that may induce to some extent hearing loss in our young population.

3. Proposal of a new regulation

The actual proposal is to lower the limit to 75 dBA for continous noise source at the distance which the toy is usually used and to limit the level at 95 dB peak for toys producing impulsive noise. Every toy should be controlled under the same experimental conditions in the manner edicted by CSA Z107.71- 1981 Standard on Consumers Small Appliances [10].

This existing Standard, already approuved by federal government and manufacturers, could be applied to sound emitted by toys. In addition, this method can be easily implemented technically and economically for both, toy manufacturers and federal responsible agency. This method of determining sound level produced by a given toy insures a uniform application and should be adopted and be part of the regulation.

Furthermore, because of the high level of risk for noise-induced hearing loss even after one single exposure, toys emitting noise from explosive source should be banned. This specific point must be included in the federal Act on hazardous products as also suggested by others reseachers in scandinavian countries [11].

Every toy sold in Canada must be tested to insure a safe noise level in the same manner the lead toxicity of toy's paint is tested by industry and government agency.

4. Conclusion

This proposal intends to reach a better achievement in protecting children's hearing integrity when it comes to noisy toys. The numerous failures identified in the actual Act should be corrected easily using a well documented safe noise level and a precise method of determining it as proposed above. These suggested legislative modifications will not impose a large economical load on federal government nor on toy manufacturers.

5. References

1. The Gazette of Canada II (1980) An Act to prohibit the advertising, sale and importation of hazardous products (1968-69. c.42, schedule part I).

2. Leroux, T. et Laroche, C. (1991) Projet de réglementation sur les jouets bruyants. Revue de littérature. Association des Consommateurs du Québec. Report granted by Consumers and Corporate Affairs Canada.

3. Organisation Mondiale de la Santé (1980) Critères d'hygiène de l'environnement 12 - Le bruit.

4. Lacombe, F. (1989) Les niveaux sonores des jouets, évaluation de la situation. University of Montréal, Faculté de Médecine, Ecole d'orthophonie et d'audiologie.

5. Douek, E., Dodson, H.C. Bannister, L.H. and Ashcraft, P. (1976) Effects of incubator noise on the cochlea of the newborn. Lancet, nov. 20, pp. 1110-1113.

6. Stennert, E., Schulte, F.J. and Vollrath, M. (1977) Incubator noise and hearing loss. Early Human Development, vol. 1, pp. 113-115.

7. Bess, F.H., Peek, B.F. and Chapman (1979) Further observations on noise levels in infant incubators. Pediatrics, vol. 63(1), pp. 100-106.

8. Uziel, A. (1985) Non-genetic factors affecting hearing development. Acta Otolaryngol (Stockholm), supp. 421, pp. 57-61.

9. Gupta, D. and Vishwakarma, S.K. (1989) Toy weapons and fire crakers: A survey of hearing loss. Laryngoscope, vol. 99, pp. 330-334.

10. CSA Standard Z107.71-M1981 (1981) Measurement and rating of the noise output of consumer appliances. Canadian Standard Association.

11. Axelsson, A. and Jerson, T. (1983) How much noise can children stand. An investigation of noise from toys. The National Swedish Board for Consumer Policies.

[Work done for the Quebec Consumers Association and granted by Consumers and Corporate Affairs Canada].

ACOUSTICAL ANALYSIS OF NASAL RESONANCE PATTERNS IN SPEECH

Anne Putnam Rochet
Department of Speech Pathology & Audiology

Bernard L. Rochet
Department of Romance Languages
University of Alberta, Edmonton

1. Background and Introduction

Under normal speaking circumstances, a nasal quality is associated with the production of nasal consonants in spoken English, and with a nasal consonant or vowel in spoken French. In addition, the influence of a nasal consonant tends to "spill over" to vowels that precede or succeed it, a phenomenon known as anticipatory or carry-over assimilation nasality, respectively. A certain amount of assimilation nasality is normal in languages where nasal consonants are a part of the speech sound repertoire. There are limits to what is perceived as normal, however, within and across languages. English and French, for example, differ with respect to phonemic and assimilation nasalization characteristics; therefore, inappropriate nasalization can distort the intelligibility of French spoken by anglophones, and vice versa. Within a language, less than the expected amount of nasality or assimilated nasality during speech is referred to as "hyponasal" resonance, and more than the expected amount as "hypernasal" resonance. Disorders of resonance, particularly hypernasality, degrade speech intelligibility in any language.

Historically, the acoustical characteristics of normal or deviant nasal resonance have been difficult to document or quantify instrumentally. Speech scientists, linguists, teachers of French or English, and speech-language pathologists have had to rely primarily on listeners' identification (i.e., auditory perceptions) of normal, hypo- or hypernasal resonance in the study of nasality patterns across languages and in speakers whose resonance is distorted. Although this subjective method does have social validity, it is not always reliable across repeated measures and not easy to incorporate systematically into speech research or second-language teaching protocols. Therefore, interested investigators continue to seek instrumental methods to document and quantify normal and deviant nasal resonance patterns reliably in connected speech, to complement the subjective, qualitative assessment of resonance balance within and across spoken languages.

This paper describes a dual-channel, analog/digital analysis system that we have applied to the study of oral/nasal resonance patterns in Canadian English and European French, for normative data against which to compare speakers of either language who have deviant nasal resonance, and as a basis from which to teach persons learning to speak English or French as a second language.

2. Instrumental Array

The oral and nasal acoustical components associated with subjects' productions of test utterances are transduced by means of two uni-directional microphones positioned in front of the mouth and nose and separated by a metal plate (Kay Elemetrics Nasometer 6200) and recorded on separate channels of an FM tape recorder (Hewlett-Packard 3964A). The oral and nasal signals for a given token on the FM recorder are low-pass filtered (@ 4800 Hz via matched Frequency Devices 901 filters) and digitized at 10 kHz via CSpeech waveform analysis software (Milenkovic, 1990) supported by an IBM-AT. The vowel portions of the oral and nasal components of each digitized signal are isolated and stored as CSpeech files. These files are converted to rms values by means of software customized for operation in MS-DOS, and the degree of nasalance is established by comparing rms amplitudes of corresponding oral and nasal data across the duration of a vowel in 5 ms steps, according to the formula:

$$\% \text{ nasalance} = [(\text{nasal rms}/\text{nasal} + \text{oral rms}) \times 100].$$

Figure 1 schematizes the oral/nasal data acquisition, analog-to-digital conversion and comparative analysis sequence.

3. Representative Data

Thirty normal adults, 15 speakers of Canadian English and 15 of Standard French have been recorded using this system (Rochet & Rochet, 1991). The data base consists of English vowels /i, I, E, a, u/ and French vowels /i, E, a, u, y/ embedded in the contexts CVC, NVC, CVN and NVN, where V= one of the target vowels, C= a non-nasal obstruent, and N= /n/ or /m/. Each word is produced as the terminal item in a carrier phrase, e.g., "A half keen." or "Neuf quines." and ten repetitions of every token are obtained from each subject. Figure 2 illustrates raw data for the non-nasal (CVC) utterance, "A half keet," produced by a female speaker and digitized in CSpeech. Figure 3 illustrates an edited version of that utterance in which just the syllable "keet" has been isolated; further editing isolates the vowel nucleus for rms conversion and temporal analysis. Figure 4 shows the syllable "neet," a carry-over (NVC) nasality context. Figure 5, "keen," illustrates an anticipatory (CVN) nasality context, and in Figure 6, "neen," the vowel is surrounded by nasal consonants in the NVN context. Figures 7 and 8 are examples of the final product of data analysis in which assimilation nasality patterns for the English and French speakers are compared graphically with respect to the proportions of vowels common to both languages that are nasalized (i.e., nasalance >0.5) following the nasal consonant in the NVC context (Figure 7), and in anticipation of the nasal consonant in the CVN context (Figure 8).

Such data not only illustrate the differences in assimilation nasality patterns within each language as a function of vowel height but also allow assimilation nasality patterns between languages to be compared for differences that are salient to second language teaching, perception and production.

4. References

Milenkovic, P. (1990). Department of Electrical and Computer Engineering, University of Wisconsin, Madison, WI 53705 U.S.A.

Rochet, A.P. and Rochet, B.L. (1991). The effect of vowel height on patterns of assimilation nasality in French and English: Quantification and interpretation. Proceedings of the XIIth International Congress of Phonetic Sciences, Aix-en-Provence, France.

Figure 1

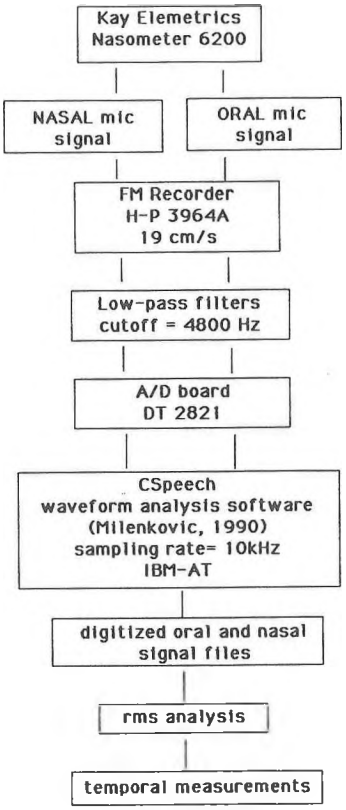

Figure 2

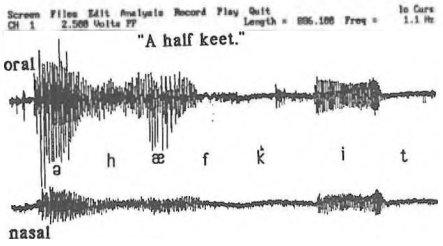

Figure 3

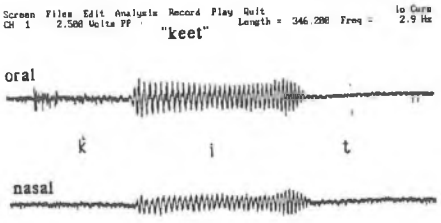

Figure 4

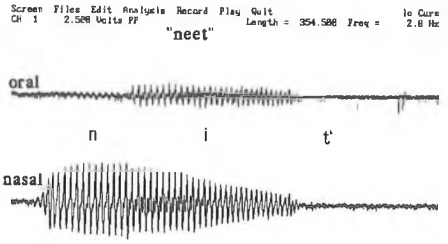

Figure 5

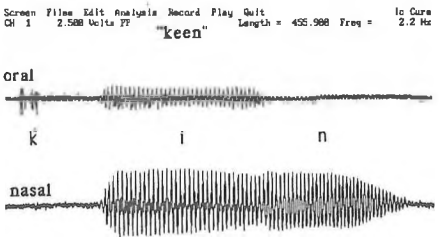

Figure 6

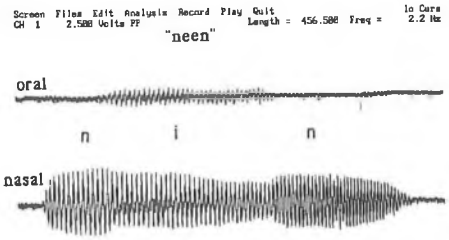

Figure 7

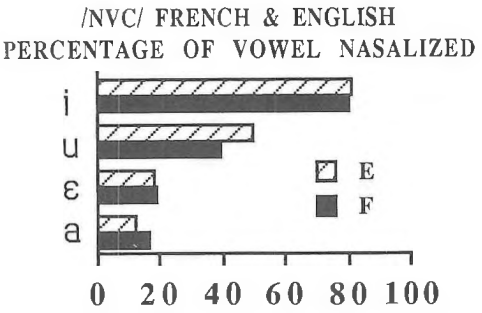

Figure 8

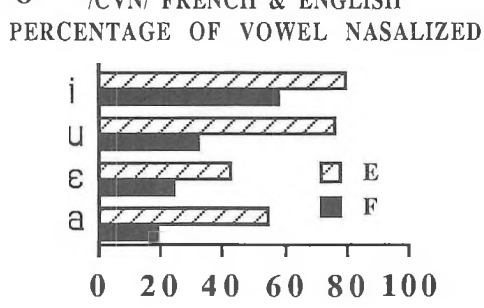

DEVELOPMENTAL ASPECTS OF SECOND FORMANT TRAJECTORIES

Megan M. Hodge
Glenrose Rehabilitation Hospital, Edmonton, Alberta

1. Introduction

This investigation was based on the premise that the development of spatial-temporal control for speech production is governed by principles similar to those that characterize the development of spatial-temporal control for coordinated action in other skilled movements. Accordingly, it is predicted that as speech skill increases, an increase in the accuracy, speed, consistency and economy of speech movements should be evident. Correspondingly, measures of perceptual and acoustic correlates of these same phenomena should be sensitive to developmental changes in speech skill.

This paper presents the results of an acoustic investigation of the relationship between increasing talker age and the "speed" of speech movements, i.e., the speed at which the size and shape of the vocal tract changes to produce the sequences of consonant and vowel sounds in the speech signal. The speaking rates of young children are typically slower than those of adults [1]. One factor contributing to the slower speaking rates of children is their greater syllable durations, compared to adults. The purpose of this investigation was to determine if the greater syllable durations of children are attributable to slower rates of articulatory movement as indexed by second formant (F2) transition rate. The specific hypotheses to be tested were that as talker age increased to young adulthood (a) an increase in F2 transition rate (corresponding to an expected increase in speed of articulator movement), and (b) a decrease in the intra-subject variability, in F2 transition rates, would be observed.

Changes or "transitions" in the locations of the first (F1) and second (F2) formants in the speech signal over time have been used to make qualified inferences about the relative extents, durations and rates of change in vocal tract position as talkers produce a sequence of speech sounds [2, 3]. Changes in the frequency of the energy region corresponding to F1 are associated with changes in the degree of major vocal tract constriction and those corresponding to F2 are associated with changes in the anterior-posterior site of major vocal tract constriction. Over the course of an utterance, a trajectory of the changes in formant frequency can be obtained.

A prerequisite to testing predictions about relationships between measures of speech spectra such as formant frequencies, and increasing talker age is to identify satisfactory spectral normalization procedures. This is necessary to eliminate the absolute resonant frequency differences that result from vocal tract size differences so that interage differences in magnitudes of spectral change that are due to vocal tract size alone are not misinterpreted as developmental differences in speech production behaviors. The normalization procedure used involved a transformation of frequency measures in Hertz to the Bark scale using the method described by Syrdal [4]. The spectral measures compared across speakers were formant transition extents, defined as the amount of change or difference from the onset to the offset of the consonant-vowel transition for the opening gesture of the first syllable in the word "baby".

2. Outline of the Experiment

Twenty males in each of four age groups (2.5-3.5 years; 5-6 years; 9-10 years and 20-30 years) and 10 males between 14-22 months served as subjects (N=90). All subjects included passed a hearing, speech and language screening appropriate to their chronological age. Multiple productions of the word "baby" were recorded from each subject. Recordings were obtained in a sound-treated booth using a Shure Model 10A head-mounted microphone or a Sony Electret 150 microphone connected to a Sony Model 399 reel-to-reel tape recorder running at 19 cm/s.

Spectrograms were prepared for five repetitions of the word for each subject in the four older groups and for 3 to 5 repetitions for each subject in the youngest age group. The Kay 7800 and 5500 Digital Sonographs were used to generate the spectrograms, using filter bandwidth and dynamic range settings that provided the clearest resolution of the formant pattern. Each spectrogram was prepared for further analysis by marking the vowel segment in the first syllable from the first to the last clearly defined glottal pulse. The interval between these two points provided the duration of the vocalic portion of the syllable. The mid-point of F2 was then hand-traced from the begining to the end of this interval. These marked spectrograms were then analyzed by means of a computer program that processed and stored data on a graphics tablet connected to a mainframe Harris computer. The data for each utterance were stored in a file that included an identifier for each measure and a listing of time (x axis) and frequency (y axis) points. Following entry of the formant trajectories, the frequency data in the files were converted to Bark values. Formant transition rate was determined by calculating the extent of spectral change from the onset to the offset of the formant transition of interest and then dividing this extent by the time interval between these two points, i.e., the formant transition duration. The onset value was defined as the first spectral value in the trajectory and the offset value was defined as the first occurence of maximal spectral change, in the direction of interest, rounded to the nearest 0.01 Bark.

3. Summary of Results

a) As shown in Table 1, durations of the vocalic portion of the syllable were greatest for the one year-olds (M=208 s) and least for the adults (M=164).

b) Mean F2 transition extents were greatest for the three youngest age groups and least for the nine year-olds. Similarly, F2 transition durations were greatest for the three year-olds and

least for the nine year-olds (see Table 1).

c) Mean F2 transition rates were similar across the five age groups, ranging from 0.113 Bark/ms for the one year-olds to 0.0096 Bark/ms for the three year-olds (see Table 1). The adults and the one year-olds had the greatest F2 transition rates. A perceptual analysis of the tokens revealed that many of the one year-olds' productions were characterized by an /i/ rather than an /e/ vowel quality in the first syllable, i.e., /bibi/ rather than /bebi/.

d) The intra-subject standard deviations for F2 transition rates across the multiple repetitions of the word exhibited the expected age trend, i.e., as age increased, the mean intra-subject standard deviation decreased. However, when the intra-subject standard deviations were compared for a subset of the time-matched subjects from each age group (vowel durations ranging from 155-200 ms), the two youngest groups still demonstrated the greatest mean intra-subject standard deviations, but the four older age groups did not show a well-defined age trend.

Age (yrs)	Extent (Bark)	Duration (ms)	Rate (Bark/ms)	Vowel Duration (ms)
1	1.21	103	.0013	208
	(.41)	(29)	(.0031)	(64)
3	1.22	128	.0096	203
	(.51)	(33)	(.0035)	(34)
5	1.20	124	.0101	205
	(.33)	(24)	(.0027)	(32)
9	0.91	95	.0100	172
	(.26)	(32)	(.0031)	(42)
Adults	1.14	106	.0111	164
	(.29)	(27)	(.0023)	(32)

Table 1. Group means and standard deviations of the F2 transition rates for the first CV in "baby".

Age (yrs)	All Subjects		Time-Matched Subjects	
	M	SD	M	SD
1	.0053 (n=10)	.0022	.0061 (n=4)	.0035
3	.0033 (n=20)	.0019	.0058 (n=6)	.0038
5	.0026 (n=20)	.0017	.0017 (n=6)	.0008
9	.0025 (n=20)	.0013	.0023 (n=6)	.0011
Adults	.0023 (n=20)	.0014	.0027 (n=6)	.0013

Table 2. Group means and standard deviations of the intra-subject standard deviations of F2 transition rates in the first CV of "baby". Data for a subset of time-matched subjects are also reported.

4. Conclusions

a) First it is obvious that the results did not support the initial hypothesis, i.e., that an increase in the rate of spectral change, and inferred increase in rate of articulatoy speed, would be observed as talker age increased. Rather, F2 transition rates appeared relatively stable across the four older age groups. As F2 slope has been associated with the intelligibility of an utterance [5], F2 transition rate may be determined by phonetic identity and as such, not influenced by increasing control of the articulators. However, F2 transition extents and durations appeared to be postively related, i.e., the greater the extent, the greater the duration, and these values generally decreased with increasing age. Thus, the longer durations of the vocalic portions of the younger children's syllables appeared to be associated with greater extents of F2 frequency change rather than slower F2 transition rates, compared to the adults. Stated a different way, the adults exhibited spectral and temporal "vowel reduction" compared to the children.

b) The high F2 transition rates of the one year-olds appear to reflect the greater F2 values associated with the high front vowel /i/ and suggest that these children were not producing the more finely graded movement for the mid-front vowel /e/ in the first syllable of the word "baby".

c) As expected, the intra-subject trial to trial variability in F2 transition rates decreased monotonically as age increased. However, when vowel duration was controlled, this relationship was not evident for the four older groups. This finding supports the point [6] that caution needs to be exercised when using variability measures to index speech sensorimotor development when (a) there is a dependent relationship between the size of the mean and standard deviation of the distribution of the measure of interest, and (b) there are potential differences in the shapes of the distributions to be compared.

5. References

1. Haselager, G, Slis, I Rietveld, A. An alternative method of studying the development of speech rate. Clinical Linguistics and Phonetics. 1991; 5:53-64
2. Weismer, G, Kent, RD, Hodge, M, Martin, R. The acoustic signature for intelligibility test words. Journal of the Acoustical Society of America. 1988;84:1281-1291
3. Kent, RD, Weismer, G, Kent, J, Rosenbek, J. Toward phonetic intelligibility testing in dysarthria. Journal of Speech and hearing Disorders: 54:482-500
4. Syrdal, A. Aspects of a model of the audiotory representation of American English vowels. Speech Communication. 1985;4:121-135
5. Kent, RD, Kent, J, Suffit, G, Brooks, B, Rosenbek, J. Relationships between speech intelligibility and the slope of second formant transitions in dysarthric subjects. Clinical Linguistics and Phonetics. 1989;3:347-358
6. Munhall, K. Articulatory variability. In P. Square-Storer (Ed) Acquired apraxia of speech in aphasic adults: Theoretical and clinical issues. 1989:64-83

THE ROLE OF PHONETIC CONTEXT IN THE ARTICULATION OF SEMIVOWELS BY PRESCHOOL CHILDREN

Elzbieta B. Slawinski Psychology Department, The University of Calgary

Introduction

One of the most important tasks children face during preschool years is learning how to speak intelligibly. Children's early speech is characterized by a number of differences from that of adults, such as various types of phoneme, and in particular consonant, misarticulations including omissions, substitutions, and distortions. Therefore, "it might be imagined that if there were any major issue in child phonology for which study of consonants alone was sufficient it would be that of how correct consonant production is acquired. In fact, the typical focus on consonant acquisition independent of vowel acquisition involves the tacit assumption that consonants are context independent" (Davis & MacNeilage, 1990, p 16). The phonetic context which involves a certain degree of coarticulation can facilitate or even interfere with correct production of the phonetic segment. Coarticulatory influences can be due to the anticipatory effect of an upcoming phonetic segment or to inertial carry-over effect of a preceding segment. Recasens (1989) demonstrated that anticipatory coarticulations reflect phonemic preprogramming while carry-over effects are mainly due to articulatory constraints. Therefore, the effect of phonetic context could explain why misarticulations are often inconsistent.

One of more frequent children's misarticulations is a gliding of prevocalic liquid. Some aspects of /r/ misarticulations due to coarticulation can be understood by knowing the extent to which individual phonemic segments restrict the position of the various articulators. The /r/ productions are characterized by the tongue tip pointed upward and slightly backward in the mouth cavity, or by bunching of the tongue in the center or near the front of the mouth cavity. Therefore, the production of the phoneme /r/ is very demanding on articulators, as the palatal /r/ strongly restricts the blade, dorsum and body of the tongue. The glide /w/, which is close to the phoneme replacing /r/ during misarticulations, is characterized by a gradual move from a rounded and narrowed configuration to the lip shape required by the following vowel, simultaneously with a change in tongue position from high-back to the position for the following vowel. Thus it seems a plausible assumption that the vocalic quality of consonants' neighbors, which constitute the totality of their active environment, affect the consonants' production.

The present study addresses the following questions about children's production of the phoneme /r/: 1) How are misarticulated phonemes different from those that are correctly produced? 2) Does the phonetic context of the following vowel influence phoneme production?

Method

1. Subjects.

The subject population consisted of two groups of 5 preschool children with normally developing articulation skills, ranging in age from 3 years 3 months to 4 years 2 months. The children were monolingual speakers of English, and had no history of speech or language difficulties. The first (control) group consisted of children with a mean age of 3 years 7 months, highly intelligible speech and no misarticulation. The second (misarticulated) group consisted of children with a mean age 3 years 9 months, was also characterized by highly intelligible speech, with the exception of /r/ misarticulations.

2. Stimuli.

A set of four objects or pictures corresponding to words beginning with the /r/ phoneme and followed by four different vowel environments (/i/, /e/, /ae/, and /a/) were chosen as stimuli (e.g. rock, rabbit, read).

3. Procedure.

The procedure for collecting the pertinent data was divided into two steps: 1) gathering samples of speech; 2) analyzing speech to determine the nature of physical differences between samples of the /r/ phonemic segment and its misarticulations. A set of 4 objects or pictures representing the stimuli words were placed in front of the seated child. The children were then asked to name these. Five tokens of each of the words with /r/ in the initial position followed by vowels /i/, /e/, /ae/, and /a/ were collected in a random manner and recorded.

4. Acoustical analysis.

Tokens were digitized using a MAC II computer with 20kHz sampling rate, 12-bit quantization and a 9.6-kHz low-pass filter. The samples were classified as being an /r/ or a misarticulated /r/. Spectrograms of these samples were analyzed in the frequency and time domains, 25 ms Hamming window, frequency range from 0 Hz to 10 kHz, and high-frequency shaping. Using criteria discussed by Chaney (1988), the transition onset point of the consonant was

defined as the starting point of directional shift in the F2 transition. Transition termination was defined as the point where transition reached the vowel steady state. At such determined points spectra were analyzed, and frequencies of onsets and offsets of the F2 transition were measured. A similar method was applied to determine the onset and offset of F3 transitions.

Results

The analyses of the /r/ productions showed that the percentage of misarticulation for the entire subject population was dependent on the context of the following vowel. When /r/ was followed by a front vowel, the misarticulation percentage was 32.6%. This error rate increased to 40% when the vowel was produced in the back of the vocal cavity. Moreover, differences in the number of misarticulations were found among /r/ articulations followed by the front vowels. The highest error rate of 37% was associated with the low vowel /ae/, followed by 32% (high vowel /i/), and 28% (middle vowel /e/).

Acoustic analyses showed strong lingual coarticulatory effects for /r/ articulated subjects and no such effect for /r/ misarticulated subjects. For the /r/ articulated group, significantly different onset frequencies of the F3 transition were found in four vocalic environments ($F(3,44)=3.38$ $p<.05$). This result was due mainly to the higher onset frequency of the F3 transition (2222 Hz) in the environment of the back vowel /a/, as compared to lower onset frequencies in the vocalic environment of front vowels (/ae/-2174 Hz; /i/-1954 Hz; and /e/-1949 Hz). The differences between onset frequencies of F3 and F2 transitions (cue for /r/ recognition) were context dependent ($F(3,44)=5.053$ $p<.5$). (/ae/-991 Hz; /i/-705 Hz; /e/-654 Hz; and /a/-968 Hz). However, the /r/ articulated children did not show differences in F2 transition duration, which was on average (for the four vocalic contexts) equal to 65 msec. Moreover, onset frequencies of the F2 transition did not differ significantly in the four vowels contexts, and could be described by a mean of 1245 Hz. The group of misarticulated children did not demonstrate significant differences dependent on phonemic context on any of the above described measures. However, differences between onset frequencies of F3 and F2 transitions varied depending on the following context. The mean differences were equal to 2009 Hz, 2086 Hz, 2356 Hz, and 2542 Hz for /ae/, /i/, /e/, and /a/ vocalic contexts respectively. Thus, the /r/ misarticulated phonetic segment was produced in a similar manner in all examined phonetic contexts, with mean for transition duration (average for four vowel context conditions) of 57 msec, and a mean onset frequencies for F2 and F3 transitions of 1201 Hz and 3449 Hz respectively. Furthermore, the statistical analysis showed significant differences in the onset frequencies of the F3 transitions between the /r/ and its misarticulations in all four vocalic contexts. The perceptual test, which examined discrimination of ten minimal-pair r/w approximant consonant contrasts demonstrated that the /r/-articulated group scored on average 96% on perceptual task while misarticulated group scored on average 82%.

Summary and discussion

The results of the present study indicate that r/w substitutions in CV syllable do not occur in an unpredictable manner, but instead are influenced by the vowel context. When /r/ is followed by a phoneme articulated at the front of the mouth cavity, the error percentage of misarticulation is significantly smaller then when the /r/ is followed by a phoneme articulated at the back of the mouth cavity. Misarticulations occur in conditions that require a significant change in the configuration of articulators. The acoustic analyses support Chaney's study (1988), that strong lingual coarticulatory effects depending on the following vowel are present for the /r/ phonetic segment, but they are absent for the /r/-misarticulations. Thus, the /r/ articulating children's consonant-vowel coarticulation must be due to the greater overlap between their consonant and vowel lingual gestures, that is, e.g., to greater fronting of the tongue body before /i/ and greater backing of the tongue body before /a/. These results are indicative of better controlled processes of the phonemic preprogramming among children articulating the /r/, compared to the /r/-misarticulated children. This study's findings that the /r/-misarticulated children scored lower on the phonemic contrast perceptual task compared to the /r/-articulated children, supports the point of view that the perception of phonemic contrast precedes its production.

Bibliography

Chaney, C. (1988). Acoustic analysis of correct and misarticulated semivowels. Journal of Speech and Hearing Research, 31, 275-287.

Davis, B.L.,& MacNeilage, P.F. (1990). Acquisition of correct vowel production: A quantitative case study. Journal of Speech and Hearing Research, 33, p.16.

Recasens, D. (1989). Coarticulatory mechanisms for tongue-dorsum activity in running speech. Journal of Acoustical Society of America, Suppl.1, 85, S148.

REPRESENTATION OF SPEECH SIGNALS IN THE DISORDERED PERIPHERAL AUDITORY SYSTEM

Donald G. Jamieson, Margaret F. Cheesman and Stefan Krol
Hearing Health Care Research Unit, Communicative Disorders
University of Western Ontario, London, Ontario, Canada

1. INTRODUCTION

The obvious limits on invasive, physiological research with human subjects restrict study of the representation of sounds in the disordered auditory system to two approaches. First, psychophysical techniques can be used to **measure** the response of the human auditory system to speech. Second, computational models can be used to **simulate** speech processing in the human peripheral auditory system. We have applied both approaches, using identical stimuli.

1.1 Physiological Models

Our model of the disordered peripheral auditory system is based closely on that described by Kates (in press) and, for comparison with normal hearing, we have also implemented a model developed by Payton [8;9]. The Kates model is a digital one, operating in the time domain, that concatenates several submodels, each representing a different part of the peripheral auditory system. Thus, the contributions of various parts of the auditory system -- the middle ear, basilar membrane (BM), inner and outer hair cells (IHC and OHC) and their synaptic junctions to auditory-nerve fibers --- are simulated, and can be studied separately. The composite model simulates the signal transformations that occur at each stage of the system, based on biophysical, biomechanical and electrophysiological observations.

The input to the model is an acoustic signal, represented as the pattern of sound pressure at the tympanic membrane. The output of the model is the neural firing rate in the auditory nerve. The processing of the sound by the BM is modeled as a cascade of filter sections. Each section is a third-order bandpass filter with parameters chosen to match the BM tuning. The output at each point on the membrane is the result of processing in all previous filter sections and is further sharpened by a second filter when the BM response is converted into a neural firing pattern by the inner hair cells. In Kates' model, this transduction is represented by a modification of Allen's [1] electrical circuit model. This model is closely connected with calcium ion kinetics during transduction. The inner hair cell (IHC) model transforms the mechanical input to the hair cell into the instantaneous firing rate of a single neural fiber. Four neural fibers are attached to each hair cell: two high-spontaneous rate fibers (50 and 75 spikes/sec) and two low-spontaneous rate fibers (5 and 10 spikes/sec). The output at each point on the BM is the arithmetic mean of the outputs of the four fibers attached to the hair cell. A novel feature of Kates' model is the feedback between the hair cells and the BM; the intensity of firing modifies the parameters of the BM filters, simulating the action of the OHCs. Adjusting this feedback path can mimic the effects of OHC damage; adjusting the resistance of hair-cell circuits can simulate damage to the IHCs.

In the Kates' model the sampling rate is determined, in principle, only by the temporal scale of investigated acoustic phenomena and digital signal processing requirements (Nyquist theorem). Kates used 40 kHz; in our studies we used 42 kHz in order to match the 14 kHz sampling rate signals used psychophysical studies. This is an advantage over Payton's model, which requires that the acoustic input be sampled at least every 0.0065 ms.

In the Payton model, the middle ear portion follows Guinan & Peake [4], who derived an analog circuit having the frequency response characteristics observed in the motion of the middle ear ossicles of anesthetized cats. A two-dimensional BM model and added sharpening mechanism were used to spatially distribute and filter stimulus frequencies.

The equations and solution methods for the cochlear fluid and BM motions are taken from Allen & Sondhi [2], and an FFT is applied. Values of the material and dynamic parameters for the cochlea were chosen to approximate an empirical cochlear place/frequency map based on anatomical measurements from cats [6]:

$$\text{resonance frequency} = 456.*(10**(2.1*(1.-x/L) - 0.8)$$

where x is the distance from the stapes and L is the length of the BM. Using this approach, the active frequencies of the model vary from 119 Hz to 57 kHz -- well beyond the range of useful human hearing. (Similar Greenwood-type formulae with coefficients matching human hearing data are used in Kates' model to place the center frequencies of 112 BM filters). Payton used 20 points on the BM, between $x/L=0.35$ and $x/L=0.825$, covering the frequency interval 270 Hz to 6800 Hz. An improved cochlear map for the present version of this 20-place model was derived from calculations of the synchronization index of the firing rate, with the frequency having the maximal index for a given place being taken as a resonance frequency. The displacement of any point along the BM resembles the output of a sharp bandpass filter with a low frequency tail. This stage of auditory signal processing improves the resolution of tuning curves, making them sharper, to more closely approximate empirical results (the so-called "second filter").

The output of the final stage, that of the excitation of the neural fibers, is modelled in three stages, following Payton [9] and Smith-Brachman [10]: 1) the signal is first passed through a half-wave rectifier; 2) this output is then lowpass filtered; 3) neurotransmitter release into the synaptic cleft is simulated.

The probability of neural firing as a function of time is proportional to the amount of neurotransmitter released by the first of three reservoirs in the model. In our model, the amount of neurotransmitter is transformed to generate a sequence of neural spikes under the assumption that spike generation is a nonstationary Poisson process. This transformation permits period histograms and inter-spike histograms to be generated.

1.2. Models of Disordered Speech

The modelled output of the normal and disordered auditory periphery was computed for synthetic fricative-vowel syllables for which psychophysical estimates of the auditory representation had been obtained previously [3]. The representations of these speech stimuli are of particular interest because the perception of the fricative portion is stongly dependent on the transition and vowel frequencies [7].

2. METHOD

Stimuli were synthetic fricative-vowel (/ʃ/ and /s/; /i/ and /u/) syllables selected based on physical parameters and on subjects' identifications and judgements of the perceptual similarity of a larger set of fricative sounds [3]. These syllables represented conditions under which the vowel context affected the perception of the fricative.

Psychophysical masking patterns were obtained using 10-ms pure tones with 5-ms raised-cosine rise and fall ramps. Seventeen probe frequencies were used, ranging from 1 kHz to 5 kHz in 0.25 kHz steps. Probes were positioned at several temporal locations in the masker; probe delays are expressed relative to the end of the fricative/onset of the vowel.

Monaural probe thresholds in the presence of the three synthetic speech maskers were obtained using a method of adjustment. Further details of the procedure are available in Cheesman [3].

2.3 Application of the Models

2.3.1 Payton model

2.3.1.1 Interpolation of Sampled Data As the speech signals of interest were sampled at 14kHz, when applying the Payton model the sampling period was adjusted to be 0.071 ms, rather than the required $\leq$0.0065 ms. To satisfy this requirement, 12 points were interpolated between each pair of sampled data points using linear interpolation. This action reduced the sampling period to 0.00595 ms, with 4200 samples within each 25 ms segment of the signal.

2.3.1.2 Stimulus Scaling Because the intensity of firing depends on the level of the input signal, it is important to ensure that each portion of the signal is appropriately scaled. This was accomplished by calculating the root mean square amplitude across the signal and using this value to normalize each sample, by dividing by the root mean square value.

2.3.1.3 Processing. To approximate the psychophysical procedure as closely as possible, the first 250 ms of the signal were processed through the model, and the firing rate calculated at each of six specific time points. Specifically, the **mean** firing rate was calculated for each of the following 10 ms intervals, measured from signal onset: 95 to 105 ms, 120 to 130 ms, 145 to 155 ms, 170 to 180 ms, 195 to 205 ms, and 220 to 230 ms. These calculations were made at each of 20 frequencies (i.e., for the output associated with each of 20 basilar membrane locations), to generate neural analogs to the psychophysical masking patterns.

2.3.2 Kates model

Application Kates' model to our stimuli was more straightforward. It required the interpolation of 3 points in order to match 42 kHz sampling rate.

3. RESULTS AND DISCUSSION

3.1. Masking Patterns

Several consistent patterns were evident in each of the masking patterns. The masking patterns showed good representation of the frication noise and the vocalic portion of the syllables. At the junction of the fricative and vowel, portions of the lower frequency vowel and fricative information were present in the patterns.

3.2. Model Output

The model described above was applied to process the speech signals described above, in order to compare psychophysical measures of the auditory representation of speech with firing rates patterns. In general we have seen good correspondence between the data obtained through the psychophysical and modelling approaches, with the auditory model appearing to be somewhat more sensitive than the normal ear to the acoustic properties of the speech signal. As one example, the transition from fricative noise to vowel region is very sharp in the model.

In the normal ear, firing rate is synchronized with the first and second formant (F1 and F2) for voiced speech sounds. When the OHCs are damaged, the firing rate decreases and most timing information is lost, with synchronization being observed only for F1. In addition, a strong onset response in the low frequency fibres disappears when OHCs are damaged, suggesting that the OHC/BM feadback is responsible for the onset response.

When the stereocillia are damaged in a significant proportion of the IHCs in a particular region of the cochlea, timing information appears to remain intact in the neural output, but the intensity of firing is substantially reduced, possibly below the difference threshold.

4. REFERENCES

[1] ALLEN, J.B.(198), "A hair-cell model of neural response", in Peripheral Auditory Mechanisms, edited by E. de Boer and M.A.Viergever, the Hague: Martinus Nijhoff Publishers, 1983.

[2] ALLEN, J.B., & SONDHI, M.M. (1979), "Cochlear macromechanics: Time domain solutions", *Journal of the Acoustical Society of America, 66*, 123-132.

[3] CHEESMAN, M.F. (1989), "The auditory representation of context-conditioned fricatives", Doctoral Dissertation, University of Minnesota.

[4] GUINAN, J.J. & PEAKE, W.T. (1967), "Middle-ear characteristics of anaesthetized cats", *Journal of the Acoustical Society of America, 41*, 1237-1261.

[5] KATES, J.M. (1991), "A time domain digital cochlear model",IEEE Transactions on Acoustics Speech and Signal Processing, in press.

[6] LIBERMAN, M.C. (1982), "The cochlear frequency map for the cat: Labeling auditory-nerve fibers of known characteristics frequency", *Journal of the Acoustical Society of America, 72*, 1441-1449.

[7] MANN, V.A. & REPP, B.H. (1980), "Influence of the vocalic context on perception of the [ʃ]-[s] continuum", *Perception & Psychophysics, 28*, 213-228.

[8] PAYTON, K.L. (1986), "Vowel processing by a model of the auditory periphery", *Ph. D. Thesis, John Hopkins University*, Baltimore.

[9] PAYTON, K.L. (1988), "Vowel processing by a model of the auditory periphery: A comparison to eight-nerve responses", *Journal of the Acoustical Society of America, 83*, 145-162.

[10] SMITH, R.L., BRACHMAN, M.L. (1982), "Adaptation in auditory-nerve fibers: A revised model", *Biological Cybernetics, 44*, 107-120.

6. ACKNOWLEDGEMENTS

We are grateful to Ketan Ramji and Lucy Kieffer for technical assistance and to J. Kates and K. Payton for providing code for the auditory model. The work was supported, in part, by grants from NSERC to MFC and from NSERC, URIF and Unitron Industries Ltd. to DGJ.

Correspondence should be addressed to Dr. D.G. Jamieson, Hearing Health Care Research Unit, Department of Communicative Disorders, University of Western Ontario, London, ON, CANADA, N6G 1H1.

DISCRIMINATION OF STATIC AND DYNAMIC FREQUENCY CHANGES BY CHILDREN AND YOUNG ADULTS

Jane F. MacNeil and Elzbieta B. Slawinski, The University of Calgary, Calgary, Alberta.

Introduction

Although there is much research documenting discrimination of pure tone frequencies, there is less work assessing dynamic frequency glides. Investigation of this nature is relevant, not only to real listening environments where signal frequencies, or spectral components, rapidly change, but also to speech perception where the correct identification of phonemes is dependent upon the sensitivity of the auditory system to respond to rapid changes of short duration frequency sweeps (formant transitions) that are critical for distinguishing consonants.

Audiological studies have shown that consonant discrimination tends to deteriorate with age before vowel recognition does (Working Group on Speech Understanding and Aging, 1988). Since consonants are characterized by formant transitions, the ability to differentiate rapidly changing components is implicated in this decline. The fact that vowel discrimination remains largely intact further suggests that the mechanisms employed to discriminate steady state signals (which characterize vowel segments) are not the same as those which differentiate dynamic signals. Evidence that the thresholds for steady state signals are lower than thresholds for gliding stimuli (Horst, 1989) additionally supports the hypothesis of the involvement of two different mechanisms.

Developmental aspects are an important focus in the study of auditory sensitivity. Elliott et al (1989) reported that young children required significantly larger differences than did young adults to differentiate signals which simulated the second formant of speech. In contrast, little improvement in masked thresholds beyond 10 years of age has been noted (Schneider et al, 1989). With respect to rapidly changing signals, some research has centered on factors such as discriminating glides from steady states, and upward glides from downward glides (Dooley & Moore, 1989, Schouten & Pols, 1989), but discrimination of dynamic signals as a function of age has received little focus.

The purpose of the present study is to evaluate the ability of children and young adults to distinguish steady state and unilaterally gliding frequency signals corresponding to the second formant of speech. Due to the difficulty of separating language from perceptual skills when actual speech signals are used, this study used signals which were dynamic and had frequency characteristics analogous to some aspects of speech but that occurred in isolation. Information derived from these fundamental auditory abilities constitutes the basis for understanding more complex auditory performance.

Method

Stimuli

Stimuli were 50 ms in duration and synthesized on a Micro Vax II computer. Digital outputs were sampled at 20 KHz , 16 bit resolution, and lowpass filtered at 3 KHz. A continuum of 17 signals increasing in 10 Hz steps was generated for both sets of signals. Gliding tones had a constant onset frequency of 900 Hz and diverged to varying offset frequencies of 950 Hz to 1110 Hz in 10 Hz steps. The frequencies of the steady state stimuli corresponded to the offset frequencies of the gliding set.

Subjects

Twenty three subjects : 13 adults (mean age 25.8 years, range 19-38 years), and 10 children (mean age 9.4 years, range 8-10 years) participated in this study. Data from 2 adults were eliminated from the final analysis due to their inability to discriminate any of the signals; as well, data from 2 of the children were also eliminated: one due to an attentional disorder, and the other because of failure to complete the experimental session. All subjects had normal hearing (better than +10 dB HL) for a range of frequencies from 500 Hz to 8 KHz determined with a Bruel and Kjaer audiometer (Model 1800).

Procedure

A two cue, two alternative forced-choice same-different paradigm designed to determine the smallest differences that subjects could discriminate between frequency changes was used. On each trial, subjects were presented with two stimuli separated by 500 ms and asked to determine if they were the 'same' or 'different'. Stimuli were presented monaurally via Kross Pro/4x headphones at the most comfortable listening level for each subject in a double walled sound attenuating anechoic chamber . For all of the children, the experimenter was also present in the chamber. Calibration of sound pressure levels was accomplished with a Bruel and Kjaer impulse precision sound level meter and a Bruel and Kjaer artificial ear positioned over the headphones;linear scale readings were taken with a 0.5 in microphone. Average sound pressure variation was 76 dB SPL with a deviation of +/- 4 dB across subjects.

Each condition consisted of 200 trials; 160 trials of 'different' stimuli, and 40 catch trials to avoid subjects developing a proclivity towards responding 'different' and to provide a metric of bias. The first stimulus in a continuum served as the constant stimulus and was presented on every test trial although its position as either first or second member of the pair was randomly varied.

Just noticeable differences (JNDs) were measured relative to the constant stimulus; therefore, for the gliding stimuli this meant that the JNDs were relative to the stimulus that had the smallest frequency change. A short practice session to familiarize subjects with the stimuli and procedure preceded the beginning of each experimental session. Individual psychometric functions were plotted with percentage correct as a function of stimulus separation in Hz, and these functions were used to specify thresholds for each age group for each stimulus type. Criterion for threshold was defined as the stimulus separation corresponding to the 70% correct position and was determined by fitting a nonlinear function to the data.

Results

Discrimination of frequency differences was evaluated in terms of JNDs and the results for each subject were based on an average of 400 trials (2 conditions X 200 trials). Each point on the psychometric function (Figure 1) is based upon 110 responses for the adults (10 trials of each stimulus difference X 11 listeners) and 80 responses for the children (10 X 8 listeners). For all subjects a nonlinear function was fit to the data and the 70% correct.position was determined. A multivariate analysis of variance (MANOVA) was conducted on the interpolated threshold data. There was a significant effect for group, $F(1,17) = 32.901$, $p < .001$, and signal type, $F(1,17) = 13.286$, $p<.001$. The interaction of group and signal type was not significant ($F=2.035$).

Adults had significantly lower thresholds than did children, and for both groups the thresholds for steady state stimuli were lower than those for sweeping stimuli. For steady tones, the adults needed smaller acoustic differences (M = 22.6 Hz, SD = 10.4 Hz) than did the children (M = 59 Hz, SD = 9.8

Hz). For sweeping tones, the thresholds are higher for both groups, but are still lower for the adults (M = 35 Hz, SD= 13 Hz) than for the children (M = 64 , SD = 19 Hz). A shift to the left in the psychometric functions of the adult data suggests an increased sensitivity relative to children. As well, the functions for the steady tones are to the left of the sweep tones demonstrating a greater sensitivity for discrimination of steady frequency changes compared to discrimination of dynamic frequency changes.

Figure 1. Psychometric Functions for Group and Signal Type

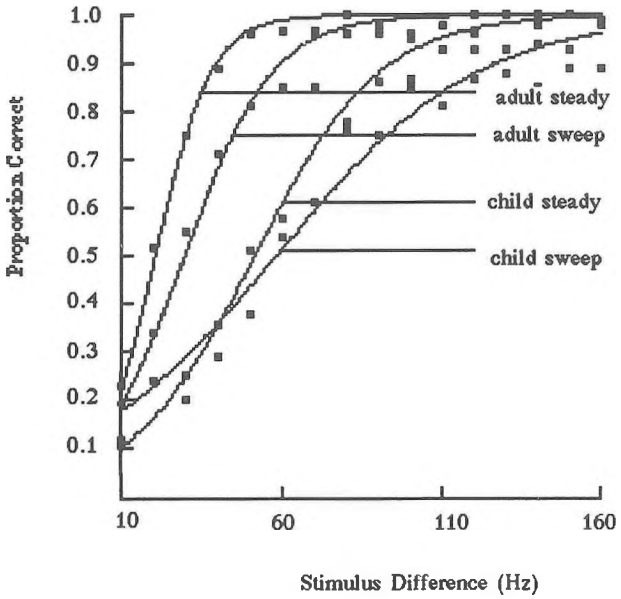

An analysis of the catch trial performance did not reveal any significant differences across groups ($p>.05$) or signal type ($p>.05$). This tentatively suggests that subjects did not adopt a more stringent criterion for any condition, nor did confidence in their decisions change across conditions. The important indication is that the relatively poorer auditory discrimination of children compared to that of adults is a function of general auditory processing and not specific features of the task or response bias.

Conclusions

(1) Thresholds for just noticeable differences have an age-related component to them. Even by 10 years of age, children require significantly larger acoustic differences than do young adults in order to be able to distinguish either steady state or gliding signals. The implication of this pattern of age differences is the presence of an unidentified, but crucial, developmental component. These findings support the results of Elliott et al (1989) who also documented age-related aspects involved in the discrimination of complex sounds.

(2) The increase in threshold which some listeners demonstrate has been attributed to a broadening of the auditory filter (Moore, 1982), but Irwin et al (1986) reported that the auditory filters of 10 year old children were not significantly wider than those of young adults. It appears that these changes are cognitive in nature and reflect more central aspects of auditory processing. The results of this study show that even at 10 years of age, some auditory abilities have not yet attained adult-like sensitivity.

(3) The pattern of children's results resembles that of the adults. For both groups, thresholds for steady state signals were lower than that for frequency glide signals. This supports the hypothesis that two different mechanisms encode steady state and gliding signals respectively and that these mechanisms are not as developed in children as they are in adults. This also concurs with the data from some hearing impaired studies where listeners with sensorineural hearing loss may perform well on one dimension, but poorly on another, again suggesting the involvement of two different processes.

(4) The poorer discrimination of gliding stimuli versus steady stimuli is consistent with research on speech perception which demonstrates poorer consonant discrimination as opposed to vowel discrimination. These results may help to explain why consonant perception deteriorates before vowel perception does. Frequency discrimination, however, is only one of many factors involved in the perception of speech, but knowledge of fundamental processing mechanisms assists in the comprehension of more complex auditory behavior. These findings may further enhance understanding of why certain listeners (particularly children and elderly people) despite having good pure tone sensitivity as measured by conventional audiological methods, experience difficulty in understanding speech or processing other complex auditory signals. It is apparent that significantly more acoustic information is needed by children, for example, in order to differentiate dynamic signals.

(5) The lack of differences among the catch trial data for both the adults and the children suggests that the poorer auditory discrimination of children is a reflection of general auditory processing , and not attributable to task difficulty or response bias.

References

Dooley, G. J. & Moore, B.C.J. (1988). Detection of linear frequency glides as a function of frequency and duration, Journal of the Acoustical Society of America, 84(6), 2045-2057.

Elliott, L.L., Hammer, M.A., Scholl, M.E. & Wasowicz, J.M. (1989). Age differences in discrimination of simulated single-formant frequency transitions, Perception & Psychophysics , 46(2), 181-186.

Horst, J.W. (1989). Detection and discrimination of frequency modulation of complex signals, Journal of the Acoustical Society of America , 85(5), 2022-2030.

Irwin, R.J., Stillman, J.A., & Schade, A. 1981. The width of the auditory filter in children, Journal of Experimental Child Psychology , 41, 429-442.

Moore, B.C.J. (1982). An Introduction to the Psychology of Hearing , (2nd ed). New York: Academic Press.

Schneider,B.A., Trehub, S. E. & Morrongiello, B.A. & Thorpe, L.A. (1989). Developmental changes in masked thresholds, Journal of the Acoustical Society of America, 86(5), 1733-1742.

Schouten, M.E.H. & Pols, L.C.W. (1989). Identification and discrimination of sweep formants, Perception & Psychophysics , 46(3), 235-244.

Working group on speech understanding and aging. (1988). Speech understanding and aging, Journal of the Acoustical Society of America , 83(3), 859-895.

ACOUSTICAL CUES IN /R-W/ DISCRIMINATION

Laurie K. Fitzgerald & Elzbieta B. Slawinski
University of Calgary, Department of Psychology

1. Introduction

There has been a great deal of controversy concerning the categorical perception of the semivowels /r/ and /w/. Although research has clearly shown that the above two phonemes are perceptually differentiated from one another on the basis of primarily two acoustical features, namely the onset frequency and transition duration of their respective second (F2) and third (F3) formants, the same has not elucidated, however, the "primacy" or perceptual "weight" of either of these two cues. That is to say, it has not been definitively specified which feature represents the more salient cue underlying the /r-w/ phonemic distinction. Consequently, when ever there has been discrepant results in the /r-w/ perceptual literature, an explanation which often surfaces relates to the acoustical characteristics of the stimuli used in the studies. Discordant results are commonly attributed to differences in the acoustical properties of the stimuli employed. In some studies, the stimuli utilized contained only formant onset frequency information whereas in other studies, the stimuli contained only the formant transiton information. In an attempt to better understand the role the two cues play in the phonemic perception of /r/ and /w/, the present study was undertaken. It was hoped that by comparing identification performances on continua with formant transition information alone, formant onset frequency information alone, and then a combination of both types of information, some light may be shed on the above issue. Working from the premise that the preceding speculation was correct, it was hypothesized that a main effect for continuum type would be exhibited.

2. Method

Subjects: The subjects were 35 male and female adults between the ages of 18 and 35. All were native speakers of English, and all had normal peripheral hearing.

Stimuli: Three 7-step male adult /r-w/ continua were synthesized via the Klatt Cascade/Parallel Software Program (Klatt, 1980). The stimuli in the continua corresponded to the words rock and walk and were 330 msec in duration. The parameter values used in the synthesis of the three continua's endpoint stimuli were patterned after Klatt(1980) guidelines and those obtained from an acoustical analysis of an adult males' recorded versions of rock and walk. The parameter values of the vowel nucleus /a/ and the stop /k/ were held constant across the continua. The stimuli were also matched for pitch, intonation, and amplitude contour. The acoustic tokens in the three continua did vary, however, according to F2 and F3 onset frequencies and F2 and F3 transitions durations. In the first continuum (C1), the acoustic tokens varied with respect to both F2 and F3 onset frequencies and F2 and F3 transition durations. F2 onset frequency varied from 1070 Hz in the endpoint stimulus corresponding to a clear token of the word rock to 650 Hz in the endpoint stimulus corresponding to a clear token of the word walk. F3 onset frequency varied in the same manner from 1460 Hz to 2150 Hz. F2 transition duration varied from 15 msec in the endpoint stimulus corresponding to a clear token of rock to 75 msec in the endpoint stimulus corresponding to a clear token of walk. Similarly, the transition duration of F3 varied from 75 msec to 15 msec. In the second continuum (C2), the acoustic tokens varied only with respect to F2 and F3 onset frequencies, and the durations of the second and third formant transitions were kept constant at a value of 45 msec. In the third continuum (C3), the acoustic tokens varied only with respect to F2 and F3 transition durations, and the onset frequencies of the second and third formants were kept constant at 860 Hz and 1805 Hz respectively.

Upon completion of synthesis, two sets of 35 trials were prepared for each continua, in which the 7 stimuli in each respective continuum was presented 5 X each in random order.

Procedure: The testing was done on an individual basis and was conducted in the Audition and Speech Laboratory at the University of Calgary. Prior to testing, subjects underwent audiometric screening. Normal performance was defined as thresholds 20 dB or lower for the frequencies of 1000, 2000, and 4000 Hz.

The test proper consisted of a two-alternative, forced-choice identification task embedded in a pseudo video-game. The video-game was played on a Apple II MacIntosh computer and involved listening to the stimuli of the continua over a loudspeaker and then identifying whether the sound heard was rock or walk by choosing a corresponding picture within the video-game.

Each subject performed an identification task with each continuum type, with the trial sets and task order counterbalanced across subjects. All three identification tasks were completed in one sitting, with a 5 minute break between the running of the second and third task. A formal training protocol was not implemented in the study, but as a means of acquainting the subjects with the nature of the task and Mac controls, 4 "dry-runs" of the video-game involving randomized endpoint stimuli were conducted with each of the three identification tasks. On average, testing took twenty minutes to complete.

3. Results

All inferential statistics were computed with the Statview Software Program on an Apple II Macintosh computer.

The mean percentages of /r/ responses were computed for all three continua and plotted as a function of stimulus number. The identification function of the two-cue continuuum was different than that evidenced in either of the two one-cue continua. Although in all three continua stimuli 1-4 were identified as /r/, as evidenced by the high percentage of /r/ responses for those stimuli, and conversely, stimuli 5-7 as /w/, as evidenced by the low percentage of /r/ responses for those stimuli, the percentages of /r/ responses for stimulus 3 in the two, one-cue continua were lower than that exhibited in the one, two-cue continuum. Stimulus 3 had a 99% identification rate in C1, the continuum containing both onset frequency and transition duration formant information. In contrast, the continua containing information soley on onset frequency (C2) or transition duration (C3) had response rates of only 78 and 79% respectively.

In addition to characterizing the subjects perceptual categorizations as a function of stimulus number and /r/ response percentage, phonemic boundaries, which mark the 50% point between sound categories, were calculated for each individual for each continuum. This was done by means of interpolating the stimulus number at the 50% crossover on the unsmoothed response functions. Mean category boundaries for each continuum were obtained by averaging the individual

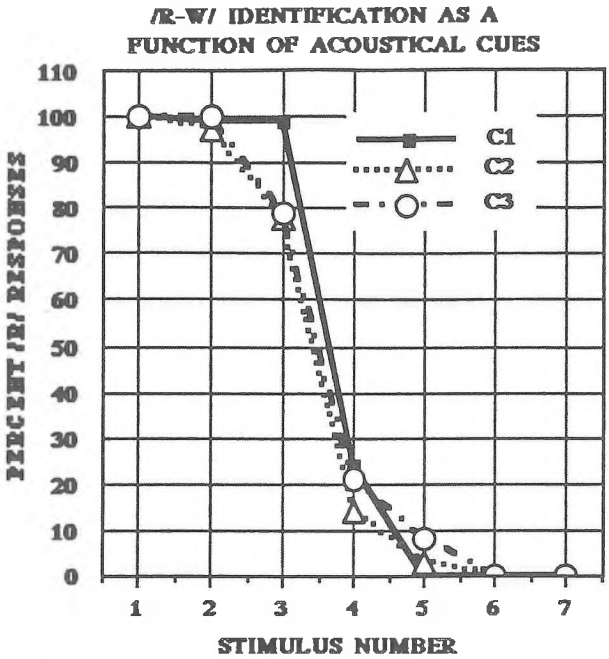

category boundaries. The mean phonemic boundary values were 3.73, 3.41, and 3.54 for C1, C2, and C3 respectively. A repeated measures analysis of variance on the factor of continuum type revealed the latter to be signficant ($F(2,68) = 8.568$; $p < .0005$). The mean phonemic boundary value corresponding to C1 was significantly different from the mean phonemic boundaries evidenced in C2 (Scheffe $F=8.483$; $p < .05$) and C3 (Fisher PLSD=.158; $p<.05$). The mean phonemic boundaries of C2 and C3, however, were not significantly different from one another.

4. Conclusions

(1) The finding that perceptual categorization of /r/ and /w/ varied as a function of two cue vs one cue availability implies that caution should be exercised when comparing data obtained on /r/ and /w/ stimuli incorporating only one of the differentiating salient acoustical dimensions vs incorporating both. This finding also suggests that the two cues are perceived in relation to one another. In turn, this provides support for the theory espoused by Wood (1975) and Soli (1980) that perception of speech sounds does not precede directly and independently from acoustical cues but rather is mediated by higher order coding levels which incorporate dependencies among acoustical cues. It is recognized, however, that the present study's support for the above theory is limited given the nature of the experimental task employed. A more stringent test would involve a trading relations design as described below in point (4).

(2) The finding that perceptual categorization of /r/ and /w/ did not vary as a function of which individual cue, formant onset frequencies or formant transition durations, was available for the same, suggests that the latter are perceptually equivalent as discriminative cues for /r/ and /w/.

(3) Because the data was collapsed across individuals, it was not possible to determine if the two cues were perceptually equivalent at the level of the individual. It would be interesting to investigate the possible existence of different individual processing strategies and/or perceptual biases brought to play in the phonemic perception of /r/ and /w/. Research conducted on stop consonant discrimination suggests that individual perceptual biases toward spectral vs temporal cues do in fact occur (Fourcin 1988). Furthermore, it appears that the perceptual biases eliminate the discriminative advantage of two-cue availability.

(4) Further research could involve a more rigorous test of the discriminative equivalence of the above two acoustical properties via a trading relations experiment. In such a study, the two acoustical dimensions could be combined in such a way as to cue the opposing phoneme ie. one dimension's parameters would be typical of /r/ and the other's parameters would be typical of /w/. Perceptual equivalence of the two cues would be evidenced by a 50% indentification rate to all of the stimuli within the continuum.

5. References

Fourcin, A. (1988). Links between voice pattern perception and production. In B.A.G. Elsendorn & H. Bouma (Eds.), Working models of human perception (pp. 67-91). Toronto: Academic Press.

Klatt, D.H. (1980). Software for a cascade/parallel formant synthesizer. The Journal of the Acoustical Society of America, 67 (3), 971-995.

Soli, S.D. (1980). Some effects of acoustic attributes of speech on the processing of phonetic feature information. Journal of Experimental Psychology: Human Perception and Performance, 6, 622-638

Wood, C.C. (1975). A normative model for redundancy gains in speeded classifications: Applications to auditory and phonetic dimensions in speech discrimination. In F. Wrestle, R.M. Shiffrin, J.J. Castellan, H. Landman, and D.B. Pisoni (Eds.), Cognitive Theory . Potomac: Eribaum.

A COMPUTER-DRIVEN PROGRAM TO IMPROVE SPEECH PERCEPTION AND SPEECH PRODUCTION SKILLS

Susan Rvachew
Alberta Children's Hospital

Introduction

Several studies have shown that a subgroup of misarticulating children has significant difficulties with the phonemic perception of speech sounds (Broen, Strange, Doyle, & Heller, 1983; Rvachew & Jamieson, 1989). It has been suggested that some of these children employ subperceptual category boundaries in both the perception and production of their error sound contrasts (Hoffman, Daniloff, Bengoa, & Schuckers, 1985). Subsequently, Chaney (1988) has recommended the use of perceptual training that focuses on the child's own misarticulations and teaches these children to identify standard phonemic categories. The purpose of this study is to evaluate the effectiveness of sound identification training in facilitating correct production of "sh" by phonologically delayed preschoolers.

Description of the Training Programs

Three groups of auditory stimuli were recorded from adults and children. Group 1 consists of correct productions of the word "shoe" and incorrect productions of the word "shoe" (e.g. /tu/, /tsu/, /su/ etc.). Group 2 stimuli are one correct version each of "shoe" and "moo" while Group 3 stimuli are one correct version each of "cat" and "Pete". All words were digitized (sf=20 kHz) using the Canadian Speech Research Environment (CSRE; Jamieson, Nearey, & Ramji, 1989). In addition, 9 sets of graphic feedback stimuli were developed. For example, one set depicts a duck pond in which birds appear one at a time. An AST 386C computer equipped with signal processing hardware and CSRE were used to present the words to the children over headphones. The child's task was to listen to each word and then indicate whether the word was correct or incorrect by pointing to the appropriate symbol on the monitor. Children assigned to the Group 3 stimili listened for the word "cat" while the remaining children listened for the word "shoe". Correct responses were rewarded by presentation of the graphic feedback pictures described above.

Subjects

The subjects were 14 boys and 5 girls ranging in age from 3 years - 8 months to 5 years - 5 months. All children were awaiting treatment for phonological delay. Every child was unstimulable for the "sh" sound during pretesting. Where possible, the children were matched according to chronological age, receptive language age, expressive language age, presence of a significant history of otitis media, and severity of phonological impairment. Children were randomly assigned to 1 of the 3 groups within their respective pairs or triads. Unmatched children were independently assigned to groups at random. The group sizes are 6, 8, and 5 children for Group 1, 2, and 3 respectively. There were no significant differences between groups with respect to any of the subject variables noted above.

Procedure

All children attended 6 weekly treatment sessions. Each session consisted of 60 perception training trials, with the stimuli determined by group assignment, and 60 production training trials. Production training followed a traditional sequence of steps from isolation (level 1) through (potentially) conversational speech (level 9). Following completion of the treatment program, a digitized recording of "sh" produced in isolation was obtained from each child. CSRE was used to determine the centroid for each "sh" production.

Results

Statistical analysis of the data will not be possible until at least 5 triads of matched subjects are completed. The raw data to date is revealing clear trends however. The mean centroids (in Hz) are as follows: Group 1 = 4202, Group 2 = 3654, Group 3 = 4906. All of the children who listened to "shoe" and "moo" produced perceptually correct "sh" sounds following therapy, and all but 2 of their "sh" samples yielded centroids below 4000 Hz. One Group 3 subject and four Group 1 subjects produced correct "sh" sounds. The centroids of the "sh" sounds produced by these groups were higher than 4000 Hz, with 2 exceptions in Group 1. For each matched pair or triad, the Group 2 centroid was the lowest.

Discussion

This study is revealing that identification training for correct "sh" sounds facilitates production learning by phonologically delayed preschoolers. In particular, children who identified the words "shoe" and "moo" were most likely to learn to produce "sh" sounds which were perceptually correct, and which had centroids appropriately below 4000 Hz. This result is consistent with Grieser & Kuhl's (1989) finding that infants' learning of equivalence classification of vowel categories is enhanced when the training stimuli are prototypical exemplars of the vowel classes being taught. The superiority of the "shoe-moo" treatment is also consistent with Gierut's (1990) maximal opposition approach to phoneme learning, in which sound contrasts that involve a major class distinction are taught.

This study also has implications for the use of acoustic analysis to document clinical outcomes and to guide the therapeutic process. With the ready availability of personal computers and software such as CSRE this is increasingly practical. As Huer (1989) has noted, however, more rigorous study of the acoustic characteristics of children's misarticulations is required. The standard acoustic cues for identifying /r/ and /S/ do correspond to clinician's perceptual judgements on the average, but a disturbing number of exceptions do occur. For example, in this study two children produced perceptually correct "sh" sounds that had centroids above 5000 Hz. One distorted "sh" sound had a centroid below 4000 Hz.

Acknowlegdement

This research funded by the M.S.I. Foundation (Edmonton, Alberta).

References

Broen, P. Strange, W., Doyle, S. & Heller, J.H. (1983). Perception and production of approximant consonants by normal and articulation delayed preschoolers. Journal of Speech and Hearing Research, 26, 601-608.

Chaney, C. (1988). Identification of correct and misarticulated semivowels. Journal of Speech and Hearing Disorders, 53, 252-261.

Gierut, J.A. (1990). Differential learning of phonological opposition. Journal of Speech and Hearing Research, 33, 540-549.

Grieser, D. & Kuhl, P.K. (1989). Categorization of speech by infants: support for speech-sound prototypes. Developmental Psychology, 1989, 577-588.

Hoffman, P.R., Daniloff, R.G., Bengoa, D., & Schuckers, G.H. (1985). Misarticulating and normally articulating children's identification and discrimination of synthetic [r] and [w]. Journal of Speech and Hearing Disorders, 50, 46-53.

Huer, M.B. (1989). Acoustic tracking of articulation errors: [r]. Journal of Speech and Hearing Disorders, 54, 530-534.

Jamieson, D.G., Nearey, T.M., & Ramji, K. (1989). CSRE: A speech research environment. Canadian Acoustics, 17, 23-35.

Rvachew, S. & Jamieson, D.G. (1989). Perception of voiceless fricatives by children with a functional articulation disorder. Journal of Speech and Hearing Disorders, 54, 193-208.

COMPUTER MODELLING OF LEXICAL TONE PERCEPTION

Fangxin Chen and Anton J. Rozsypal
Department of Linguistics, University of Alberta

1. Introduction

Theoretical importance and practical implications of research on computer speech recognition generate considerable interest in this field among linguists, psychologists, and communication engineers alike. The long-term aim is to design a model reflecting the speech perception process and eventually simulate it by a computer program able to perform speaker-independent speech recognition. The present study focuses on one aspect relevant for tone languages, the recognition of lexical tones. The language chosen is Mandarin Chinese (MC).

MC is basically a monosyllabic contour-tone language. A syllable encoded with a lexical tone constitutes an independent semantic unit (morpheme). There are four lexical tones in MC citation form: level tone (Tone 1), rising tone (Tone 2), falling-rising tone (Tone 3) and falling tone (Tone 4).

To build our tone-perception model, two aspects of tone were investigated: perceptual dimensions and domain. The perceptual dimensions specify which acoustic cues contribute to the lexical tone perception and how these cues are represented in the auditory system. Tone domain determines where in the syllable the lexical tone is physically located.

For signal editing, analysis and subject testing, the Alligator program, developed in our Department, was used. The stimuli were synthesized on the Wavelet Speech Synthesizer, one of the Alligator signal generating modules (Rozsypal, 1987).

2. Perceptual Dimensions of Tone

To explore the perceptual dimensions of tone, three experiments were conducted. The first experiment examined how pitch contour determines tone perception. A continuum of MC syllables were synthesized with fixed duration and initial fundamental frequency f_i and linear pitch contour slopes ranging from negative to positive slopes. The stimuli were presented to the Mandarin-speaking subjects for tone category identification. The results show that although lexical tone perception relies primarily on auditory detection of linear frequency glides, phonetic tone categorizations do not coincide exactly with the auditory thresholds for non-linguistic tone detection. This suggests that lexical tone is processed not merely by the peripheral auditory system, but that a more central levels of the auditory system must be involved. The asymmetry between the frequency thresholds for rising and falling tone detection also suggests that articulatory constraints on tone production plays an important role in the formation of lexical tone categories. The second experiment explored the interrelationship among pitch contour slope, duration, and initial frequency in lexical tone perception. Two continua of synthesized MC syllables were prepared. In the first continuum, f_i was fixed at 100 Hz; the duration was increased from 40 ms to 200 ms in 20 ms steps; the final fundamental frequency f_f was increased from 100 Hz to 150 Hz in 5 Hz steps, except for syllables with 40 ms duration, in which case f_f was increased from 100 Hz to 200 Hz in 10 Hz steps. In the second continuum, f_i was set to 200 Hz; duration was increased from 40 ms to 200 ms in 20 ms steps; f_f was increased from 200 ms to 250 ms in 5 Hz steps, except for syllables with 40 ms duration, for which f_f was increased from 200 Hz to 300 Hz in 10 Hz steps. These two sets of continua were presented to the subjects for tone identification. The results indicate that the interrelationship among pitch slope, tone duration and the initial frequency can be described by the formula

$$\frac{\Delta f \, T}{\log f_i} = C_j \, ,$$

where Δf is the difference between f_f and f_i of the pitch glide and T is the tone duration. The constant C_j assumes a particular value for each tone category denoted by the index j. This equation indicates that the frequency shift threshold Δf for tone detection is inversely proportional to the tone duration T and directly proportional to the logarithm of f_i. The validity of this formula is restricted: the duration of the glide T must be at least about 40 ms long. The minimal duration is required for perceiving a stable tone (Doughty & Garner, 1948). This means that for a male voice range the syllable must be about four periods or longer to have a tonal quality. For a female voice range, the duration threshold of tonality is about seven periods. On the other hand, for tone duration greater than 100 ms, Δf becomes fairly constant and will not change markedly. Similar results were reported in a non-linguistic tone experiment (Dooley & Moore, 1988). This relationship between Δf and T leads to the hypothesis that the human listener's temporal window in lexical tone processing is about 100 ms. The third experiment was conducted to determine whether there is any correlation between intensity contour and lexical tone perception. A list of 28 MC syllables in four tones, read by ten Mandarin-speaking subjects of both sexes, were recorded. The syllables were digitized and their intensity contours extracted. These were classified into nine basic intensity patterns. The matching of intensity contour and tone category indicated that MC syllables with falling-rising and falling-level intensity contours were associated only with Tone 3. Consequently, they can be used as a reliable acoustic cue for Tone 3 perception.

3. Domain of Tone

Before discussing the domain of MC tone, a brief description of MC syllable structure seems appropriate. This structure can be expressed by the following syllable structure rules, where elements within square brackets are optional:

Syllable - [Initial] + [Medial] + Rhyme;
Initial - Consonant;
Medial - Glide (j, w, ɥ);
Rhyme - Nucleus + [Coda];
Nucleus - Vowel;
Coda - Nasal (n, ŋ);

Following is an illustration of how the MC syllable 'huang /hwaŋ/' can be diagrammed by the MC syllable structure rules:

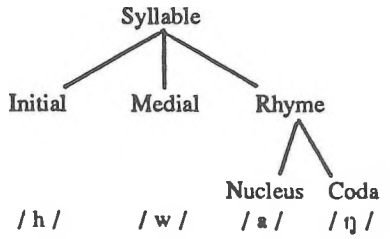

To establish the domain of lexical tones, two approaches were taken. In a perceptual experiment, a list of natural MC syllables in the four tones were recorded and digitized. Either the Initial, Medial or Coda was gated out from the syllables and only the remainders were presented to the subjects. The subjects were then asked to indicate the tone categories of the remainders of the syllables. According to the confusion matrices based on the original tone categories of the syllables and the reported tone categories judged by the subjects, the removal of Initial or Medial had little effect on subjects' tone perception, while the elimination of Coda seriously affected subjects' tone judgements. In the second approach, the pitch contours of a list of natural MC syllables in the four tones were extracted and the characteristic lexical tone patterns were located in the segmental environment. The results of both approaches indicate that the relevant tone contour pattern is contained in the Rhyme part of a syllable, which confirms Howie's (1974) argument. In speech production, the speaker's intended tone might be 'distorted' by the segmental environment, mainly the initial voiced consonant, due to articulatory factors. Intrinsic tone perturbations of this nature appear to have been established as tone variants through language exposure.

4. Computer Tone Recognition

Based on the above findings, we designed a computer program written in Turbo Pascal language, modelling the perceptual aspects of linguistic tone recognition. A 100 ms sliding window was used to simulate the human ear's temporal window in scanning the pitch contour of the input syllable. The pitch slope within this window was computed according to the following formula for the linear regression slope,

$$Slope = \frac{n \Sigma t_j f_j - \Sigma t_j \Sigma f_j}{n \Sigma t_j^2 - (\Sigma t_j)^2},$$

where n is the number of periods within the moving window, t_j are the time values for the end of the j-th period within the moving window, and f_j are the corresponding frequency values. The period index j ranges from 1 to n. In case the pitch glide duration was shorter than 100 ms, the remaining t_j values within the window were increased by constant steps of the average period duration of the segment and the corresponding 'missing' f_j values were set to the initial frequency value f_i. This automatically reduced the slope value within the moving window, reflecting the interrelationship between duration and frequency change in tone detection. The critical slope boundary values for the detection of Tone 1 (level tone), Tone 2 (rising tone), and Tone 4 (falling tone) were determined by analyzing 360 words in citation form spoken by ten Mandarin speakers of both sexes and normalized with respect to the initial fundamental frequency. Recognition of Tone 3 (falling-rising) required detection of both falling and rising pitch slope, where the falling pitch slope must precede the rising one. In tone scanning, the pitch contour within the initial voiced consonant was disregarded as irrelevant to lexical tone recognition.

Besides pitch contour, the tone recognition program also analyzed the intensity contour of the input syllable. The input syllables were divided into three equally long parts and the average values of intensity in each part were calculated. According to the ratios of average intensity values between each two parts, about nine different intensity contours could be identified, in which falling-rising or falling-level intensity contours served as reinforcement for Tone 3 decisions.

To test the reliability of the above procedure, a list of 180 words in citation form with different tones spoken by five new speakers was recorded and submitted to the tone recognition procedure. A correct recognition rate of 98% was obtained. The only confusions encountered were between Tone 2 and Tone 3, the same confusion pattern as found in human listeners (Kiriloff, 1969; Zue, 1976).

References

Doughty, J.M., and Garner, W.R. (1948). "Pitch Characteristics of short Tones. II. Pitch as a function of tonal duration," J. Exp. Psych. **38**, 478-494.

Blicher, D.L., Diehl, R.L., and Cohen, L.B. (1990). "Effects of syllable duration on the perception of the Mandarin Tone 2 / Tone 3 distinction: Evidence of auditory enhancement," Journal of Phonetics, **18**, 37-49.

Diehl, R.L, and Walsh, M. A. (1989). "An auditory basis for the stimulus-length effect in the perception of stops and glides," J. Acoust. Soc. Am., **85**, 2154-2164.

Dooley, G.J., and Moore, B.C.J. (1988). "Detection of linear frequency glides as a function of frequency and duration," J. Acoust. Soc. Am. **84**, 2045-2057.

Howie, J.M. (1974). "On the domain of tone in Mandarin," Phonetica, **30**, 129-148.

Kiriloff, C. (1969). "On the auditory perception of tones in Mandarin," Phonetica, **20**, 63-67.

Kewley-Port, D., Watson. C.S., and Foyle, D.C. (1988). "Auditory temporal acuity in relation to category boundaries; Speech and nonspeech stimuli," J. Acoust. Soc. Am., **83**, 1133-1145.

Rozsypal, A.J. (1987). "Wavelet speech synthesizer," *Proceedings, Acoustics Week '87*, 62-67. Canadian Acoustics Association, Calgary, Alberta.

Zue, V.W. (1976). "Some perceptual experiments on the Mandarin tones," J. Acoust. Soc. Am. **60**, Suppl.1, S45 (Abstract).

EFFECT OF CONSONANT AND VOWEL CONTEXT ON MANDARIN CHINESE VOT: PRODUCTION AND PERCEPTION

Bernard L. Rochet and Yanmei Fei
Department of Romance Languages, University of Alberta

1.0 Introduction:
The following is a preliminary report on a study of voice onset time (VOT) in Mandarin Chinese. The issues to be focused on here are the effects of consonantal place of articulation and vowel quality on VOT duration (at the production level) and cross-over boundary values (at the perceptual level).

2.0 Subjects:
Ten native speakers of Mandarin Chinese were recruited from various departments at the University of Alberta. All of them completed the recordings which yielded the production data, and eight of them completed the perceptual tests.

3.0 Materials:
The production data were derived from the subjects' readings of a randomized word-list and were recorded on a good quality cassette recorder (Sony TC-D5 PROII), via a Beyer 111 dynamic microphone in a soundproof room. The words recorded consisted of an initial occlusive (/p, t, k, b, d, g/) and a high vowel (/i/ or /u/) or a low vowel (/a/).

The stimuli used for the perceptual tests were synthesized in cascade at a 10 kHz sampling rate, using Klatt's cascade/parallel speech synthesizer (Klatt 1980), implemented on an IBM AT microcomputer, with Canadian Speech Research Environment software. Several continua were used, 3 each for labial and dental occlusives (for the vowels /i/, /a/, and /u/); and 2 for the velar occlusives (for the vowels /u/ and /a/ only, because velar occlusives do not occur before the vowel /i/ in Mandarin Chinese). In each continuum, VOT values were incremented in 100 ms steps from -60 ms (lead VOT) to +130 ms (lag VOT).

4.0 Measurements:
The signals recorded for each subject were digitized at a sampling rate of 22 kHz, and temporal measurements of VOT were obtained from these digitized units by means of waveform analysis sofware developed at the University of Alberta. The results were analyzed by means of repeated measures ANOVAs.

5.0 Results:
5.1.0 Production
5.1.1 The voiceless aspirated occlusives
Mean VOT durations for the voiceless aspirated occlusives /p/, /t/ and /k/ are shown in Figure 1 (for the vowels /a/ and /u/). Significant main effects were found for both PLACE ($F[2, 198] = 18.44$, $p<.01$) and VOWEL ($F[1, 94] = 19.341$, $p<.01$), with no significant two-way interaction. Tukey HSD tests confirmed that VOT for /k/ (at 110.3 ms) was significantly greater than for /t/ (98.7 ms, $p<.01$) and for /p/ (99.6 ms, $p<.01$). On the other hand, the VOT values for /p/ and /t/ were not significantly different. When the following vowel was /u/, the mean VOT duration was 106.7 ms, compared with 99.1 ms when the following vowel was /a/.

Figure 2 shows the effects of the three vowels /i/, /a/, and /u/ on the preceding initial occlusives /p/ and /t/ (in this case, the consonant /k/ is not represented because it does not occur before the vowel /i/). The nature of the VOWEL had a significant effect on the VOT values of the preceding consonants ($F[2, 196] = 6.248$, $p<.01$), while the PLACE of articulation of the consonant was not significant. The two-way interaction was significant ($F[2, 196] = 3.343$, $p<.05$). Tukey HSD tests for main vowel effects indicated significantly longer VOT values (105.6 ms) when the following vowel was /i/ than when it was /a/ (96.1 ms; $p<.01$), while no other comparisons reached significance (with /u/ at 102.6 ms).

5.1.2 The voiceless unaspirated occlusives
Very similar patterns were observed for the occlusives /b, d, g/, for which the mean VOT values are summarized in Figures 3 and 4. For both series (/b, d, g/ and /p, t, k/), the velar is characterized by a longer VOT than the dental and the labial. As far as vowel effect is concerned, occlusives followed by the low vowel /a/ are always accompanied by a shorter VOT than those followed by the high vowels /u/ and /i/. Both series also show an interaction between place of articulation and identity of the vowel: specifically, the longest voicing lags occur before /u/ for the labials, and before /i/ for the dentals.

5.2.0 Perception
Mean cross-over boundary values for the labial, dental, and velar occlusive series (/p-b/, /t-d/ and /k-g/) are shown in Figure 5 (for the vowels /a/ and /u/). Significant main effects were found for both PLACE ($F[2, 14] = 25.865$, $p<.001$) and VOWEL ($F[1, 7 = 116.227$, $p<.001$), with a significant two-way interaction ($F[2, 14] = 13.598$, $p<.001$). Tukey tests confirmed that the cross-over boundary for the velars (at 37.2 ms) was significantly higher than that for the dentals (25.3 ms, $p<.01$). The boundary for the labials (33.9 ms) was also significantly higher than that of the dentals ($p<.01$), but there was no significant difference between the boundaries of the velars and labials. For the vowels, a following /u/ was associated with a significantly higher cross-over boundary (39.1 ms) than a following /a/ (25.2 ms).

Mean cross-over boundary values for the labial and dental series are shown in Figure 6 (for the vowels /i/, /a/, and /u/). The nature of the VOWEL had a significant effect on the cross-over boundary values of the preceding consonant ($F[2, 14] = 50.234$, $p<.001$), while the PLACE of articulation of the consonant was not significant. The two-way interaction was significant ($F[2, 14] = 19.94$, $p<.001$). Tukey tests for main vowel effects indicated that /i/ was associated with a higher cross-over boundary (41.3 ms) than /u/ (35.2 ms), which in turn was characterized by a higher boundary than /a/ (24.0 ms; $p<.01$).

A comparison of Figures 1, 3 and 5, and 2, 4 and 6 respectively suggests that the interaction between consonant place of articulation and vowel quality observed for the production data is also at work in perception.

6.0 Discussion:
The present results are in keeping with trends reported for VOT durations in other languages. In particular, the occurrence of longer voicing lags with velars observed here is a common phenomenon. The tendency for high vowels to be associated with longer VOT values and the interaction between consonant place and vowel quality have also been documented by Rochet et

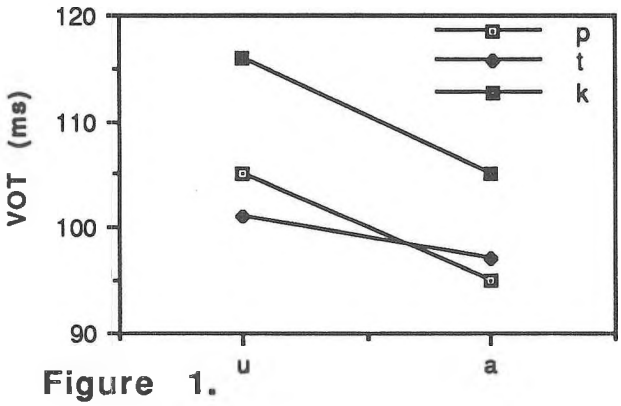

Figure 1.

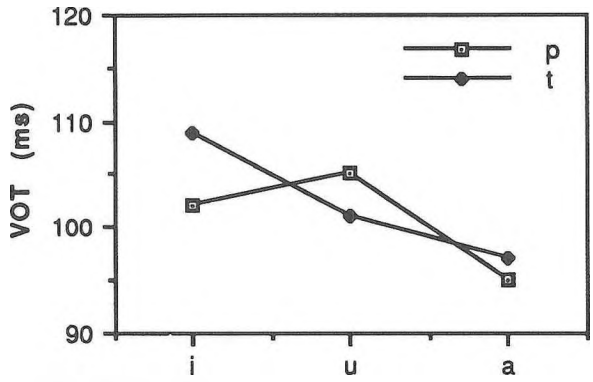

Figure 2.

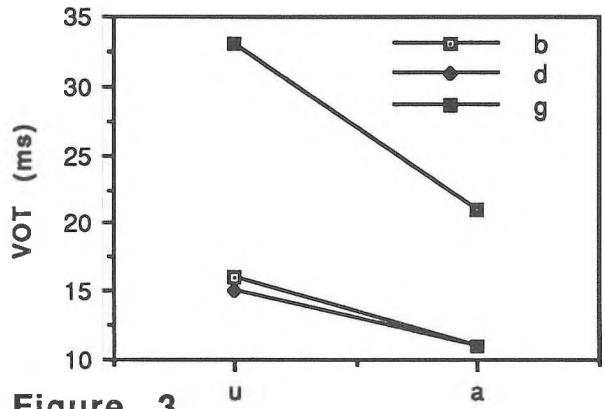

Figure 3.

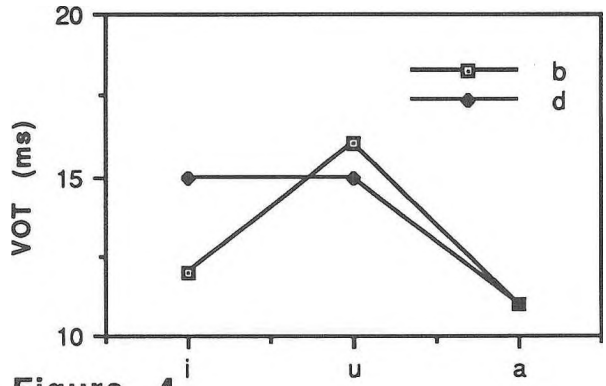

Figure 4.

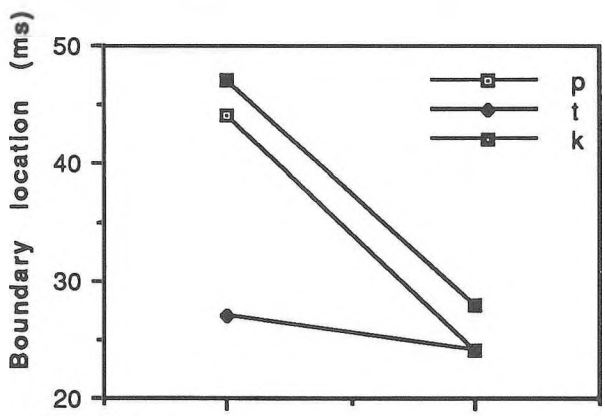

Figure 5.

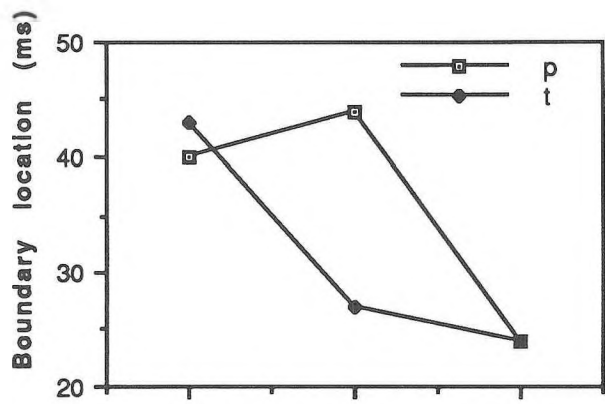

Figure 6.

al. (1987) and Fischer-Jørgensen (1972), respectively.

The parallelism noted in the present study between the patterns of variation of VOT duration (in production) and cross-over boundary location (perception) has rarely been observed (but see Summerfield 1975). Further research is needed to establish in what languages and under what conditions VOT characteristics are mirrored or ignored in perception.

7.0 References:

Fischer-Jørgensen, E. (1972). "'ptk' et 'bdg' français en position intervocalique accentuée." In A. Valdman, ed., Papers in Linguistics and Phonetics to the Memory of Pierre Delattre. The Hague: Mouton. Pp. 143-200.

Klatt, D. (1980). "Software for a cascade/parallel formant synthesizer." JASA 67: 971-995.

Rochet, B., T. Nearey, & M. Munro (1987). "Effects of voicing, place and vowel context on VOT for French and English stops." JASA 81: S65.

Summerfield, Q. (1975). "How a full account of segmental perception depends on prosody." In A. Cohen et al., eds., Structure and Process in Speech Perception. New York: Springer-Verlag. Pp. 51-68.

A DEMISYLLABLE-BASED TEXT-TO-SPEECH SYNTHESIS SYSTEM FOR ENGLISH

S.J. Eady, P. Ollek and J.R. Woolsey

Speech Technology Research Ltd., Suite D, 1623 McKenzie Avenue, Victoria, B.C. V8N 1A6, Canada

Introduction

Synthesis of English speech by computer can be accomplished in several different ways, depending on the size of the speech units that are used to produce voice output. The most widely used units for speech synthesis are phonemes (i.e., small speech units corresponding to individual phonetic items) [1]. An alternate method of producing computer-generated speech is to concatenate entire words of English in a method called "word-concatenation" synthesis [2]. A third strategy, the one described in this paper, is to use intermediate-sized units corresponding to half syllables, called "demisyllables" [3].

Demisyllables as Units of Synthesis

In demisyllable synthesis, each syllable of a word is composed of an initial demisyllable, which comprises the initial consonant and the first part of the following vowel, plus a final demisyllable, which includes the remaining portion of the vowel and any following consonants. The examples below illustrate this point:

SYLLABLE	INITIAL DEMISYLLABLE	FINAL DEMISYLLABLE
"bet"	BE	ET
"set"	SE	ET
"quench"	KWE	ENCH

Since all words of English are composed of syllables, and all syllables can be created from demisyllables, then it follows that this method can be used to produce any English word. This paper describes the various components that have been developed for microcomputer-based speech synthesis using demisyllables.

Hardware Requirements

The Demisyllable Synthesis System is designed for use on an IBM AT or compatible with a minimum of 640K of RAM. In addition, it also requires a TMS-320C25 DSP chip and a digital-to-analog converter. In its current configuration, the system will run on the Loughborough TMS320C25 Development Board or on the Kay Elemetrics CSL hardware.

Demisyllable Inventory

The inventory of demisyllable speech units consists of approximately 1400 prerecorded items that were produced in monosyllabic words by a male speaker of English. The recorded demisyllables were then digitized and encoded using pitch-synchronous LPC (10-pole, covariance method) [4].

Each encoded demisyllable unit consists of a number of 10-msec speech frames, and each frame contains quantized values for energy, pitch and 10 LPC reflection coefficients. Quantization of these values results in a storage requirement of 14 bytes per frame, and a corresponding transmission rate of 1400 bytes per second. The entire demisyllable inventory requires about 450 kilobytes of storage.

Text-to-Demisyllable Conversion

Voice output from the demisyllable synthesis system is initiated through a text-input module that accepts standard English orthographic text, as well as punctuation marks and symbols that commonly occur in written text (e.g., $, %, @, etc.). When text is input to the system, each word or symbol is first translated into its constituent demisyllable units. In addition, for each word, the system determines the stress pattern and the part of speech. All of this processing is done using a set of rules that have been developed for this purpose [5].

Demisyllable-to-Speech Rules

When an English sentence is entered into the text-input module described above, its constituent words are automatically translated into demisyllable units, and the designated units are then retrieved from the demisyllable inventory files.

Demisyllables are then transformed into complete sentences of English by means of a set of rules that are summarized below and described in greater detail elsewhere [6]. The rules are applied in the order given. The general strategy is to work from the smallest units (i.e., demisyllables) to progressively larger, more complex units (i.e., syllables, words and sentences).

Syllable Creation

The first step in the conversion from demisyllables to sentences is the creation of syllables. Each syllable is created by concatenating an initial and a final demisyllable from the demisyllable inventory. Since all initial demisyllables end in a vowel and all final demisyllables begin with a vowel, this concatenation is achieved quite simply by joining the two vocalic segments together and performing a spectral smoothing across the boundary between them.

Word Creation

Words are produced from the newly-created syllables by means of three different steps, which are described as follows:

1. Syllable Linking: A set of syllable-linking rules is used to modify phonetic segments at syllable boundaries within a word. These rules are formulated in terms of ten phonetic classes (i.e., voiced and voiceless stops, affricates and fricatives, as well as nasals, liquids, semivowels and vowels). Depending on the phonetic classes involved, the syllable-linking rules may act to delete certain speech frames, to smooth the energy contour at the boundary or to perform a spectral smoothing (i.e., smoothing of LPC reflection coefficients) at the syllable boundary.

2. Adjustment of Syllable Durations: The second stage in word creation is the adjustment in the length of each syllable in a word. This duration adjustment is required so that the syllables will have lengths that are appropriate for the stress pattern of the word in question.

3. Word-Level Pitch Assignment: The final step in the creation of words from demisyllables, is the assignment of appropriate pitch contours. As with duration adjustments,, the pitch contour of an English word is determined primarily by the stress pattern of its constituent syllables (see [6] for further details).

Sentence Creation

After words have been created from demisyllable units, the next task is to produce complete sentences from these words. This process involves three different steps.

1. Word Concatenation: The first step is to join together the word units that have been created by the components described above. When the words are concatenated, a set of word-linking rules is applied. These rules are very similar to the syllable-linking rules described above, in that they act to modify phonetic segments at syllable boundaries. In this case, however, the syllables in question are at word boundaries.

2. Sentence-Level Pitch Contour: This component is designed to provide an appropriate intonation pattern for each synthesized sentence. The method used here is very similar to that previously developed for a word-concatenation synthesis system (see [2] for details). In short, it works by overlaying a sentence-level pitch contour on top of the word-level pitch contours that are produced during the word-creation stage. The pitch level of each word is adjusted, depending on its function in the sentence. In addition, certain "tonic" pitch contours are applied at the end of each sentence to differentiate statements (which end in a falling pitch) from questions (which have rising terminal pitch contours). A third tonic contour, called a continuation rise, is also available, and may be used in the middle of a sentence at major clause boundaries.

3. Sentence-Level Timing Adjustment: The final step in sentence creation is the adjustment of word durations at different locations in a sentence. This primarily involves an increase in duration on the final word of a sentence or on any word within a sentence that occurs before a pause.

This "pre-pausal" lengthening is accomplished by adjusting the frame size of the demisyllable items that constitute the word in question. As noted above, the default frame size is 10 msec. By increasing this value to 15 msec, we can effect a 50% increase in the duration of a word or syllable. Frame-size adjustment of this magnitude is used to produce a duration increase for words that occur before a pause.

Summary

The microcomputer-based system described here has been developed to generate English speech from unlimited text input. The system uses prerecorded demisyllables as units of synthesis. With an inventory of approximately 1400 demisyllables, it can generate all possible syllables and words of the English language. By combining these units to form continuous speech, the system can produce any English sentence.

Acknowledgement

This work was supported by the Science Council of British Columbia, by NRC Canada and by NSERC of Canada.

References

[1] Klatt, D.H. (1987). "Review of text-to-speech conversion for English," Journal of the Acoustical Society of America, vol. 82, pp. 737-793.

[2] Eady, S.J., Dickson, B.C., Urbanczyk, S.C., Clayards, J.A.W. and Wynrib, A.G. (1987). "Pitch assignment rules for speech synthesis by word concatenation," Proceedings of the IEEE International Conference on Acoustics, Speech and Signal Processing, vol. 3, pp. 1473-1476.

[3] Lovins, J.B., Macchi, M.J. and Fujimura, O. (1979). "A demisyllable inventory for speech synthesis," Speech Communication Papers Presented at the 97th Meeting of the Acoustical Society of America, J.J. Wolf and D.H. Klatt (eds.), pp. 519-522.

[4] Hunt, M.J. and Harvenberg, C.E. (1986). "Generation of controlled speech stimuli by pitch-synchronous LPC analysis of natural utterances," Proceedings of the 12th International Congress on Acoustics, paper A4-2.

[5] Hemphill, T. and Ollek, P. (1990). "Text-to-demisyllable conversion in the STR text-to-speech synthesis system,," STR Technical Report No. SS9001.

[6] Eady, S.J., Hemphill, T., Woolsey, J. and Clayards, J. (1989). "Development of a demisyllable-based speech synthesis system," Proceedings of the IEEE Pacific Rim Conference on Communications, Computers and Signal Processing, pp. 463-466.

CANADIAN-DESIGNED SOFTWARE FOR SPEECH ANALYSIS AND SYNTHESIS

B.C. Dickson, A.G. Wynrib, R.C. Snell, S.J. Eady, and J.A.W. Clayards

Speech Technology Research Ltd., Suite D, 1623 McKenzie Avenue, Victoria, B.C. V8N 1A6, Canada

Introduction

This paper describes a microcomputer-based system, called **Computerized Speech Lab (CSL)**, which has been designed for analysis and synthesis of speech signals. The system, which runs on an IBM AT-compatible computer, consists of executable software modules and a hardware module that plugs into the host computer.

Hardware Module

The hardware for the system consists of an external module and a printed circuit board that fits into a slot in the host computer. The external module provides for signal conditioning and volume control on two channels. The external module connects to the printed circuit board, which has a DSP16A chip for 16-bit data acquisition and playback at sampling rates between 2.5 and 51.2 kHz on each channel. The DSP16A also handles digital filtering and downsampling in order to control aliasing. A TMS-320C25 digital signal processing chip is also included on the printed circuit board for high-speed data processing.

Software Modules

The software for this system has been designed to make a wide range of operations easily accessible to the user. The software operates in a windows-type environment using pull-down menus and a mouse. Commands may be entered by choosing from the selections in the pull-down menus, by user-defined function keys or by command strings input at the keyboard. Further flexibility is achieved by allowing the software to run through a series of command files or macros, which combine many commands into one instruction.

System Features

The system provides the user with numerous features for handling speech signals:

1. Signal Acquisition and Playback

The software provides capabilities for dual-channel speech acquisition, disk storage, retrieval and playback with user-selected sampling frequencies.

2. Speech Editing

The program also provides capabilities for speech editing, including mixing, subtracting, digital filtering, amplitude scaling, time warping, appending, splicing and downsampling. Editing also includes the ability to apply window weighting to the edges of splices for glitch-free cuts.

3. Speech Analysis

The software includes routines for analysis of energy, pitch, FFT spectrum, LPC frequency response, LPC formant history and colour or grey-scale spectrograms. Results of analyses can be displayed in graphic or numerical modes. An example of a spectrogram analysis is displayed in Figure 1.

4. Phonetic Transcription

In addition, there is a Phonetic Transcription feature for producing International Phonetic Alphabet (IPA) standardized character sets which are time-linked to the speech waveform. An example of such a phonetic transcription is shown in Figure 1.

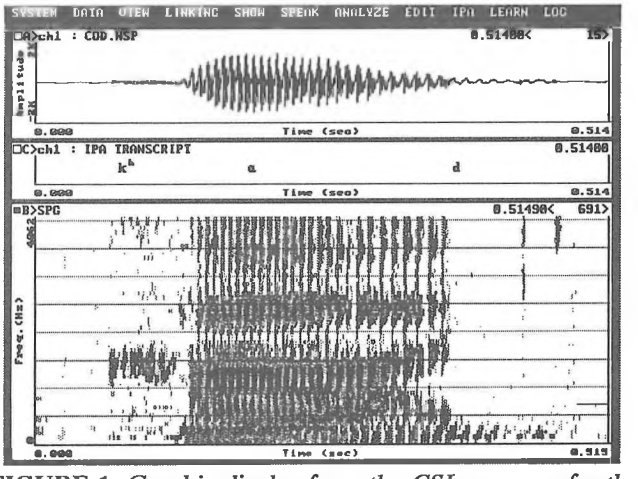

FIGURE 1: *Graphic display from the CSL program for the word "cod", showing the speech waveform (top), IPA transcription (middle) and spectrogram (bottom).*

5. Parameter Manipulation

The LPC Parameter Manipulation/Synthesis module (also called **ASL**) provides a number of different speech processing and data manipulating capabilities which allow the user to investigate the properties of a speech signal. This module uses linear predictive coding (LPC) for analysis and resynthesis of speech data. Synthesis is of high quality using the residual-excited pitch-synchronous LPC approach.

Parameters that can be manipulated in this module include energy, pitch, duration, formant frequencies and formant bandwidths. Parametric values resulting from LPC analysis may be examined and edited in three different modes. In addition, waveforms resulting from analysis and synthesis may be compared in a fourth mode. Three of these four modes are illustrated in Figures 2, 3 and 4.

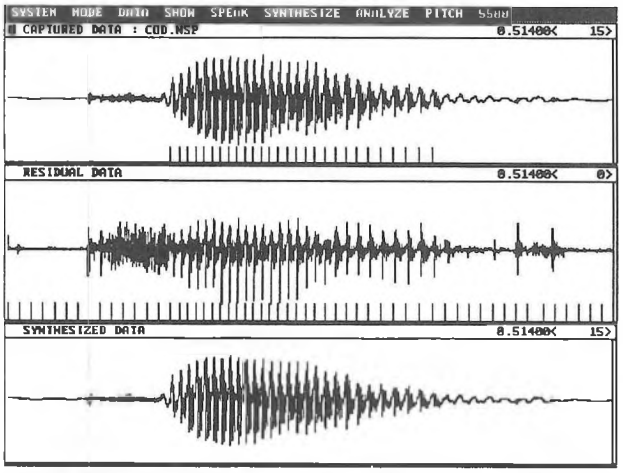

FIGURE 2: *Graphic display from the ASL module of the CSL program for the word "cod", showing the original speech waveform (top), the LPC residual waveform (middle) and the resynthesized speech waveform (bottom).*

Figure 2 shows a sample display from the **Waveform** mode of the ASL module. The top waveform in this figure is the original digitized speech data that has been produced by a male speaker. The vertical striations beneath the waveform illustrate the locations of pitch pulses during voiced portions of the speech signal. These pitch locations are used as frame boundaries for the pitch-synchronous LPC analysis that has been performed on this data. The LPC residual waveform resulting from analysis is displayed in the middle viewscreen of Figure 2. This waveform can be used as the excitation for resynthesis of the speech data. The waveform at the bottom of the figure is the result of resynthesizing the speech data using the residual-excitation approach. Note that, since none of the synthesis parameters has been changed in this case, the two waveforms in the top and bottom viewscreens of Figure 2 should be identical. In fact, listening tests show that the two signals are perceptually indistinguishable.

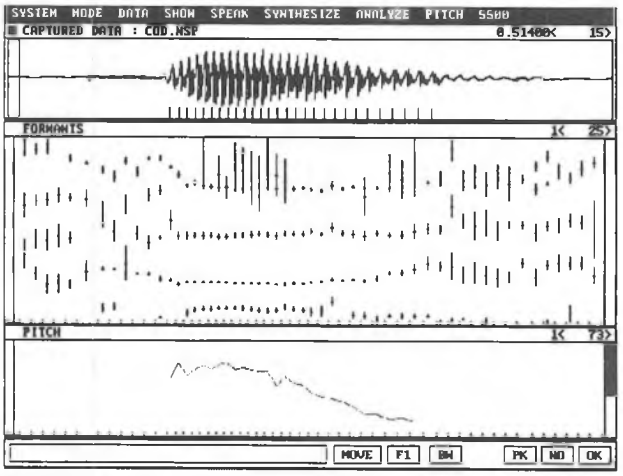

FIGURE 3: *Graphic display from the ASL module for the word "cod", showing the speech waveform (top), formant frequencies derived from LPC analysis (middle) and pitch contour (bottom).*

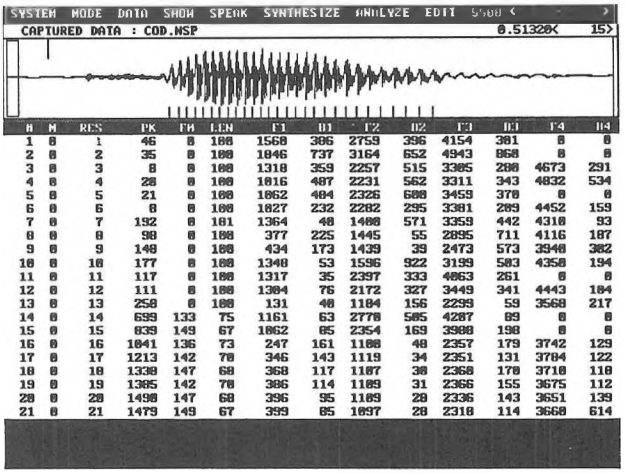

N	M	RES	PK	FM	LEN	F1	B1	F2	B2	F3	B3	F4	B4
1	0	1	46	0	100	1568	306	2759	396	4154	301	0	0
2	0	2	35	0	100	1046	737	3164	652	4943	868	0	0
3	0	3	0	0	100	1318	359	2257	515	3305	200	4673	291
4	0	4	28	0	100	1016	407	2231	562	3311	343	4032	534
5	0	5	21	0	100	1062	404	2326	600	3459	370	0	0
6	0	6	0	0	100	1027	232	2282	295	3301	289	4452	159
7	0	7	192	0	101	1364	40	1400	571	3359	442	4310	93
8	0	8	90	0	100	377	225	1445	55	2895	711	4116	187
9	0	9	140	0	100	434	173	1439	39	2473	573	3940	382
10	0	10	177	0	100	1340	53	1596	922	3199	503	4358	194
11	0	11	117	0	100	1317	35	2397	333	4063	261	0	0
12	0	12	111	0	100	1304	76	2172	327	3449	341	4443	184
13	0	13	258	0	100	131	40	1104	156	2299	59	3568	217
14	0	14	699	133	75	1161	63	2778	585	4287	89	0	0
15	0	15	839	149	67	1062	85	2354	169	3988	198	0	0
16	0	16	1041	136	73	247	161	1188	48	2357	179	3742	129
17	0	17	1213	142	70	346	143	1119	34	2351	131	3784	122
18	0	18	1338	147	68	368	117	1187	38	2368	178	3718	118
19	0	19	1385	142	70	386	114	1189	31	2366	155	3675	112
20	0	20	1498	147	68	396	95	1189	28	2336	143	3651	139
21	0	21	1479	149	67	399	85	1097	28	2318	114	3668	614

FIGURE 4: *Graphic display from the ASL module for the word "cod", showing the speech waveform (top), and numerical values resulting from LPC analysis (bottom).*

Figure 3 illustrates the **Formants** mode of the ASL module. This mode provides the means for graphic editing of the parameter contours that result from LPC analysis. The figure displays the original speech waveform at the top, the pitch contour at the bottom and a time-history display of formant frequencies in the middle. Pitch and formant parameters can be modified by redrawing the pertinent contours using a mouse. Resynthesis of a new speech signal can be done quickly to provide immediate feedback to the user.

Figure 4 displays the **Numeric Values** mode of the ASL module. As can be seen in the figure, this mode provides a waveform display at the top and a list of numerical values resulting from LPC analysis at the bottom. Each column of data represents a separate LPC parameter. The parameters include residual frame number, energy, fundamental frequency, frame length, formant frequencies and formant bandwidths. Each of these parameters can be modified by entering new numerical values on a frame-by-frame basis or by marking a column and smoothing between endpoints. As in the Formants mode, resynthesis following parameter manipulation provides instant feedback on the effects of parameter changes.

Summary

The **Computerized Speech Lab** is a microcomputer-based system that provides a wide range of functions for the analysis and synthesis of speech signals. The software for this system has been designed and developed in Canada and is currently being sold to speech researchers around the world.

Acknowledgement

The software described here was developed by Speech Technology Research Ltd. under contract to Kay Elemetrics Corp.

AN IMELDA BASED VOICE RECOGNITION SYSTEM: A STEP TOWARDS EFFECTIVE VOICE RECOGNITION FOR PERSONS WITH SEVERE DISABILITIES

Gary E. Birch[1], Dariusz A. Zwierzynski[1], Claude Lefebvre[1], and David Starks[2]

[1]The Neil Squire Foundation
Research and Development Division
4381 Gallant Avenue
North Vancouver, B.C.
Canada
V7G 1L1

[2]Canadian Marconi Company
415 Legget Drive
P.O. Box 13330
Kanata, Ontario
K2K-2B2

1. Introduction

The Neil Squire Foundation has worked individually with well over 3000 adults with severe physical disabilities in assisting them to effectively use computer based technical aids. The Foundation recognizes the significant potential voice recognition represents in solving many human/machine interface problems and therefore, researchers in the Foundation have endeavoured to keep abreast of voice recognition technology. For many severely disabled persons, the ability to use spoken commands to control their environment is a very enticing concept. This interface capability can greatly enhance their ability to pursue a career, obtain an education, or enjoy recreational activities.

2. Background

Through interaction with the Foundation's clients we have had experience with various commercially available voice recognition systems, ranging from medium to high end systems, in various applications. As attractive as voice recognition first appears, the Foundation currently, except in special circumstances, discourages its application. We estimate that we have had well over 200 hours of direct individual involvement with severely disabled persons who were utilizing speech input. Through this experience we have encountered several limitations with currently available systems which have resulted in simply too much frustration for a majority of our clients. Primarily, these include lack of robustness to background noise, change in speaker emotion and speaker fatigue as well as generally complicated and unfriendly user training/application software. Researchers from the University of Tennessee, Centre of Excellence for Computer Applications [1], came to similar conclusions about the problems besetting speech input for persons with severe disabilities. Interestingly, one of the most significant problems cited was the lack of user friendly support software packages.

This experience lead the Foundation to become involved in the development of an IMELDA based voice recognition system that would potentially overcome these limitations. This system is being jointly developed by the Speech Research Centre of the National Research Council of Canada, the Canadian Marconi Company and the Neil Squire Foundation. The theoretical premises and the functional design of the recognition system were originally developed at the NRC. We are also developing a P.C. based user friendly training software package designed to work with the recogniser hardware.

3. IMELDA

Our speech recogniser represents a hybrid system in that it employs a discriminant network in the front-end component and dynamic time warping technique in the back-end component. The front-end discriminant network first extracts the invariant acoustic features from the speech signal. It then passes them on to the back-end component where they are compared with the stored templates through the DTW technique for the final recognition.

The front-end processing is a conventional fast-fourier-transform-based spectral filter-bank analysis followed by a linear transformation. The linear transformation developed and tested at the NRC laboratory is a linear discriminant network [2]. It is very efficient at extracting invariant features for reliable speech recognition, especially when the speech is distorted or spoken in high background noise. The linear discriminant network was called IMELDA, which stands for Integrated MEL-scale linear Discriminant Analysis because it combines various mel-scale spectral representations into a single set of discriminant functions. The mel scale is a frequency scale of the human ear. The computation of the linear discriminant transformations involves the between-class with the within-class covariance information of the spectral features [3].

The original idea behind using LDA to derive a robust linear discriminant transform for speech recognition applications in the NRC Speech Research Centre dates back to a paper written by Dr. Melvyn J. Hunt in 1979 [4]. There, he suggested that the distance measures in speech recognition should be based on within-class variances in speech sounds.

A within-class matrix (W) is derived by non-linearly time-aligning the individual examples of words to their corresponding averaged word models (templates). Two main assumptions underlie the computation of the W matrix. The first is that the aligned frame pairs belong to the same class. This assumption is made possible by non-linearly time-aligning two tokens, differing in their temporal structure, which maximises their phonetic similarity. The second assumption is that template frames represent class centroids, and that the parameters in the corresponding frames of the individual examples of the word in question are distributed about the template values according to a multivariate Gaussian distribution with equal variance in all directions. This implies a spherical symmetry of the probability density functions and hence it is possible to use Euclidean squared distances. Even though it is not possible to consider each template to be a separate class, the estimation for the between-class matrix can be effected by computing the covariance over all the parameters in the frames of all the templates in the vocabulary.

The end result of the IMELDA computation is a reduced set of orthogonal discriminant vectors which focus on the features which most effectively differentiate between speech sounds. In summary, the linear transformation of the output of the mel-scale filter-bank is achieved by multiplying a matrix of discriminant functions by the vector of log energies contained in a frame of the filter-bank output. The transformed feature vector is then used with Euclidean distance calculations to determine the optimal discrimination between template frames.

To test the mainframe implementation of the IMELDA recognition system, we compared its performance to two well respected commercial systems in a digit string recognition test where we voluntarily distorted the speech signal to simulate speech distortions found in noisy environments. In one case, we added white noise to the speech signal such that the SNR was set approximately to 15dB. In the other case, we changed the spectral balance ('tilt') of the speech signal by 6 dB/octave, by processing speech through a pre-emphasis filter. The IMELDA system demonstrated a profound advantage in the tests with distorted speech and it was also superior in speaker independent tests for both clean and distorted speech. [3] (see Table 1).

Male Continuous Word Recognition Percentage Errors (%)

Representation	Speaker-Dependant			Speaker-Independent		
	Quiet	Noise	Tilt	Quiet	Noise	Tilt
IMELDA	0.2	0.6	0.1	1.8	4.1	1.4
commercial.1	1.2	1.2	23.6	9.3	12.0	50.7
commercial.2	N/A	N/A	N/A	N/A	N/A	N/A

Male Isolated Word Recognition Percentage Errors (%)

IMELDA	0.1	0.5	0.0	0.3	1.9	0.4
commercial.1	0.4	1.3	20.0	5.0	10.0	45.2
commercial.2	0.7	16.4	12.4	8.5	26.7	26.5

***Table 1** Continuous and isolated digit recognition test results for 1352 digits by 9 male speakers. The test material was presented in three conditions: undegraded (Quiet), with white noise added to give a 15 dB SNR (Noise), and with a 6 dB/octave spectral tilt applied (Tilt). The commercial.1 system had a finely adjusted noise mask to achieve the good test noise results. Since commercial.2 is an isolated word type, results for continuous-word recognition would not be meaningful.*

4. Hardware

The IMELDA speech recognition algorithms have been implemented in hardware and are packaged in a 10" x 5" x 6" enclosure. This hardware recogniser was designed as a real-time prototype platform so that we could demonstrate IMELDA as well as develop, test, and evaluate the ongoing research efforts. Our goal is to achieve the same level of recognition performance with the hardware as with the mainframe implementation.

Two digital signal processor circuit cards are used. One for the signal processing aspects of IMELDA and the other for the continuous word pattern matching algorithm. This approach allows a high degree of development flexibility. In fact there is 40% spare capacity on one processor. However, the pattern matching algorithm is so computationally expensive that the number of words that can currently be recognised in real-time is limited to 30 words. We will be investigating techniques to increase the active vocabulary size.

Preliminary evaluations of the recogniser indicate that we are approaching the baseline established on the mainframe despite some limitations imposed by the hardware. The hardware recogniser has a lower mathematical dynamic range because it uses fixed point arithmetic rather than floating point and it employs a bandwidth limiting audio codec. The dynamic range was addressed by choosing the Analog Device ADSP-2100A DSP processor with its 40 bit multiply-accumulator which extends the dynamic range during long series of consecutive math operations and by using the block-floating point technique for the FFT implementation of the Mel-scale filterbank. The limited precision actually assisted the 'back-end' processing of the distance calculation in the pattern matching algorithm. This is reflected in Table 2 which compares pattern matching algorithm performance of the mainframe with the hardware.

Isolated Digits for speaker 'aa'

Platform	Quiet	Noise	Tilt
Mainframe	0/80	3/80	1/80
Hardware	0/80	1/80	1/80

***Table 2** Mainframes vs. Hardware results for speaker 'aa'. Number of errors over 80 digits spoken in three different conditions.*

The audio codec limits the speech bandwidth from 200 Hz to 3400 Hz. Fortunately, the IMELDA transform derives most of its information from the vocal tract resonances (formants) which reside within this range. The IMELDA transform for the hardware prototype has been derived from speech processed through this audio interface and, hence, the spectrum is weighted accordingly.

5. User Interface Software

The user interface software is implemented on a P.C. based platform and it communicates to the hardware through a serial link. This software handles the presentation and execution of the various functions of the recognition system in an orderly manner.

The first iteration of this software was intended to be a support tool for the hardware developers as well as a generalized user interface. As such, a certain degree of computer competence was assumed in the first iteration. The issue of how to handle novice computer users has be taken into consideration in the design process, but the user interface features necessary to support them have not been fully incorporated into the current version of the software.

The main functions for the program were determined to be: 1) File creation and handling capabilities for user vocabulary files 2) Edit capabilities for the vocabulary files 3) Syntax specification and editing capabilities 4) "Terminate-and-stay-resident" (TSR) code that accepts recognition results from the hardware and generates the corresponding command level macros for the user's application 5) Training mode for training each of the acoustic templates 6) Define mode for binding acoustic templates to keystroke macros 7) Embedded and isolated word training modes.

The basic flow and presentation for the program were laid out based on the operation of the voice recognition hardware and the experience of the NSF engineers with other commercial voice recognition systems. As a result, the interface was designed so that it operated in a menu driven graphical environment. Essentially, the user lays out word groups on a graphics screen in block elements. The user then specifies the syntax for a vocabulary by connecting word groups together in the order in which he/she wants word groups to be recognized. The user interface software will then generate the appropriate data file to specify the syntax of the vocabulary. This data file is then downloaded to the recognizer and used as part of the recognition process. This syntax definition method greatly simplifies data entry for novice users as it is more intuitive in nature and puts the burden of generating the syntax description file on the interface software.

6. Conclusions and Future Directions

Testing of the mainframe implementation of the IMELDA recognizer has demonstrated that it deals well with simulated noisy backgrounds and tilted speech. These results indicate that an IMELDA based recognizer will be able to address the identified limitations of other commercially available recognizers for persons with severe disabilities related to background noise and speaker variability (potentially related to changing emotion and fatigue). Initial testing of the hardware prototype recognizer has indicated that results comparable to the mainframe implementation can be achieved. The user interface software has been designed and implemented in such a manner as to overcome the limitations of generally complicated and unfriendly support software. Current work is focused on the improvement of the user training software and the performance of the recogniser in harsh environments where there is high background noise. Once these improvements are implemented, future work will involve an evaluation of the hardware and the software interface on a population of persons with severe physical disabilities. Other future work will include: increasing the active vocabulary size, continued development of speaker independence capabilities and implementation of robust keyword activation.

7. References

1. V.A. Thomason, P.S. Chopra, S.M. Farajian, and M.A. Abazid, "Application of Voice Recognition Devices for Computer Access and Programming", Proc. RESNA, ICAART-88, Montreal, Canada, 1988, pp. 370-371.

2. Hunt, M. J. and Lefebvre, C., Distance measures for speech recognition, Aeronautical Note, NAE-AN-57, Ottawa, March, 1989.

3. Hunt, M. J., Evaluating the performance of connected-word speech recognition systems, Proc. IEEE Int. Conf. Acoustics, Speech and Signal Processing (ICASSP-88), Vol. 1, pp. 215-218, New York, April, 1988.

4. Hunt, M. J., A statistical approach to metrics for word and syllable recognition, J. Acoust. Soc. Am., Salt Lake City, Vol. 66, pp. S535-536, 1979.

Hierarchical Non-Stationarity in a Class of Doubly Stochastic Models with Application to Automatic Speech Recognition

L. Deng
Department of Electrical and Computer Engineering
University of Waterloo, Waterloo, Ontario, Canada N2L 3G1 deng@ccng.waterloo.edu

Abstract

In this paper we introduce the concept of two-level (global and local) hierarchical nonstationarity for describing the complex, elastic, and highly dynamic nature of speech signals. A general class of doubly stochastic process models are developed to implement this concept. In this class of models, the global nonstationarity is embodied through an underlying Markov chain (or any other scheme capable of providing nonlinear time warping mechanisms) which governs the evolution of the parameters in a set of output stochastic processes. The local nonstationarity is realized by assuming state-conditioned, time-varying first and second order statistics in the output data-generation process models. To provide practical algorithms for speech recognition which allow the model parameters to be reliably estimated, the local nonstationarity is represented in a parametric form. Simulation results demonstrated close fitting of the model to the actual speech data. Results from speech recognition experiments provided evidence for the effectiveness of the model in comparison with the standard HMM, which is a degenerated case — with single-level nonstationarity — of the proposed model.

I. Introduction

Traditional stochastic models have been developed to deal only with stationary sources, or at best, with nonstationary observations which can be directly transformed into stationary observations by simple time differentiation [2]. Only with the advent of hidden Markov models (HMMs) has it become possible to model nonstationary sources in a reasonably satisfactory manner.

Nonstationary behaviors are exhibited in the HMM via the evolution of the underlying Markov chain. This is a powerful mechanism for representing acoustic signals in natural speech since it parallels patterns of change of the phonetic content contained in the acoustic signal. However, in the HMM setup no mechanism is provided to handle detailed variations in the highly dynamic speech signal given a fixed phonetic content. This is true of all the stochastic models for speech developed so far, including the best known Baum's and Liporace's HMMs [1, 6] and Poritz's hidden filter model [7]. These models all assume the state-conditioned stationarity for the observation data and they rely solely on the (hidden) Markov chain to fit the overall speech nonstationarity.

Acoustic signals in actual speech exhibit a clear nature of hierarchical nonstationarity. At the global level, nonstationarity is exhibited when phonetic contents change over time in a relatively slow fashion. A Markov chain is well equipped to describe such changes. The local nonstationarity, on the other hand, manifests itself generally at the allophonic or at the microstructural level. The effects of such local nonstationarity are especially pronounced in transitional segments of speech whose production involves strong articulatory dynamics (e.g. glides, diphthongs, and CV/VC transitions) [5]. Both the standard HMM and the hidden filter model are a handicap in handling the local nonstationarity.

The purpose of this paper is to propose a general class of stochastic models which are capable of capturing both the global nonstationarity and the local nonstationarity in the speech signal in a parametric form.

II. The Hierarchical Nonstationary Model

The global nonstationarity in this class of models, as with the standard HMM, is implemented by a homogeneous Markov chain. The local or state-conditioned nonstationarity is implemented by an autoregressive output process where both the first-order statistic (mean) and the second-order statistic (autocorrelation function) are made a function of time via time-varying mean function and time-varying autoregression coefficients. We call this model the *hierarchical nonstationary model*, or HN-model for short.

The HN-model consists formally of the following parameter quadraples $[\mathbf{A}, \mathbf{\Theta}, \mathbf{\Psi}, \mathbf{\Sigma}]$:

1. Transition probabilities, $a_{ij}, i, j = 1, 2, ..., N$ of the homogeneous Markov chain with a total of N states;
2. Parameters Θ_i in the time-varying mean functions $g_t(\Theta_i)$ of the output data-generation process, as dependent on state i in the Markov chain;
3. Parameters Ψ_i in the time-varying autoregression coefficients (with a fixed regression order p) $\phi_t(\Psi_i)$ of the output data-generation process, as dependent on state i in the Markov chain;
4. Covariance matrices, Σ_i, of the zero-mean, Gaussian, IID driving noise $R_t(\Sigma_i)$, which are also state dependent.

Given the above model parameters, the observation vector sequences, $O_t, t = p+1, p+2, ..., T$ are generated from the model according to

$$O_t = g_t(\Theta_i) + \Sigma_{k=1}^{p} \phi_t(\Psi_i) O_{t-k} + R_t(\Sigma_i), \qquad (1)$$

where state i at a given time t is determined by the evolution of the Markov chain characterized by a_{ij}.

III. Parameter Estimation for the HN-Model

As with the standard HMM, we use the EM algorithm to obtain an iterative solution to maximum likelihood estimates for the parameters in the HN-model. Each iteration in the EM algorithm consists of two steps. In the E step, the auxiliary function $Q(\Phi|\Phi_0)$ is obtained:

$$Q(\Phi|\Phi_0) = E[log P(O_1^T, \mathcal{S}|\Phi)|O_1^T, \Phi_0], \qquad (2)$$

where the expectation is taken over the "hidden" state sequence $\mathcal{S}$. For the HN-model, algebraic manipulations on (2) lead to the simplified form of Q

$$\begin{aligned} Q \quad = \quad & \sum_{i=1}^{N} \sum_{j=1}^{N} \sum_{t=1}^{T-1} P(s_t = i, s_{t+1} = j|O_1^T, \Phi_0) \log a_{ij} \\ & + \sum_{i=1}^{N} \sum_{t=1}^{T} P(s_t = i|O_1^T, \Phi_0) N_t(i), \end{aligned} \qquad (3)$$

where $N_t(i)$ stands for the log likelihood

$$\begin{aligned} -\frac{D}{2} log(2\pi) \quad & -\tfrac{1}{2} log|\Sigma_i| - \tfrac{1}{2}[O_t - g_t(\Theta_i) - \Sigma_{k=1}^{p} \phi_t(\Psi_i) O_{t-k}]^{Tr} \\ & \Sigma_i^{-1}[O_t - g_t(\Theta_i) - \Sigma_{k=1}^{p} \phi_t(\Psi_i) O_{t-k}]. \end{aligned} \qquad (4)$$

Estimates of the model parameters are obtained in the M step via maximization of (3). Re-estimation formulas for the transition probabilities and for the residual covariance matrices are very similar to those in the standard HMM and are thus omitted. Re-estimation of the parameters in the time-varying mean functions and in the regression coefficients requires solution of a system of equations which is derived below.

By removing optimization-independent terms and factors in (3), an equivalent objective function is obtained as

$$\begin{aligned} Q_e(\Theta_i, \Psi_i) = \sum_{i=1}^{N} \sum_{t=1}^{T} \gamma_t(i) & [O_t - g_t(\Theta_i) - \Sigma_{k=1}^{p} \phi_t(\Psi_i) O_{t-k}]^{Tr} \\ & \Sigma_i^{-1}[O_t - g_t(\Theta_i) - \Sigma_{k=1}^{p} \phi_t(\Psi_i) O_{t-k}], \end{aligned} \qquad (5)$$

where $\gamma_t(i) = P(s_t = i|O_1^T, \Phi_0)$, which can be computed efficiently by the use of the forward-backward algorithm [1].

The re-estimation formulas are obtained by jointly solving

$$\frac{\partial Q_e}{\partial \Theta_i} = 0; \quad \frac{\partial Q_e}{\partial \Psi_i} = 0, \quad i = 1, 2, ..., N. \tag{6}$$

Using the chain rule for differentiation, (6) becomes

$$\sum_{t=1}^{T} \gamma_t(i)[O_t - g_t(\hat{\Theta}_i) - \Sigma_{k=1}^{p} \phi_t(\hat{\Psi}_i) O_{t-k}] \frac{\partial g_t(\hat{\Theta}_i)}{\partial \hat{\Theta}_i} = 0, \tag{7}$$

and

$$\sum_{t=1}^{T} \sum_{s=1}^{p} \gamma_t(i)[O_t - g_t(\hat{\Theta}_i) - \Sigma_{k=1}^{p} \phi_t(\hat{\Psi}_i) O_{t-k}] O_{t-s}^{T\tau} \frac{\partial \phi_t^{T\tau}(\hat{\Psi}_i)}{\partial \hat{\Psi}_i} = 0 \tag{8}$$

for $i = 1, 2, ..., N$.

We now let $g_t(\Theta_i)$ and $\phi_t(\Psi_i)$ take specific forms of time function. Polynomial functions are the simplest choices, which convert (7) and (8) to a coupled linear system of equations for solving the polynomial coefficients. That is, let

$$g_t(\Theta_i) = \sum_{m=0}^{M} \mathbf{B}_i(m) t^m, \quad \phi_t(\Psi_i) = \sum_{l=0}^{L} \mathbf{H}_i(l) t^l, \tag{9}$$

where $\mathbf{B}_i(k)$ is a D-dimensional vector and $\mathbf{H}_i(k)$ is a $D \times D$ matrix, both associated with state i in the Markov chain and with polynomial order k. Then the model parameters Θ and Ψ are just two sets of the polynomial coefficients, $b_d(m), m = 0, 1..., M$, and $h_{uv}(l), l = 0, 1, ..., L; d, u, v = 1, 2, ..., D$.

Substituting (9) into (7) and (8), we obtain the linear vector system for the re-estimate of the polynomial coefficients

$$\sum_{t=1}^{T} \gamma_t(i)[\mathbf{O}_t - \sum_{m=0}^{M} \hat{\mathbf{B}}_i(m) t^m - \sum_{k=1}^{p} \sum_{l=0}^{L} \hat{\mathbf{H}}_i(l) t^l O_{t-k}] t^u = 0,$$

for $u = 0, 1, ..., M$, coupled with the linear matrix system

$$\sum_{t=1}^{T} \sum_{s=1}^{p} \gamma_t(i)[\mathbf{O}_t - \sum_{m=0}^{M} \hat{\mathbf{B}}_i(m) t^m - \sum_{k=1}^{p} \sum_{l=0}^{L} \hat{\mathbf{H}}_i(l) t^l O_{t-k}] t^v O_{t-s}^{T\tau} = 0,$$

for $v = 0, 1, ..., L$.

We have so far implemented the model which contains only the component of time-varying means, or the above model with $\mathbf{H} = \mathbf{0}$.

IV. Application to Speech Recognition

Preliminary speech recognition experiments have been carried out to evaluate the HN-model described above. In an E-set recognition experiment using words as the speech units [5], we found that with a large amount of training data, the HN-model performs the nearly same as the standard HMM containing a large number of states. However, with only two tokens to train each word model, the standard HMM suffers from the undertraining problem but the HN-model does not. In the second set of experiments, we intend to improve the previously developed locus model [4] by using the quadratically time-varying mean functions in the HN-model to fit formant transition data. The model in [4] requires the linearity assumption on the acoustic transition data but with the HN-model, polynomial fitting to the data of any order can be implemented with mathematical tidiness to reliably estimate the "locus" parameters.

V. Discussion

The statistical properties of the standard HMM, the hidden filter model, and the currently developed HN-model can be compared to appreciate the increasing level of generality in the model development. The standard HMM is a local IID model, which has a very simple statistical structure. It contains locally constant (degenerated) mean functions. The hidden filter model generalizes the standard HMM in just providing time-origin independent (and hence remains a locally stationary model), exponentially decaying functions in the second-order statistics. The first-order statistics remain the same as those in the standard HMM. The HN-model developed in this paper generalizes the above models in providing locally time-varying first-order and second-order statistics, and hence a locally nonstationary model.

The HN-model provides a mechanism for dealing with two levels of nonstationarity in the signal to be modeled: the global nonstationarity as controlled by the Markov chain, and the local nonstationarity as accommodated by the state-conditioned time-varying statistics up to the second order. The first order statistic is important since it catches the general trend for the dynamic movement of speech data over time. In the standard HMM [3], states are intended and can only be used to represent piece-wise stationary segments of speech although the acoustic realization of many types of speech sounds exhibits highly dynamical trends and varies in a truly continuous manner. Such trends can be much more efficiently and accurately described by time-varying mean functions, rather than using many HMM states to approximate the trends piece-wise constantly.

The theoretical significance of the correlation function lies in the fact that any random process, in a second-order theory with which we assume state-conditioned speech data are in conformity, identifies itself with this function. Intuitively, we argue for close relationships between the correlation function $\rho(\tau)$ and speech frame (Y_t) dependence as follows: If $\rho(\tau)$ has large values at τ, then the acoustic data in a speech frame would have strong influences on those in another speech frame which is τ frames away. For instance, suppose $\rho(\tau)$ has a large positive value; then if Y_t is greater than the mean value, $Y_{t+\tau}$ would tend to be forced to move above the mean value so as to keep $\rho(\tau)$ positive.

In view of the close relationship between the properties of the actual speech signal and those provided by the HN-model, and of essentially the same computational complexities between the standard HMM and the HN-model, we predict strong utilities of the HN-model in speech recognition. Our preliminary experiments are consistent with this prediction.

References

[1] L.E. Baum. "An inequality and associated maximization technique in statistical estimation for probabilistic functions of Markov processes", *Inequalities*, Vol. 3, pp. 1–8, 1972.

[2] G.E.P. Box and G.M. Jenkins. *Time Series Analysis—Forecasting and Control*, Holden-Day, San Francisco, CA, pp. 67–72, 1976.

[3] L. Deng, P. Kenny, M. Lennig, and P. Mermelstein. "Phonemic hidden Markov models with continuous mixture output densities for large vocabulary word recognition," *IEEE Trans. Signal Processing*, Vol. 39, No. 7, July, 1991, pp. 1677–1681.

[4] L. Deng, P. Kenny, M. Lennig, and P. Mermelstein. "Modeling acoustic transitions in speech by state-interpolation hidden Markov models," *IEEE Trans. Signal Processing*, scheduled to appear in February, 1992.

[5] L. Deng and K. Erler. "Structural Design of HMM Speech Recognizer Using Multi-Valued Phonetic Features: Comparison with Segmental Speech Units," submitted to *J. Acoust. Soc. Am.*.

[6] L.A. Liporace, "Maximum likelihood estimation for multivariate observations of Markov sources," *IEEE Trans. Information Theory*, Vol.28, pp. 729-734, 1982.

[7] A.B. Poritz, "Hidden Markov models: A guided tour," *Proc. IEEE Internat. Conf. on Acoustics, Speech, and Signal Processing*, New York, New York, April 11–14, 1988, pp. 7–13.

EXPLOITING PAUSES IN CONTINUOUS SPEECH RECOGNITION

Douglas O'Shaughnessy
INRS-Télécommunications, Université du Québec
3 Place du Commerce, Verdun, Québec H3E 1H6

1. Introduction

Most automatic speech recognition systems to date have required that speakers carefully pronounce their speech, in order to obtain good recognition performance. The task of automatic recognition of spontaneous, natural or conversational speech differs from that of careful or read speech in several ways, the most obvious difference concerning hesitation phenomena. In spontaneous speech, people often start talking and then think along the way. This causes spontaneous speech to have a variable speaking rate (both within and across sentential utterances); at times, such speech exhibits interruptions. The specific interruption phenomena studied in this paper are hesitation pauses (both filled and unfilled) and utterance restarts. Pauses are simple interruptions in the flow of speech, where a significant delay occurs in the delivery of the speech between words. In restarts, the speaker repeats or corrects some words (usually in addition to pausing).

A primary application of this study of hesitation phenomena lies in improving the performance of automatic recognizers, given an input of spontaneous speech (e.g., verbal conversations with computer databases). Speech researchers have often expressed interest in exploiting the intonation of spoken utterances in the recognition process, but have been deterred by the complex nature of how intonation (including pauses) relates to the text of an utterance. Even straightforward phenomena such as unfilled pauses (i.e., silence periods - which are generally easy to identify, if long enough) are not reliable indicators to the syntactic or semantic sentence structure of an utterance.

2. Speech database studied

In the context of our investigation into voice dialog access to databases, we are currently examining an application involving a simulated travel agent. A naive user (the speaker) is given the task of arranging a trip involving air travel via commerical airlines, by verbally interacting with a "computer travel agent." Thus, the user formulates verbal questions (and commands) on the fly, in a spontaneous fashion, as if in conversation with a travel agent. The current system does not reply verbally, but rather outputs information from a database onto a computer screen. The database is a version of the Official Airline Guide actually used by travel agents (it was furnished as part of a project supported by DARPA - the US Defence Advanced Research Projects Agency). The spoken data consists of more than 30 adult male and female speakers, each speaking about 30 utterances, each ranging in length from a few words to several dozen words. Many utterances are quite fluent, and exhibit no pause phenomena. However, about half contain pauses, and many have more than one hesitation phenomenon.

3. Previous studies on hesitation phenomena

In examining a corpus of speech produced by people spontaneously describing images, Levelt [1] found that 18% of the speech restarts occurred within a word, which was then corrected in the restart; i.e., the speaker paused in the middle of the "problem word" and restarted the utterance (e.g., "...go to the ye-, to the orange node"). In 51% of the cases, the speaker halted immediately after the word to be corrected, while 31% of the time the speaker stopped one or more words after the problem word (e.g., "...from green left to pink - er, from blue left to pink"). Most of the interruptions at word boundaries occurred at major syntactic boundaries. Within-word interruptions, on the other hand, did not even preserve syllable boundaries; i.e., speakers tended to stop immediately upon realizing that a problem existed, even if that meant stopping before a vowel could be pronounced in the current syllable. Levelt found that "uhh" occurred in 30% of restarts. He noted that uttering such a neutral sound (i.e., filling the pause) may help the speaker prevent an interruption by another speaker. The implication is that listeners often interpret unfilled pauses (i.e., silence) as a cue to start speaking, but they would not interrupt a filled pause. Levelt noted that restarts can be either marked prosodically by changes in intonation (between the speech before and after the pause) or unmarked prosodically (i.e., no change in intonation). Cases of simple mispronunciation tended to be unmarked, whereas lexical changes (replacement of a word with a different sense) were marked. While Levelt's work is of direct relevance here, it gives few quantitative details other than simple statistics of occurrence; in particular, F0 and durational distributions are rarely mentioned.

Deese [2] noted that hesitation pauses occur less often in planned (non-spontaneous) than unplanned speech. He defined such a pause as occurring in a syntactically inappropriate location and lasting between 100 ms and 300 ms. Our results below dispute these assertions: some occur at syntactic boundaries, and hesitation pauses can last well beyond 300 ms. Deese suggested that filled pauses lend an air of diffidence and humility, whereas unfilled pauses suggest assurance and superiority. In comparing planned and unplanned speech, he found that planned speech had more total pauses (10.3 per 100 words, vs. 8.8 for unplanned speech), while having fewer restarts (3.8 per 100 words, vs. 5.0 for unplanned speech). He found that pauses ranged from about 50 ms to 5 s (we found similar pause lengths here). Without giving quantitative results, he noted that long filled pauses tended to be segmented into syllables (i.e., "uhh umm uhh" rather than "uhhhhhh" or "ummmm"). Mispronunciations (words uttered incorrectly rather than chosen incorrectly) occurred at a rate of 1.5 per 10,000 words; mistaken words occurred at 2.5 per 10,000 words.

Hauptmann and Rudnicky [3] investigated ways in which humans differ in speaking to computers as opposed to speaking to other humans. They found that the average utterance to a computer was longer (6.1 words vs. 5.5 words to a human). Filled pauses occurred at a rate of 4 per thousand words when talking to a computer, and 15 per 1000 to a human. Almost all filled pauses occurred just before a definite reference to a name.

A few researchers have reported success in identifying major syntactic boundaries using prosodic means. 90% success rates are noted for English using prepausal lengthening [4,5] and for French using pitch patterns [6] and vowel durations [7]. Few details are described in this literature, however, and none exploit hesitation phenomena. Furthermore, the English results were based on read speech (not the spontaneous speech of our study) and assumed knowledge of the text corresponding to the speech (which would not be the case in an automatic recognition system).

A study of hesitations in spontaneous French speech [8] noted many similarities to English, and gives an idea how often hesitations occur. They found that a false start (as well as a simple word repetition) occurs on the average every 60 syllables, that a filled pause occurs on average every 22 syllables, and that an unfilled pause happens every 6.5 syllables on average. Thus, hesitation phenomena are very frequent in spontaneous speech and must be addressed in a recognition system attempting to handle such speech.

4. Experimental results

The grammaticality of a pause cannot be reliably separated based on silence duration. Both grammatical and ungrammatical sentence-internal pauses ranged from 100 ms to 3900 ms, with much overlap between the two classes. The 46 syntactic pauses examined averaged 900 ms (median = 800 ms), while the 22 ungrammatical ones averaged 715 ms (median = 600 ms). While there is a definite tendency toward longer silences at syntactic boundaries, a clearer distinction is found in the prepausal word; speakers tend to plan ahead for grammatical pauses and take action prior to the pause. One might expect that speakers would lengthen the final word before a planned pause (i.e., traditional prepausal lengthening) [9], while less often lengthening a word prior to a hesitation. Such a distinction did not occur in duration, but rather in the pitch contour. Very few ungrammatical pauses had a continuation rise in F0 (fundamental frequency) just prior to the pause, whereas 80% of the grammatical pauses were accompanied by a prior F0 rise of 10-40 Hz. These are reliable F0 patterns that can easily be extracted, and do not involve extracting F0 during unvoiced-voiced transitions (where F0 estimators have their greatest difficulties).

Not all pauses are as easy to locate as silences: filled pauses resemble words in continuous, spontaneous speech. A phonetic distinction is made here between filled pauses at major syntactic boundaries and those within syntactic units. Filled pauses at major boundaries were found in the range of 200-500 ms; those within syntactic units were shorter on average (e.g., 170-320 msec). Thus the ranges overlapped, but the syntactic nature of the filled pause could be distinguished by analyzing the silence periods adjacent to the filled pause: for the ungrammatical filled pause, a preceding unfilled pause was very brief (0-350 ms), as was any ensuing silence (0-500 ms). Each grammatical filled pause was preceded by a silence exceeding 275 ms; a long prior silence (> 700 ms) led to a relatively short filled pause (< 300 ms), whereas a short prior silence correlated with a long filled pause (> 300 ms). The spectral pattern of a filled pause was a uniform vowel during its duration (e.g., a steady schwa), possibly followed by the steady nasal /m/. Filled pauses all had falling (5-20 Hz) or flat F0 patterns, at relatively low F0 levels. Ones at syntactic boundaries tended to start higher in F0 and then fall, whereas filled pauses internal to a syntactic unit had lower F0 patterns. All had F0 ending in the bottom 15% of the speaker's F0 range.

5. Conclusion

Simple rules to exploit hesitation phenomena in recognition of spontaneous, continuous speech have been described. The acoustic measurements required (silence durations, F0 during vowels) are robust enough to be practical even for speech in noisy environments. The durations of pauses and F0 behavior in prepausal syllables allow reliable discrimination of whether a pause is occurring at a major syntactic boundary. Earlier results comparing pause statistics in English and French [8] suggest that the results here could be applied as well to French speech.

6. References

[1] W. Levelt, Speaking: From Intention to articulation. Cambridge, MA: MIT Press, 1989.

[2] J. Deese, Thought into speech: The Psychology of a language. Englewood Cliffs, NJ: Prentice-Hall, 1984.

[3] A. G. Hauptmann and A. I. Rudnicky, "Talking to computers: an empirical investigation," International Journal of Man-Machine Systems. vol. 28, pp. 583-604, 1988.

[4] C. W. Wightman and M. Ostendorf, "Automatic recognition of prosodic phrases," in Conference Proceedings of the IEEE International Conference on Acoustics, Speech, and Signal Processing, pp. 321-324, 1991.

[5] P. J. Price, C. W. Wightman, M. Ostendorf, and J. Bear, "The use of relative duration in syntactic disambiguation," in Conference Proceedings of the International Conference on Spoken Language, pp. 13-16, 1990.

[6] J. Vassière, "On automatic extraction of prosodic information for automatic speech recognition system," Conference Proceedings of Eurospeech-89, pp. 202-205, 1989.

[7] N. Carbonell, "On the use of prosodic knowledge for continuous speech recognition and understanding," Conference Proceedings of Eurospeech-89, pp. 522-252, 1989.

[8] F. Grosjean et A. Deschamps, "Analyse des variables temporelles du français spontané," Phonetica. vol. 28, pp. 191-226, 1973.

[9] T. Crystal and A. House, "Segmental durations in connected-speech signals," Journal of the Acoustical Society of America. vol. 84, no. 4, pp. 1553-1585, 1988.

A NON LINEAR ANALYSIS FOR CLEAN AND NOISY SPEECH

Jean Rouat, Yong Chun Liu and Sylvain Lemieux
Dépt des sciences appliquées, Université du Québec à Chicoutimi,
CHICOUTIMI, Québec, Canada, G7H 2B1

1.Introduction

The research in speech analysis is recognized to be an important aspect in the area of speech processing, with applications in speech coding, speech recognition, etc. Depending on the application, the speech analyzer has to extract the most appropriate parameters. This paper will focus on the problem of speech analysis with possible applications in speech recognition. It is known that speaker-independent recognition of continuous speech is a very complicated task which has not yet been fully mastered. The better the quality of the analysis, the easier it becomes to recognize what has been spoken.

The automatic "demodulation" of speech with nonlinear operators, based on perceptive knowledge is a problem which has not yet been fully addressed, and speech "demodulation" might assist the researcher in the understanding of speech and / or in the design of a simple and efficient speech analysis.

2.Modulation

Research work on automatic demodulation of speech can be justified because of the hypothesis proposing that the humain brain has neural cells specialized in Amplitude Modulation (AM) and Frequency Modulation (FM) detection [1] [7] [8].

It is known from previous studies (see [5], for example) that fluctuations in the envelope rather than in the fine structure of the speech signal carry the information regarding speech intelligibility. The fluctuations of the envelope of a speech signal are dependent on the relative frequency, the relative energy and the relative phase of the formants (for voiced speech). This suggests again an analysis based on a model of speech "modulation".

3.Nonlinear operators

Recently Kaiser [2] proposed a nonlinear operator (called Teager energy operator) able to extract the energy of a signal based on mechanical and physical considerations. It has been shown [3] that this operator is able to tract the envelope of an amplitude or frequency modulated signal.

Another nonlinear operator has been proposed [6] (called "Dyn") based on perceptive considerations. This operator shows surprising ability to enhance the FM-AM modulation in speech, and can be compared to the Teager energy operator. One could consider that the Teager operator is the envelope of the Dyn operator for vowels. Figure 1 illustrates this idea. Depending on the application, one can use the Dyn or the Teager operators. The top section of Fig. 1. shows four pitch periods taken from the original speech (/i/) of a male speaker (pitch frequency = 130Hz). The second section presents the band-pass-filtered speech [4] with a center frequency of 2300Hz. The third section shows the output of the Dyn operator on the band-pass-filtered speech. And the fourth section illustrates the output of the Teager energy operator on the same band-pass-filtered speech. The Dyn and the Teager operators show the modulated energy pulses characteristics of the speech signal.

Is there a link between these pulses and the formants? Are these pulses characteristic of a nonlinear coupling between the glottal source and the vocal tract? Is it possible to use these nonlinear operators to extract an information suitable for speech recognition? Most of these questions do not have a clear answer yet. And this paper proposes an analysis which can be used to answer the above questions.

4.The analysis

The actual version of the analyzer is comprised of a bank of twenty filters from 300Hz to 3300Hz. These filters simulate the frequency analysis performed by the cochlea. There are rounded exponential filters with the Equivalent Rectangular Bandwidths (ERB) proposed by Moore and Glasberg [4]. The output of each filter is then processed by either the Dyn operator or by the Teager Energy operator depending on the application, see [6] for more details.

This model is very simple and no attempt has been made to represent the exact transduction mechanism from the inner hair cells (for afferent information) or from the outer hair cells (for active feedback). The Dyn operator needs one multiplication and one addition per sample and the Teager operator, two multiplications and one addition per sample.

5.Comments

Figure 2 shows the output of the model for three pitch periods from the transition /d//i/ in the syllable "di" from a male speaker.
It can be seen that the formant information is preserved and that high-frequency components are enhanced in comparison with low-frequency components. The pulses of energy are better seen in high-frequency. From Figure 2, it can be seen that the low-frequency components are not in phase with the high-frequency components.

6.Conclusion

A new analysis has been proposed based on nonlinear transformations of the signal and on perceptive know ledge. It has been shown that this analysis preserves the formant structure [6] on the frequency dimension and has a very good time resolution. This analysis gives a three dimensionnal representation of speech: "mechanical energy", Bark scale and time scale. In comparison with a spectrogram representation, this analysis shows a more important redundancy in frequency (Bark scale) and in time (modulation) and consequently should be more resistant to noise.

7.References

[1] Gardner, R.B. and Wilson J.P. (1979). Evidence for direction-specific channels in the processing of frequency modulation. J. Acoust. soc. Amer. 66, p. 704.
[2] Kaiser, J.F. (1990). On a simple algorithm to calculate the 'energy' of a signal. Proceedings of IEEE-ICASSP'90, Albuquerque, pp. 381-384.

[3] Maragos, P. Quatieri, T. and Kaiser, J.F. (1991). Speech nonlinearities, modulations and energy operators. Proceedings of the IEEE - ICASSP'91, Toronto, pp. 421-424.
[4] Moore, B.C.J. and Glasberg, B.R. (1983). Suggested formulae for calculating auditory-filter bandwidths and excitation patterns. J. Acoust. Soc. Am. 74, pp. 750-753.
[5] Plomp, R. (1988). Effect of amplitude compression in hearing aids in the light of the modulation-transfer function. J. Acous. Soc. Amer. 83 (6), pp. 2322-2327.
[6] Rouat, J. (1991). Dyn: a nonlinear operator for speech analysis. Université du Québec à Chicoutimi, dépt des sciences appliquées, rapport interne.
[7] Tansley, B.W. and SUFFIELD, J.B. (1983). Time course of adaptation and recovery of channels selectively sensitive to frequency and amplitude modulation. J. Acoust. Soc. Amer. '74, p. 765.
[8] Wakefield, G.H. and Viemeister, N.F. (1984). Selective adaptation to linear frequency-modulated sweeps: Evidence for direction-specific FM channels ? J. Acoust. Soc. Amer. 75, p. 1588.

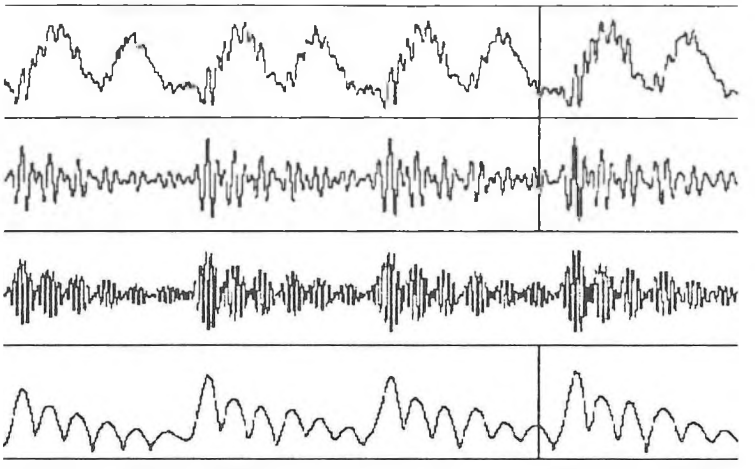

Fig. 1 : nonlinear operators on band-pass-filtered speech, C.F. 2300Hz

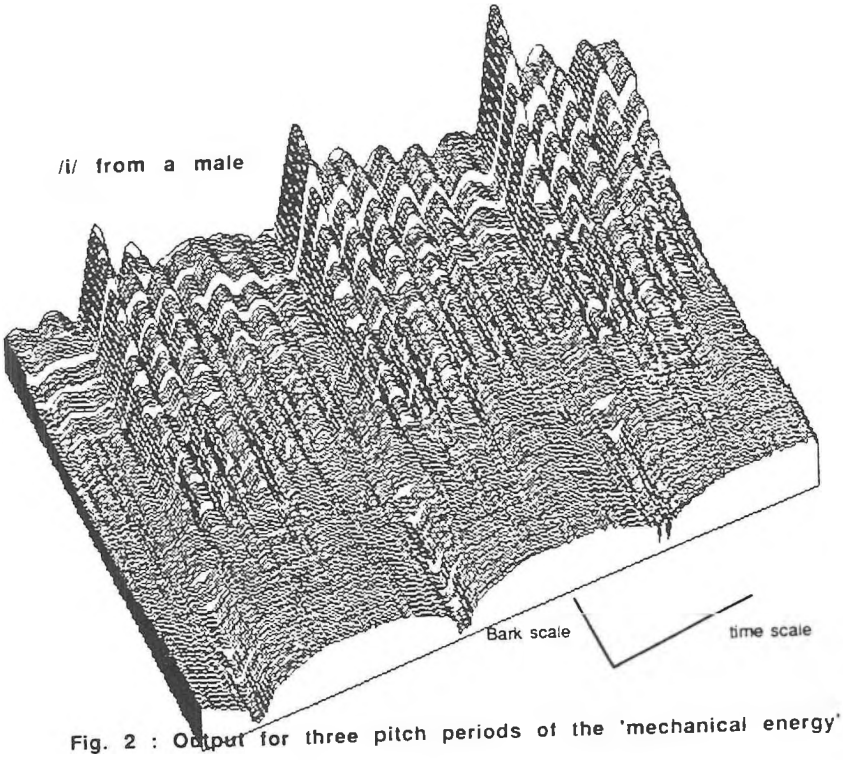

Fig. 2 : Output for three pitch periods of the 'mechanical energy'

ACOUSTICAL INTERFACE™ SYSTEM

precision acoustical measurements with your FFT, scope or meter

PS9200 POWER SUPPLY

■ Dual Channel ■ 9V "Radio" Battery
■ Portable ■ 50 Hours Operation
■ Low Noise ■ LED Status Indicator

7000 SERIES MICROPHONES

■ Type 1 Performance ■ ¼, ½ and 1 Inch Models

4000 SERIES PREAMPLIFIERS

■ 2Hz to 200kHz ± 0.5db ■ Removable Cable ■ PS9200 and 7000 Series Compatible

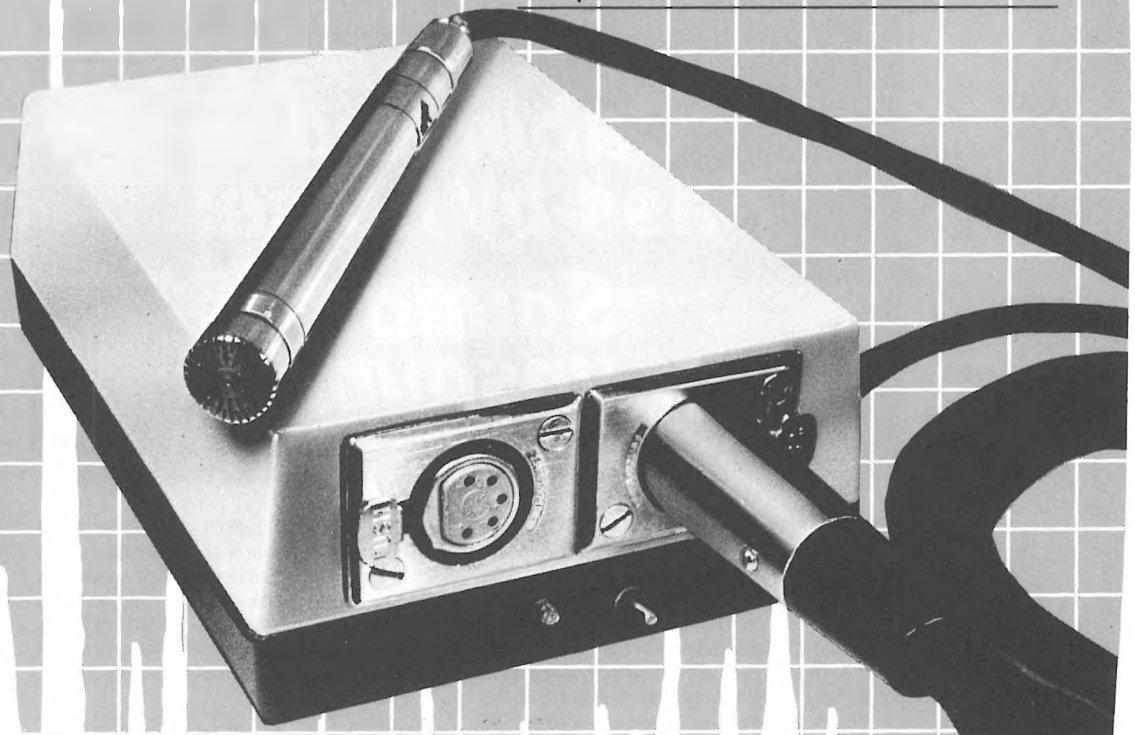

NEW LOW COST PRECISION MEASUREMENTS

■ **SINGLE CHANNEL SYSTEM UNDER $1,200**
■ **DUAL CHANNEL SYSTEM UNDER $2,000**
(½ or 1 inch microphones)

ACO Pacific, Inc.
2604 Read Avenue
Belmont, CA 94002
(415) 595-8588

ACOUSTICS BEGINS WITH ACO

The Canadian Acoustical Association
l'Association Canadienne d'Acoustique

ANNUAL GENERAL MEETING / ASSEMBLEE GENERALE ANNUELLE

Date / Date:	October 10 / 10 octobre 1991
Time / Heure:	3:30 p.m. / 15h30
Place / Endroit:	Ramada Renaissance Edmonton, Alberta

AGENDA / ORDRE DU JOUR

1. Welcome
2. Reading of the Minutes
3. Report of the President (B. Dunn)
4. Report of the Executive Secretary (W. Sydenborgh)
5. Report of the Treasurer (G. Bolstad)
6. Report of the Editor of *Canadian Acoustics* (M. Hodgson)
7. Report of the Membership Chairperson (M. Zagorski)
8. Preliminary summary report of Canadian Acoustics Week 1991 (G. Bolstad)
9. Prizes: Postponed to banquet
10. Report from Chairperson of Education Committee (S. Abel)
11. Report on International INCE and Inter-Noise '92 (T. Embleton)
12. Report of the Overall Prize Review Committee (A. Behar) / Decision on future policy
13. Discussion of Science Fair Policy (A. Cohen)
14. Status Report on 1994 International Congress of Audiology (B. Dunn)
15. Report on International Conference on Spoken Language Processing (B. Dunn)
16. Canadian Acoustics Week 1992 and other future meetings
17. Other business:

    Business arising from the Minutes
    Business arising from the Board Meeting
    New business

18. Elections

The Canadian Acoustical Association
l'Association Canadienne d'Acoustique

BOARD OF DIRECTORS MEETING / REUNION DES DIRECTEURS

Date / Date:	October 10 / 10 octobre 1991
Time / Heure:	10:00 a.m. / 10h00
Place / Endroit:	Ramada Renaissance Edmonton, Alberta

AGENDA / ORDRE DU JOUR

1. Report of the President (B. Dunn)

2. Report of the Executive Secretary (W. Sydenborgh)

3. Report of the Treasurer (G. Bolstad)

4. Report of the Editor of *Canadian Acoustics* (M. Hodgson)

5. Report of the Membership Chairperson (M. Zagorski)

6. Report on Canadian Acoustics Week 1991 (G. Bolstad)

7. Prizes:

   Directors Award (C. Laroche)
   Postdoctoral Prize (S. Abel)
   Bell Speech Prize (L. Brewster)
   Underwater Acoustics Prize (D. Chapman)
   Student Presentations (A. Behar)
   Eckel Award (M. Hodgson)

8. Report from Chairperson of Education Committee (S. Abel)

9. Report on International INCE and Inter-Noise '92 (T. Embleton)

10. Report of the Overall Prize Review Committee (A. Behar) / Discussion of the efficient administration and advertising of prizes.

11. Information on Science Fairs (A. Cohen)

12. Status Report on 1994 International Congress of Audiology (B. Dunn)

13. Report on International Conference on Spoken Language Processing (B. Dunn)

14. Halifax chapter (D. Chapman)

15. Report of the nominating committee (S. Abel)

16. Canadian Acoustics Week 1992

17. New business

NEWS / INFORMATIONS

CONFERENCES

Inter-Noise 91 (Costs of Noise): Sydney, Australia, December 2-4, 1991. Contact: Christine Bourke, Conference Secretariat, University of New South Wales, P.O. Box 1, Kensington, NSW 2033, Australia.

International Conference on Sonar Signal Processing, Institute of Acoustics: Leicestershire, U.K., December 16-18, 1991. Contact: Professor J.W.R. Griffiths, Dept. of Electronic Engineering, University of Technology, Loughborough LE11 3TU, U.K. Telephone: (0509) 222830. Telex: 34319. Fax: (0509) 22830.

2nd International Congress on Recent Developments in Air- and Structure-Borne Sound and Vibration: Acoustical Society of America Institute of Noise Control Engineering, March 4-6, 1992. Contact: For further information call (205) 844-4820.

2nd French Congress on Acoustics: Arcachon, France, April 14-17, 1992. Contact: Congres Français d'Acoustique, Mécanique Physique, Universite de Bordeaux I, 33405 Talence Cedex, France. Telephone: (33) 56 84 62 26. Telefax: (33) 56 84 69 64.

DGLR/AIAA 14th Aeroacoustics Conference: Aachen, Germany, May 11-14, 1992. Contact: Dr. John Seiner, Acoustics Division, NASA Langley Research Center, Mail Code 166, Hampton, Virginia 23665-5225, USA. Telephone: (804) 864-6274. Fax: (804) 864-7687.

Eurosymposium. "The Mitigation of Traffic Noise in Urban Areas": Palais des Congres Nantes, France, May 12-15, 1992. Contact: Y. Delanne, L.C.P.C., Centres de Nanates 8 P 19, 44340 Bouguenais, France. Telephone: (33) 40 84 59 01. Fax: (33) 40 84 59 96.

6th International Conference on Hand-Arm Vibration: Bonn, Federal Republic of Germany, May 19-22, 1992. Contact: 6th HAV - Berufsgenossenschaftliches Institute fur Arbeitssicherheit - BIA, Alte Heerstrasse 111, D-5205 Sankt Augustin 2. Telex 49/2241/23102. Telefax: (49) 2241 231234.

Acoustical Society of America: Salt Lake City, Utah, May 11-15, 1992. Contact: Murray Strasberg, Acoustical Society of America, 500 Sunnyside Blvd., Woodbury, NY 11797, USA.

14th International Congress on Acoustics: Beijing, China, September 3-10, 1992. Contact: ICA Secretariat, Institute of Acoustics, P.O. Box 2712, Beijing 100080, China. Fax: 256-1457.

COURSES

Acoustics & Noise Control: Seven Springs, Pennsylvania, October 21-15, 1991. Contact: AVNC, Continuing Education Division, 250 Shagbark Drive, R.D. #1, Cheswick, PA 15024..

Signal Processing: Seven Springs, Pennsylvania, October 21-15, 1991. Contact: AVNC, Continuing Education Division, 250 Shagbark Drive, R.D. #1, Cheswick, PA 15024.

CONFERENCES

Conférence Inter-Noise 91 (Les Coûts du Bruit): Sydney, Australie, du 2 au 4 décembre 1991. Contacter: Christine Bourke, Conference Secretariat, University of New South Wales, P.O. Box 1, Kensington, NSW 2033, Australie.

Conférence internationale sur le traitement des signaux de sonar, Institute of Acoustics: Leicestershire, Grande-Bretagne, du 16 au 18 décembre 1991. Contacter: Professor J.W.R. Griffiths, Department of Electronic Engineering, University of Technology, Loughborough LE11 3TU, Grande-Bretagne. Téléphone: (0509) 222830. Télex: 34319. Télécopieur: (0509) 22830.

2e Congrès international sur les derniers progrès dans le domaine des vibrations et des sons aériens et des corps: Acoustical Society of America / Institute of Noise Control Engineering, du 4 au 6 mars 1992. Renseignements: (205) 844-4820.

2e Congrès français d'acoustique: Arcachon, France, du 14 au 17 avril 1992. Contacter: Congrès français d'acoustique, Mécanique physique, Université de Bordeaux I, 33405 Talence Cedex, France. Téléphone: (33) 56 84 62 26. Télécopieur: (33) 56 84 69 64.

14e Conférence DGLR/AAIAA sur l'aéroacoustique: Aachen, Allemagne, du 11 au 14 mai 1992. Contacter: Dr. John Seiner, Acoustics Division, NASA Langley Research Center, Mail Code 166, Hampton, Virginie 23665-5225, E-U. Téléphone: (804) 864-6274. Télécopieur: (804) 864-7687.

Eurosymposium sur la maîtrise du bruit routier en milieu urbain: Palais des congrès, Nantes, France, du 12 au 15 mai 1992. Contacter: Y. Delanne, L.C.P.C., Centre de Nantes 8 P 19, 44340 Bouguenais, France. Téléphone: (33) 40 84 59 01. Télécopieur: (33) 40 84 59 96.

6e Conférence internationale sur les vibrations dans les bras et les mains: Bonn, Allemagne, du 19 au 22 mai 1992. Contacter: 6th HAV - Berufsgenossenschaftliches Institute fur Arbeitssicherheit - BIA, Alte Heerstrasse 111, D-5205, Sankt Augustin 2. Télex: 49-2241-23102. Télécopieur: (49) 2241-231234.

Conférence de l'Acoustical Society of America: Salt Lake City, Utah, du 11 au 15 mai 1992. Contacter: Murray Strasberg, Acoustical Society of America, 500 Sunnyside Blvd, Woodbury, NY 11797, E-U.

14e Congrès international sur l'acoustique: Beijing, Chine, du 3 au 10 septembre 1992. Cotnacter: ICA Secretariat, Institute of Acoustics, P.O. Box 2712, Beijing 100080, Chine. Télécopieur: 246-1457.

COURS

Acoustics & Noise Control: Seven Springs, Pennsylvanie, du 21 au 25 octobre 1991. Contacter: AVNC, Continuing Education Division, 250 Shagbark Drive, R.D. #1, Cheswick, PA 15024, E-U.

Underwater Acoustics and Signal Processing: Penn State, November 4-8, 1991. Contact: Dr. Alan D. Stuart, Short Course Chairman, Penn State Graduate Program in Acoustics and Applied Research Laboratory, P.O. Box 30, State College, PA 16804. Telephone: (814) 863-4128. Fax: (814) 865-3119.

Training Cource in Noise Control: Orlando, Florida, November 18-22, 1991. Contact: Hoover and Keith Inc., 11381 Meadowglen, Suite 1, Houston, Texas 77082. Telephone: (713) 9876.

Mechanical Vibration: Seven Springs, PA, March 2-6, 1992. Contact: AVNC, Continuing Education Division, 250 Shagbark Drive, R.D. #1, Cheswick, PA 16094.

NEW PRODUCTS

The American Institute of Ultrasound in Medicine (AIUM) announces the publication of two new guidelines for performance of ultrasound examinations. *Guidelines for Performance of the Pediatric Neurosonology Ultrasound Examination*, and the *Guidelines for Performance of the Ultrasound Examination of the Female Pelvis*.

These new guidelines are available for $6.00 each for AIUM members and $20.00 each for non-0members. Postage and handling are included. To order, simply call, fax, or write to AIUM, Publications Department, 11200 Rockville Pike, Suite 205, Rockville, MD 20852-3139. Telephone: (301) 881-2486. Fax: (301) 881-7303. American Express, MasterCard and VISA are welcome.

ANNOUNCEMENT

The Institute of Noise Control Engineering will be providing the opportunity for interested persons to take the INCE "Fundamentals Exam" (for Affiliate Membership) and the INCE "Professional Exam" (for Membership) during Acoustics Week in Edmonton, AB (1991 October 7-11). If you are interested in taking either exam, please call or fax the number below immediately:

Richard J. Peppin, P.Engl
Vice President, Membership
INCE
5012 Macon Road, Rockville, MD 20852 USA
(301) 495-7738 phone, -7739 FAX

Signal Processing: Seven Springs, Pennsylvanie, du 21 au 25 octobre 1991. Contacter: AVNC, Continuing Education Division, 250 Shagbark Drive., R.D. #1, Cheswick, PA 15024, E-U.

Underwater Acoustics and Signal Processing: Penn State, du 4 au 8 novembre 1991. Contacter: Dr. Alan D. Stuart, Short Course Chairman, Penn State Graduate Program in Acoustics and Applied Research Laboratory, P.O. Box 30, State College, PA 16804. Téléphone: (814) 863-4128. Télécopieur: (814) 865-3119.

Training Course in Noise Control: Orlando, Floride, du 18 au 22 novembre 1991. Contacter: Hoover and Keith Inc., 11381 Meadowglen, Suite 1, Houston, Texas 77082. Téléphone: (713) 496-9876.

Mechanical Vibration: Seven Springs, Pennsylvanie, du 2 au 6 mars 1992. Contacter: AVNC, Continuing Education Division, 250 Shagbark Drive. R.D. #1, Cheswick, PA 15024, E-U.

NOUVEAUX PRODUITS

L'American Institute of Ultrasound in Medicine (AIUM) annonce la publication de deux guides pour la prise d'échographies: *Guidelines for Performance of the Pediatric Neurosonology Ultrasound Examination* et *Guidelines for Performance of the Ultrasound Examination of the Female Pelvis*.

Ces nouveaux guides sont disponibles au prix de 6 $ l'unité pour les membres de l'AiUM et de 20 $ pour les non-membres. Ce prix inclut les frais de poste et de manutention. Pour les commander, contacter: AIUM, Publications Department, 11200 Rockville Pike, Suite 205, Rockville, MD 20852-3139. Téléphone: (301) 881-2486. Télécopieur: (301) 881-7303. Cartes American Express, MasterCard et VISA acceptées.

ANNONCE

L'Institut de génie en contrôle du bruit (INCE) offre la possibilité aux personnes intéressées, de compléter "l'Examen Fondamental" INCE (pour les membres affiliés) et "l'Examen Professionnel" INCE (pour les membres) lors de la Semaine de l'Acoustique à Edmonton (7-11 octobre 1991). Si vous êtes intéressés à passer l'un ou l'autre examen, veuillez composer le numéro de téléphone ou de FAX ci-bas, le plus tôt possible:

Richard J. Peppin, P.Eng.
Vice President, Membership
INCE
5012 Macon Road, Rockville, MD 20852 E-U
(301) 495-7738 (téléphone)
(301) 495-7739 (FAX)

EMPLOYMENT

As a service to readers we will publish, at no charge, advertisements from employers looking for staff, and from individuals seeking employment. To take advantage of this service, simply send your advertisement to the Editor-in-Chief. Individuals wishing to remain anonymous may request the use of a file number, to be managed by the Editor.

Acoustical Consultants Required

Well-respected West Coast firm has openings for two engineers, architects or scientists. The first requirement is for a junior consultant and requires at least one year working experience in the field of acoustics and/or post-graduate training in acoustics. Initially, work would consist largely of residential site evaluations and HVAC noise control design. Diversification into other areas would follow. Ability to work and communicate effectively with clients is an important requirement of this position. The second position is for a senior consultant and requires at least 7 years experience in architectural acoustics. Additional experience in sound system design, industrial/marine noise control or environmental noise assessment would be an asset. Contact:

Barron Kennedy Lyzun & Associates Ltd.
The Professional Centre
250 - 145 West 17th Street
North Vancouver, BC V7M 3G4

L'Université de Sherbrooke sollicite des candidatures pour un poste de

Professeur(e) en génie mécanique

Poste ouverte dans le secteur vibro-acoustique dans le cadre de l'établissement d'une chaire en acoustique.

Profil des fonctions

- Enseignement au 1er cycle dans les domaines de la mécanique appliquée: dynamique, systèmes mécaniques, vibrations, acoustique industrielle. Enseignement au 2è et 3è cycles dans les domaines de l'acoustique et des vibrations.

- Recherches fondamentales en vibroacoustique et recherches appliqueés dans le thème de la réduction du bruit à la source. Participation aux projets financés par la chaire à des contrats et aux concours réguliers des organismes subventionnaires. Supervision d'étudiants de 2è et 3è cycles.

Qualifications requises

Doctorat en génie mécanique avec spécialisation en acoustique ou vibroacoustique. Avoir une expérience reconnue du bruit à la source. Membre de l'Ordre des ingénieurs du Québec ou qualifications pour le devenir. Maîtrise de la langue française.

Traitement - Selons les normes en vigeur.

Exigences particulières - La candidature sera soumise pour approbation par le CRSNG.

Avant le 31 octobre 1991, prière de faire parvenir votre curriculum vitae ainsi que les noms et adresses de trois personnes susceptibles de fournir des recommandations, à:

Monsieur le doyen, Faculté des sciences appliquées
Université de Sherbrooke, Québec J1K 2R1
Fax: (819) 821-7903

EMPLOIS

A titre de service aux lecteurs nous publierons, sans frais, les annonces d'employeurs qui cherchent du personnel, et d'individus qui sont à la recherche d'un emploi. Pour bénéficier de ce service, envoyez simplement votre annonce au rédacteur en chef. Les individus désirant demeurer anonymes peuvent demander un numéro de dossier, géré par le rédacteur.

Employment Sought

Well-trained graduate with M.Eng. in acoustics seeks a professional career as an acoustical engineer. Experienced in architectural acoustics and occupational noise assessment. Familiar with acoustic theory, instrumentation, noise control design, as well as computers and software routines. Please contact:

Mr. Li Junping
Centre for Building Studies
Concordia University
1455 de Maisonneuve Blvd. W.
Montreal, Quebec H3G 1M8
(514) 848-7919 (office)
(514) 342-2263 (residence)

Le Groupe d'Acoustique et Vibrations de l'Université de Sherbrooke, un chef de file au Canada, regroupe une vingtaine de personnes dont 4 professeurs, 3 attachés de recherche et une dizaine d'étudiants. En vue de la constitution d'une chaire en acoustique qui sera financée conjointement par le Conseil de recherches en sciences naturelles et en génie (CRSNG) et par l'Institut de recherche en santé et sécurité au travail (IRSST), le laboratoire d'acoustique et vibrations est à la recherche de candidats pour combler les postes suivantes:

2 Postes de chercheur postdoctoral

- Recherche fondamentale en vibroacoustique

- Exigences - titulaire récent d'un doctorat en Acoustique ou Vibroacoustique
  - langues: français ou anglais

- Rémunération - selon les normes du CRSNG

2 Postes d'assistant de recherche

- Recherche appliquée en contrôle du bruit et des vibrations

- Exigences - titulaire d'une maîtrise ou d'un doctorat en acoustique ou vibroacoustique
  - parler et écrire courrament le français

- Rémunération - selon les normes du CRSNG

Avant le 31 octobre 1991, prière de faire parvenir les pièces suivantes: un curriculum détaillé; une copie des résultats académiques de 1er, 2è, 3è cycles; une copie de mémoire et de thèse (si possible); deux lettres de références, à:

Jean Nicolas, Professeur titulaire
GAUS (Groupe d'Acoustique et Vibrations)
Département de génie mécanique
Université de Sherbrooke
Sherbrooke, Québec J1K 2R1
Tél: (819) 821-7157
Fax: (819) 821-7163

Representatives Wanted

Scantek, Inc., the exclusive North American distributor of Norsonic (formerly Norwegian Electronics), RION, Castle Associates, RTA Technology, Braunstein & Berndt and others is searching for one or more representatives in Canada to handle its entire line. We offer a strong and diverse line, a strong customer base, and unsurpassed support and service. For further information call or write:

Richard J. Peppin, P.Eng.,President
Scantek, Inc., 916 Gist Avenue
Silver Spring, MD, USA 20910
Tel: (301) 495-7738
Fax: (301) 495-7739

Manager

A well-established, well-equipped western-Canadian acoustical consultant is seeking a Manager to assume full responsibility for operating the company. Eligibility for membership in APEGGA and at least 3 years experience in acoustical consulting are required. Management and market experience are a definite asset. Partnership and eventual full ownership are open to negotation. Contact:

Bolstad Engineering Associates Ltd.
9249 - 48th Street
Edmonton, Alberta T6B 2R9
Tel: (403) 465-5317
Fax: (403) 465-5318

Wanted : Career

Acoustical Engineer Solicits Challenging Career

Knowledgable in highway noise control techniques and analysis. Practical experience using transducers and instrumentation measuring techniques, such as sound intensity, for analyzing acoustical and vibration phenomena. University education in engineering. Member of:

Association of Professional Engineers of Ontario (APEO)
Canadian Acoustical Association
Institute of Noise Control Engineering
Acoustical Society of America

Reply with confidence and confidentiality to:

Acoustical Engineer
4 Ludlow Avenue
Toronto, Ontario M8Z 3S8

INSTRUCTIONS TO AUTHORS
PREPARATION OF MANUSCRIPT

Submissions: The original manuscript and two copies should be sent to the Editor-in-Chief.

General Presentation: Papers should be submitted in camera-ready format. Paper size 8.5" x 11". If you have access to a word processor, copy as closely as possible the format of the articles in Canadian Acoustics 18(4) 1990. All text in Times-Roman 10 pt font, with single (12 pt) spacing. Main body of text in two columns separated by 0.25". One line space between paragraphs.

Margins: Top - title page: 1.25"; other pages, 0.75"; bottom - 1" minimum; sides, 0.75".

Title: Bold, 14 pt with 14 pt spacing, upper case, centered.

Authors/addresses: Names and full mailing addresses, 10 pt with single (12 pt) spacing, upper and lower case, centered. Names in bold text.

Abstracts: English and French versions. Headings, 12 pt bold, upper case, centered. Indent text 0.5" on both sides.

Headings: Headings to be in 12 pt bold, Times-Roman font. Number at the left margin and indent text 0.5". Main headings, numbered as 1, 2, 3, ... to be in upper case. Sub-headings numbered as 1.1, 1.2, 1.3, ... in upper and lower case. Sub-sub-headings not numbered, in upper and lower case, underlined.

Equations: Minimize. Place in text if short. Numbered.

Figures/Tables: Keep small. Insert in text at top or bottom of page. Name as "Figure 1, 2, ..." Caption in 9 pt with single (12 pt) spacing. Leave 0.5" between text.

Photographs: Submit original glossy, black and white photograph.

References: Cite in text and list at end in any consistent format, 9 pt with single (12 pt) spacing.

Page numbers: In light pencil at the bottom of each page.

Reprints: Can be ordered at time of acceptance of paper.

DIRECTIVES A L'INTENTION DES AUTEURS
PREPARATION DES MANUSCRITS

Soumissions: Le manuscrit original ainsi que deux copies doivent être soumis au rédacteur-en-chef.

Présentation générale: Le manuscript doit comprendre le collage. Dimensions des pages, 8.5" x 11". Si vous avez accès à un système de traitement de texte, dans la mesure du possible, suivre le format des articles dans i'Acoustique Canadienne 18(4) 1990. Tout le texte doit être en caractères Times-Roman, 10 pt et à simple (12 pt) interligne. Le texte principal doit être en deux colonnes séparées d'un espace de 0.25". Les paragraphes sont séparés d'un espace d'une ligne.

Marges: Dans le haut - page titre, 1.25"; autres pages, 0.75"; dans le bas, 1" minimum; aux côtés, 0.75".

Titre du manuscrit: 14 pt à 14 pt interligne, lettres majuscules, caractères gras. Centré.

Auteurs/adresses: Noms et adresses postales. Lettres majuscules et minuscules, 10 pt à simple (12 pt) interligne. Centré. Les noms doivent être en caractères gras.

Sommaire: En versions anglaise et française. Titre en 12 pt, lettres majuscules, caractères gras, centré. Paragraphe 0.5" en alinéa de la marge, des 2 cotés.

Titres des sections: Tous en caractères gras, 12 pt, Times-Roman. Premiers titres: numéroter 1, 2, 3, ..., en lettres majuscules; sous-titres: numéroter 1.1, 1.2, 1.3, ..., en lettres majuscules et minuscules; sous-sous-titres: ne pas numéroter, en lettres majuscules et minuscules et soulignés.

Equations: Les minimizer. Les insérer dans le texte si elles sont courtes. Les numéroter.

Figures/Tableaux: De petites tailles. Les insérer dans le texte dans le haut ou dans le bas de la page. Les nommer "Figure 1, 2, 3,..." Légende en 9 pt à simple (12 pt) interligne. Laisser un espace de 0.5" entre le texte.

Photographies: Soumettre la photographie originale sur paper glacé, noir et blanc.

Références: Les citer dans le texte et en faire la liste à la fin du document, en format uniforme, 9 pt à simple (12 pt) interligne.

Pagination: Au crayon pâle, au bas de chaque page.

Tirés-à-part: ils peuvent être commandés au moment de l'acceptation du manuscrit.

The Canadian Acoustical Association

l'Association Canadienne d'Acoustique

SUBSCRIPTION INVOICE

Subscription for the current calendar year is due January 31. Subscriptions received before July 1 will be applied to the current year and include that year's back issues of Canadian Acoustics, if available. Subscriptions received from July 1 will be applied to the next year.

Check ONE Item Only:

CAA Membership	$35
CAA Student membership	$10
Corporate Subscription	$35
Sustaining Subscription	$150

Total Remitted $_____

INFORMATION FOR MEMBERSHIP DIRECTORY

Check areas of interest (max 3):

1. Architectural Acoustics _____
2. Electroacoustics _____
3. Ultrasonics & Physical Acoustics _____
4. Musical Acoustics _____
5. Noise _____
6. Psycho/Physiological Acoustics _____
7. Shock & Vibration _____
8. Speech Communication _____
9. Underwater Communication _____
10. Other _____

PLEASE TYPE NAME AND ADDRESS BELOW:

VEUILLEZ ECRIRE VOTRE NOM ET VOTRE ADRESSE CI-DESSOUS:

FACTURE D'ABONNEMENT

L'abonnement pour la présente année est dû le 31 janvier. Les abonnements reçus avant le 1 juillet s'appliquent à l'année courante et incluent les ancient numéros (non-épuisés) de l'Acoustique Canadienne de cette année. Les abonnements reçus à partir du 1 juillet s'appliquent à l'année suivante.

Cocher la case appropriée :

Membre individuel	
Membre étudiant(e)	
Membre de société	
Abonnement de soutien	

Versement total

RENSEIGNEMENT POUR L'ANNUAIRE DES MEMBRES

Cocher vos champs d'intérêt (max. 3):

1. Acoustique architecturale _____
2. Electroacoustique _____
3. Ultrasons, acoustique physique _____
4. Acoustique musicale _____
5. Bruit _____
6. Physio/psychoacoustique _____
7. Chocs et vibrations _____
8. Communication parlée _____
9. Acoustique sous-marine _____
10. Autre _____

Telephone number (_____) _____ Numéro de téléphone
Facsimile number (_____) _____ Numéro de télécopieur
E-Mail number _____ Numéro de courier électronique

Faites parvenir ce formulaire à l'adresse suivante en prenant soin d'y joindre un chèque fait au nom de L'ASSOCIATION CANADIENNE D'ACOUSTIQUE:

Make cheques payable to THE CANADIAN ACOUSTICAL ASSOCIATION. Mail this form with payment to:

W.V. Sydenborgh
H.L. Blachford Ltd.
2323 Royal Windsor Drive
Mississauga, Ontario L5J 1K5

The Canadian Acoustical Association
l'Association Canadienne d'Acoustique

SUSTAINING SUBSCRIBERS / ABONNES DE SOUTIEN

The Canadian Acoustical Association gratefully acknowledges the financial assistance of the Sustaining Subscribers listed below. Annual donations (of $150.00 or more) enable the journal to be distributed to all at a reasonable cost. Sustaining Subscribers receive the journal free of charge. Please address donation (made payable to the Canadian Acoustical Association) to the Associate Editor (Advertising).

L'Association Canadienne d'Acoustique tient à témoigner sa reconnaissance à l'égard de ses Abonnés de Soutien en publiant ci-dessous leur nom et leur adresse. En amortissant les coûts de publication et de distribution, les dons annuels (de $150.00 et plus) rendent le journal accessible à tous nos membres. Les Abonnés de Soutien reçoivent le journal gratuitement. Pour devenir un Abonné de Soutien, faites parvenir vos dons (chèque ou mandat-poste fait ou nom de l'Association Canadienne d'Acoustique) au rédacteur associé (publicité).

Acoustec Inc
935 rue Newton, suite 103
Québec, Québec G1P 4M2
Tél.: (418) 877-6351

Barman Swallow Associates
1 Greenboro Dr., Suite 401
Rexdale, Ontario M9W 1C8
Tel.: (416) 245-7501

Barron Kennedy Lyzun & Assoc.
#250-145 West 17th Street
North Vancouver, BC V7M 3G4
Tel.: (604) 988-2508

Bilsom International Ltd.
60 St. Clair Ave. E., Suite 1002
Toronto, Ontario M4T 1N5
Tel.: (416) 922-7807

H.L. Blachford Ltd.
Noise Control Products
Engineering / Manufacturing
Mississauga: Tel.: (416) 823-3200
Montreal: Tel.: (514) 866-9775
Vancouver: Tel.: (604) 263-1561

Bolstad Engineering Associates
9249 - 48 Street
Edmonton, Alberta T6B 2R9
Tel.: (403) 465-5317

Bruel & Kjaer Canada Limited
90 Leacock Road
Pointe Claire, Québec H9R 1H1
Tel.: (514) 695-8225

J.E. Coulter Associates Engineering
200 Finch Ave. W., Suite 201
North York, Ontario M2R 3W4
Tel.: (416) 250-6565

Dalimar Instruments Inc.
P.O. Box 110
Ste-Anne-de-Bellevue
Québec H9X 3L4
Tél.: (514) 453-0033

Eckel Industries of Canada Ltd.
Noise Control Products, Audiometric
Rooms - Anechoic Chambers
P.O. Box 776
Morrisburg, Ontario K0C 1X0
Tel.: (613) 543-2967

Electro-Medical Instrument Ltd.
Audiometric Rooms and Equipment
349 Davis Road
Oakville, Ontario L6J 5E8
Tel.: (416) 845-8900

Hatch Associates Ltd.
Attn.: Tim Kelsall
21 St. Clair Ave. E.
Toronto, Ontario M4T 1L9
Tel.: (416) 962-6350

Hugh W. Jones & Associates
374 Viewmount Drive
Allen Heights
Tantallon, Nova Scotia B0J 3J0
Tel.: (902) 826-7922

Industrial Metal Fabricators Ltd.
Environmental Noise Control
288 Inshes Avenue
Chatham, Ontario N7M 5L1
Tel.: (519) 354-4270

Larson Davis Laboratories
1681 West 820 North
Provo, Utah, USA 84601
Tel.: (801) 375-0177

Mechanical Engineering Acoustics and Noise Unit
Dept. of Mechanical Engineering
6720 30th St.
Edmonton, Alberta T6P 1J3
Tel.: (403) 466-6465

MJM Conseillers en Acoustique Inc.
M.J.M. Acoustical Consultants Inc.
Bureau 440, 6555 Côte des Neiges
Montréal, Québec H3S 2A6
Tél.: (514) 737-9811

Nelson Industries Inc.
Corporate Research Department
P.O. Box 600
Stoughton, Wisconsin, USA 53589-0600
Tel.: (608) 873-4373

OZA Inspections Ltd.
P.O. Box 271
Grimsby, Ontario L3M 4G5
Tel.: (416) 945-5471

Scantek Inc.
Sound and Vibration Instrumentation
916 Gist Avenue
Silver Spring, Maryland, USA 20910
Tel.: (301) 495-7738

Spaarg Engineering Limited
Noise and Vibration Analysis
822 Lounsborough Street
Windsor, Ontario N9G 1G3
Tel.: (519) 972-0677

Tacet Engineering Limited
Consultants in Vibration & Acoustical Design
111 Ava Road
Toronto, Ontario M6C 1W2
Tel.: (416) 782-0298

Triad Acoustics
Box 23006
Milton, Ontario L9T 5B4
Tel.: (800) 265-2005

Valcoustics Canada Ltd.
30 Wertheim Court, Unit 25
Richmond Hill, Ontario L4B 1B9
Tel.: (416) 764-5223

Vibron Limited
1720 Meyerside Drive
Mississauga, Ontario L5T 1A3
Tel.:(416) 670-4922

Wilrep Ltd.
1515 Matheson Blvd. E.
Mississauga, Ontario L4W 2P5
Tel.: (416) 625-8944